Regulation of DNA Cleavage by the ATPase Domain of DNA Topoisomerase II

BY

MATTHEW GILBERTSON
B.A. Biology, Saint Olaf College 2009
M.P.H. Epidemiology and Global Communicative Diseases,
University of South Florida, 2012

THESIS

Submitted as partial fulfillment of the requirements
for the degree of Doctor of Philosophy in Biopharmaceutical Sciences
in the Graduate College of the
University of Illinois at Chicago, 2019

Defense Committee:

   John L. Nitiss, PhD, Chair and Advisor, Biopharmaceutical Sciences
   William T. Beck, PhD, Biopharmaceutical Sciences
   Leslyn Hanakahi, PhD, Biopharmaceutical Sciences
   Arnon Lavie, PhD, Biochemistry
   Andrew Riley, PhD, Medicinal Chemistry

ACKNOWLEDGEMENTS

me to imagine doing all that I have accomplished over the past several decades without their help. My mom, Barb Gilbertson, deserves a special thank you for her assistance in editing this behemoth.

Finally I thank my wife, Rachel Gilbertson. My wife and I have traveled the journey towards this Ph.D. for almost half of our relationship and I don't think there are sufficient words in this document to express my gratitude and admiration for her constant support and love that has enabled me to achieve this accomplishment.

Contributions of Authors

Chapter 1 is an introduction chapter that highlights relevant topics that are covered in my dissertation and sets up the research questions that were the focus of the research presented. Chapter 2 represents a large unpublished collaborative project for which I was a primary author and driver of research. The MBT530 class of Spring 2015 helped to carryout the initial steps of the genetic screen. Kim Cuaresma, Abhishek Deshpande, Hannah Miles, Dr. Karin Nitiss, Radhika Patel and I collaborated to carry out the clonogenic survival assays on etoposide sensitive yeast isolates. I carried out the purification and biochemical analysis of Top2 mutant proteins. We sent mutant purified protein to Dr. Fenfei Leng, Florida International University to carry out the experiments presented in figure 2.11 part D and E. Chapter 3 represents a large unpublished collaborative project between the John L. Nitiss and Sue Jinks-Robertson's laboratories. Dr. Anna Rogojina identified the self-poisoning mutant allele in yeast Top2 and purified the mutant proteins. I carried out the biochemical characterization experiments shown figure (3.3) with the mutant proteins. I carried out the exploration of etoposide-induced mutagenesis in yeast and characterized the large mutations. Radhika Patel isolated large mutations in yeast expressing a self-poisoning allele of yTop2. Nicole Stantial, from Sue Jinks-Robertson's laboratory, at Duke University, carried out the experiments described in figures (3.7 and 3.8). Chapter 4 represents a project to characterize a Top2 mutant allele identified in a human neurological disease. Hannah Miles, Dr. Karin Nitiss and I constructed the mutant alleles in yeast expression vectors and carried out the yeast transformations and complementation experiments described in figures (4.1 and 4.2). Lokha Boopathy assisted with the fluctuation assays described in figure 4.3. I purified and characterized the mutant proteins with assistance from Hannah Miles. Chapter 5 represents the discussion of the research presented in the preceding chapters, my conclusions and future directions for research in this field.

TABLE OF CONTENTS

LIST OF FIGURES

ASD	Autism spectrum disorders
ADP	Adenosine diphosphate
AEBSF	4-Benzenesulfonyl fluoride hydrochloride
AML	Acute myeloid leukemia
AMP-PNP	Adenylyl-Imidophosphate
ATP	Adenosine triphosphate
cDNA	Complementary DNA
CNV	Copy Number Variations
DMSO	Dimethyl sulfoxide
DNA	Deoxyribonucleic acid
DSB	Double stranded break
DTT	Dithiothreitol
EDTA	Ethylenediaminetetracetic acid
FRET	Förster resonance energy transfer
HAP	Hydroxyapatite
HR	Homologous recombination
ICE	*In vivo* complex of enzyme
ICRF	Imperial cancer research fund
KCL	Potassium chloride
KO	Knock out
LC50	Lethal concentration 50%
mAMSA	N-(4-(acridin-9-ylamino)-3-methoxyphenylmethanesulfonamide

MDR	Multi-drug resistance
MLC	Minimum lethal concentration
MLL	Mixed lineage leukemia
MMEJ	Microhomology-mediated end joining
NHEJ	Non-homologous end joining
Ni-NTA	Nickel-nitrilotriacetic acid
OE	Overexpression
ORF	Open reading frame
PCELL	Phosphocellulose
PCR	Polymerase chain reaction
PMSF	Phenylmethylsulfonyl fluoride
SSB	Single strand break
TE	Tris-EDTA
Top2	Topoisomerase II
Top2α	Human topoisomerase II alpha
Top2β	Human topoisomerase II beta
WT	Wild type

SUMMARY

DNA topoisomerases play a crucial cellular role by processing DNA topology. DNA metabolism inherently creates a variety of topological DNA structures (supercoils, knots and catenanes) that frequently require processing. The DNA topoisomerases are a class of enzymes that alter DNA topology by initiating transient strand breaks in the DNA. DNA topoisomerases initiate these DNA breaks by performing a transesterification reaction using their active site tyrosine to form a covalent link with DNA. The human type II DNA topoisomerases, topoisomerase II alpha and beta (Top2α and Top2β) function as larger homodimers and initiate a double-strand break in the DNA which allows them to passage a second DNA molecule through the break. To finish their catalytic reaction the enzymes efficiently re-ligate the break reversing the covalent linkage to release the DNA molecule.

The DNA topoisomerases are of great interest to the scientific and medical communities as they can be targeted by a variety of small molecules in both eukaryotic and prokaryotic cytotoxic therapies. Small molecules like etoposide and doxorubicin stabilize Top2α and Top2β when the enzymes are covalently linked to DNA, leading to DNA damage and cell death. Therefore, this class of inhibitors is referred to as Top2 poisons. Targeting Top2 is therapeutically effective but is accompanied with several severe side effects such as secondary malignancies and cardiotoxicity. At present, the molecular details of how Top2 poisons trap the covalent complex are not well understood.

This research develops the results of a screen to identify mutants of Top2α that are hypersensitive to etoposide. Many mutations were identified far from the etoposide

binding site, some of which demonstrated cross-sensitivity to mAMSA. I purified and biochemically characterized several of the identified mutant proteins and found that many of the mutations in the ATPase domain appear to affect the regulation of DNA cleavage. These results implicate the ATPase domain as an allosteric regulator of DNA cleavage.

We additionally sought to determine the DNA repair pathways that lead to the mutagenic consequences of Top2 poisoning the pathways. To study this issue we exposed yeast to etoposide and selected for *CAN1* mutations that would confer resistance to L-canavanine, a toxic analog of arginine. We identified that etoposide-induced mutations included a high proportion of DNA duplications. These kinds of mutation are frequently observed in patients that develop secondary malignancies associated with targeting topoisomerase 2. Additionally, we found that this class of mutation was suppressed in yeast lacking essential NHEJ cofactors and *TDP1*. These results suggested that NHEJ repair along with *TDP1* is likely involved in the misrepair of Top2 mediated DNA damage associated with secondary malignancies.

A recently identified allele of Top2β (His63Tyr) was associated with global developmental delay and autism spectrum disorder[1]. This was an excellent candidate to study a potential link between Top2β and neuronal neural defects. We constructed the Top2β His63Tyr mutant allele in a yeast expression vector and characterized the allele. We found the expression of the mutant allele was not tolerated in a DNA repair deficient yeast strain indicating a deleterious phenotype. Yeast carrying the mutant allele exhibited significantly higher recombination rates. The purified mutant enzyme was also found to produce extraordinarily high levels of drug-independent DNA cleavage. These results

suggested the etiology of the disease was via Top2-mediated induction of DNA damage during neuronal development.

1 INTRODUCTION

Research on etoposide hypersensitive Top2 alleles and mutagenic consequences of etoposide exposure must begin with review of DNA topology with respect to topoisomerase biologic roles, mechanisms, crystal structure and biochemistry as well as topoisomerase targeting agents and drugs. The extension of research on DNA topology begins with understanding topoisomerases.

1.1 DNA topoisomerases

The discovery of the double helical structure of DNA in 1953 was a monumental scientific advancement but was accompanied by several structural concerns that at the time were not easy to explain[2]. One challenge was the complex nature of DNA toplogy. The structure of the double helix inherently leads to topological formations and unique DNA tangles within the cell[3]. The extent of the DNA topology problem was initially highlighted by the demonstration that the *E.coli* chromosome is circular[4]. The semiconservative mechanism of DNA replication on the circular chromosomes results in catenanes, which are interlocking circles of DNA, that fail to separate at anaphase (Figure 1.1 C)[5–7]. Additionally, bi-directional replication fork progression results in the production of positive DNA supercoils that could interfere with DNA metabolism (Figure1.1 A)[8–10]. These concerns were validated by observation of topological structures in DNA isolated from several organisms[11,12]. Some organisms such as mesophilic bacteria and archaea maintain their DNA as negatively supercoiled, this tendency appears to promote DNA melting to facilitate transcription and initiation[10,11,13].

Figure 1.1 DNA topological structures

A. Relaxed

(−1)
(−1)
Negative Supercoils
(-)

(+1)
(+1)
Positive Supercoils
(+)

B.
(+1)
(+1)
(+1)
Knotted

C.
(+1)
(+1)
Catenated
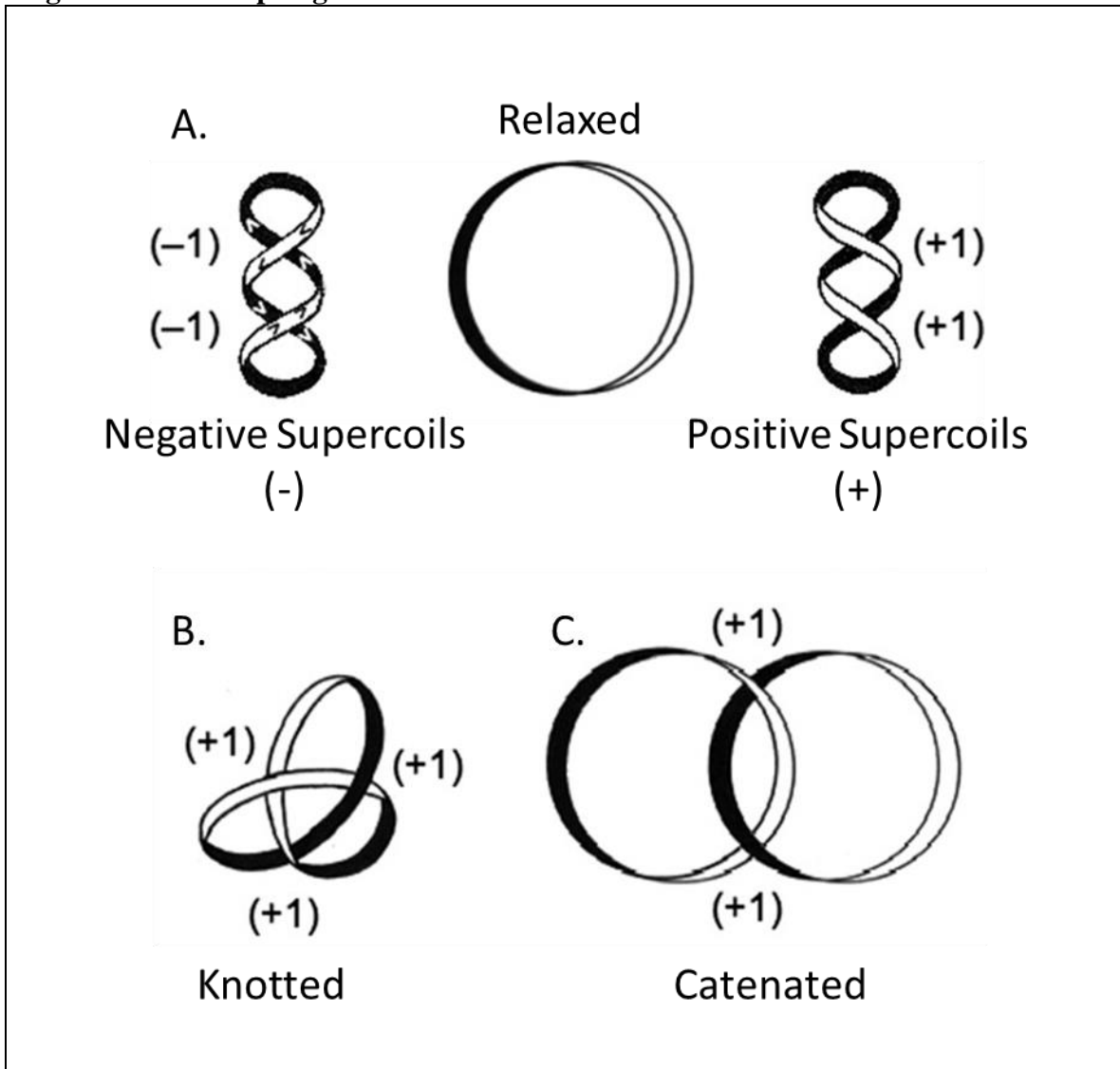
Deweese JE, Osheroff MA, and Osheroff N. DNA Topology and topoisomerases: Teaching a "knotty" subject. Biochemistry and Molecular Biology Education. 2008 Feb; 37(1): 2–10

Figure 1.1 DNA topological structures. An illustration of the DNA topological structures, the DNA helices are shown as circular ribbons. **A.** "Relaxed" DNA lacking torsional stress is neither underwound nor overwound. Underwinding DNA results in negative supercoils whereas overwinding DNA results in positive supercoils. **B.** DNA can form intermolecular knots and tangles **C.** Circular DNA can form interlocked catenanes.

John Wiley and Sons Online Library has licensed me to reuse this figure in my thesis in print and electronic formats. John Wiley & Sons, License # 4563130776724

The subsequent discovery of DNA topoisomerase enzymes was key to explaining the complexities of DNA topology[8]. The DNA topoisomerases are a group of enzymes capable of processing DNA topological structures such as knots, supercoils and catenanes (Figure1.1A). DNA topoisomerases play crucial roles in DNA metabolism (replication, transcription and meiosis)[14]. These enzymes transform DNA topology by initiating transient DNA strand breaks[15]. The enzymes catalyze a DNA strand passage mechanism through the strand breaks to effectively alter DNA topology. DNA topoisomerases as a class of enzyme are predicted to be present in all life forms given the structure of DNA and mechanisms of DNA metabolism[16].

The DNA topoisomerases are of particular research interest because they are targeted in many cytotoxic therapies by small molecules[17]. Agents like camptothecin, ciprofloxacin, etoposide and doxorubicin target topoisomerase and have been utilized for many years in anti-tumor or antibiotic therapies[18,19]. Despite the clinical longevity of many of these agents, interest in novel topoisomerase targeting agents remains high[20–24]. Many topoisomerase targeting agents are associated with severe side effects limiting the extent of their clinical applications[25,26].

Six DNA topoisomerases proteins and one topoisomerase-like protein have been identified in human cells (Top1, Top1 mitochondrial, Top2α, Top2β, Top3α, Top3β and Spo11) (Table 1.1)[16,27,28]. All DNA topoisomerase enzymes utilize an active site tyrosine to perform a nucleophilic attack on the phosphodiester DNA backbone[16,26,28]. As a result the topoisomerase proteins become covalently bound to DNA by a phospho-tyrosyl linkage during catalysis[29–33]. The six known human topoisomerases are subdivided into types based on the molecular details of the DNA breakage reaction.

The type I enzymes effect the relaxation of DNA supercoils by initiating transient single strand breaks (SSB) in DNA[34–36]. The type I enzymes are further subdivided into type IA and type IB which differ in both mechanism and structure[35–39]. The type IA enzyme forms a 5'phosphotyrosyl protein-DNA covalent linkage whereas the IB enzymes become covalently linked to the 3'phosphotyrosyl protein-DNA[29,40]. The type IA enzymes catalyze a single strand break through which is passed a single-stranded DNA molecule. The type IA enzymes catalyze the relaxation of negative supercoils and unknotting of single stranded or nicked DNA strands[15,34]. Humans have two type IA topoisomerase enzymes topoisomerase III alpha (Top3α) and topoisomerase III beta (Top3β). The type IB enzymes act as "DNA swivelases" by allowing the free 5' end of DNA to rotate about intact DNA strand[3,41]. The type IB enzymes process positive and negative DNA supercoils[3,41]. There are two human topoisomerase type IB enzymes, topoisomerase I (Top1) and mitochondrial topoisomerase I (Top1mt). Top1 plays a role in processing DNA topology in both DNA replication and transcription[27]. Top1mt functions as a topoisomerase for mitochondrial DNA[42].

The type II topoisomerase enzymes initiate transient double strand breaks (DSB) in DNA and thus can process a wide array of DNA topological structures because they can passage a second double stranded DNA duplex through the break[43–46]. The type II enzymes break DNA by forming a covalent 5' phosphotyrosyl protein-DNA linkage to each of the DNA strands and require ATP for their catalytic activity[47–54]. These two DNA strand breaks are offset by a 4-nucleotide overlap[55]. In humans the type II enzymes function as homodimers with each subunit initiating a single strand break by coordinating with essential elements of the opposing subunit[56]. The type II enzymes process positive

5

and negative DNA supercoils, knots and catenanes[27,54,57]. The type II topoisomerases are also subdivided as IIA and IIB[28,58]. While there have been no type IIB topoisomerase enzymes discovered in humans, Spo11, a topoisomerase-like enzyme shares homology in the DNA binding domain with other type IIB topoisomerases[59,60]. Initiator of meiotic double strand breaks (Spo11), is active during meiosis and facilitates the induction of enzyme mediated DNA double strand breaks that lead to meiotic recombination[3,59,60]. Type IIB topoisomerases (Topo VI) have been discovered in numerous organisms, primarily in archea and plant species, although several eubacterial species that carry this enzyme have also been identified[58,61,62]. There are two type IIA topoisomerases in human cells, human topoisomerase II alpha (Top2α), topoisomerase II beta (Top2β).

.

Table 1.1 Human DNA topoisomerases

Classification	Enzyme	Cofactors	Covalent DNA linkage	Yeast Ortholog	DNA substrates	Knockout Phenotype (Mouse)
Type IB	Top1	None	3'	Top1	DNA supercoils$^{+/-}$	Early embryonic lethal[63]
Type IB	Top1mt	None	3'	Top1	DNA supercoils$^{+/-}$	Viable[64]
Type IIA	Top2α	Mg^{2+} and ATP	5'	Top2	DNA supercoils$^{+/-}$ DNA knots DNA catenanes	Early embryonic lethal[65]
Type IIA	Top2β	Mg^{2+} and ATP	5'	Top2	DNA supercoils$^{+/-}$ DNA knots DNA catenanes	Late embryonic lethal[66]
Type IA	Top3α	Mg^{2+}	5'	Top3	DNA supercoils^{-} Hemicatenanes Double Holliday Junctions D loops	Embryonic lethal[67]
Type IA	Top3β	Mg^{2+}	5'	Top3	DNA supercoils^{-} RNA knots R loops	Viable[68]

1.2   Topoisomerase II

The eukaryotic DNA topoisomerase II (Top2) enzymes catalyze an ATP dependent reaction to relax and unknot topological DNA structures. These enzymes function as large homodimers and play a critical role in the separation of replicated chromosomes. Only one Top2 isoform appears to be present in lower eukaryotes (*S. cerevisiae, C. elegans, D. melanogaster*)[69,70]. Expression of two Top2 isozymes appears to be limited to higher eukaryotes (vertebrates)[71].

Humans express two topoisomerase II (Top2) isozymes, which share a large degree of homology in peptide sequence and structure[72–74]. Genomic analysis suggests the two genes are the result of a duplication event[75,76]. Both proteins function as large homodimers, the Top2α monomer is ~170kDa, polypeptide length 1531 amino acids (aa) and the Top2β monomer is ~180kDa, polypeptide length 1626aa[77–82]. Top2α and Top2β isozymes share ~70% identity[76,81]. These enzymes share a highly similar catalytic mechanism and are capable of processing the same types of DNA topological substrates[57,71].

Subtle biochemical differences have been identified in the two Top2 enzymes. These two proteins exhibit distinct expression patterns during the cell cycle and are further differentiated by nuclear localization[83,84]. The Top2α enzyme is essential for survival in dividing cells[85,86]. Expression of Top2α protein fluctuates dramatically, from barely detectable levels in non-dividing cells to its highest levels near G2/M phase[83,87,88]. In contrast, Top2β enzyme is dispensable for viability and expression level is not linked to cell cycle progression[83,89,90]. Top2α purified protein has demonstrated preferential relaxation of positive DNA supercoils with ~10 fold greater efficiency than Top2β[91]. The

observed differences between isoforms highlight their roles in DNA metabolism, Top2α
is tied closely to DNA replication and chromosomal segregation and Top2β is highly
involved in DNA transcription[92,93].

1.2.1   <u>Biological roles of topoisomerase II</u>

Understanding role topoisomerases play in cells underlies the research completed
in this study and begins with examination of the processes of DNA replication,
termination, chromosomal segregation, and transcription. Eukaryotic systems such as
Saccharomyces cerevisiae have proven to be incredibly powerful tools to explore the
biological roles of topoisomerases in these processes.

<u>Replication</u>

DNA topoisomerase activity is required during DNA replication[94]. The semi-
conservative mechanism of DNA replication unwinds the DNA double helix inherently
altering DNA topology. Unwinding the DNA helix with the replication fork produces
over-winding ahead of the replication fork, a manipulation that produces positive DNA
supercoils ahead of the replication fork (Figure 1.2)[95,96]. Top1 and Top2α are both
capable of processing positive DNA supercoils[97,98]. Studies in *Saccharomyces* suggest
that either Top1 or Top2 can remove the positive DNA supercoils, as the loss of either
individually does not significantly affect DNA replication[99]. Loss of both Top1 and Top2
results in the complete inhibition of DNA replication[99–101].

As DNA synthesis progresses (elongation), positive supercoils are continually
generated ahead of the replication fork requiring the activity of Top1 and Top2α[94,95]. The
positive supercoils can be absorbed by the twisting of the daughter chromatids behind the
replication fork, called precatenanes (Figure 1.2)[96,102,103]. *In vitro* both of the Top2

isoforms are capable of processing positively supercoiled and catenated DNA[91]. Cells

depleted for Top2α demonstrated delayed chromosomal segregation leading to the

formation polyploidy in mitosis[104]. Top2β dissociates from chromosomes during DNA

replication[71,93,105]. However, by exchanging the C-terminal regions (CTR) of the Top2α

and Top2β proteins, Top2β (with α CTR) will complement for Top2α deficiency in

mammalian cells[93]. These observations indicated that the specialization of biological

roles between the two isozymes may be based primarily on enzyme nuclear localization

and that localization is influenced by the CTR of the proteins.

Figure 1.2 DNA topological structures in replication
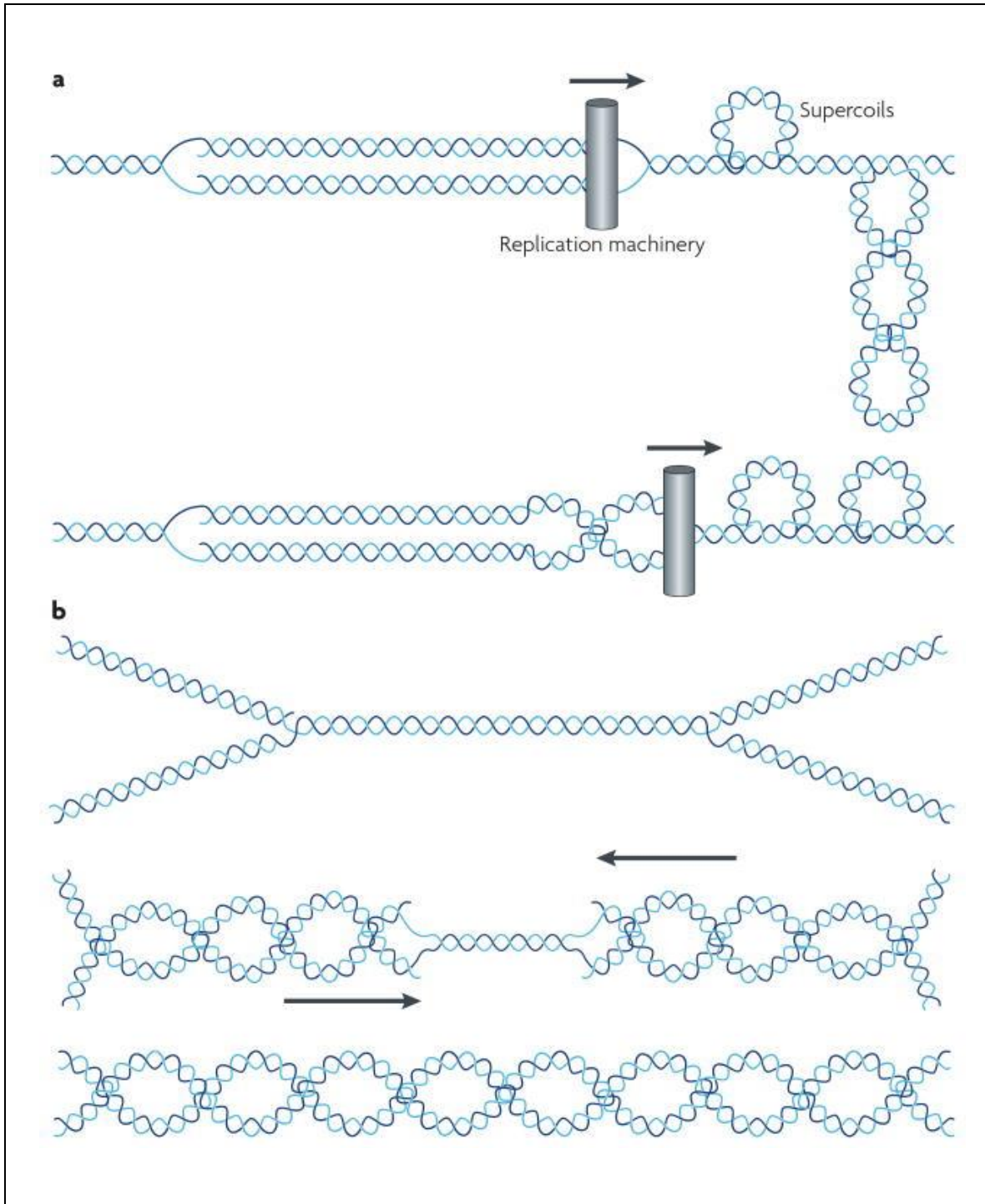
Nitiss JL. DNA topoisomerase II and its growing repertoire of biological functions.
Nature Reviews Cancer. 2009 May; 9(5): 327–337

Figure 1.2 DNA topological structures in replication. An illustration of the DNA topological structures associated with DNA replication **A.** The assembly of DNA replication machinery separates the helical DNA strands as the replication fork advances during DNA synthesis. Most of the topological tension produced by overwinding the DNA in front of the replication fork is relieved by the formation of positive DNA supercoils. The positive DNA supercoils are a substrate for Top1 and Top2 strand passage. The topological tension is also relieved by the slow rotation of the replication fork generating pre-catenane structures with the newly synthesized daughter DNA strands. **B.** Eukaryotic DNA replication is bi-directional meaning replication forks will converge. Upon the termination of DNA replication the two daughter chromatids are interwoven as catenanes. These DNA catenanes are a substrate for Top2.

Termination of DNA replication requires Top2 activity[106,107]. As DNA replication is bidirectional and begins at multiple locations on eukaryotic chromosomes, DNA replication forks converge[108]. A converging pair of replication forks will produce positive supercoils with a rapidly shrinking region of DNA for topoisomerases to catalytically process[57]. While Top1 and Top2 both process positive supercoils, yeast Top2 is recruited to the termination region (TER) sites and yeast expressing a catalytically inactive Top2 fail to complete DNA replication[106,109,110]. This observation would indicate that Top2 activity is required for termination of replication. However, yeast depleted for Top2 complete DNA replication then fail to segregate chromosomes during in mitosis, suggesting that an inactive enzyme interferes with the termination of replication[106]. The remaining positive supercoils between converging forks can be transformed into the intertwining of the two daughter DNA strands as precatenanes. Upon the termination of DNA replication the sister chromatids are catenated DNA molecules and require Top2 action for separation[103]. Taken together these observations highlight the essential role Top2α plays in DNA replication and termination[86,104,111].

Chromosomal segregation

The Top2 protein is known to play a role in chromosome condensation and chromosomal segregation[112]. Human chromosomal DNA are sufficiently large to require dense packaging in order to fit within the nucleus of each cell[94]. Critical to chromosomal segregation during mitosis is the involvement of the structural maintenance of chromosomes (SMC) proteins, which form complexes that include either cohesin or condensin. Top2 has been shown co-localize with these complexes to chromosomes[113–116]. Top2 likely co-localizes during compaction of the chromatin in due to the associated

topological stresses involved in the process. In addition Top2 is necessary for the separation of the sister chromatids during anaphase[117].

Top2 plays a crucial role in DNA replication by separating the intertwined sister chromatids. Failure to adequately separate replicated chromosomes results in mitotic delay suggestive of a decatenation checkpoint in G2 of the cell cycle[118]. Cells depleted for Top2 demonstrate mitotic errors like polyploidy and chromosomal mis-segregation but not mitotic delay[104,106,119]. Catalytic inactivation of Top2 leads to G2 cell cycle arrest suggesting that the presence of Top2 is required for the activation of the decatenation checkpoint[120,121]. Phosphorylation of Top2α Ser-1524 has been reported to be required for activation of the decatenation checkpoint as it is involved in the recruitment of MDC-1 (mediator of DNA damage checkpoint protein-1) to chromatin[122]. Several enzymes closely associated with DNA damage response have also been identified as potentially being involved in the decatenation checkpoint (BRCA1, PTEN, and ATR)[118,123,124].

Transcription

DNA topoisomerases play an integral role in DNA transcription and gene expression as supercoiling affects the efficiency of DNA transcription[11,125–130]. DNA supercoils are generated by DNA transcription, in a mechanism similar to the advancement of the replication fork. As the transcription machinery progresses, positive supercoils are generated ahead of the fork and negative supercoiling are generated behind the fork (Figure 1.2)[131]. Studies using *Saccharomyces cerevisiae* have elucidated a considerable number of details exploring a role for DNA topoisomerases in DNA transcription[130,132]. In yeast, Top1 and Top2 are independently dispensable for the

completion of transcription however loss of either leads to substantial inhibition of DNA elongation by RNA Polymerase II[133].

The Top2β protein has been identified to play a unique but poorly understood role in DNA transcription of select genes. Top2β is recruited to the promoter region of some hormonally activated genes along with a complex containing several proteins associated with DNA repair [134–138]. This complex has been shown to form a prolonged DNA double strand break in the promoter regions of several hormone response genes and producing extensive γh2AX phosphorylation (signaling the activation of DNA damage response pathways)[134,135,139]. The recruitment of this complex appears to be required for the efficient transcription of these genes[135]. The biological role of these seemingly programed double strand breaks is poorly understood and merits further investigation. Recent work has further described the participation of Top2β in the transcription of long genes[125]. Top2β is essential for the transcription of genes during neuronal development.[92,140,141] Top2β -/- mouse pups are stillborn as they fail to enervate the diaphragm[92]. De novo mutations in DNA topoisomerase genes have been linked to children diagnosed with autism spectrum disorders[125,142,143]. A recently described de novo heterozygous mutation (His63Tyr) in Top2β was identified as the disease causing gene in a patient with developmental delay[1]. These studies highlight the importance of Top2β during transcription as well as neural development.

1.2.2 Top2 catalytic mechanism

The Top2 homodimer carries out strand passage activity by coordinating a series of conformational changes involving the close coordination of several domains of the enzyme[144,145]. Figure 1.3 illustrates our current understanding of how Top2 performs its

catalytic cycle. Top2 initiates the catalytic mechanism by binding two segments of double stranded DNA[43,44,146,147]. Top2 cleaves one of these segments to form a gate in the DNA called the gate segment or G-segment. The second DNA segment is passed through the gate and is called the transfer segment or T-segment. The mechanism by which the enzyme accomplishes strand passage quickly grows complex. In addition to DNA the enzyme requires two additional cofactors for catalysis: ATP and a divalent metal cation[148].

Figure 1.3 DNA topoisomerase II catalytic mechanism

A. DNA Topoisomerase II Strand passage

B. DNA Topoisomerase II Catalytic Mechanism

T Segment
G Segment
ATP
ADP
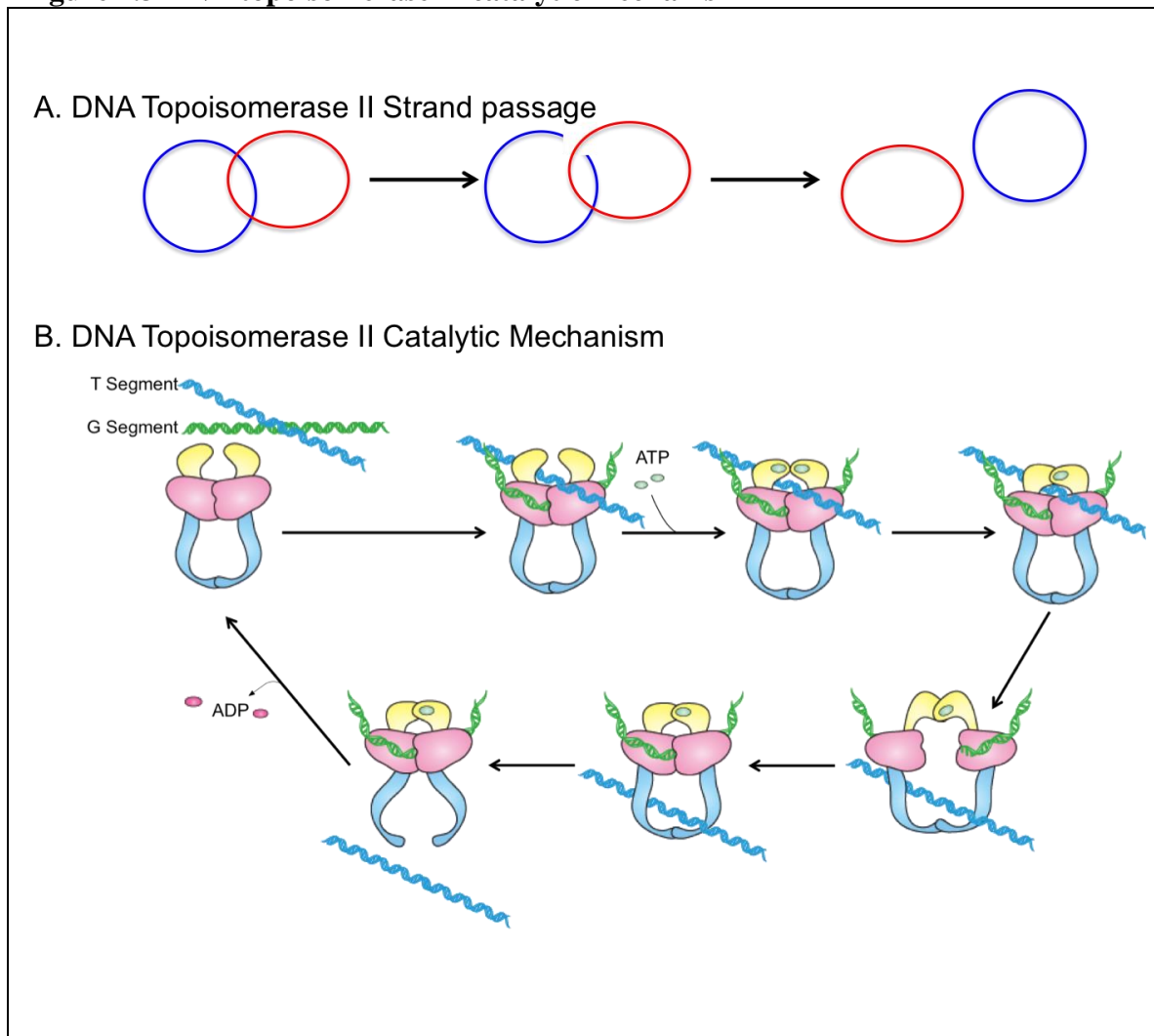
Figure 1.3. A. DNA Topoisomerase II catalyzes topological DNA transformations by initiating a transient double strand break in a DNA duplex, passaging a second DNA duplex through the break, and then efficiently relegates the DNA duplex. **B.** The catalytic mechanism involves Top2 first binding a DNA duplex labeled the G-segment (green). In the presence of a divalent cation (Magnesium) Top2 cleaves both DNA strands by carrying out a transesterification reaction where the active site tyrosine performs a nucleophilic attack on the phosphodiester backbone of DNA. Resulting in a covalent 5'phosphotyrosyl linkage between each subunit and a single strand of the G-segment. Top2 binds two ATP molecules promoting the dimerization of the N-terminus (closed clamp) of the homodimer thereby capturing the second DNA duplex labeled the T-segment (blue). One ATP molecule is rapidly hydrolyzed and the catalytic core of the enzyme (red) separates to allow the passage of the T-segment. Following this strand passage the catalytic core synapses the g-segment DNA and the 3'OH performs a nucleophilic attack on the phosphotyrosyl bond resulting in the religation of the DNA g-segment. The T-segment exits the reaction through the c-terminus of the protein. Following strand passage a second ATP hydrolysis occurs, releasing the ADP and opening the closed clamp to release the G-segment or capturing another T-segment for additional catalytic cycles.

The enzyme binds two ATP molecules in the ATPase domain, promoting the dimerization of the N-terminus of the protein. This conformation shift is called the closed clamp conformation and encloses the T-segment[149,150]. The ATP molecules are hydrolyzed sequentially, suggesting their participation in different processes of the catalytic reaction[151]. ATP hydrolysis is stimulated in the presence of DNA[149,152–155].

Top2 initiates a transesterification reaction where the active site (Tyr805 Top2α, Tyr 821 Top2β) performs a nucleophilic attack on the sugar-phosphate backbone of DNA (G-segment) with the assistance of the essential divalent cation positioned by the TOPRIM (topoisomerase-primase) domain of the opposing subunit (Figure 1.3 A)[156,157]. This reaction results in a covalent 5' phophotyrosyl protein-DNA intermediate[29–33]. The strand breaks made by each subunit are staggered by a 4-nucleotide overlap[55]. The energy of this reaction is conserved which allows the cleaved DNA to be ligated freely after strand passage. The T-segment of DNA traverses through the "DNA" gate formed by the G-segment (strand passage)[43,45]. Top2 must undergo a large conformational shift to accommodate the passage of a DNA duplex (T-segment) through the central core of the enzyme[55,72,158]. This conformational shift involves the dissociation of ~1800-2560 Å^2 (Top2β- Top2α) of the protein dimerization interface (~50%), forcing the enzyme to rely on the N-Gate and C-Gates of the protein for dimer stability[55,72,158,159].

After strand passage, the enzyme brings the covalently bound DNA ends together and the 3' end hydroxyl group of the DNA performs a nucleophilic attack on the covalent phosphotyrosyl linkage[57]. The completion of this reaction removes the covalent link between the protein and DNA by ligating the G-segment. Top2 targeting agents appear to interfere with the enzymes DNA breakage ligation reaction[17]. Small molecules like

etoposide appear to block DNA religation by stabilizing Top2 while it is covalently linked to DNA[17]. While the specific molecular details of drug action are not fully understood, Top2 poisons generate high levels of DNA damage by stabilizing Top2 DNA cleavage, thus blocking further progression through the catalytic cycle[19]. If Top2 poisons are removed from the reaction, Top2 is capable of completing the reaction cycle[160].

Having completed strand passage and religation, the enzyme hydrolyzes the second ATP molecule[151]. The N-gate dissociates after the release of the two ADP molecules allowing a conformation shift would allow for the release of the G-segment or the capture of a new T-segment for another catalytic cycle[161,162]. Top2 will perform a single catalytic cycle when bound to AMP-PNP, a non-hydrolysable analog of ATP or bisdioxopiperizines[163]. These data indicated the second ATP hydrolysis is likely involved in the dissociation of the ATPase domain dimer and that neither ATP hydrolysis event is actually required for strand passage.

1.2.3 Top2 biochemistry

Top2 biochemical studies have made immense contributions to elucidating an array of molecular details within the catalytic mechanism, protein-DNA interaction, and mechanisms of drug action[27,164]. Many of the contributions biochemical studies have made to our understanding of Top2 have been discussed already in describing the protein structure and catalytic mechanism; however, there are several important characteristics that need to be highlighted in greater detail.

Interactions with DNA

Topoisomerases catalyze DNA strand passage which 'relaxes' supercoiled DNA producing a collection of DNA topoisomers distributed close to the lowest level of free

energy[30,57]. Because of their 'swivelase' mechanism the type 1B topoisomerases produce

the predicted Boltzmann distribution of topoisomers near thermodynamic equilibrium

(covalently closed DNA that differ in topological winding number near topologically

relaxed DNA)[165,166]. The distribution of DNA topoisomers produced by the type II

enzymes were much narrower than expected in what is referred to as topological

simplification[167]. In an effort to explain this phenomenon, one model proposed a sharp

bend in the DNA G-segment which could explain the observed distribution of DNA

topoisomers[168]. Structural analysis of the co-crystalized Top2-DNA later demonstrated a

150° bend in the DNA G-segment providing direct evidence in support of this

hypothesis[56].

An essential aspect of this model, however, is that DNA strand passage is

unidirectional, the T-segment captured by the N-terminus of the enzyme upon binding

ATP and then would leave through the C-terminus[44]. Using the yTop2 crystal structure,

Roca et. al designed a disulfide bridge that would fuse the C-terminal protein

dimerization interface (yTop2 Asn1043Cys Lys1127Cys)[43,157]. The purified mutant

yTop2 protein could only relax DNA after treatment with 2-mercaptoethanol which

disrupted the disulfide bonds, providing direct evidence for the 'two gate reaction

mechanism'[43]. These findings indicated the dynamics of the gates between the subunits

of the Top2 homodimer are critical to the enzyme.

Top2 mobility/conformation states

Recent work with single-molecule Foster Resonant Energy Transfer (sm-FRET)

experiments have examined the dynamics of the breakage reunion core of *Drosophila*

Top2 as the enzyme carries out strand passage[161]. These studies utilized the 150° DNA

bend by attaching a fluorophore and quencher to the DNA. By measuring fluctuations in the efficiency of energy transfer, DNA gate dynamics were assessed in the breakage reunion core[161,169,170]. Top2 targeting agents appear to shorten the dwell time in the closed conformation state demonstrating an interference with the ligation of the DNA G-segment[161,169]. Also, dimerization of the N-gate with AMP-PNP corresponded to a reduction in FRET signaling, suggesting the opening or partial opening of the breakage reunion core[169].

Divalent cations and DNA cleavage

As discussed earlier, the DNA cleavage reaction requires a divalent cation cofactor. The physiological divalent cation involved in DNA cleavage is likely Mg^{2+}; however biochemical studies have shown Mn^{2+}, Ca^{2+}, and Co^{2+} work as substitute cofactors[148,171,172]. Mn^{2+}, Ca^{2+}, and Co^{2+} generate greater levels of DNA cleavage than Mg^{2+} and combinations of these metals stimulate DNA cleavage at an even greater level[172–174]. These data support a two divalent metal cation model for Top2 mediated DNA cleavage and suggest that divalent metal cations strongly influence the Top2 DNA cleavage-ligation equilibrium[173,174].

1.2.4   Top2 crystal structure

The catalytic mechanism of Top2 strand passage described above requires a series of conformation changes throughout the enzyme[175]. Structural analysis of the eukaryotic Top2 has profoundly improved the interpretation of Top2 biochemistry and led to a better understanding of the catalytic mechanism overall[57]. Much of what we know about the structure of Top2 is through the work of James Berger who published the first crystal structure of the breakage reunion domain of yeast Top2 in 1996 (Table 1.2)[157]. This

structure demonstrated the geometry and dynamics of Top2 dimerization[43,157]. An important advancement in our understanding of Top2 activity was the publication of the yeast Top2 enzyme catalytic core crystal structure by Dong and Berger in 2007 showing yeast Top2 protein bound to DNA (Table 1.2)[56]. James Berger also published the yeast ATPase domain in 2003 and eventually the catalytically active yeast Top2 structure bound to DNA in 2012(Figure 1.4 A)[176,177]. As ~ 40% of the *S. cerevisiae* Top2 amino acid sequence is identical to the human enzyme, this work has served as a framework for the interpretation of biochemical discoveries regarding eukaryotic Top2[81]. Presently no full-length structure has been solved for the human enzymes, yet crystal structures of key fragments of Top2α and Top2β proteins have been solved[72–74,159,178].

The ATPase domain (amino acids ~30-265) (Figure 1.4 B) belongs to the GHKL, (gyrase, heat shock protein 90, histidine kinase, and mutL) superfamily[179]. This domain binds to and hydrolyzes ATP. The ATPase domain contains one of the major dimerization interfaces in the protein called the N-gate. When bound to nucleotide, this domain adopts a closed clamp conformation, with the dimerization of the N-terminal domains thereby capturing a T-segment[44,150,176,177,180–182]. Adjacent to the ATPase domain is the transducer domain (aa ~266-428), which plays a role in ATP binding and hydrolysis[183–186]. The transducer domain consists primarily of a group of alpha helices that connect the ATPase domain to the catalytic core of the enzyme[177]. At present we have three crystal structures of the Top2α ATPase and Transducer domains bound to nucleotide (ADP, ADP with SO_4, or AMP-PNP) (Table1.2)[159,180].

Structural analysis of the yTop2 crystal structure indicated the hole formed between the N-gate in the closed conformation and catalytic enzyme core is too narrow to

23

accommodate B form DNA (diameter ~20 Å) (Top2α gap diameter: 17 Å)[159,177,187].

Furthermore, a yTop2 mutant protein incapable of DNA cleavage could not trap a T-segment with an AMP-PNP induced closed-clamp[146,187].

Several domains make up the enzymes catalytic core: TOPRIM (aa ~455-572), winged helix (WHD) (aa ~765-865), and tower (aa ~895-1000) (Figure 1.4 C). These domains serve as a major dimerization interface between the two subunits[43,157]. The catalytic core of the enzyme, also called the breakage reunion core is responsible for coordinating DNA binding, cleavage and religation. The catalytic transesterification (DNA breakage) reaction requires the participation of domains involving both Top2 subunits. Integral to transesterification is the positioning of divalent metal cations, which allow the nucleophilic attack on DNA forming the covalent protein-DNA intermediate[148,173,188]. The TOPRIM domain possesses an essential DxD motif (Asp541, Asp543 and Asp545 in Top2α, Asp557, Asp559 and Asp561 in Top2β) that position the divalent cation so it can participate in DNA cleavage[188]. The physiological divalent cations used by Top2 are Mg^{2+}; however, Mn^{2+}, Ca^{2+}, and Co^{2+} have been shown to also support DNA cleavage *in vitro*[148,171–173]. DNA cleavage by the homodimer involves the TOPRIM domain of one subunit interacting with the opposing subunits' active site tyrosine[156,157]. The TOPRIM domain is named for the ~100 conserved amino acid residues shared by topoisomerases, bacterial primases, and OLD family nucleases[188].

Connected to the TOPRIM domain is the winged helix domain (WHD) which contains the active site tyrosine (Tyr805 Top2α and Top2β Tyr826). The winged helix domain along with the adjacent tower domain form a positively charged groove that binds the DNA G-segment [28,56,189]. These two domains cooperatively induce a sharp bend

in the DNA (150°) and are responsible for the alignment of the 3'OH DNA end at the religation step of strand passage.

Attached to the catalytic core of the enzyme is a coiled coil domain (aa~1020-1180), which contains the C-gate, another major dimerization interface (Figure 1.4 C). This dimerization interface likely functions as an anchor to keep the two subunits together during strand passage[43,144]. The C-gate dissociates post-strand passage to allow for the release of the DNA T-Segment. C-terminal to the coiled coil domain is the C-terminal domain of the enzyme. This domain is disordered on existing Top2 structures and is also the most variable region of the Top2 protein across species and isozymes. The C-terminal domain is believed to serve some undetermined function in strand passage as well as participate in enzyme localization[190].

Table 1.2 Eukaryotic Top2 crystal structures

Structure Name	Protein	Description	Year [Citation]
1BGW	yTop2	Breakage Reunion Domain	1996 [157]
1BJT	yTop2	Breakage Reunion Domain	1999 [144]
1QZR	yTop2	ATPase Domain in complex with ANP-PNP and ICRF-187	2003 [176]
1PVG	yTop2	ATPase Domain in complex with ANP-PNP	2003 [176]
1ZXM	Top2α	ATPase Domain in complex with AMP-PNP	2005 [159]
1ZXN	Top2α	ATPase Domain in complex with ADP	2005 [159]
2RGR	yTop2	Breakage Reunion Domain in complex with DNA	2007 [56]
3L4J	yTop2	Breakage Reunion Domain in complex with DNA	2010 [174]
3L4K	yTop2	Breakage Reunion Domain in complex with DNA and the divalent cation	2010 [174]
3QX3	Top2β	Breakage Reunion Domain in complex with DNA and Etoposide	2011 [73]
4FM9	Top2α	Breakage Reunion Domain in complex with DNA	2012 [72]
4GFH	yTop2	Catalytically active Top2 bound to DNA and AMP-PNP	2012 [177]
4G0U	Top2β	Breakage Reunion Domain in complex with DNA and Amsacrine	2013 [74]
4G0V	Top2β	Breakage Reunion Domain in complex with DNA and Mitoxantrone	2013 [74]
4G0W	Top2β	Breakage Reunion Domain in complex with DNA and Ametantrone	2013 [74]
4J3N	Top2β	Breakage Reunion Domain in complex with DNA	2013 [74]
4R1F	Top2α	ATPase Domain in complex with ADP and SO_4	2014 [180]
5GWI	Top2β	Breakage Reunion Domain in complex with DNA and Etoplatin N2α	2017 [178]
5GWJ	Top2β	Breakage Reunion Domain in complex with DNA and Etoplatin N2β	2017 [178]

5GWK	Top2α	Breakage Reunion Domain in complex with DNA and Etoposide	2017 [178]
5ZRF	Top2β	Breakage Reunion Domain in complex with DNA: Novel Conformation	2018 [158]
5ZQF	Top2β	Breakage Reunion Domain in complex with DNA: Novel Conformation	2018 [158]
5ZEN	Top2β	Breakage Reunion Domain in complex with DNA: Novel Conformation	2018 [158]
5NNE	hBRD4 and Top2α	Co-crystal structure of hBRD4 and Top2α C-terminal domain fragment (aa 1198-1207)	2019 [191]
6CA8	pfTop2	Breakage Reunion Domain: Plasmodium Falciparum	2019[192]

Figure 1.4 The structure of topoisomerase II

A.

B.

C.
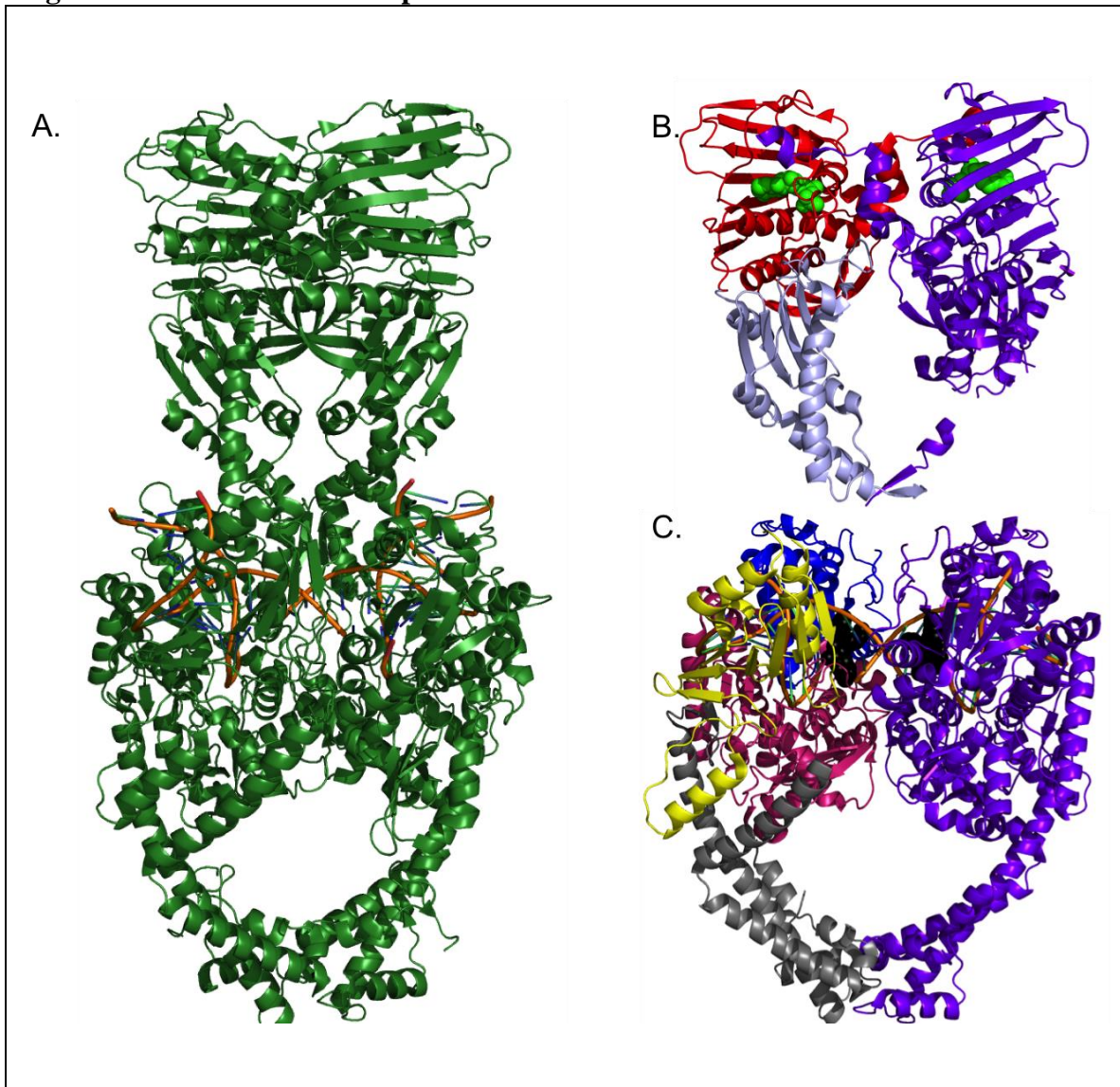
Figure 1.4 The crystal structure/domain organization of eukaryotic Topoisomerase II **A.** The structure of catalytically competent yeast Top2 in complex with double stranded DNA (orange) bound to AMP-PNP (not shown) (PDB molecule: 4GFH)[177]. This structure shows the architecture and domain organization of a functional Top2 enzyme with all three of the major dimerization interfaces 'closed'. **B.** The crystal structure of the Top2α N-terminal ATPase protein fragment (~aa29-426) in complex with ADP (green) (PDB molecule: 1ZXN)[159]. This structure shows the ATPase (red) (~aa30-265) and transducer (light blue) (~aa 266-428) domains of Top2α as well as the interactions with the opposing subunit of the homodimer (purple) as a closed clamp conformation. **C.** The crystal structure of the catalytic enzyme core of Top2α in complex with DNA (orange) and etoposide (black) (PDB molecule: 5GWK)[178]. This structure shows the domain organization in the catalytic core TOPRIM (blue) (~aa455-572), WHD (pink)(~aa765-865), Tower (yellow) (~aa895-1000), Coiled-Coil (Grey) (~aa1020-1180). This structure shows the alignment of the TOPRIM domains coordinating with the active site tyrosine (Tyr805) (Top2α) of the opposing subunit in order to accomplish the DNA breakage reaction. This structure also shows the interactions with the opposing subunit of the homodimer (purple) including two of the three major dimerization interfaces of the protein.

1.3   Topoisomerase II targeting agents

The DNA topoisomerases were discovered in 1971 by Dr. James Wang[8,193]. In the intervening 40 years this class of enzymes has maintained a high level of research interest because of the discovery of active anti-tumor agents like etoposide and doxorubicin approved for therapeutic use in 1983 and 1974, respectively[194–197]. These two small molecules and many of their derivatives are used as broad-spectrum anti-neoplastic agents[18]. Because of the utility of these agents in anti-cancer therapies a key discovery was their shared therapeutic target, Top2. Top2 targeting agents are also used in antibiotic therapies in both contexts these agents are used to cause DNA damage and cytotoxicity[17,18,198].

There are two distinct classes of Top2 targeting small molecule agents: catalytic inhibitors and topoisomerase poisons (Figure 1.5)[199]. These classes are distinguished based on the mechanism of generating cytotoxicity. Top2 catalytic inhibitors follow a conventional mechanism of small molecule drug action by reducing the catalytic activity of the Top2 enzyme[200]. Mammalian cells depleted for Top2α or treated with Top2 catalytic inhibitors result in chromosomal mis-segregations or mitotic delays, likely killing cells by depriving cells of critical Top2 acitivty[104,118,120,121].

The topoisomerase poisons lead to high levels of DNA breakage by subverting the catalytic activity of the enzyme converting it into a form of unique DNA lesion[18,201,202]. Topoisomerase poisons stabilize the enzyme while it is covalently linked to DNA, resulting in a prolonged covalently attached DNA-protein intermediate that shelters a DNA break[50,203–207]. Cells exposed to Top2 poisons produce mostly protein-linked DNA strand breaks leading them to commit to apoptosis[201,202,205,206,208–211]. This DNA lesion

serves as a barrier to DNA metabolism (transcription and replication) and can lead to further DNA damage from replication fork collapse and transcriptional stress[212,213].

1.3.1 **Top2 poisons**

Numerous small molecules have been identified that can incite the trapping of Top2 as a covalent complex with DNA. Top2 poisons vary greatly in chemical scaffold and exposure quickly leads to high levels of Top2 mediated DNA breakage[204,206]. Several of these compounds are approved for therapeutic use to target human or bacterial cells in therapies designed to cause cell death via DNA damage[204,205,214,215].

For many years the precise molecular mechanisms of Top2 poisoning have remained poorly understood. Many Top2 poisons can bind DNA (intercalators) or the apo Top2 enzyme as well as the DNA-enzyme covalent complex. Structural analysis of crystalized Top1 in complex with DNA and a Top1 poison (camptothecin) indicated a ternary complex where the poison functions as an interfacial inhibitor that blocks DNA ligation[216]. Several pieces of evidence suggested that Top2 poisons may bind at the site of DNA Top2 cleavage[217,218]. Given the chemically diverse nature of Top2 poisons and the characterization of point mutations that affected drug sensitivity, the interfacial inhibition model was similarly proposed for Top2[50,199,204,208,219–221].

The interfacial inhibition model predicts drug binding at the DNA-protein interface to form a ternary complex that displaces key residues involved in the DNA breakage/reunion reaction[222,223]. This model could explain the observations that Top2 poisons demonstrate a preference of DNA sequence at cleavage sites depending on the Top2 isoform and poison[224–228]. Structural analysis of the catalytic cores of Top2β and Top2α co-crystallized with DNA and etoposide gives strong evidence in support of this

model[73,74,178]. These structures show two drug molecules inserted into the base stack between the 5'Phophotyrosine and 3'OH DNA ends essentially blocking DNA ligation.

The Top2 poisons are divided as either intercalative or non-intercalative referring to the nature of their relationship with DNA[18]. The intercalating poisons sit at the -1 and +1 bases of DNA during Top2 catalysis and disrupt normal DNA base stacking[229,230]. This action interferes with the interfacial geometry between the DNA and protein required for religation of the DNA during catalysis. Because of their interaction with DNA the intercalating poisons have demonstrated a strong preference for the -1 and +1 DNA bases[228].

The DNA intercalating Top2 poisons are diverse in chemical scaffold. Certain derivatives of anthracyclines have been approved for use in anti-tumor therapies, these include: daunorubicin, doxorubicin, epirubicin and mitoxantrone (Figure 1.5)[17]. Daunorubicin is approved for use in acute myeloid leukemia (AML), acute lymphoblastic leukemia (ALL), and chronic myelogenous leukemia (CML) as well as Kaposi's sarcoma. Doxorubicin is approved for use in a wide array of anti-tumor therapies including: leukemia, lymphoma, myeloma, neuroblastoma, sarcoma, and Wilm's tumor as well as cancers of the bladder, breast, endometrium, lung, ovary, stomach, and thyroid[231]. Epirubicin is approved for use against breast cancers and occasionally used in place of doxorubicin[232]. Mitoxantrone is approved for use in acute leukemia and non-Hodgkin's lymphoma as well as metastatic breast or prostate cancers as a second line therapy[233]. Several intercalating Top2 poisons (amonafide, ellipticine and mAMSA) are not used clinically but are potent Top2 poisons and remain relevant in a research capacity

(Figure 1.5)[234]. Amonafide exhibited some anti-tumor activity in a phase III clinical trial but is no longer in clinical development due to toxicity associated with its metabolites[235].

The non-intercalating Top2 poisons include the epipodophyllotoxins (etoposide and teniposide) and fluoroquinolones (ciprofloxacin) (Figure 1.5)[236,237]. The epipodophyllotoxins are semi-synthetic derivatives of podophyllotoxins (microtubule inhibitors) and are used in several anti-cancer settings[238]. Etoposide is approved for use in refractory testicular tumors and as a first line therapy in small cell lung cancer[17]. Etoposide is occasionally also used to treat lymphoma, non-lymphocytic leukemia and glioblastoma[17]. Teniposide is approved for use in the treatment of refractory ALL[239]. Fluoroquinolones are well known for their antibiotic application against prokaryotes and several derivatives (such as CP115,953) have been shown to have activity against the eukaryotic enzyme[240–242]. In a recent phase III clinical trial another quinolone with activity against the eukaryotic enzyme (Vosaroxin) demonstrated increased overall survival and increased complete response rates in combination with cytarabine in patients with refractory/early relapsed acute myeloid leukemia[243].

1.3.2 <u>**Top2 catalytic inhibitors**</u>

Many small molecules have been identified as catalytic inhibitors of Top2. The bisdioxopiperazines are the best-characterized chemical scaffold of the Top2 catalytic inhibitors. Of these dexrazoxane (ICRF-187) is the only FDA approved Top2 catalytic inhibitor (Figure 1.5)[244]. Bisdioxopiperazines stabilize the dimerization of the N-terminal ATPase domain as a closed clamp conformation[245]. This activity traps the enzyme on the G-segment of the DNA and prevents additional catalytic cycles as the enzyme cannot capture any additional DNA. The clinical indication for dexrazoxane is to mitigate the

cardiotoxic side effects of doxorubicin. In yeast, dexrazoxane appears to achieve cell killing by poisoning the activity of Top2[244,246,247]. However, catalytic inhibitors have been shown to antagonize Top2 poison activity[248]. Resveratrol, well known as the potentially healthful active compound found in red wine, is structurally related to bisdioxopiperazines. Resveratrol, however, works in an contrary fashion by blocking the dimerization of the ATPase domain, inhibiting the closed clamp conformation and the ATPase activity of the enzyme[247].

The remaining Top2 catalytic inhibitors are abundant, chemically diverse and fall into two classes: ATP competitive inhibitors such as the phosphomimetics or purine analogs and agents that prevent DNA cleavage. These agents are not selective for Top2 likely because the ATPase domain of Top2 belongs to the GHKL superfamily[179]. Notable members of this category are purine analogs such as QAP1 and 8-Cl-ATP, however, these agents can vary widely in chemical scaffold (ie. novobiocin and daurinol) (Figure 1.5)[249,250]. 8-Cl-ATP is currently undergoing phase I and II clinical trials for application colorectal cancer and solid tumors[251]. Several small molecules initially thought to be catalytic inhibitors as they target the Top2 ATPase domain (8-Cl-ATP, emodin and salvicine) have been identified potentially causing DNA damage via Top2 poisoning (Figure 1.5)[249,252,253].

Notable catalytic inhibitors of Top2 that work by inhibiting DNA cleavage include: aclarubicin (a derivative of anthracycline) and merbarone (Figure 1.5). Aclarubicin inhibits Top2 from binding DNA, a prerequisite for DNA scission[254]. In contrast, merbarone has no effect on DNA binding but appears to block DNA cleavage[255].

Figure 1.5 DNA topoisomerase II targeting drugs

A. Daunorubicin, Epirubicin, Etoposide, Teniposide, Doxorubicin, Mitoxantrone, CP115,953, Ciprofloxacin, Amsacrine (mAMSA), Amonafide, Ellipticine

B. 8-Cl-ATP, Dexrazoxane (ICRF-187), Resveratrol, Emodin, Salvacine

C. Merbarone, QAP1, Aclarubicin, Novobiocin
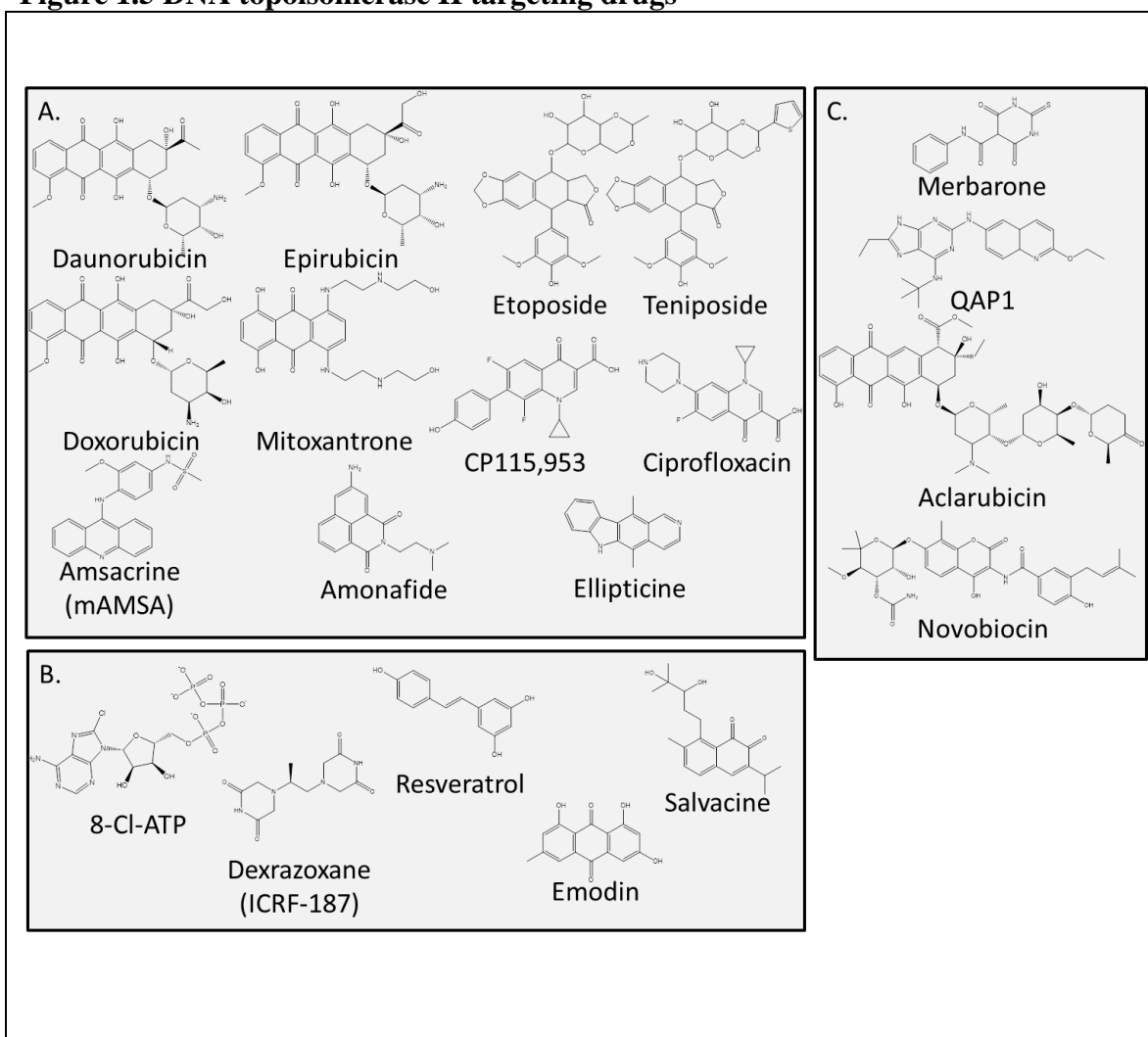
Figure 1.5 The chemical structures of DNA Topoisomerase II targeting agent's represent a wide variety of chemical scaffolds **A.** The DNA Topoisomerase II poisons work by stabilizing Top2 while it forms a covalent complex with the DNA. These agents generate high levels of double strand and single strand breaks in cells. **B.** The DNA Topoisomerase II catalytic inhibitors that may also work as weak Top2 poisons. These agents are believed to bind to the N-terminal region of Top2. The mechanism of action of these inhibitors is by trapping the enzyme in a conformation state that prevents further catalytic activity. Emodin, salvacine, and 8-Cl-ATP have been identified as agents that trigger DNA strand breaks and could operate as Top2 poisons[249,252,253,256]. There is additional evidence to suggest that dexrazoxane kills cells in a mechanism similar to that of the top2 poisons[257]. **C.** The DNA Topoisomerase II catalytic inhibitors work by decreasing the catalytic activity of Top2. The mechanism of action of these agents is less unified. QAP1, a purine analog and novobiocin, an aminocourmarin, competitively inhibit the ATPase activity of Top2. Aclarubicin, merbarone and novobiocin have other significant cellular targets. Aclarubicin blocks DNA binding by Top2 and Merbarone blocks DNA cleavage without affecting DNA binding.

1.3.3 Repair of Top2 mediated DNA damage

Top2 poisons generate high levels of DNA damage (both single and double strand breaks) to generate therapeutic cytotoxicity[17,28]. Repair of Top2 mediated DNA damage occurs in three major phases (recognition, removal and DNA repair)[18]. Recognition of Top2 mediated DNA damage requires cells first to distinguish a difference between the transient covalent complex that occurs with catalysis and a covalent complex that is trapped by small molecules or other mechanisms[18]. The mechanisms that recognize trapped Top2 covalent complexes are not well understood, however, they may be associated DNA-tracking machinery (ie. transcription or replication factors) as the trapped Top2c works as a block to DNA metabolism[18]. The Top2 covalent complexes stabilized by Top2 targeting drugs are reversible *in vitro* and likely remain so until a certain stage of the removal process[258–260].

Cells exposed to Top2 poisons have been shown to introduce post-translation modifications (PTM) to the Top2cc such as sumoylation and poly-ubiquitination[261,262]. While these PTM are involved in the recognition of the trapped Top2cc some sumoylation modifications are also important to the regulation of enzyme activity[117,263,264]. Sumoylation and subsequent polyubiquitination of the Top2 enzyme have been demonstrated to be important for the proteolytic degradation of the trapped Top2cc by the proteolytic pathway likely involving degradation of Top2 by the 26s proteasome[27].

Two pathways have been identified in cells as being capable of processing the Top2cc for removal: the proteolytic pathway and nucleolytic processing pathway[18]. The mechanistic basis for these pathways is to remove the Top2 DNA lesion by degrading the

protein (proteolysis) or cutting the DNA to remove the bulky protein adduct (nucleolytic)[18]. The tyrosyl-DNA phosphodiesterase proteins (TDP1 and TDP2) have been identified as specialized enzymes that can hydrolyze the 5' phosphotyrosyl linkage between the protein and DNA[17,18,265]. Removal of the 5' phosphotyrosyl linkage may also occur through the endonucleolytic activity MRE11 in the MRN complex or CtIP[266,267]. Factors that participate in the recognition and processing of the Top2cc have been identified as candidates for inhibition as they synergize with Top2 poisons[265,268,269]. After the Top2 protein-DNA adduct is processed and removed cells repair the DNA strand breaks by homologous recombination or non-homologous end joining DNA repair pathways.

1.4 Clinical Applications and limitations of targeting Top2

1.4.1 Clinical Applications of targeting Top2

Top2 targeting agents are used as effective cytotoxic therapies due to there ability to cause DNA damage[17,28]. Etoposide and doxorubicin are some of the best known and most widely used Top2 targeting agents and were approved for use in anti-neoplastic therapies over 40 years ago[194–197]. Top2 targeting agents are commonly used in combination therapies with other DNA damage agents such as platinum drugs (ie. cisplatin) or bleomycin[270,271]. These agents have a clear clinical utility as anti-tumor agents but their current clinical application is limited due to the negative consequences associated with their use[17,18].

1.4.2 Limitations of targeting Top2

Clinical therapeutic use of Top2 as an anti-cancer agent is severely limited by several clinically documented side effects (cardiotoxicity and secondary

malignancies)[272–274]. Top2 poisons like doxorubicin and etoposide have been shown to target both human isoforms, thus it has been difficult to dissect the etiology of these side effects[17,18,275,276].

One of the most serious of these side effects includes the development of secondary malignancies typically presenting as acute myeloid leukemia (AML)[273,274,277,278]. These secondary malignancies are typically characterized as drug induced chromosomal translocations usually involving the MLL1/KMT2A gene and ~50 partner loci[277,279]. The development of AML is characterized by a latency period of ~2 years as opposed to the ~5-7 year latency associated with alkylating agents[277]. The development of therapy induced acute myeloid leukemia (t-AML) has not yet been linked to any genetic risk factors or cumulative Top2 poison dose however the dosing schedule is somehow linked to t-AML etiology[280–282]. The Top2β isoform is also strongly linked to t-AML, although there is currently no direct evidence. Top2β has been shown to be required for the production of etoposide induced DSBs at genes (RUNX1) identified as breakpoint regions for t-AML cases[283]. Another study showed that etoposide induced chromosomal rearrangements were dependent on Top2β in skin cells[284]. One of the prevailing models for t-AML translocations involves shared transcription machinery between MLL1 and proximal partner loci [278]. The roles of topoisomerases in genome instability, and my work on using novel topoisomerase mutants to explore the effects of topoisomerase targeting agents will be discussed in greater detail in Chapter 3.

A second significant side-effect of targeting Top2 is the development of acute cardiomyopathy in treated patients[285]. Cardiomyopathy is predominantly linked to anthracycline therapies[286–288]. The etiology was slightly more difficult to elucidate given

that anthracyclines are strongly linked to oxidative stress (also associated with cardiotoxicity)[272,285,289]. Several studies have suggested that treatment with dexrazoxane (Top2 catalytic inhibitor) can ameliorate/protect patients from top2 therapy associated cardiotoxicity[165,289–293]. Top2β again is strongly tied to the development of these major side effects. In cardiomyocytes Top2β is ubiquitously expressed while Top2α is not, suggesting that Top2β would be responsible for the cardio toxic effects targeting top2[294]. Mice carrying cardiomyocytes conditionally deleted for Top2β by Cre-*loxp* were protected from the cardio toxic effects of doxorubicin [272]. These data provide strong supporting evidence to link Top2β to cardiotoxicity, as Top2α gene is also essential in mice and it could not be deleted.

1.4.3 Resistance to Top2 targeting drugs

A major issue all therapies face is the development of drug resistance; Top2 targeting agents are no exception. Several mechanisms have been identified to contribute to cellular resistance to Top2 targeting agents.

1.1.1.1. *Mechanisms of resistance*

Consistent with previously identified resistance mechanisms, alterations to the expression or efficiency of drug export proteins that produces lower levels of drug accumulation within cells will lead to drug resistance[295–299]. A major mechanism of this is through the overexpression of the ATP-binding cassette (ABC) proteins[300]. The ABC proteins are a family of membrane transport proteins capable of exporting many different molecules from cells and when overexpressed can generate multidrug resistance[301]. Several ABC transport proteins have been identified to play a role in generating

resistance to Top2 targeting agent like doxorubicin or in (ABCB1/MDR1 and ABCC1/MRP1)[302–305].

In contrast to other therapies, resistance to Top2 targeting drugs can also occur from decreased levels of expression or catalytic activity. Ectopic expression of inactive forms of yTop2 confers etoposide resistance in yeast[306]. Similarly, co-treatment with catalytic inhibitors and Top2 poisons demonstrate an antagonistic relationship[248]. These findings are consistent with Top2 poisoning as the mechanism of drug action through Top2 mediated DNA damage. Biochemical characterization of drug resistant mutant Top2 alleles has provided some insights into the molecular details of drug action.

As discussed in previous sections, the biochemical characterization of Top2 mutant proteins has provided many of the details of Top2 biology. Thus many Top2 mutant proteins have been characterized with the interest of exploring the catalytic mechanisms of activity, interaction with Top2 targeting drugs and locations of drug binding (Appendix A)[307]. Not all of the previously characterized mutant enzymes focused solely on drug resistance or sensitivity. Several alleles of yeast Top2 have been identified to convey temperature sensitive (*ts*) activity. These *ts* yeast Top2 alleles have proven to be incredibly useful tools to measure the sensitivity of human Top2 isoforms and were instrumental in isolating the mechanisms of drug action for Top2 targeting drugs[86,198,306,308–311]. Identification and analysis of novel mutant enzymes alleles related to Top2 targeting is an ongoing focus of current topoisomerase research. As the characterization of these mutant proteins with altered sensitivity to Top2 poisons pertains closely to the research presented in chapter 2, the mutant enzymes and what we have learned from them are discussed in the introduction to that chapter.

1.5 <u>Introduction summary</u>

The DNA topoisomerase proteins provide critical functions by processing DNA topology in cells. Topological structures like supercoils knots and catenanes are processed by a strand-passage mechanism involving transient DNA strand breaks. DNA topoisomerase 2 functions are extremely important to cells. These enzymes serve as bonafide cellular targets for wide variety of small molecule agents. These agents represent a wide array of known drug scaffolds, highlighting multiple potential strategies for poisoning the Top2 enzymes. Numerous studies have focused on the biochemical characterization of the Top2 enzymes with the goal of better understanding the mechanism of drug action and unperturbed enzyme reaction. Many of which have used yeast and mutant enzymes to characterize these

In the following chapters I will begin with a review of notable mutant protein characterizations and then present work I have carried out in an effort to advance the understanding of the Top2 enzyme through research focused on: characterization of purified mutant Top2α proteins that convey etoposide hypersensitivity to yeast (Chapter 2), exploration of the mutagenic consequences of targeting topoisomerases II with etoposide in yeast (Chapter 3), and the characterization of a recently identified mutation in Top2β (His63Tyr) associated with global developmental delay in humans (Chapter 4). My final chapter (5) will integrate the findings of the preceding chapters and detail the mechanistic insights gained by this research and explore the potential applications of this knowledge.

2 CHARACTERIZATION OF ETOPOSIDE HYPERSENSITIVE TOP2 ALLELES

2.1 <u>Summary</u>

The biochemical characterization of mutations in DNA topoisomerase II has helped to decipher details of drug action and enzyme biology. Biochemical analysis of hypersensitive mutant alleles has revealed that Top2 targeting chemical scaffolds have the potential to target both eukaryotic and prokaryotic enzymes[312,313]. These details have highlighted similarities in the mechanisms of topoisomerase targeting drug activity as well as illustrated that existing drugs could be modified to exert therapeutic effects against either of the prokaryotic/eukaryotic enzymes. Analysis of hypersensitive mutant alleles has also expanded our perception of how distal parts of the enzyme could contribute to Top2 targeting drug sensitivity[313,314]. Overall, the characterization of drug hypersensitive mutant proteins has provided a different angle from which to approach the study of Top2 targeting drugs and has proven to be a valuable tool to understanding enzyme biology[314].

The goal of the work presented in this study was to expand on previous efforts to study etoposide drug action by isolating a large number of mutations in Top2α that confer hypersensitivity to etoposide. We hypothesized that analysis of mutant proteins that confer hypersensitivity would provide a unique tool to characterize the details that are important to etoposide activity and provide an opportunity to explore additional details of enzyme biochemistry.

This yeast-based study identified 83 alleles of Top2α (excluding duplicates) that convey hypersensitivity to etoposide that were distributed throughout the Top2α catalytic

domains. We identified several clusters of mutations by their close proximity on the available Top2α crystal structures. Many of the clusters were distant from the proposed etoposide binding site and may identify regions of the protein important for sensitivity to numerous Top2 targeting drugs. We found that many of the etoposide sensitizing mutations identified here also conveyed a corresponding level of sensitivity to mAMSA. Together these findings suggested this group of mutations likely affected Top2 catalysis rather than drug binding.

We selected several of the more sensitive Top2α mutations identified by this screen for purification and further characterization. Biochemical analysis of these mutant proteins identified several interesting characteristics that were shared by other mutations in the same regions. Several purified mutant enzymes (Asp374Gly and Thr377Ile) demonstrated a decreased ATP requirement for catalytic activity. A previously characterized mutant in this region (Asp48Asn) shared this characteristic as well as a greater sensitivity to etoposide when expressed in yeast. These mutant enzymes also demonstrated a lack of DNA stimulated ATP hydrolysis activity that is shared with other etoposide sensitizing mutant proteins. Our results indicated that this group of mutant proteins exhibit altered utilization of ATP hydrolysis, which could dysregulate the catalytic mechanism leading to etoposide sensitivity. Furthermore, these results suggest that the ATPase domain plays a role in the regulation of enzyme mediated DNA cleavage.

2.2 <u>Introduction</u>

The biochemical characterization of drug hypersensitive mutant DNA Topoisomerase II has provided valuable insights into the mechanisms of enzyme catalysis and dynamics of drug action[240,312,315,316]. Previous research has characterized a large number of Top2 mutant proteins Appendix A[307]. Many of the eukaryotic Top2 mutant proteins previously characterized were selected for analysis based on their ability to confer resistance to Top2 targeting drugs; these studies are summarized and referenced in Appendix A. While some of the identified mutant proteins demonstrated differential sensitivities to Top2 poison many have been generalized into 3 major categories based on the proposed role of the amino acid residues involved (drug binding, DNA binding, and effect on catalytic activity)[73].

2.2.1 <u>Characterization of notable Top2 mutant proteins</u>

Analysis of mutant eukaryotic Top2 enzymes that alter drug sensitivity have provided details regarding the mechanisms of drug action as well as developed tools to study the enzyme in the future. In this section I highlight several notable Top2 mutant proteins as well as describe several genetic screens that have helped to guide the approach we took with our research.

Top2 targeting drug sensitive and resistant mutations

Topoisomerase targeting agents were initially studied in mammalian cells. A standard pharmacologic approach is the selection of cell lines resistant to the agent of choice. When mammalian cell lines were selected for resistance were obtained, an interesting pattern of sensitivity was seen. The cell lines were resistant to all classes of topoisomerase II targeting agents, but had relatively normal sensitivity to other classes of

agents. For example, Human leukemia cells (CEM/VM-1) were selected for resistance to teniposide and demonstrated high levels of cross-resistance to etoposide, anthracyclines, mitoxantrone and mAMSA[305]. A potential explanation was that the cell lines carried specific alterations in Top2, either in levels of expression, or mutations that change intrinsic sensitivity of the enzyme to inhibitors. Both types of alterations were seen. In the CEM/VM-1 cells, a mutation changing Arg450Gln was identified[317]. Subsequently an additional mutation, changing Pro803Ser was identified[317]. Similar results were obtained with other cell lines; e.g., Zwelling 1991[318]. While these mutations provided strong evidence that Top2 was the principal target of these agents, this approach was unlikely to lead to the identification of enough mutant alleles to provide a detailed biochemical picture of potential mutants that alter drug sensitivity.

The laboratory of Dr. John Nitiss developed yeast based genetic system was developed to isolate mutant alleles of Top2 to overcome a reduction in catalytic activity[319]. This system utilized temperature sensitive yeast alleles to select for mutants with sufficient catalytic activity to complement the temperature sensitive deficiency of Top2 in the yeast. This approach was able to isolate three mutant alleles of yTop2, of which two were resistant to both mAMSA and etoposide[319].

The yeast genetic system described above was also used to select for yeast Top2 alleles that grow in the presence of CP115, 953 in an effort to analyze the molecular details of differentially sensitive alleles of Top2[320]. The yTop2 Gly437Ser allele was identified in these yeast cells to convey resistance to CP115, 953, mAMSA, etoposide, and ellipticine. Biochemical analysis of the purified Gly437Ser mutant protein however revealed that the enzyme was hypersensitive to Top2 poisons *in vitro*. As the mutant

46

protein had wild type levels of catalytic activity, the drug resistance phenotype was suggested to be due to the decreased stability of the mutant protein, thereby decreasing the expression levels of the protein *in vivo*[320].

Despite the use of yeast along with vectors that overexpress Top2, many isolated mutants confer resistance through a reduction of Top2 catalytic activity[306]. For example, in an early drug resistance screen using overexpression of Top2, yTop2 was randomly mutagenized *in vitro* and transformed cells were selected for resistance to etoposide. This study found 129 yeast isolates identified as resistant to etoposide, all of which were cross-resistant to amsacrine. Of these, 36 of the isolates were randomly selected for further characterization of which 19 (52%) demonstrated at least a 4-fold reduction in relaxation activity in cell lysates[307]. These results supported the notion that a reduction in Top2 catalytic activity was a frequent mechanism of resistance to Top2 poisons and suggested that biochemical analysis following large mutant screens would be complicated by a large number of mutants that were resistant solely due to reduced enzyme activity.

Recently, a quinolone resistance screen was carried out to explore the alterations required for the yeast and human Top2 enzymes to be selective for ciprofloxacin and/or vosaroxin[321]. This screen utilized next-generation sequencing to identify the mutations in the yeast and human Top2 isozymes. Many mutations were identified in the ATPase domain; therefore the researchers purified the catalytic core (DNA binding and DNA cleavage domain) of yTop2, Top2α and Top2β. They found that catalytic core Top2β was extremely sensitive to fluoroquinolone poisoning, suggesting that ATPase domain plays a role in regulating drug resistance[321].

One of the most commonly identified quinolone resistant mutations is Ser83Trp in DNA Gyrase (a prokaryotic Top2)[322,323]. Biochemical analysis of the Ser83Trp mutant protein revealed that Top2 targeting drugs that do not usually exhibit any effect on DNA Gyrase could inhibit the enzyme's strand passage activity and exhibit elevated levels of DNA cleavage[240,323]. These findings suggested that the important biochemical domains were conserved between eukaryotic and prokaryotic orthologs. Therefore, the orthologous mutation was constructed in the conserved Ser740 residue of yTop2 and was shown to similarly convey resistance to quinolones and an unexpected hypersensitivity to etoposide[199,240]. The differential sensitivity to Top2 poisons suggested that Ser-740 was near the etoposide-binding site. The mutation was also constructed in the conserved residue of Top2α (Ser763Trp), yeast expressing this allele were sensitized to etoposide[316].

Several mutations have been identified that can convey differing levels of resistance or sensitivity to Top2 poisons. A mutation (Thr744Pro) in the neighboring α-helix in yTop2 results in increased sensitivity to several Top2 poisons including norfloxacin and oxolinic acid, which the eukaryotic enzyme is not usually sensitive to[312]. The yTop2 Thr744Pro mutant allele additionally sensitized cells to mAMSA and CP115, 953 but not etoposide. Molecular modeling of the Thr744Pro mutant protein suggested the displacement of key residues that participated in enzyme catalysis. Another mutation identified in yTop2 (His1011Tyr) conveys resistance to CP119, 953 and etoposide, hypersensitivity to ellipticine but does not alter sensitivity to mAMSA[313]. These mutations suggest that the details of drug interaction maybe subtly different between non-intercalating and intercalating agents.

The laboratory of Dr. John Nitiss carried out a yeast based genetic screen to identify mAMSA hypersensitive alleles of yTop2. This screen utilized an *in vivo* recombination technique to create a library of yeast carrying mutagenized yTop2 plasmids[314]. The major advantage of this approach was the ability to target specific regions of the Top2 coding sequence for mutagenesis. We adapted this approach to Top2α in the work that is described in this chapter. Using this approach several yTop2 alleles (Pro473Leu, Gly737Val and Leu1025Ile) were identified that confer sensitivity to mAMSA. Pro473Leu and Gly737Val did not confer cross-sensitivity to etoposide and were biochemically characterized. In the presence of mAMSA the Pro473Leu allele generated low levels of double strand breaks and high levels of single strand breaks. This finding indicated that hypersensitivity could be achieved by generating single strand breaks and additionally highlighted that trapping Top2 as a single strand-bound covalent complex was an important mechanism of cell killing[314].

Biochemical analysis of drug hypersensitive Top2 alleles has already provided several key details about drug action. We hypothesized that by studying and characterizing etoposide hypersensitive Top2α alleles we would learn more about the molecular dynamics of drug action as well as important details about the unperturbed Top2 reaction.

2.3 Materials and methods

2.3.1 Growth medium

Yeast extract peptone dextrose adenine (YPDA) medium is a complete synthetic media used for yeast growth. YPDA medium was prepared by mixing 10g yeast extract (BD Difco, 212750), 20g bacto-peptone (BD Difco, 211677), 20g dextrose (glucose)

(Alfa Aesar, A168828), 2ml 0.5% adenine solution in ddH$_2$O at a final volume of 1

liter[324]. Agar plates of the medium were prepared by adding 17g of bacto-agar (Fisher

Scientific Bioreagents, BP1423-500) to 1 liter of medium prior to sterilization. YPDA

medium was sterilized by autoclaving at 250˚C for 25 minutes. Molten agarose medium

was allowed to cool to 55˚C in a water bath, poured into 60mm petri dishes at room

temperature to set.

        Transformed *Saccharomyces cerevisiae* strains were grown on selective synthetic

dropout medium. The selective medium was prepared by omitting the appropriate factors

that allow for the selection of auxotrophic yeast ie. SC-LEU⁻ is synthetic media lacking

only leucine but containing all other contents. Yeast synthetic dropout medium was

prepared by dissolving 1.7g yeast nitrogen base without $(NH_4)_2SO_4$ (BD Difco, 233520),

5.0g $(NH_4)_2SO_4$ (FisherScientific Bioreagents, 7783-20-2), 20.0g dextrose (glucose), and

an appropriate amount of yeast synthetic dropout powder (Table 2.1) in ddH$_2$O at a final

volume of 1 liter. The appropriate amount of yeast synthetic dropout powder depends

component that is being omitted ie. for SC-Ura⁻ medium the dropout powder will lack

uracil and therefore 0.77g/L was used, as uracil would account for 0.2g/L of the dropout

powder. The pH of the medium was adjusted to pH 6.0 with NaOH. Agar plates of the

medium were prepared by adding 17g of bacto-agar to 1 liter of medium prior to

sterilization. Synthetic dropout medium was sterilized by autoclaving at 250˚C for 25

minutes. Synthetic dropout medium with galactose was made identically to synthetic

dropout medium except that 20g of dextrose was replaced with 20g of galactose (Sigma

Aldrich, G0625).

SC-Ura⁻ agar medium with drug was made identically to SC-Ura⁻ agar medium except with the addition of etoposide (Sigma-Aldrich, E1383) or ciprofloxacin (Santa Cruz Biotechnology, 85721-33-1) after the sterilized agarose medium cooled to 55˚C in a water bath, mixed, then poured into 60mm petri dishes at room temperature to set. Drug concentrations were as indicated for individual experiments.

SC-Ura⁻ induction medium was prepared by dissolving 1.7g yeast nitrogen base without $(NH_4)_2SO_4$, 5.0g $(NH_4)_2SO_4$, 0.77g of SC-Ura⁻ synthetic dropout powder (Table 2.1), 30ml 100% glycerol (Fisher Bioreagents, 56-81-5), and 23.5ml lactic acid (Sigma-Aldrich, W261106) in ddH_2O at a final volume of 1 liter. The pH of the medium was adjusted to pH 6.0 with NaOH pellets (Acros Organics, 131-73-2). The medium was sterilized by fast-flow sterifilter (Thermo Fisher, 595-4520).

Table 2.1 Yeast complete synthetic media

Drop-out powder	mg/L	Source, CAS#
Adenine	10	Sigma, A9126
L-Argninine HCl	50	Sigma, A5131
L-Aspartic Acid	80	Sigma, A9256
L-Histidine HCl	20	Sigma, H8125
L-Isoleucine	50	Sigma, I2752
L-Leucine	100	Sigma, L8000
L-Lysine HCl	50	Sigma, L5626
L-Methionine	20	Sigma, M9625
L-Phenylalanine	50	Sigma, P2126
L-Threonine	100	Sigma, T8625
L-Tryptophan	50	Sigma, T0254
L-Tyrosine	50	Sigma, T3754
Uracil	20	Sigma, U0750
L-Valine	140	Sigma, V9500
Total	**0.79 g/L**	

E. coli growth media was prepared by mixing 25g of liquid broth (LB) medium (Fisher Bioreagents, BP1426-500) in ddH_2O at a final volume of 1 liter. The pH of the medium was adjusted to pH 7.0 with NaOH. Agar plates of the medium were prepared by

adding 17g of bacto-agar to 1 liter of medium prior to sterilization. The medium was sterilized by autoclaving at 250˚C for 25 minutes. LB medium containing a selective antibiotic was prepared identically except that the medium was allowed to cool to ~55˚C after sterilization at which point an antibiotic, ampicillin or kanamycin (50µg/ml) was added. Ampicillin or kanamycin were used depending on the selective marker in the plasmid of interest.

2.3.2   <u>Yeast vectors and plasmid construction</u>

All yeast expression plasmids used in this chapter have been described previously and are summarized in Table2.2[183,247,311,314,325–327]. The plasmids described here were propagated in DH5α *E. coli* grown on LB medium with ampicillin (50µg/mL) for selection. The pMJ1 plasmid, a yeast expression plasmid carrying Top2α under the control of the *TOP1* promoter, was modified to create a library of mutations in Top2α[326]. The modifications and uses of pMJ1 are covered in greater detail in the etoposide screen description (Section 2.4.1).

Plasmids were introduced to yeast strains using yeast lithium acetate transformations as described Appendix B[328–330]. Most of the plasmids outlined in Table 2.2 carry the *URA3* marker; yeast that carry and express the plasmids grow on SC-URA⁻ media. The pGal:RAD52 plasmid instead carries *LEU2* which selects for yeast that carry and express the plasmid on SC-Leu⁻ media[314,327]. Plasmids pMJ1, yCP50, and yCPlac33 carry a yeast centromere to maintain low copy number and mitotic stability in yeast[325,326]. Plasmid (pCH1042) is an integrating plasmid, which replaces endogenous yeast *top2* with the *top2-4* temperature sensitive allele and *URA3*[311,331].

Table 2.2 Yeast expression plasmids used in chapter 2

Yeast expression plasmid	Description
α12URAB	Top2α with N-Terminal 6xHis tag under the control of the yeast GAL1 promoter
pCH1042	Integrating plasmid, converts endogenous yeast *top2* to *top2-4* by gene replacement
pCM1	Top2α under the control of the yeast *GAL1* promoter
ypGAL:*RAD52*	*RAD52* under the control of the yeast *GAL1* promoter
pMJ1	Top2α overexpression the control of the yeast *TOP1* promoter
yCP50	Yeast centromere containing shuttle vector (used as empty vector control)
yCPlac33	Yeast centromere containing shuttle vector (used as empty vector control)

2.3.3 Yeast strains

S. cerevisiae strains (JEL1t1, JN332a, JN362a and YMM10) are described in Table 2.3. JEL1t1 is a yeast protein overexpression and purification strain[240,332]. JEL1t1 is derived from the NKY879 (MATa *leu2 trpl urd52 prbl-1122 pep4*) strain of *S. cerevisae*[152]. NKY879 was used as it was a protease deficient yeast strain and proteolysis is often an important contributing factor to overall yield during Top2α protein purification[152,333]. JEL1t1 carries the *GAL4* gene under the control of the *GAL10* promoter integrated at the *his3* locus. This leads to elevated expression levels of *Gal4* protein during galactose induction. The *Gal4* protein activates promoters including the *GAL1* promoter used by yeast expression vectors described earlier[334]. *Gal4* overexpression leads to 5-10 fold greater expression in JEL1t1 compared to NKY879[152]. The JEL1t1 strain carries a deletion of the *top1* gene which is disrupted by *LEU2*[331,335]. Top2α purified from this strain lacks potential yeast *Top1* protein contamination that might interfere with the plasmid relaxation assay to analyze Top2 activity.

JN362a is a *S. cerevisiae* haploid yeast strain that has been used to study topoisomerase targeting agents in yeast[336]. The JN332a and JN394 strains are isogenic to JN362a except deleted for *rad52*[311]. Since *RAD52* is essential for homologous recombination in yeast, JN332a is DNA repair deficient and therefore more sensitive than JN362a to double strand DNA damage including damage arising from trapped topoisomerases[311,336–339].

YMM10 is a *S. cerevisiae* haploid strain engineered to carry nine gene deletions that encode for a group of membrane-bound drug-efflux proteins identified by Karl Kuchler[295,340–342]. These nine proteins belong to the ATP-binding cassette (ABC) superfamily associated with multiple drug resistant (MDR) phenotypes observed in both eukaryotes and prokaryotes[295,340]. The loss of these drug efflux pumps in YMM10 has been shown to increase sensitivity to etoposide, most likely by increased drug accumulation[342].

Table 2.3 Yeast parental strain genotype

Yeast Strain	MAT (a/α)	Genotype	Year Published (Citation)
JEL1t1	a	*trp1, leu2, ura3-52, pbr1-1122, pep4-3, his3:: pGAL10GAL4, top1::LEU*	1993[152]
JN362a	a	*ura3-52 leu2 trp1, his7 adel-2, ISE2*	1992[311]
JN332a	a	As JN362a but *rad52::TRP1*	1992[311]
JN394t2-4	a	As JN362a but *rad52::LEU2 top2-4*	1992[311]
YMM10	a	*ura3-52; his3-Δ200; leu2-Δ1; trp1-Δ63; lys2-801amb; ade2-101oc; Δpdr18::hisG-URA3-hisG; Δpdr12::hisG; Δsnq2::hisG; pdr5::TRP1; Δpdr10::hisG; Δpdr15::loxP-KANMX-loxP; Δyor1::HIS3; Δbat1::HIS3; Δycf1::HIS3*	2001[343]
YMM10 t2-4	a	As YMM10 but *top2-4*	2001[343]

2.3.4   **Random mutagenesis of plasmid DNA**

We generated a collection of internally deleted Top2α plasmids from pMJ1 by

using PCR to amplify the backbone of pMJ1 with the two primers targeting novel

restriction half-sites (Bio-Rad iProof, 1725310) (PCR conditions and primers Table 2.4).

The internally deleted Top2α constructs (pMJ1 Δ199-386, pMJ1 Δ356-681, Δ576-925,

Δ902-1161 amino acids) were gel isolated and ligated so they could be propagated in *E.*

coli. This created a novel restriction site marking the internally deleted gene segment.

Table 2.4 Top2α plasmid deletions construct primers and PCR conditions

Deleted region of Top2α and PCR conditions	Primer Name	Primer Sequence (5'-3')
Δ199-386: 55°C ann, 165 secs elong, 11 Kb product (Bio-Rad iProof)	F-199-Xho1	GAGCTTTGGATCAACATGCC
	R-199-Xho1	GAGTTCCATCTCACCAGCTC
Δ359-756: 59°C ann, 165 secs elong, 11 Kb product (Bio-Rad iProof)	F-359-PMJ1-517AA	GTGGGTCTTCAGTACAAGAA AAACTATG
	R-359-PMJ1-517AA	GTGATTTTTCACCTGATGTG CTTTTAC
Δ576-925: 59°C ann, 165 secs elong, 11 Kb product (Bio-Rad iProof)	F-576-Xho1-925-hTOP2gap	GAGCTTCCCGTCAGAACATG GAC
	R-576-Xho1-925-hTOP2gap	CCCTCGAGTGATAAATTCCT CCAGAAAACGATG
Δ902-1161: 59°C ann, 165 secs elong, 11 Kb product (Bio-Rad iProof)	F-902-Xhol-1161aa	GAGTCCATCAGATTTGTGGA AAGAAG
	R-902-Xho1	GAGCCAGTTCTTCAATAGTA CCCTTG

We amplified segments of the Top2α gene (Amino acids 199-386, 356-681, 576-

925, 902-1161) using error-prone PCR (GeneMorph II Random Mutagenesis Kit, Agilent

200550) to generate ~1 mutation per DNA fragment (PCR conditions and primers

Table2.5). The PCR products were gel isolated and purified using the GeneJet Gel

Extraction kit (Thermo Scientific, K0691).

Table 2.5 Error-prone PCR conditions and primers

Region of Top2α and PCR conditions	Primer Name	Primer Sequence (5'-3')
Δ199-386: 48°C ann, 60 secs elong, 671 bp product, 500ng of target DNA, 25 PCR cycles	Alpha-18	TTACTGTGGAAACAGCCAGTAGA
	Alpha-1200R	TTTGATAAATTTTTCACTCAATTGGCATG
Δ359-756: 48°C ann, 60 secs elong, 714 bp product, 500ng of target DNA, 25 PCR cycles	Alpha-1001F	TGACTAAACTTGTTGATGTTGTGAAG
	Alpha-15	CCTCCAGAAAACGATGTCGCAG
Δ576-925: 48°C ann, 75 secs elong, 1.2 Kb product, 500ng of target DNA, 25 PCR cycles	Alpha-10	AGGTGTCTTCTCGGTGCCA
	Alpha-25	GTTCCCACATCAAAGGCTTGC
Δ902-1161: 48°C ann, 60 secs elong, 1 Kb product, 500ng of target DNA, 25 PCR cycles	Alpha-7	GTGCTGAAGGAATCGGTACTG
	Alpha-23	CCTTTCCCAGGAAGTCCGA

2.3.5   Site directed plasmid mutageneis

Top2α mutations were constructed in yeast expression plasmids using an *in vivo* DNA recombination approach or oligonucleotide site directed mutagenesis[314]. Yeast plasmid DNA was extracted from yeast isolates carrying the identified mutation using the zymolase procedure described above[344,345]. The segment of DNA containing the mutated sequence was PCR amplified using the IPROOF High-fidelity PCR Kit (PCR conditions and primers Table 2.6). The backbones of pMJ1, pCM1 and α12URAB were restriction digested with BSU36I and KFL1 to produce a 10.5Kb and 11.8Kb DNA fragment, respectively, containing an internal Top2α gene deletion from amino acids 100-682 and non-complementary ends. These DNA fragments were gel isolated and co-transformed into yeast strains (JN332at2-4 also carrying pGalRAD52, YMM10 or JEL1 *top1⁻*) with the DNA insert encoding for the missing portion of the Top2α gene and the mutation of interest. JEL1t1 and YMM10 yeast are proficient for HR and typically these yeast will

accurately reconstitute the Top2α gene incorporating the identified mutation. To verify

the incorporation of the mutations, plasmid DNA was extracted from the transformed

JEL1t1 yeast by zymolase procedure and the recently inserted fragment was PCR

amplified and sequenced to verify the Top2α mutation was incorporated with no

additional alterations.

Table 2.6 Top2α primers and PCR conditions for mutant Top2α cloning

Region of Top2α and PCR conditions	Primer Name	Primer Sequence (5'-3')
Δ99-682: 51°C ann, 50 secs elong, 2.2kb product (Bio-Rad iProof)	S-1	GTGTCACCATTGCAGCCTGTAA
	Alpha-13	AAGCGAGAAGTAAAGGTTGC
Δ460-1196: 51°C ann, 75 secs elong, 3kb product (Bio-Rad iProof)	F-199-Xh01-386aa-hTOP2gap	GAGCTTTGGATCAACATGCC
	AS-4	TTCATCTGGGAAATGTGTAGCA

2.3.6 Genetic screen for etoposide hypersesnitive mutants of Top2α

We adapted genetic screen approach for Top2α from a previously published yeast

screen that selected for mAMSA hypersensitive alleles of yTop2[314]. Similar to the

mAMSA screen we co-transformed a mutagenized segment of the Top2α coding

sequence into yeast with an internally deleted linear plasmid carrying the non-

mutagenized remainder of the Top2α gene. Also similar, we increased the intrinsic

sensitivity of the yeast to Top2 poisons by overexpressing Top2α and by using a repair-

deficient yeast strain (JN332a$_{t2-4}$). As the *in vivo* functional reconstitution of the Top2α

gene required homologous recombination and this yeast strain is *rad52*-, the strain also

carried a plasmid carrying the *RAD52* gene under the control of the *GAL1* promoter. Thus

prior to the yeast transformation, JN332a$_{t2-4}$ yeast were grown in SC-Leu⁻, Galactose then

plated to SC-URA⁻, Leu⁻, Galactose agar plates at 34°C (the non-permissive temperature

for the yeast *top2-4* allele) to select for a functional Top2α protein that complements for the deficiency of yTop2[319].

2.3.7   <u>Yeast patching and replica plating</u>

Yeast transformants (yeast that formed colonies) on selective media were patched and expanded onto fresh agar plates. From these expanded colonies yeast were inoculated for further experimentation. Replica plating is a technique for testing for yeast growth under various conditions as indicated by experiment[346]. Patched yeast grown on a master plate were stamped onto sterile velvet on a block to leave imprints of the colonies. Naïve agar plates were pressed to the velvet to transfer the patched colonies to the fresh plates containing various selection parameters as indicated by experiment. After 1-2 days yeast growth is assessed and compared to positive or negative controls as appropriate.

2.3.8   <u>Measurment of Top2 targeting drug sensitivity in yeast</u>

Yeast spot test. The yeast spot test was used to validate yeast etoposide sensitivity[347]. Yeast isolates identified by the etoposide sensitivity screen to be sensitive to etoposide were inoculated into SC-URA⁻ media and grown overnight at 34°C, shaking at ~280 rpm. Yeast cell number was determined using a hemocytometer or optical density at λ600nm, using empirically determined formulae obtained by parallel hemocytometer counts and OD600 measurements. The concentration of yeast was diluted to 2.0×10^6 cells/mL ~0.2 ODU/mL. Serial1: 5 dilutions were performed and 3μL of diluted cell culture were spotted in duplicate onto agar selective media plates containing DMSO, 10μg etoposide/ml, or 100μg ciprofloxacin/ml then incubated at 34°C for 2-3 days. Yeast sensitivity to drug was determined by comparing screen isolates to yeast carrying pMJ1

Top2α wild type or Top2α Ser763Trp as negative and positive controls for sensitivity, respectively.

Clonogenic survival assay. Yeast sensitivity to small molecules like etoposide was assessed more rigorously using the yeast clonogenic survival assay as has been described previously[198,311]. The yeast clonogenic survival assay is a quantitative assay for determining the sensitivity of yeast to an agent. Yeast were inoculated into selective media and grown overnight at the appropriate temperature (25°C, 30°C, or 34°C), shaking at ~280 rpm. Yeast concentration was determined using a hemocytometer or absorbance at λ600nm. The concentration of yeast was diluted to 2.0 X 10^6 cells/mL ~0.2 ODU/mL. Diluted cultures (2-3ml) were exposed to drug concentrations as indicated for 24 hours at the appropriate temperature, shaking at ~280 rpm. A sample of the diluted culture was serially diluted and plated to agar selective media at time 0 to establish initial cell viability. After 24 hours the drug exposed yeast were also serially diluted and plated onto agar selective media. Plated yeast were incubated at the appropriate temperature for 3-5 days until colonies formed. Yeast colonies that formed on agar plates were counted and results were reported relative to the initial number of viable colonies.

2.3.9   Identification of mutations in Top2α

Yeast plasmid DNA extraction and Top2α *PCR.* Yeast plasmid DNA was extracted from yeast isolates identified by the etoposide screen using zymolase procedure[344,345]. Yeast cell lysates were made by suspending yeast cells in a 24% zymolase solution, incubated at 37°C for 45 minutes, then boiled for 10 minutes. These cell lysates were stored at 4°C and used to provide DNA template for PCR amplification of the mutagenized region of Top2α (PCR conditions and primers Table 2.7).

Table 2.7 Top2α primers and PCR conditions

Region of Top2α and PCR conditions	Primer Name	Primer Sequence (5'-3')
Δ199-386: 57°C ann, 40 secs elong, 1.46kb product (Bio-Rad iProof)	Alpha-17	GAGATTCTAGTTAATGCTGCGG
	Alpha-15	CCTCCAGAAAACGATGTCGCAG
Δ359-756: 52.7°C ann, 40 secs elong, 1.34kb product (Bio-Rad iProof)	Alpha-18	TTACTGTGGAAACAGCCAGTAGA
	Alpha-14	CTTTGATGTGCTGGTGCCC
Δ576-925: 66°C ann, 40 secs elong, 1.59kb product (NEB Q5)	Alpha-9	GCACCAAGCATTCCTAGGAG
	F359-Pml1-756aa-hTOP2gap	GTGGGTCTTCAGTACAAGAAAACTATG
Δ902-1161: 53°C ann, 50 secs elong, 1.66kb product (Bio-Rad iProof)	Alpha-6	CAAACGGAATGACAAGCGAG
	AS-2	TTTGATTGGCTTAAATGCCAATGTAGT

Amplified DNA products were sent to UIC core facility iLAB for Sanger DNA sequencing (Sequencing primers Table 2.8). DNA sequences were analyzed for mutations against the known wild type Top2α coding sequence (NCBI RefSeq[348]) using DNA sequence alignment software (Snapgene[349], APE freeware, or DNASTAR Lasergene 9 'SeqMan'[350]).

Table 2.8 Top2α sequencing primers

Region of Top2α	Primer Name	Primer Sequence (5'-3')
Δ199-386	Alpha-16	TTGTCTCTCCCAACCACACC
	Alpha-18	TTACTGTGGAAACAGCCAGTAGA
	Alpha-20	GCTCTTCTGACCATTAGTGCAAC
	F-199-Xh01-386aa-hTOP2gap	GAGCTTTGGATCAACATGCC
Δ359-756	Alpha-2	GTGAAGTTTAAGGCCCAAGTCCAG
	Alpha-16	TTGTCTCTCCCAACCACACC
	Alpha-1200R	TTTGATAAATTTTTCACTCAATTGGCATG
Δ576-925	Alpha-6	CAAACGGAATGACAAGCGAG
	Alpha-12	CAATCGAGCCAAAGAGCTGAGC
	R681-Pml1-917aa	GTGGTAGTTTGTCCATACAAGTAATCCTC
Δ902-1161	Alpha-7	GTGCTGAAGGAATCGGTACTG
	Alpha-11	CATGTTCTGACGGGAAGCTC
	Alpha-22	TGGTGCTTTTTGACCACGTAG

2.3.10 Overexpression and purification of Top2α in yeast

S. cerevisiae strain JEL1 *top1⁻* was used for protein overexpression and purification. Cell growth and induction of Top2α protein were conducted as described prevously[33]. Transformed JEL1 top1Δ strains were grown in URA- induction media to a cell concentration measured by absorbance at 600nm ~0.7 ODU/mL. 20% Galactose was added to the cell culture (2% final concentration) to induce the yeast to produce Top2α protein, these yeast were incubated at 30°C for 10-14 hours, shaking at 280rpm. After the incubation yeast were harvested using the Beckman Coulter Avanti® J-E high-speed centrifuge, rotor JLA 10.500, 6000RPM for 15min at 4°C, frozen with liquid nitrogen and stored at -80°C. Top2α induced yeast pellets were prepared the same for both Top2α protein purification strategies.

Hydroxyapatite purification. Top2α hydroxyapatite (HAP) (Bio-Rad, 1306-06-5) purification[351]. This strategy utilizes the hydroxyapatite resin, a form of calcium phosphate that can perform a complex mixture of anionic and cationic exchange through its multiple functional groups[352]. Yeast cells were mechanically lysed by glass bead homogenization. Cell debris was pelleted by high-speed centrifuge and nucleic acids were precipitated with 10% Polymin P. Two ammonium sulfate precipitations were performed, first with a 35% precipitation, to eliminate the remaining cell debris and susceptible proteins, then using a 65% precipitation to Top2α from solution. The precipitated Top2α protein was re-suspended in sodium phosphate buffer and loaded on a hydroxyapatite chromatography column to bind and elute Top2 over a potassium phosphate gradient. Fractions containing Top2α were pooled and concentrated with a phosphocellulose (anion exchange) column (Sigma, C3145-100G). Samples were collected throughout the purification and were later assessed to measure efficacy or issues in the protein preparation. The concentrated Top2α protein was eluted in a solution of 40% glycerol (for stability), and then stored as aliquots in liquid nitrogen for later use. Protein concentration was determined using Bradford Reagent (Bio-Rad, 500-0006). The Top2α HAP purification protocol and buffer recipes are included in Appendix B.

Ni-NTA purification. Ni-NTA affinity purification is a well-established purification strategy[353]. The protein carried a 6x His tag was attached to the amino terminus of the Top2α protein (α12URAB) by a peptide linker recognizable by a *Tobacco etched virus* (TEV) protease. After protein purification the 6x His tag was cleaved from the protein[354].

Ni-NTA resins (Thermo Scientific, 88222) are agarose beads coated with nickel.

Yeast cells were mechanically lysed by glass bead homogenization. Cell debris was pelleted by high-speed centrifuge. 6 x His Top2α proteins was permitted to bind to nickel resin by gentle rocking at 4°C for 1 hour. The Top2α protein bound Ni-NTA resin was washed, then eluted with imidazole a histidine-nickel competitive inhibitor (Sigma, I0125). Buffer exchange was accomplished by protein dialysis overnight at 4°C to remove imidazole. Top2α protein was concentrated using centrifugal filter units (Millipore, UFC910024). Protein concentration was determined using Bradford Reagent (Bio-Rad, 500-0006). The Top2α Ni-NTA protocol and buffer recipes are included in Appendix B.

2.3.11 <u>Western blot antibodies and materials</u>

Purified proteins were run on a 7.5% SDS-polyacrylamide gel and transferred to a PVDF membrane (Bio-Rad, 1620177). The gel was stained in a solution of 0.1% Coomassie brilliant blue dye (Bio-Rad, 161-0400), 10% Glacial Acetic acid (Fisher scientific, 64-19-7), 50% methanol (Fisher scientific, 67-56-1) for at least 1 hour at room temperature then destained in water in a microwave for 10-20 minutes. The membranes were immunostained using rabbit anti-yeast Top2 (Topogen, Inc.) or rabbit anti-human Top2α (Bethyl Lab, BL983) followed by incubation with horseradish peroxidase (HRP)-conjugated anti-rabbit secondary antibodies (GE Healthcare, NA934).

2.3.12 <u>Topoisomerase assays</u>

Plasmid relaxation assay. The topoisomerase plasmid relaxation assay has been described previously[312]. This assay was used to measure topoisomerase catalytic activity. Using negatively supercoiled pUC18 plasmid DNA as a substrate, topoisomerases perform DNA strand passage to relax supercoils. Samples contained a reaction mixture

(50mM Tris-HCl, pH-8.0, 100mM KCl, 1mM EDTA, 8mM $MgCl_2$, 2% glycerol, 1mM ATP, 200ng of pUC18), the indicated amount of purified Top2 enzyme and drug of interest. In several experiments these core reaction components were varied to reveal specific differences between the wild type and mutant proteins. Samples were incubated at 37°C for 5 minutes then stopped with10mM EDTA and subjected to electrophoresis on a 1% agarose gel, DNA bands were visualized by UV.

Decatenation assay. The topoisomerase decatenation assay is used to measure type II topoisomerase catalytic activity and has also been described previously[312]. Similar to the plasmid relaxation assay, the reaction samples contained a reaction mixture (50mM Tris-HCl, pH-8.0, 100mM KCl, 1mM EDTA, 8mM $MgCl_2$, 2% glycerol and 1mM ATP), 200ng of Kinetoplast DNA (kDNA) (Topogen inc., TG2013-1), which is a catenated DNA substrate (interlocking rings), along with the indicated amount of purified Top2 enzyme, and the drug of interest. In several experiments these core reaction components were varied to reveal specific differences between the wild type and mutant proteins. Samples were incubated at 37°C for 5 minutes then stopped with10mM EDTA and subjected to electrophoresis on a 1% agarose gel, DNA bands were visualized by UV. The catalytic activity of type II topoisomerases (DNA duplex strand passage) uniquely allows for the separation of the kDNA substrate. Catenated kDNA will not enter the gel during gel electrophoresis while the decatenated kDNA migrates clearly visualizing the level of catalytic activity.

Plasmid cleavage assay. The topoisomerase plasmid cleavage assay is a measure of enzyme mediated DNA cleavage and has been described previously[355–357]. This assay quantifies the amount of DNA cleavage by the purified Top2 protein. Samples contained

a reaction mixture of (50mM Tris-HCl, pH-8.0, 100mM KCl, 1mM EDTA, 8mM $MgCl_2$, 2% glycerol, 1mM ATP, and 200ng of pUC18), the indicated amount of purified Top2 enzyme and drug of interest. In several experiments these core reaction components were varied to reveal specific differences between the wild type and mutant proteins. Samples were incubated at 37°C for 10 minutes then halted with pre-heated 3.3% SDS (Bio-Rad, 161-0302). After the samples were stopped the reaction mixture was treated with proteinase K (Roche, 03115844001) for at least 2 hours at 50°C. Sample DNA was extracted by a phenol, phenol-chloroform, chloroform extraction, precipitated with ethanol then resuspended in a (10mM Tris-HCl, pH 8.0, 10mM EDTA, 10%glycerol) buffer, and analyzed by gel electrophoresis on a 1% agarose gel, DNA bands were visualized by UV.

Quantitation of Top2-mediated DNA cleavage. The DNA bands observed in plasmid cleavage assays were quantitated using the GelDoc-It imaging system (UVP. Upland, Ca). Band intensity was measured for the nicked circular and linear DNA bands. Normalized levels of DNA cleavage (ng) were calculated based on the relative intensity of nicked circular and linear DNA bands to total intensity of the DNA sample. The advantage of this approach was its ability to control for variability of DNA intensity between agarose gels. However, there were limitations to this approach for quantitation of DNA cleavage. By assessing the relative intensity of specific bands compared to overall sample intensity, quantitation could be biased by incomplete or non-uniform ethidium bromide staining or impurities in agarose gel and limits the ability to use linear DNA controls. Previous versions of this assay used radioactive labeled DNA, for which quantitation was more sensitive but potentially more time consuming and hazardous.

ATP hydrolysis Assay. The topoisomerase coupled ATP hydrolysis assay has been described previously[183,358]. This assay couples the ATP hydrolyzed by the Top2 catalytic reaction to NADH absorbance. Samples contained a reaction mixture of (50mM Tris-HCl, pH-8.0, 100mM KCl, 1mM EDTA, 8mM $MgCl_2$, 2% glycerol, 200mM Phosphoenolpyruvate, 5U/mL Pyruvate Kinase, 8U/mL Lactate Dehydrogenase, 16mM NADH, 50nM purified Top2 dimer), the indicated amount of ATP and sonicated salmon sperm DNA as indicated. Salmon sperm DNA (ssDNA) (Sigma Aldrich) was prepared by dissolving in TE buffer (10mM Tris-HCl, pH-8.0, 1mM EDTA). The ssDNA was then sonicated to shear the DNA to an average size of~4kb, extracted by a phenol, phenol-chloroform, chloroform extraction, precipitated with ethanol then resuspended in TE. 100μl reactions were loaded in duplicate into a 96-well plate (Costar, 3635) and 340nm absorbance was measured for 20minutes at 37°C. The change in absorbance was calculated by a least-squares fit of the data and used to determine the rate of ATP hydrolysis (μmol ATP $\cdot$ min^{-1} $\cdot$ nmol Top2^{-1})[247].

2.4   Results

We set out to explore the molecular details of Topoisomerase II poisoning with etoposide by performing a genetic screen for drug-sensitive variants of Top2α. This screen was designed in part as a class project for the spring 2015 MBT530 class for which I served as a teaching assistant. In this role I helped with the screen design and execution; the students, however, carried out the screen itself.

The etoposide sensitivity screen was carried out in the *Saccharomyces cerevisiae* strain JN332a$_{t2-4}$[311]. This yeast strain carries a temperature sensitive allele of yTop2 (T$_{2-4}$) and is deleted for the *RAD52* gene, essential for DNA double strand break repair by

homologous recombination. Top2α expression in yeast can complement for ytop2 deficiency at the non-permissive temperature for the *top2-4* allele, 34°C. The JN332a$_{t2-4}$ yeast strain also carried an inducible plasmid (pGal1RAD52) where expression RAD52 protein is under the control of the Gal1 promoter[314]. Thus, this strain is proficient for homologous recombination when grown on galactose, but deficient when grown in glucose.

2.4.1 <u>Selection of mutations in Top2α that confer hypersensitivity to etoposide</u>

Our screen targeted 4 discrete regions of the Top2α gene for mutagenesis (amino acids 199-386, 359-756, 576-925,902-1161) with error prone PCR (Figure 2.1). With these regions our screen aimed to effectively cover the entire Top2α gene (amino acids 199-1161) except the extreme amino and carboxyl termini. We used PCR conditions to generate approximately 1 base substitution in the target sequence. The PCR products were gel isolated and co-transformed with linear plasmid backbone DNA deleted for the amplified gene segment into JN332a$_{t2-4}$ at 34°C. Selection for the transformed JN332a$_{t2-4}$ yeast at 34°C selected for Top2α alleles that complement a deficiency of yTop2[319].

We used this strategy to generate a library of yeast expressing functional mutants of Top2α (Figure 2.1). ~20,000 JN332a$_{t2-4}$ individual yeast colonies were picked and patched to agar plates containing SC-URA$^-$, Leu$^-$, Galactose along with JN332a$_{t2-4}$ yeast carrying pMJ1 wild type and Ser763Trp as positive and negative controls, respectively. These patched yeast 'master' plates were grown for 2-4 days then replica plated to agar SC-URA$^-$ plates containing either etoposide (10µg/mL), no drug or SC-URA$^-$, Leu$^-$, Galactose. Sensitivity to growth under these conditions was assessed after 24-48hours. Yeast isolates that did not grow on etoposide (10µg/mL) agar plates were identified,

those that demonstrated greater sensitivity to etoposide than those expressing wild type

Top2α were analyzed further for etoposide sensitivity using clonogenic survival.

Figure 2.1 Etoposide hypersensitive screen design
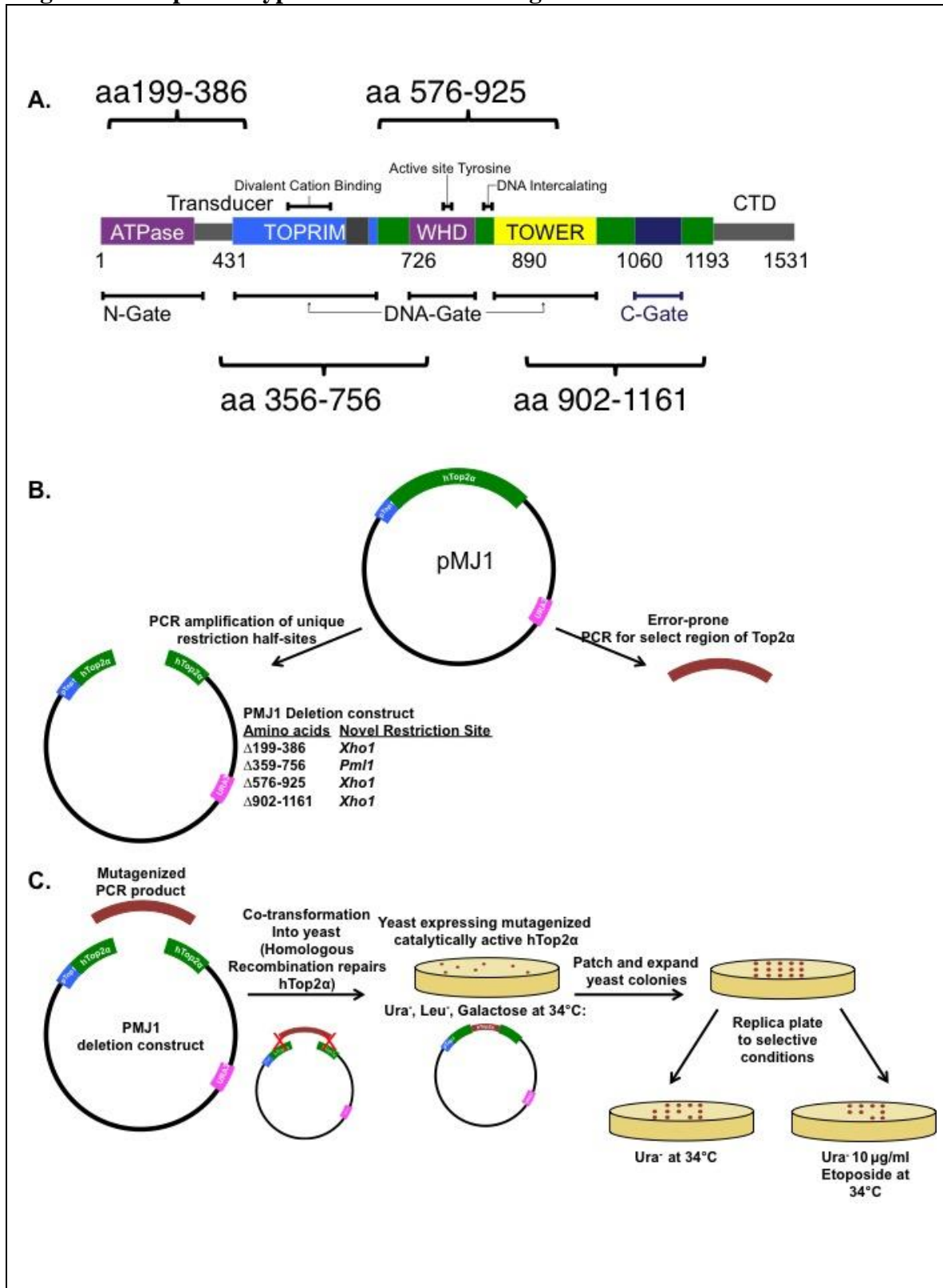
Figure 2.1 Top2α mutagenesis screen for etoposide hypersensitive alleles
A. This figure is from Wendorff TJ, et al., *J Mol Biology*, 2012[72], highlighting the regions of the Top2α coding sequence that were targeted for mutagenesis in this screen. **B.** pMJ1 plasmid DNA was PCR amplified using primers to create an internal deletion of the Top2α gene targeting DNA that would when ligated form a novel restriction site. Selected Regions of the Top2α gene were amplified with error-prone PCR to generate a mutagenized insert carrying ~1 mutation per fragment. **C.** pMJ1 deletion construct and mutagenized insert DNA were co-transformed into JN332aT$_{2-4}$ pGal1:RAD52 at 34°C. Transformed yeast colonies were patched and screened for sensitivity to etoposide by replica-plating to SC-URA$^-$ media plates supplemented with 10µg of etoposide/ml.

Elsevier has licensed me to reuse this figure 2.1 A in my thesis in print and electronic formats. Elsevier, License # 4595461272332

2.4.2   Etoposide hypersensitive yeast carrying Top2α

Our screen identified ~311 yeast isolates that were not able to grow on 10μg etoposide/mL agar plates. These isolates were potentially hypersensitive to etoposide as yeast carrying wild type Top2α were able to grow under these conditions. 251/260 (~97%) of these isolates demonstrated greater sensitivity to etoposide compared to wild type Top2α using the spot test assay (Figure2.2 A and B).

To accurately describe and compare the sensitivity of these yeast isolates to etoposide, we carried out yeast colony formation assays and determined the etoposide minimum lethal concentration (MLC). The etoposide MLC was the concentration of etoposide at which exposure to etoposide killed yeast cells (Relative Survival <100%). JN332a$_{t2-4}$ yeast expressing wild type Top2α exhibits an MLC of 100μg etoposide/mL. The results of the mutagenesis screen are summarized Table 2.9.

We performed the yeast colony formation assay with 209 of the yeast isolates from the screen (42 isolates were set aside as they either grew poorly or were potentially a clone of another colony being assessed). 186 yeast isolates exhibited greater sensitivity than yeast expressing wild type Top2α at 20μg etoposide/mL (Appendix C). We carried out the colony formation assay at least once for each of the 209 yeast isolates, we verified etoposide sensitivity in the 5 most etoposide sensitive isolates with a second colony formation assay and observed similar levels of sensitivity (MLC<5μg etoposide/mL).

We found 140 yeast isolates had an MLC ≤20μg etoposide/mL and determined that these isolates were hypersensitive to etoposide as the MLC of yeast carrying the wild type enzyme is 100μg etoposide/mL. Yeast isolates identified by the screen exhibited high levels of sensitivity to etoposide compared the wild type enzyme or Ser763Trp

71

(Figure 2.3 A). Our screen was very successful in identifying Top2α mutant alleles that confer high levels of sensitivity to etoposide therefore we decided to group the based on the level of hypersensitivity (Table 2.10). There were 19 yeast isolates that exhibited an MLC ≤5µg etoposide/mL, 48 yeast isolates that exhibited an MLC ≤10µg etoposide/mL, and 92 yeast isolates with an MLC ≤20µg etoposide/mL. We limited the number of yeast isolates listed in Table 2.10 to the 59 independently derived isolates with ≤20% relative survival at 20µg etoposide/mL as these were the most sensitive of those identified.

Table 2.9 Etoposide hypersensitive screen

Mutagenized Region of Top2α	Etoposide Sensitive Yeast Isolates	Etoposide MLC after 24 hour exposure		
		5µg etoposide /mL	10µg etoposide /mL	20µg etoposide /mL
Δ199-386	109	1	3	32
Δ359-756	78	14	13	15
Δ576-925	36	3	8	6
Δ902-1161	84	1	5	39

Figure 2.2 Representative spot test assays
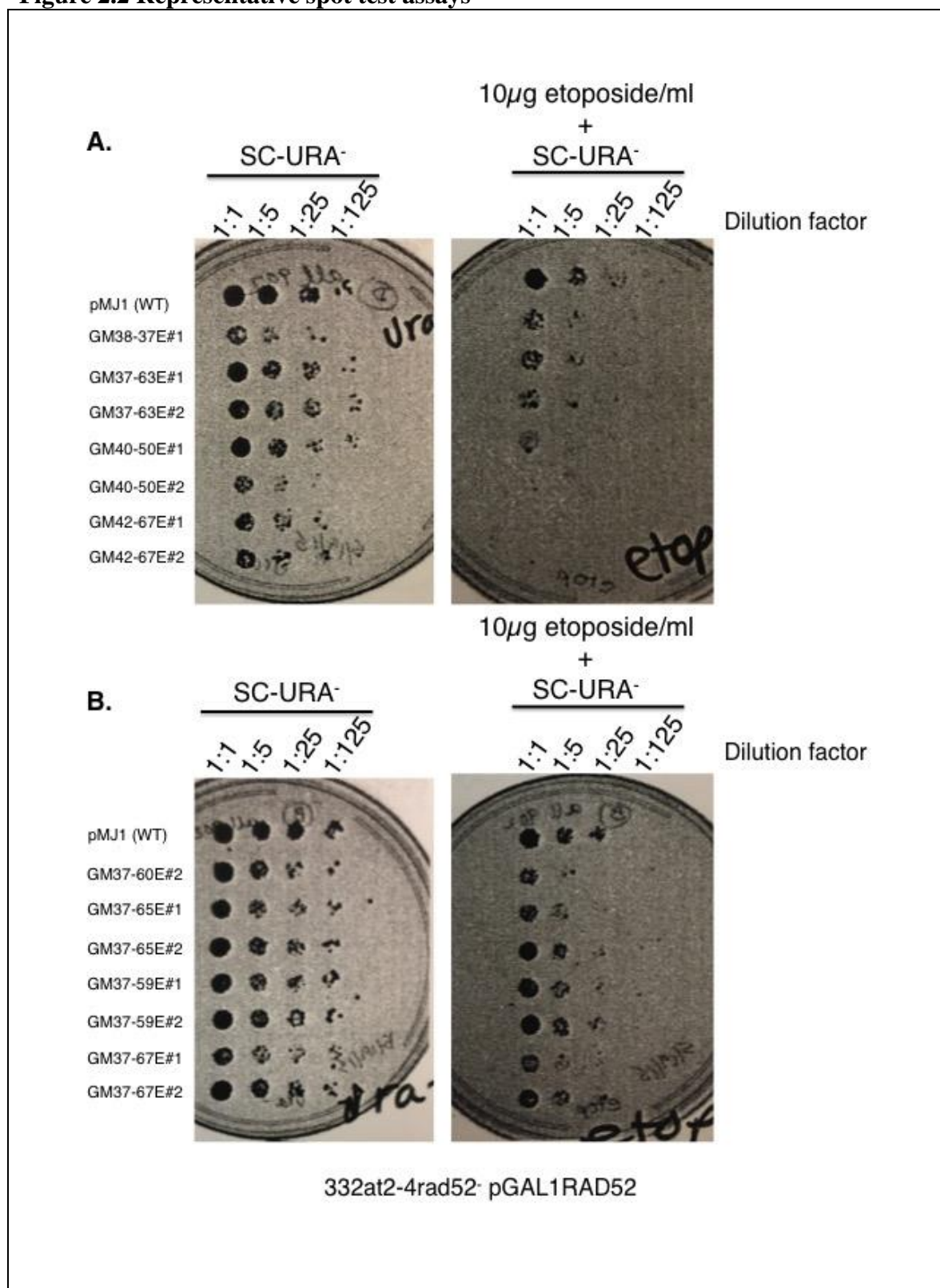
Figure 2.2 Yeast spot tests evaluated JN332a$_{t2-4}$ growth. 2µl of 1: 5 serial dilutions of $2x10^6$ yeast culture were spotted onto SC-URA⁻ plates containing either DMSO or etoposide (10µg etoposide/mL /mL). JN332a$_{t2-4}$ yeast were carrying pGAL1RAD52 and pMJ1 (Top2α: wild type or randomly mutagenized). Unique screen isolate identifier label is to the left of the plate image. **A.** Yeast growth was compared to wild type on SC-URA⁻ (DMSO or 10µg etoposide/mL). In this experiment all yeast isolates demonstrated growth sensitivity compared to wild type on the etoposide containing plate. However, yeast isolates GM38-37E#1 and GM40-50E#2 exhibited relatively poor growth on both plates potentially suggesting a weaker sensitivity to etoposide. **B.** Yeast growth was compared to wild type on SC-URA⁻ (DMSO or 10µg etoposide/mL). In this experiment the yeast isolates GM37-60E#2 and GM37-67E#1 exhibited growth sensitivity compared to wild type on the etoposide containing plate. Dr. Karin Nitiss performed these experiments.

2.4.3   Etoposide hypersensitive Top2α mutations

The genetic screen in Top2α to isolate etoposide sensitive allele identified 86 mutations Top2α that sensitize yeast to etoposide. Etoposide sensitizing mutations were found throughout the mutagenized regions Top2α. Many of the isolates identified carried single base alteration to the Top2α coding sequence. However, some were identified that carried multiple mutations (Table 2.10). This result was expected given the Gaussian distribution of mutations expected from the error-prone PCR. The yeast strain used by the screen could potentially have picked up intrinsic alterations that increased sensitivity to etoposide (such as reverting to yTop2 wild type from *top2-4*)[198]. Therefore, we verified the etoposide sensitivity conferred by mutations carried by three of the etoposide sensitive yeast isolates identified initially (A330Val Asp374Gly, Asn258Asp Ala350Gly, and Lys207Glu Met228Ile). The mutations were reconstructed by *in vivo* recombination in the parental plasmid (pMJ1) and transformed into fresh JN332a$_{t2-4}$ yeast, then analyzed etoposide sensitivity. Yeast carrying the remade plasmids exhibited similar levels of etoposide sensitivity as those isolated by the screen.

The most sensitive yeast isolate identified (~50-fold more sensitive than wild type) carried a Asn433Lys mutation in Top2α. The Asn433 amino acid residue is located near to the transducer and TOPRIM domains but is disordered on available crystal structures and is not conserved in yTop2. Many of the most sensitive yeast isolates carried Top2α mutations between amino acids 359-756. Several of the most sensitive yeast isolates (MLC carried Top2α amino acid substitutions, which were identified in multiple independently derived yeast isolates (Val364, Asp442, Val415, Asn445, Lys466,

Asp479, Gly852, Met502, Glu1109, Val470, and Thr377). Many of which were the same changes however several were different substitutions.

In three of the yeast isolates listed in Table 2.10 we were unable to recover a mutation in the Top2α mutagenized region. For these isolates we sequenced the Top2α coding sequence and were unable to find any mutations. These isolates have been set aside. We plan to recover the pMJ1 plasmid from these isolates and transform into a fresh yeast strain to determine if the elevated sensitivity to etoposide is due to other alterations on the pMJ1 plasmid.

Table 2.10 Etoposide hypersensitive Top2α mutations

Yeast Isolate #	Mutated Region	Mutated Amino Acids	Yeast Relative Survival (%) Etoposide Concentration (µg/mL)			
			0	5	10	20
pMJ1	WT	Wild type	550	510	450	480
3683	Δ359-756	N433K	320	5.0	2.7	0.60
3689	Δ359-756	V364I*, D442Y*	900	21	2.5	1.0
3641	Δ359-756	E506G	700	28	2.3	1.0
3691	Δ359-756	V415A*	770	30	10	7.9
3512	Δ359-756	N445D*	1500	40	2.7	1.1
3685	Δ359-756	D479Y*	330	56	12	1.2
3491	Δ359-756	V470L*, H498Y, G437E	380	60	11	2.5
3498	Δ359-756	D479Y*	660	65	4.4	0.50
3346	Δ359-756	D463N, K466I*	440	68	5.9	0.84
3694	Δ359-756	T377R*	180	76	32	5.9
3475	Δ199-386	Q355H	670	82	30	13
3639	Δ359-756	D442G*, I490V	400	84	26	1.2
3477	Δ359-756	V415L*	600	89	40	8.8
3653	Δ576-925	V742L, E839K	440	91	20	2.6
3655	Δ576-925	Y640H, G760S	2600	92	15	2.9
3660	Δ576-925	N866K	430	92	32	8.7
3643	Δ359-756	T372N, D442Y*, A469T, E523V	180	96	30	8.9
3518	Δ902-1161	No mutations found in coding sequence	230	100	66	16
3487	Δ359-756	D280E, E281K	660	100	66	10

Yeast isolates identified with etoposide sensitivity at 10µg etoposide/mL

Yeast Isolate #	Mutated Region	Mutated Amino Acids	Yeast Relative Survival (%) Etoposide Concentration (µg/mL)			
			0	5	10	20
pMJ1	WT	Wild type	550	510	450	480
3671	Δ576-925	A652V, G852S*, K936N	750	110	16	1.7
3390	Δ902-1161	Y960C, K1161E	640	180	25	2.6
3479	Δ359-756	D442G*	560	110	27	1.1
3481	Δ359-756	M502L*	680	160	34	6.9
3687	Δ359-756	E503G, M539V	260	110	40	3.8
3662	Δ576-925	R736G, G852C*	690	150	41	1.4
3344	Δ359-756	K466R*	130	110	41	3.0
3480	Δ359-756	M502L*, S224F	400	140	43	4.7
3350	Δ359-756	D442N*	330	140	43	21
3530	Δ902-1161	E1109K*	330	120	46	20
3681	Δ359-756	N445I*	290	160	50	18
3698	Δ576-925	K622E	580	150	53	9.2
3665	Δ576-925	T792A, F818Y	520	170	54	3.5
3348	Δ359-756	V470A*	1600	270	54	4.4
3338	Δ199-386	No mutations found in coding sequence	820	220	60	20
3632	Δ359-756	H432R	580	260	60	12
3646	Δ576-925	F790S, T858I	560	170	63	13
3502	Δ359-756	D479Y*	1100	220	65	14
3669	Δ576-925	P576L, A814V	790	340	66	10
3489	Δ359-756	V470G*	310	140	68	52
3529	Δ902-1161	K1070E*, D1170N	330	140	77	26
3651	Δ576-925	E623K, V751A	410	180	79	34
3391	Δ902-1161	A1052G	4300	870	80	26
3431	Δ199-386	T377I*	850	200	87	18
3486	Δ359-756	D374E*, S387G	420	210	92	20

3401	Δ199-386	K278M, T377I*	290	180	94	30
3695	Δ576-925	T694I, Y612C	740	230	94	19
3534	Δ902-1161	A1043D	340	180	95	17
3341	Δ359-756	A444T	800	240	97	22

**Yeast isolates identified with strong etoposide sensitivity
at 20µg etoposide/mL**

Yeast Isolate #	Mutated Region	Mutated Amino Acids	Yeast Relative Survival (%) Etoposide Concentration (µg/mL)			
			0	5	10	20
pMJ1	WT	Wild type	550	510	450	480
3462	Δ199-386	L275M	570	230	110	8.0
3541	Δ902-1161	E1109K*	2000	240	130	9.0
3540	Δ902-1161	L1025V	1300	430	110	9.7
3496	Δ902-1161	D956Y	1100	230	120	10
3470	Δ359-756	V364I*, S471P	680	210	110	10
3471	Δ359-756	V364I*	720	230	110	13
3396	Δ902-1161	No Mutations found in coding sequence	780	250	120	16
3523	Δ902-1161	E1109K*	1100	420	130	16
3436	Δ902-1161	K1070E*	1100	510	210	17.6
3322	Δ199-386	A330V, D374G*	670	270	120	18
3537	Δ902-1161	S891G	960	290	180	18

Table 2.10 Etoposide hypersensitive yeast isolates**.** The sensitivity of independently derived yeast isolates determined with a yeast clonogenic survival assay. The hypersensitive yeast isolates were divided into three categories based on their sensitivity to etoposide (relative survival: ≤ 100% at 5µg etoposide/mL, ≤ 100% at 10µg etoposide/mL, and ≤ 20% at 20µg etoposide/mL. The difference in relative survival between isolates at the bottom of one category and the top of the next are minimal. *Mutated amino acid residues identified in multiple independently derived yeast isolates

2.4.4 Top2α mutations cross-sensitive to mAMSA

Top2 targeting agents represent several chemical scaffolds we were interested to determine if the hypersensitivity exhibited by the yeast isolates identified here was specific for etoposide. Yeast carrying Top2α are sensitive to intercalating agents like mAMSA[314]. To test the specificity of etoposide hypersensitive Top2α mutations we selected the 15 most etoposide sensitive yeast isolates carrying single mutations and assessed for mAMSA sensitivity with the colony formation assay (Figure 2.3 B).

Nearly all of the yeast isolates exhibited elevated levels of sensitivity to mAMSA with an MLC 2-fold lower than yeast carrying the wild type enzyme (Figure 2.3 C). One of the Top2α mutant alleles (Glu506Gly) exhibited mAMSA sensitivity similar to yeast expressing the wild type enzyme (Figure 2.3 B). This suggested that the etoposide hypersensitivity conferred by this mutant allele was specific to etoposide. Etoposide and mAMSA are suggested to share a binding pocket even though they represent different chemical scaffolds, cross-sensitivity observed in many of these alleles might suggest that the Top2α mutations do not function by altering drug binding. The Top2α Asp479Tyr and Asn433Lys mutant alleles demonstrated the higher levels of sensitivity to mAMSA with 40-fold and 20–fold greater sensitivity than yeast carrying the wild type enzyme, respectively.

Figure 2.3 Yeast screen isolate Top2 poison sensitivity

A. Etoposide sensitivity of yeast screen isolates
Wild Type MLC: 100µg etoposide/ml

B. mAMSA sensitivity of yeast screen isolates
Wild Type MLC: 2µg mAMSA/ml
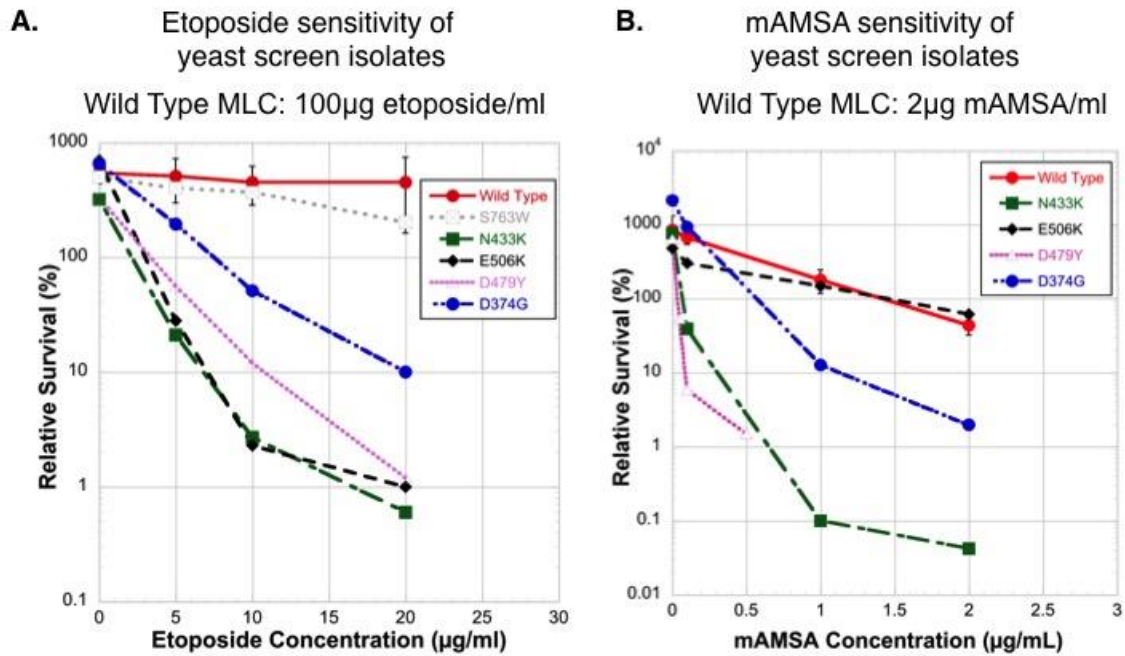
C. Etoposide Sensitive Yeast Screen Isolates Tested for mAMSA sensitivity

Top2α Mutation	Fold Change in etoposide MLC	Fold Change in mAMSA MLC
N433K	20	20
D479Y	~10-20	40
Q355H	20	2
V364I, D442Y	20	2
V415L	20	2
E506G	20	1
N866K	20	2
T377R	10	2
D442G	10	2
D442N	10	2
M502L	10	2
A1043D	10	2
A1052G	10	2
E1109K	~5-10	2
D374G	5	2

Figure 2.3 Yeast isolates identified by the etoposide hypersensitivity screen exhibited high levels of sensitivity to etoposide. Cell viability determined by the yeast colony formation assay in JN332a T$_{2-4}$ cells carrying pMJ1 after 24-hour exposure to increasing concentrations of **A.** Etoposide (0 (DMSO), 5, 10, or 20 µg etoposide/mL) **B.** mAMSA (0 (DMSO), 0.1, 1, or 2 µg mAMSA/mL). The yeast isolate carrying Asp479Tyr mutation was instead exposed to lower mAMSA concentrations (0 (DMSO), 0.05, 0.1, or 0.5 µg mAMSA/mL) to more accurately characterize the sensitivity. **C.** Table of yeast isolates tested for sensitivity to mAMSA, their minimum lethal concentration (MLC) relative to JN332a T$_{2-4}$ yeast carrying pMJ1 wild type for etoposide and mAMSA.

2.4.5   Etoposide hypersensitive mutation clusters

We mapped the Top2α amino acids identified in the etoposide sensitivity screen onto the available Top2α crystal structures (Figure2.4)[159,178]. We mapped amino acid substitutions (1-426) primarily onto structure 1ZXN of the ATPase domain bound to ADP as it had more amino acid residues solved than 1ZXM, ATPase domain bound to AMP-PNP[159]. We mapped amino acid substitutions (436-1187) primarily onto structure 5GWK of the breakage reunion domain in complex with DNA and etoposide[178]. While we initially used the 4FM9 structure we now use the 5GWK structure as it was in complex with etoposide. The 4FM9 structure differs as it shows the C-gate dimerization interface as dissociated[72].

We observed several discrete clusters of etoposide hypersensitive Top2α mutations in the Top2α protein (Figure 2.4 A). We defined the clusters as a group of 5 or more amino acid substitutions identified by the screen within 25Å. The C1 cluster (Asn370, Thr372, Asp374, Ser375 and Thr377) is located in the ATPase/Transducer domains at the N-Terminal dimerization interface and has a diameter of ~21.9Å (Figure 2.4 B). The C2 cluster (Ala330, Val334, Val338, Asp339, Ala353, Gln355, Val356, Val415) is located in the Transducer domain near the junction leading into the DNA breakage/reunion core of the enzyme, this cluster is ~20-23Å in diameter and is comprised of a barrel of 3 alpha helices (Figure 2.4 C). The C3 cluster (Asp442, Asn445, Asp463, Lys466, Ala469, Val470, Ser471, Val476, Asp479, Met539, Lys622, Glu623, Phe628, Phe790, Thr792, Lys936, Tyr960) is located at a protein dimerization interface within the DNA breakage/reunion core and is comprised of both beta sheets and alpha helices and has a diameter of ~27.8Å (Figure 2.4 D). Numerous etoposide sensitizing

mutations were identified in the coil-coil and C-gate of Top2α but these did not appear to form defined clusters.

Figure 2.4 Etoposide sensitizing amino acid clusters on Top2α crystal structures
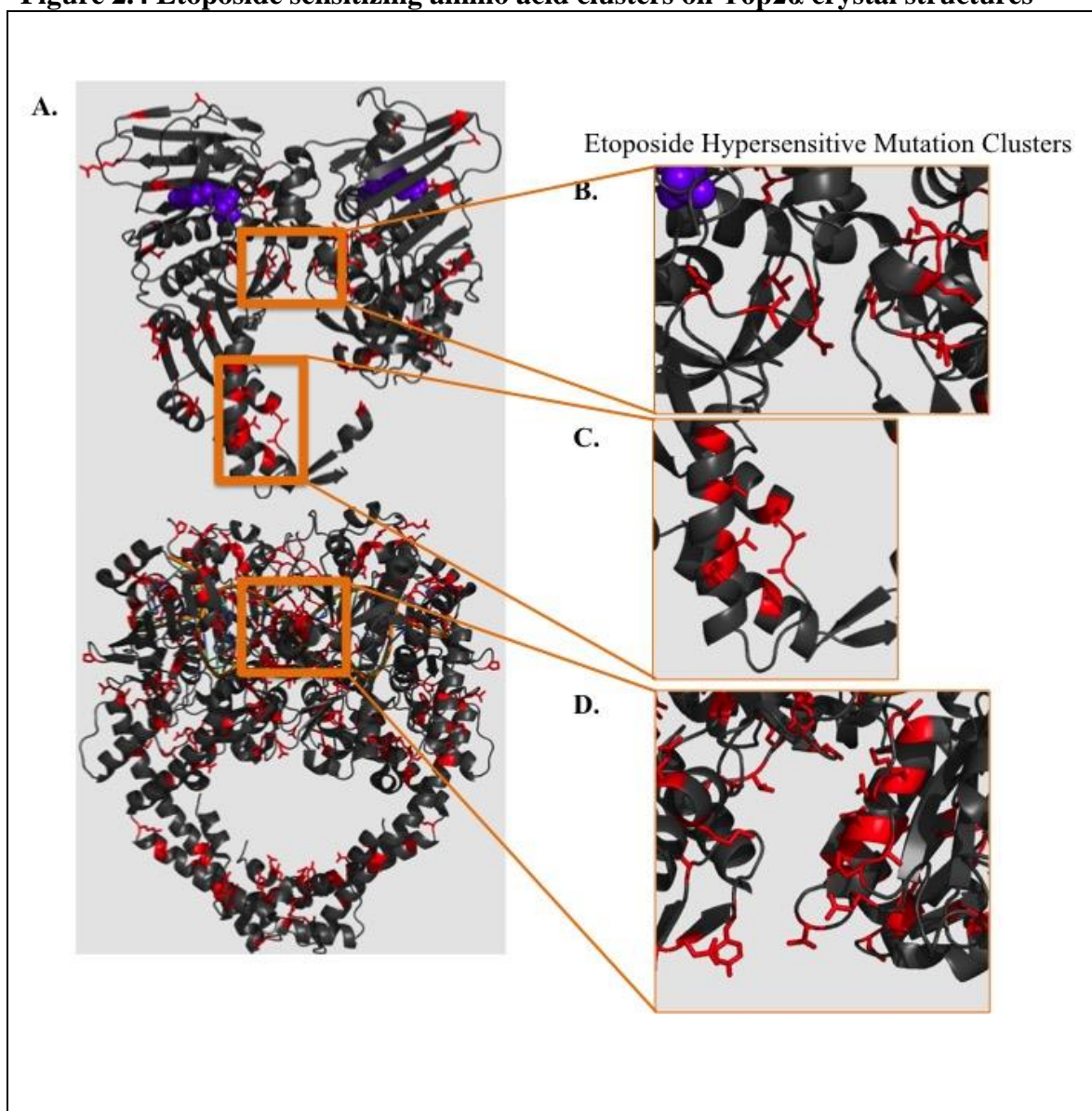
Figure 2.4 Amino acid residues identified by the etoposide sensitivity screen Top2α crystal structures. **A. Top:** Top2α ATPase domain crystal structure (1ZXN) in complex with ADP (Purple) with screen identified amino acid residues highlighted (red)[159], **Bottom:** Top2α DNA Breakage/Reunion domain in complex with DNA and etoposide (5GWK) with screen identified amino acid residues highlighted (red)[178]. **B.** Mutation Cluster C1, diameter: ~21.9Å. Highlighted amino acids: Asn370, Thr372, Asp374, Ser375 and Thr377 **C.** Mutation Cluster C2, diameter: ~20-23Å. Highlighted amino acids: Ala330, Val334, Val338, Asp339, Ala353, Gln355, Val356, Val415 **D.** Mutation Cluster C3, ~27.8Å. Highlighted amino acids: Asp442, Asn445, Asp463, Lys466, Ala469, Val470, Ser471, Val476, Asp479, Met539, Lys622, Glu623, Phe628, Phe790, Thr792, Lys936, Tyr960.

2.4.6 **Selection of mutant proteins for characterization**

To examine the Top2α biochemical properties associated with etoposide hypersensitivity we elected to purify and biochemically characterize several of the Top2α mutant proteins. We chose to start with the mutants that conferred the greatest etoposide sensitivity. We restricted our analysis to mutants that carried a single amino acid substitution because an analysis of multiple mutations would require the dissection of individual mutation contributions to biochemical properties.

We selected Leu275Met, Gln355His, Asp374Gly, Thr377Ile, Val415Leu and Asn445Asp Top2α mutant proteins for characterization (Figure 2.5). While not a parameter considered for selection, several of the mutations selected were among the amino acid residues that were identified as the mutation clusters identified earlier (Figure 2.4). The C1 mutation cluster included Asp374Gly and Thr377Ile, mutation cluster C2 included Gln355His and Val415Leu, and Cluster C3 included Asn445Asp.

Figure 2.5 Top2α mutations selected for biochemical characterization
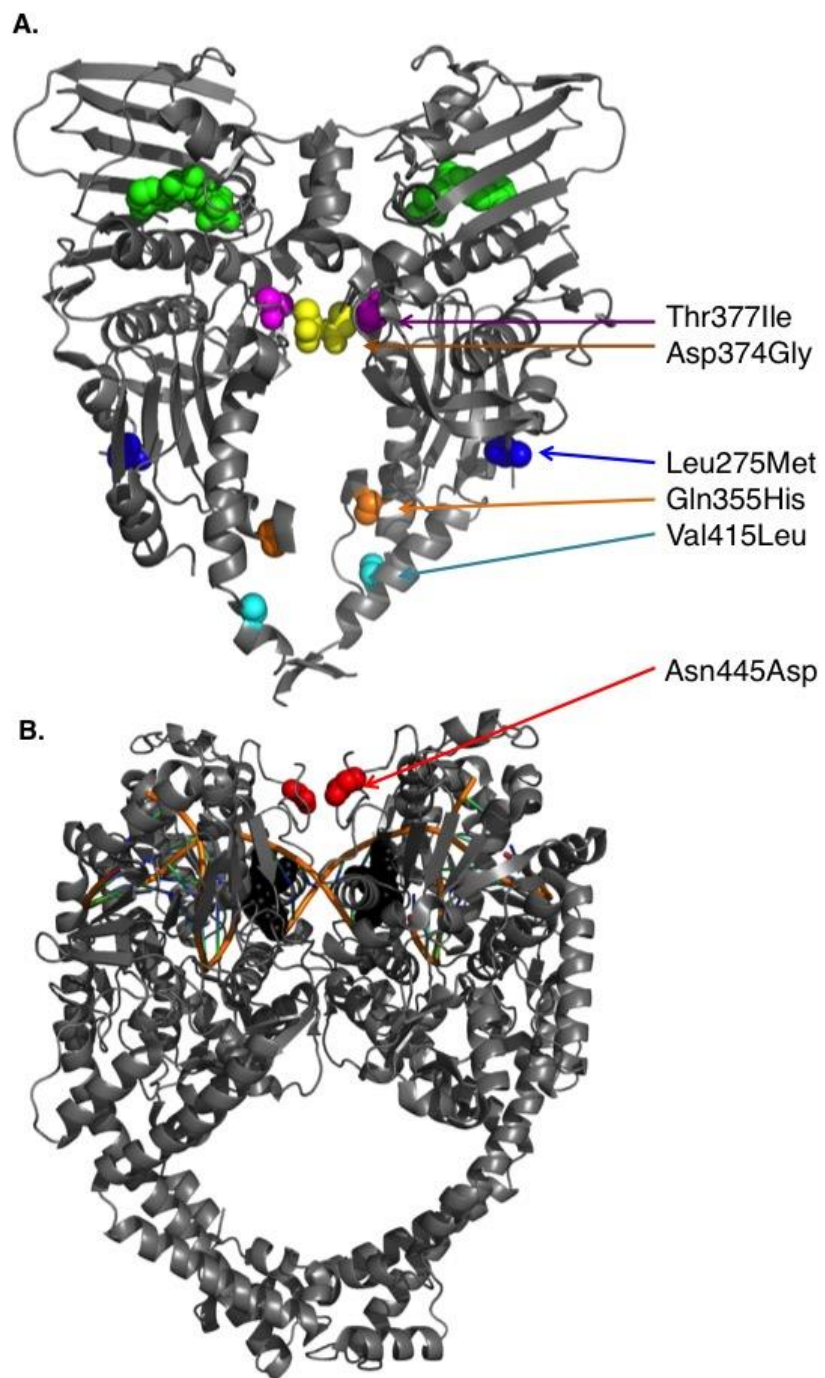
Figure 2.5 The location of amino acid residues selected for biochemical analysis. **A.** Top2α ATPase domain crystal structure (1ZXN) in complex with ADP (green) with screen identified amino acid residues highlighted (Thr377 (pink), Asp374 (yellow), Leu275 (blue), Gln355 (orange), Val415 (cyan)[159]. **B.** Top2α DNA Breakage/Reunion domain in complex with DNA and etoposide (5GWK) with screen identified amino acid residues highlighted (Asn445 (red))[178].

2.4.7 <u>Biochemical characterization of etoposide hypersensitive proteins</u>

To study the biochemical characteristics of the Top2α mutant proteins, we introduced the mutations into Top2α inducible expression plasmids pCM1 or α12URAB and overexpressed the Top2α mutant proteins in yeast strain JEL1t1. The mutant proteins were purified using hydroxyapatite or nickel affinity chromatography. Figure 2.6 shows representative Top2α mutant protein purification results from yeast on 7.5%SDS-PAGE Coomassie stained acrylamide gels.

Figure 2.6 Top2α Mutant protein purification and validation
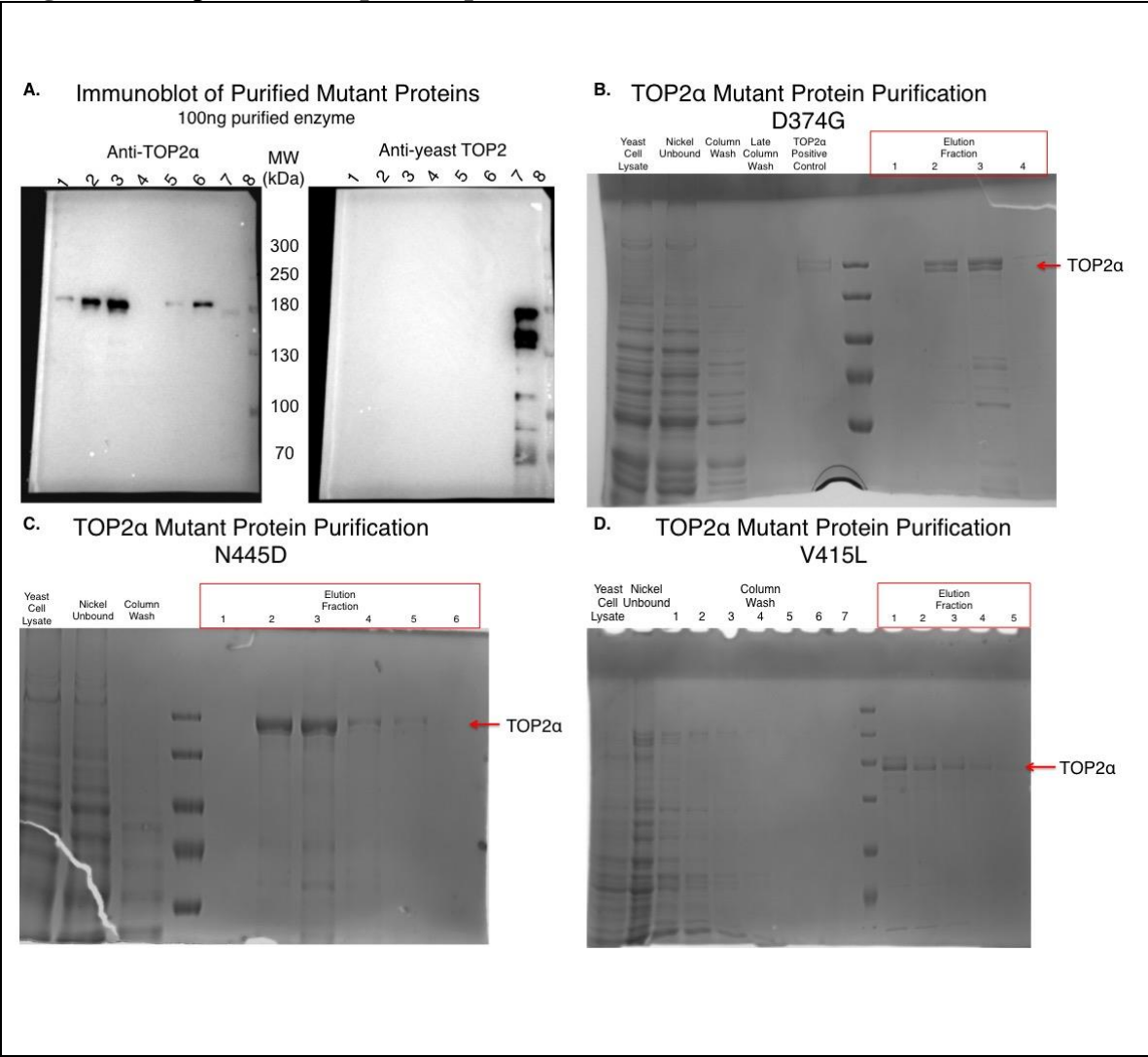
Figure 2.6 Top2α mutant protein purification and validation. The results of Top2α mutant protein purification from yeast strain JELt1 and immunoblot analysis for yeast Top2. The Top2α protein monomer is 170kDa and the yeast Top2 protein monomer is 160kDa **A.** Immunoblot analysis of purified mutant proteins for yeast Top2 contamination 100ng of each purified protein was loaded in to each well as determined by Bradford assay quantitation. Lanes: 1, Hydroxyapatite chromatography purified Top2α Asp48Asn mutant protein (purified in 2002). 2, Hydroxyapatite chromatography purified Top2α Asp374Gly mutant protein. 3, Hydroxyapatite chromatography purified Top2α wild type protein. 4, Nickel affinity chromatography purified Top2β His63Tyr mutant protein. 5, Nickel affinity chromatography purified Top2α Asp374Gly mutant protein. 6, Nickel affinity chromatography purified Top2α wild type protein. 7, Hydroxyapatite chromatography purified yeast Top2 wild type protein (purified in 2000). 8, Spectra multicolor high range protein ladder. **B.** 6xHis-TEV-Top2α Asp374Gly was overexpressed in yeast strain JELt1. Two fractions were obtained, and were proteolyzed with Tobacco Etched Virus (TEV) protease to remove the 6xHis tag then concentrated using millipore centricon 100,000 MWCO. **C.** 6xHis-TEV-Top2α Asn445Asp was overexpressed in yeast strain JELt1. Two fractions were obtained, and were proteolyzed with TEV protease to remove the 6xHis tag then concentrated using millipore centricon 100,000 MWCO. **D.** 6xHis-TEV-Top2α Val415Leu was overexpressed in yeast strain JELt1. Two fractions were obtained, and were proteolyzed with TEV protease to remove the 6xHis tag then concentrated using millipore centricon 100,000 MWCO.

2.4.8   Relaxation activity of purified mutant proteins

We first measured topoisomerase activity by assessing relaxation of negatively supercoiled plasmid DNA. In an agarose gel a negatively supercoiled plasmid will migrate more quickly during electrophoresis than relaxed DNA as it is more compact in shape[359]. Under a standard set of conditions the strand passage activity of the mutant proteins was measured and compared to wild type enzyme using the plasmid relaxation assay (Figure 2.7)[359]. The Asp374Gly mutant protein exhibited similar relaxation activity as the wild type enzyme (Figure2.7 A). Asp374Gly completely relaxed 200ng of negatively supercoiled (pUC18) plasmid DNA with 13ng of protein (within 1-2fold of wild type). The Thr377Ile mutant protein exhibited similar relaxation activity as the wild type enzyme (Figure2.7 B). Thr377Ile completely relaxed the supercoiled DNA substrate with 13ng of protein (within 1-2fold of wild type). The Gln355His mutant protein exhibited similar relaxation activity as the wild type enzyme (Figure2.7 C). Gln355His completely relaxed the supercoiled DNA substrate with 25ng of protein (within 1-2fold of wild type).

The Val415Leu mutant protein exhibited reduced levels of relaxation activity compared to wild type enzyme (Figure 2. 7 D). Val415Leu completely relaxed the supercoiled DNA substrate with 400ng of protein (4 fold less than wild type). The Asn445Asp mutant protein demonstrated reduced levels of relaxation activity compared to wild type enzyme (Figure 2. 7 E). Asn445Asp completely relaxed the supercoiled DNA substrate with 400ng of protein (8 fold less than wild type). The Asn445Asp relaxation activity results are based on two independent purifications suggesting that the reduced relaxation activity is not an artifact of the protein purification process. The

reduced relaxation activity of Val415Leu was based on a single purification, and loss of activity may have occurred during the purification process, additional purifications could be used to verify this finding.

To probe the reduced topoisomerase activity of Asn445Asp further we carried out a time-course plasmid relaxation assay. In this experiment we used a set concentration of enzyme and 200ng of supercoiled plasmid DNA, topoisomerase reactions were stopped at various time points with EDTA as before. Incomplete relaxation activity was seen with 100ng of the Asn445Asp mutant protein after 1 hour (Figure 2.7 F). These results may suggest that either a small population of the purified mutant protein remains active or that this mutant shows slow topoisomerase activity.

The time-course relaxation assay with Asn445Asp was carried out twice. All other assays were carried out at least three times. The differences in wild type relaxation activity between the assays shown in (Figure 2.7 A, C-D) were likely due to inter-experiment variability. The relaxation activity of these mutant proteins did not exhibit changes to catalytic activity after storage in liquid nitrogen.

Figure 2.7 Relaxation activity of purified mutant proteins
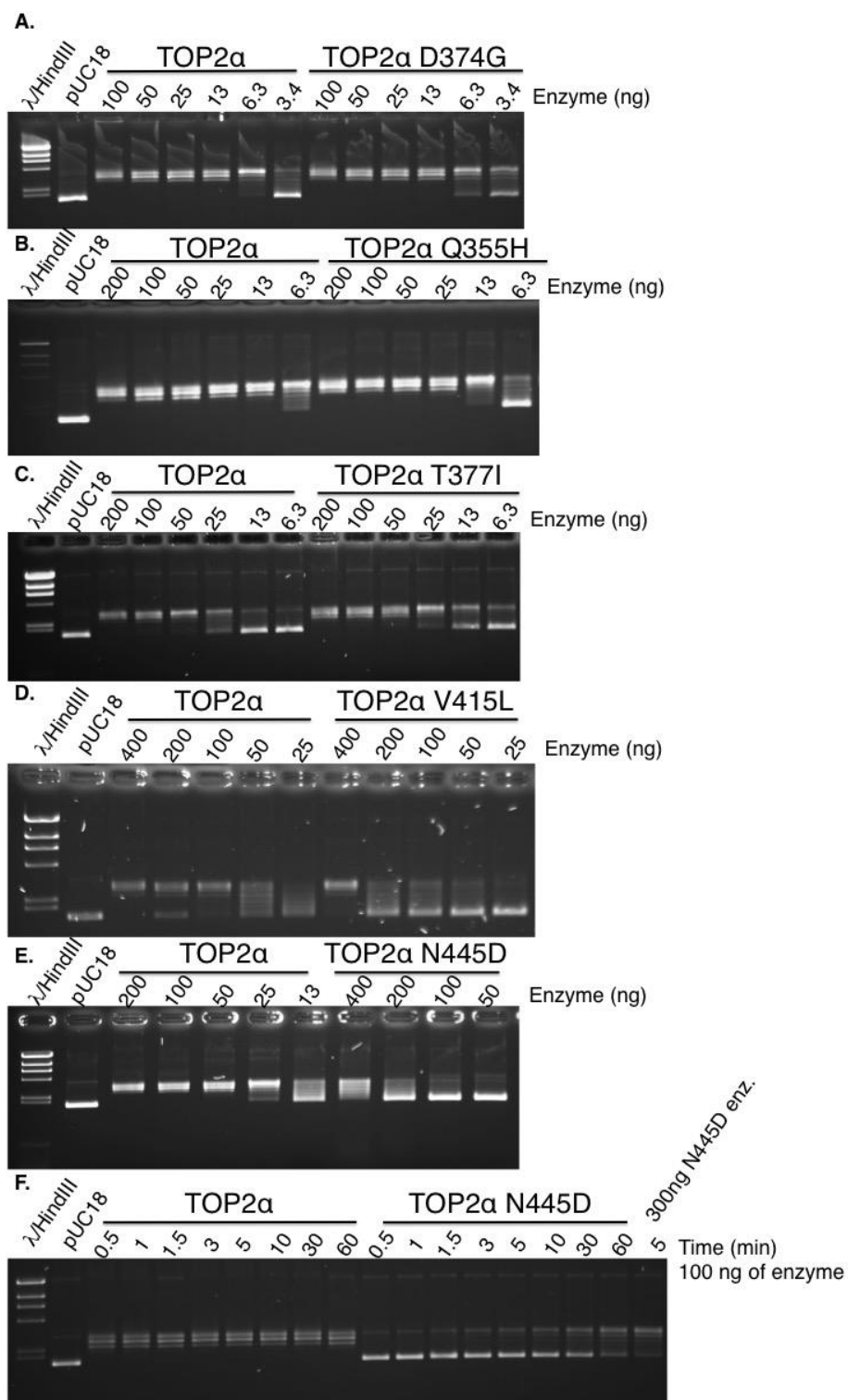
Figure 2.7 Catalytic strand passage activity of purified Top2α mutant proteins compared to wild type enzyme using 200ng negatively supercoiled plasmid DNA (pUC18) and the amount of enzyme indicated above each well. The Time-course relaxation assay with N445D was carried out twice. All other assays were carried out at least three times. **A.** Plasmid relaxation activity of the D374G mutant protein compared to wild type. Complete relaxation of pUC18 DNA was seen with 6.3ng of wild type enzyme and 13ng of D374G mutant enzyme. **B.** Plasmid relaxation activity of the Q355H mutant protein compared to wild type. Complete relaxation of pUC18 DNA was demonstrated by 13ng of wild type enzyme and 25ng of Q355H mutant enzyme. **C.** Plasmid relaxation activity of the T377I mutant protein compared to wild type. Complete relaxation of pUC18 DNA was seen 50ng of wild type enzyme and 50ng of T377I mutant enzyme. **D.** Plasmid relaxation activity of the V415L mutant protein compared to wild type. Complete relaxation of pUC18 DNA was observed 100ng of wild type enzyme and 400ng of V415L mutant enzyme. **E.** Plasmid relaxation activity of the N445D mutant protein compared to wild type. Complete relaxation of pUC18 DNA was observed 50ng of wild type enzyme and 400ng of N445D mutant enzyme. **F.** Time-course plasmid relaxation assay of the N445D mutant protein compared to wild type. 100ng of Top2 enzyme was added into each reaction for the time indicated above each well. As a comparison for relaxation activity 300ng of N445D mutant protein was add to a reaction for 5minutes (right-most lane). Complete relaxation of pUC18 DNA was observed all time points with the wild type enzyme and incomplete relaxation of the pUC18 DNA was seen with the N445D mutant enzyme after 1 hour. A similar level of relaxation activity was observed with 300ng of N445D mutant enzyme after 5min.

2.4.9 <u>Decatenation activity of mutant proteins</u>

We further characterized the topoisomerase activity of mutant proteins by measuring decatenation activity with catenated kinetoplast DNA (kDNA)[360]. The Asp374Gly mutant protein exhibited similar decatenation activity as the wild type enzyme (Figure2.8 A). Asp374Gly completely decatenated 150ng of kDNA with 13ng of protein. The Gln355His mutant protein exhibited similar relaxation activity as the wild type enzyme (Figure2.8 A). Gln355His completely decatenated 150ng of kDNA with 13ng of protein. The Thr377Ile mutant protein exhibited similar decatenation activity as the wild type enzyme (Figure2.8 B). Thr377Ile completely decatenated 150ng of kDNA with 13ng of protein.

The Asn445Asp and Val415Leu mutant proteins exhibited reduced levels of decatenation activity compared to the wild type enzyme (Figure 2.8 C). Complete decatenation of 200ng of kDNA was observed with 300ng of wild type enzyme compared to the 150ng for the Val415Leu mutant protein. These results indicated that the Val415Leu mutant protein exhibited slightly reduced (2 fold) decatenation activity. Incomplete decatenation activity of kDNA was seen with the Asn445Asp mutant protein at 600ng of enzyme. These results suggested a severe reduction in Asn445Asp topoisomerase activity, and were consistent with the previously observed reduced relaxation activity. The level of topoisomerase activity exhibited by the mutant proteins was consistent for both the relaxation and decatenation assay.

Figure 2.8 Decatenation activity of Top2α mutant proteins

98
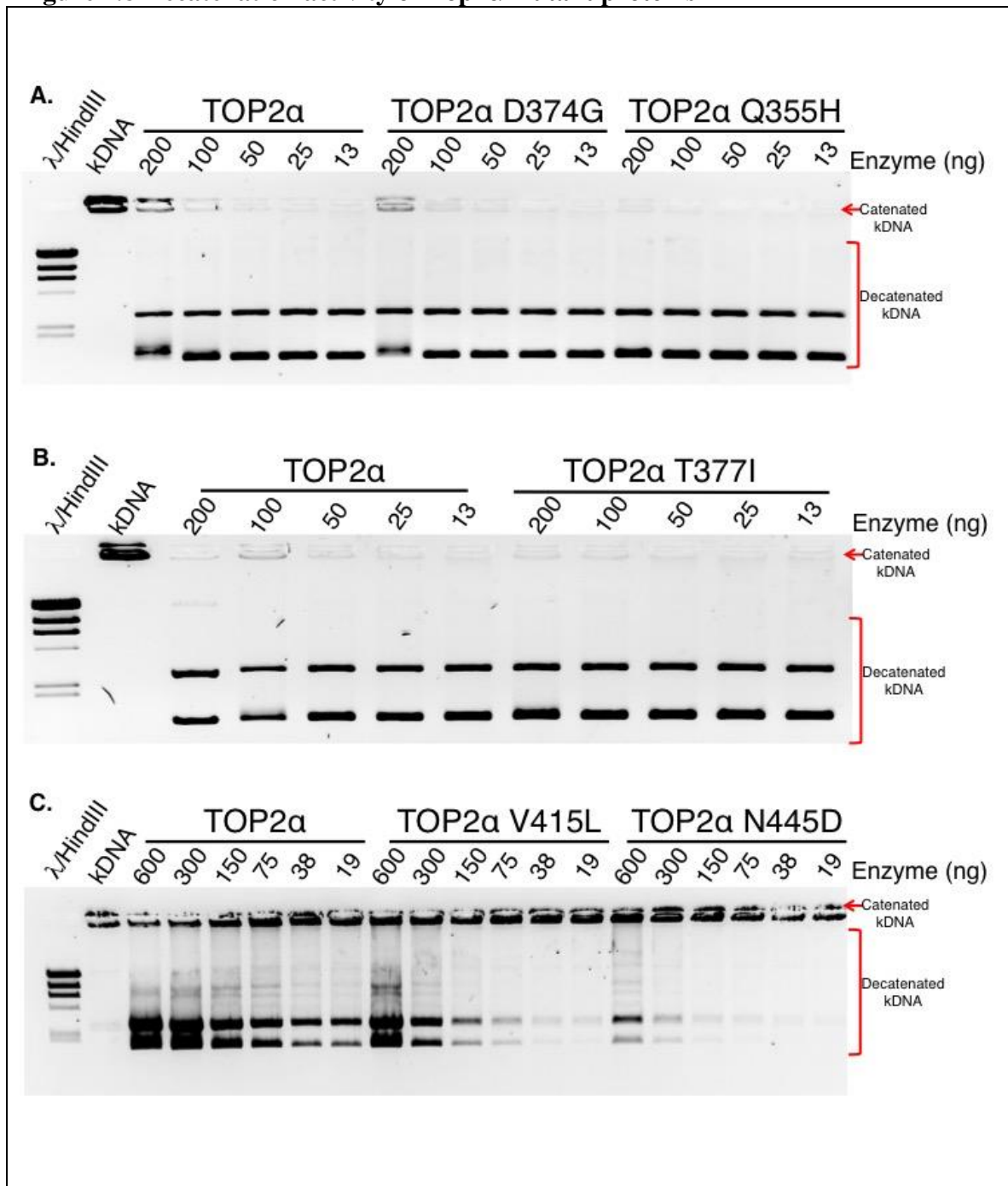
Figure 2.8 Catalytic strand passage activity of purified Top2α mutant proteins compared to wild type enzyme using catenated kinetoplast DNA (kDNA) and the amount of enzyme indicated above each well. Decatenation activity of mutant proteins was measured in at least three independent experiments. **A.** Decatenation activity of the D374G and Q355H mutant proteins compared to wild type enzyme using 150ng catenated kinetoplast DNA (kDNA). Complete decatenation activity was observed at 13ng of wild type, D374G and Q355H enzyme. **B.** Decatenation activity of the T377I mutant protein compared to wild type enzyme using 150ng catenated kDNA. Complete decatenation activity was observed at 13ng of wild type and T377I mutant enzyme. **C.** Decatenation activity of the V415L and N445D mutant proteins compared to wild type enzyme using 200ng catenated kDNA. Complete decatenation activity was observed at 300ng wild type enzyme, complete decatenation activity was observed with the V415L mutant enzyme at 600ng of enzyme. Partial decatenation activity was observed with 600ng of N445D mutant enzyme.

2.4.10 <u>Etoposide and mAMSA induced DNA cleavage in mutant proteins</u>

We next measured the levels of etoposide induced DNA cleavage with the mutant proteins *in vitro* using a plasmid cleavage assay[357]. Enzyme-mediated DNA cleavage was measured by the formation of linear and nicked DNA products as observed on an agarose gel. The DNA bands intensity were measured to determine the relative amounts of cleaved DNA (linearized and nicked). Figure 2.9 A shows Top2 mediated-DNA cleavage in the presence of etoposide. We compared the levels of DNA cleavage by the Asp374Gly and Asn445Asp mutant proteins to the wild type enzyme. Using a fixed equal concentration of Top2α protein, the Asp374Gly and Asn445Asp mutant proteins were compared to wild type enzyme (Figure 2.9 A). The mutant proteins exhibited lower levels of plasmid linearization in the presence of etoposide compared to the wild type enzyme. As expected, the relative intensity of the linear DNA band decreased for the wild type enzyme at higher concentrations of etoposide because the plasmid developed multiple Top2 mediated strand breaks and no longer ran as single band. However, both of the Asp374Gly and Asn445Asp mutant proteins exhibited greater levels of nicked plasmid DNA than the wild type enzyme (Figure 2.9 B).

Similar levels of DNA cleavage were observed in the presence of mAMSA (Figure 2.9 C and D). However, the levels of nicked DNA in the presence of mAMSA did not increase in mutant proteins in response to increasing mAMSA concentrations (Figure 2.9 D). When we controlled for equal units of enzyme strand passage activity (as determined by the plasmid relaxation assay), we found that the Asp374Gly mutant protein exhibited slightly greater levels of plasmid linearization compared to wild type enzyme and significantly higher levels of plasmid nicking (Figure 2.9 E and F).

Figure 2.9 Topoisomerase poison induced DNA cleavage with mutant proteins
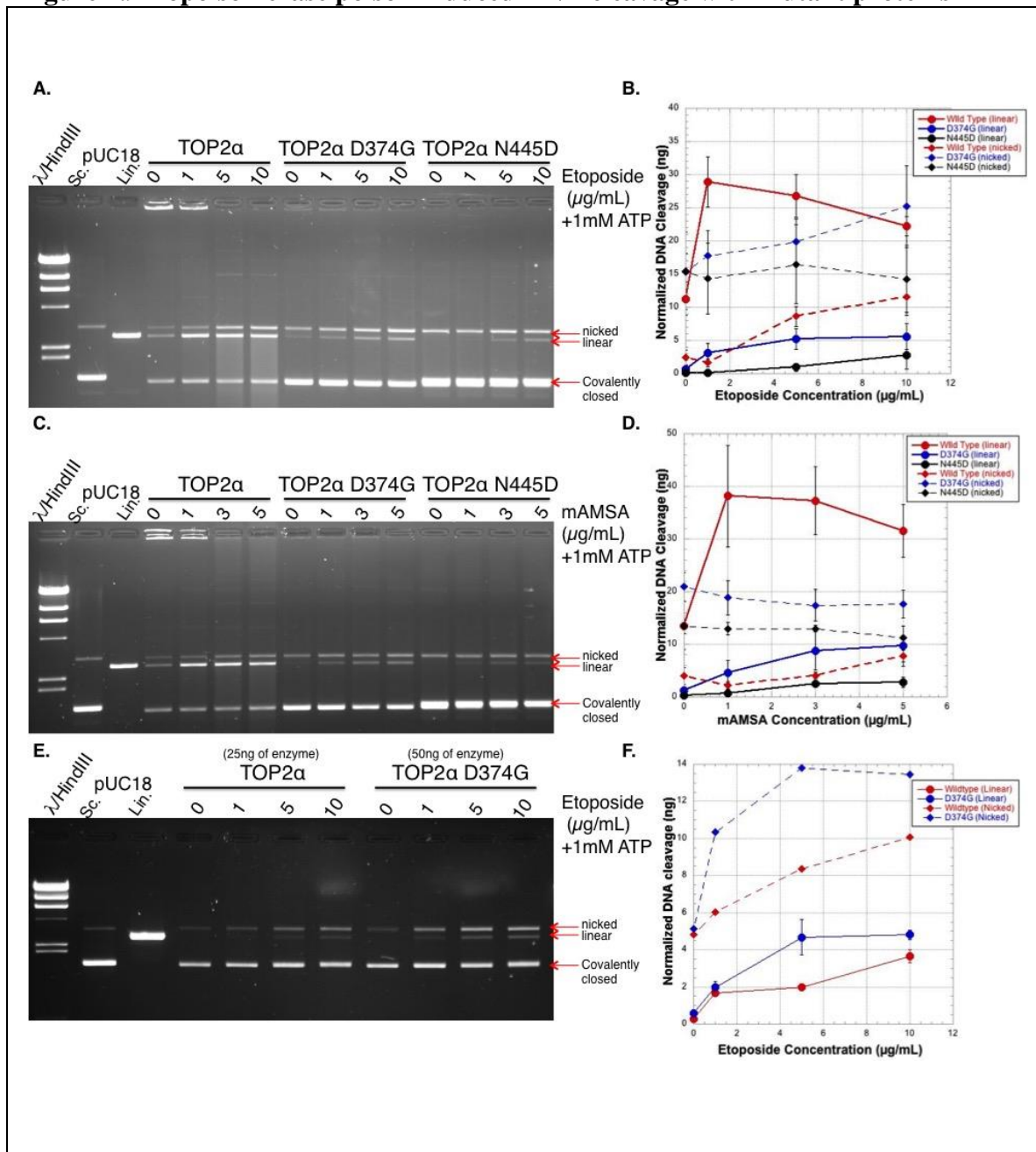
Figure 2.9 ATP-dependent Top2α mutant protein mediated DNA cleavage of 200ng negatively supercoiled plasmid DNA (pUC18) in the presence of Top2 poisons compared to wild type enzyme. The lanes labeled Sc. contain 200ng supercoiled pUC18 DNA and the lanes labeled Lin. contain 30ng ECORI linearized pUC18 DNA. The mobility of nicked, linearized and covalently closed DNA are labeled to the right of each gel. **A.** Plasmid cleavage assay with 500ng of Top2α enzyme (Wild type, D374G and N445D) and various concentrations of etoposide as indicated above each lane. 500ng of Top2α wild type enzyme produced innate levels of DNA cleavage (linear and nicked) with a dose response increase linking etoposide concentrations and intensity of the linear and nicked DNA bands. **B.** Quantitation of etoposide induced DNA cleavage described in **A.**, error bars represent the standard deviation of three experiments. At higher concentrations of etoposide the amount of linearized plasmid DNA decreased because of plasmid DNA developed multiple Top2 mediated strand breaks and were therefore lost to quantitation. **C** Plasmid cleavage assay with 500ng of Top2α enzyme (Wild type, D374G and N445D) and various concentrations of mAMSA as indicated above each lane. 500ng of Top2α wild type enzyme produced innate levels of DNA cleavage (linear and nicked) with a dose response increase linking mAMSA concentrations and intensity of the linear and nicked DNA bands. **D.** Quantitation of mAMSA induced DNA cleavage described in **C.**, error bars represent the standard deviation of three experiments. **E.** Plasmid cleavage assay, controlling for equal units of catalytic strand passage activity (based on plasmid relaxation activity) with 50ng of Top2α Asp374Gly and 25ng of wild type enzyme and various concentrations of etoposide as indicated above each well. **F.** Quantitation of etoposide induced DNA cleavage described in **E.**, error bars represent the standard deviation of at least three experiments.

2.4.11 <u>**Inhibition of Relaxation activity by catalytic inhibitors**</u>

The amino acid substitutions in several of the mutant proteins were located in the ATPase domain, distant from the DNA cleavage site. Following the location of these substitutions we next tested the sensitivity of the mutant enzymes to catalytic inhibitors that bind to the ATPase domain using the plasmid relaxation assay. Catalytic inhibition of relaxation activity by dexrazoxane (ICRF-187) was assayed using fixed enzyme concentrations and increasing concentrations of dexrazoxane (Figure 2.10 A). The Top2α wild type enzyme showed inhibition of relaxation activity at 100μM ICRF-187. The relaxation activity of the Asp374Gly mutant protein was inhibited at 50μM ICRF-187. The Gln355His mutant protein also demonstrated inhibition at 50μM ICRF-187. Catalytic inhibition of relaxation activity by vanadate, a phosphomimetics, was similarly assayed (Figure2.10 B). The Top2α wild type enzyme showed incomplete inhibition of relaxation activity at 200μM vanadate whereas the Asp374Gly showed catalytic inhibition at 50μM vanadate. These results suggested that the Asp374Gly mutant protein is hypersensitive to inhibition by these catalytic inhibitors.

Figure 2.10 Inhibition of mutant protein topoisomerase activity by Top2 catalytic inhibitors
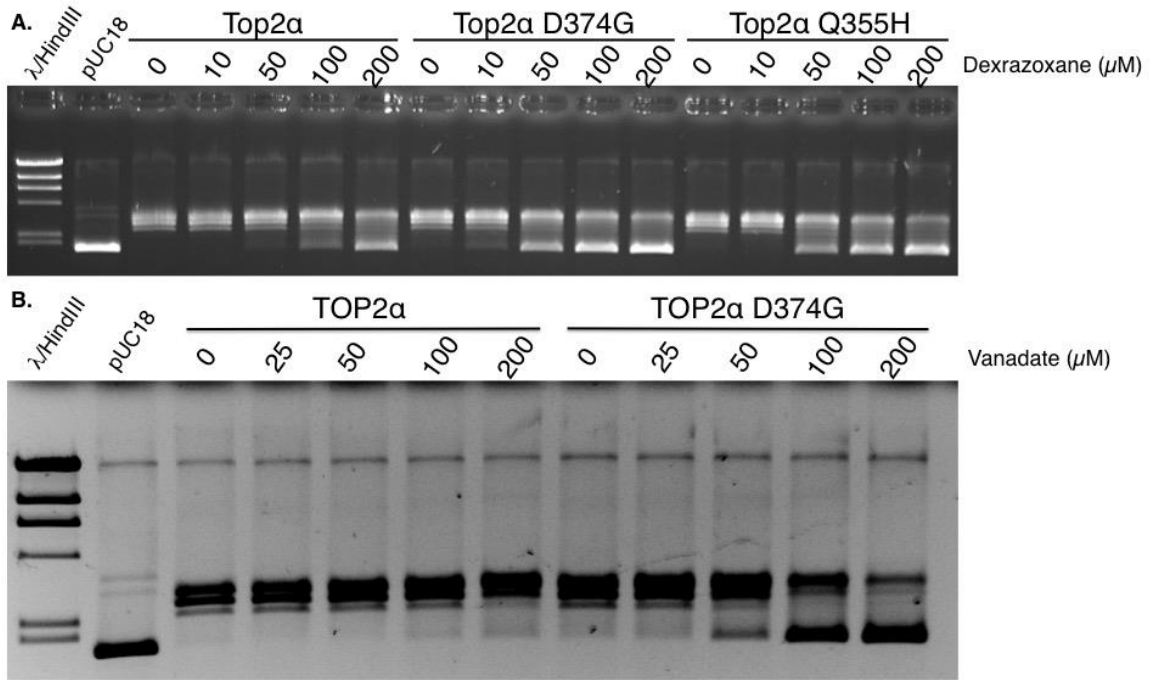
Figure 2.10 Sensitivity of mutant Top2α proteins to Top2 catalytic inhibitors. The catalytic inhibition of topoisomerase activity for wild type, D374G, and Q355H was compared using ATP-dependent relaxation of 200ng of pUC18 plasmid in the presence of Top2 catalytic inhibitors. All assays were carried out in three independent experiments. **A.** Plasmid relaxation activity with 50ng of Top2α enzyme in the presence of (0, 10, 50, 100, or 200μM) dexrazoxane (ICRF-187). Enzyme inhibition of relaxation activity is observed at 50-100μM for wild type protein, 10-50μM D374G protein, and ~50μM Q355H protein. **B.** Plasmid relaxation activity of 100ng of Top2 enzyme in the presence of (0, 25, 50, 100, or 200μM) vanadate. Enzyme inhibition of relaxation activity is observed at ~200μM for wild type protein and 50μM D374G protein.

2.4.12 <u>Previously characterized mutant alleles near the C1 cluster sensitize yeast to etoposide</u>

There are two previously characterized Top2α mutant proteins (Asp48Asn and Tyr50Phe) located near mutation cluster C1 (Asp374Gly and Thr377Ile)[183,361]. These Top2α mutant alleles were characterized by our laboratory and Asp48Asn mutant protein was previously reported to be resistant to catalytic inhibition by dexrazoxane[183]. We hypothesized that the Asp48Asn and Tyr50Phe mutant alleles would sensitize cells to etoposide. These mutant alleles were not assessed for sensitivity to etoposide during their characterization as the experimental standard at the time was to express the alleles in yeast cells deficient for *rad52*, which could not be done with Asp48Asn[183]. Therefore, we chose to measure the etoposide sensitivity of the Asp48Asn and Tyr50Phe mutant alleles in yeast strain (YMM10 $_{t2-4}$) using the clonogenic survival assay (Figure 2.11 A). The pMJ1 plasmid carrying Asp48Asn, Tyr50Phe, Asp374Gly or wild type were independently introduced into YMM10 $_{t2-4}$. Yeast expression of these mutant Top2α alleles (Asp48Asn, Tyr50Phe, and Asp374Gly) led to increased levels of sensitivity to etoposide. Yeast cells carrying Asp48Asn produced increased etoposide sensitivity (MLC: 5µg/ml etoposide) compared to yeast expressing the wild type enzyme (MLC: 10µg/ml etoposide). Yeast carrying Asp374Gly or Tyr50Phe exhibited strong sensitivity to etoposide (MLC 1µg/ml etoposide) (Figure 2.11 A). The Asp48 side chain appears to form a hydrogen bond with Thr372 (distance: 3.4 Å) on the crystal structure. To probe the importance of this interaction we constructed a series of mutations in Thr372 (alanine and aspartic acid). We expressed the mutated alleles in yeast strain (YMM10 $_{t2-4}$) to measure etoposide sensitivity using the clonogenic survival assay. Only the Thr372Asp

mutant allele sensitized yeast to etoposide (MLC: 1μg/ml etoposide). We similarly

probed the mutation requirement of Asp374 by substituting aspartic acid with leucine,

asparagine or alanine. Only the Asp374Leu allele sensitized yeast to etoposide (MLC:

1μg etoposide/ml). Other mutant alleles (Thr372Ala, Asp374Asn and Asp374Ala)

sensitized yeast cells similar to those expressing wild type enzyme (MLC 10μg

etoposide/ml).

Figure 2.11 Mutations located near to Asp374 similarly sensitize yeast cells to etoposide
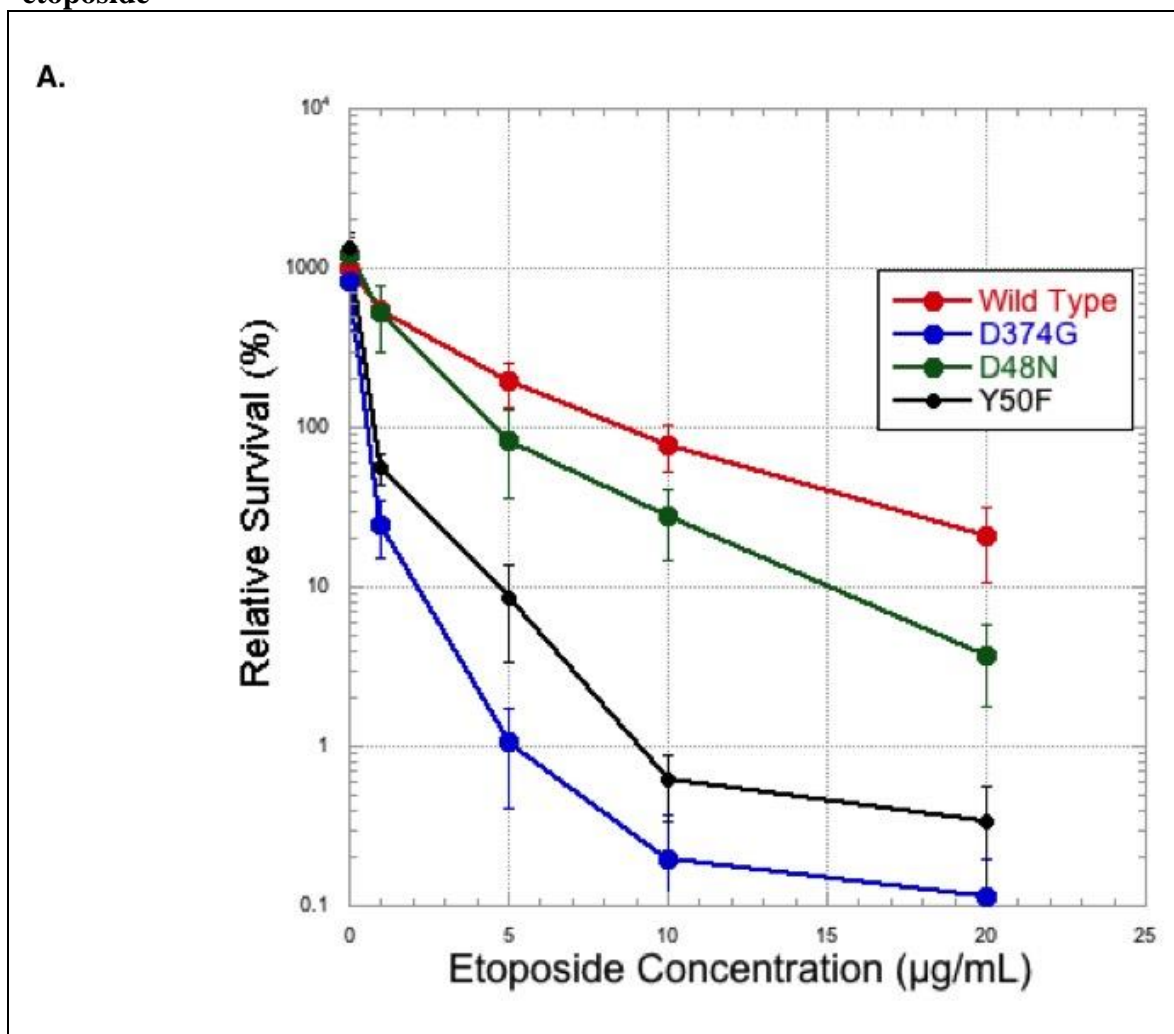
Figure 2.11 Yeast clonogenic survival assay. YMM10 $_{t2-4}$ yeast cells carrying pMJ1 with different mutations in Top2α (Wild type, Asp374Gly, Asp48Asn and Tyr50Phe). Yeast sensitivity to etoposide is represented as cell survival (%). Cell survival is the viable number of cells after 24 hour exposure to etoposide of various concentrations (0(DMSO), 1, 5, or 10μg etoposide/mL) relative to the quantity of viable yeast at T=0. Some increased sensitivity to etoposide was observed with the Asp48Asn mutant. The Tyr50Phe and Asp374Gly mutants exhibited hypersensitivity. Error bars indicate the standard error of three experiments.

2.4.13 <u>Reduced ATP utilization and defects in hydrolysis</u>

Asp48, Tyr50, Asp374 andThr377 are located near the ATP binding site[159]. We hypothesized that the Asp374Gly and Thr377Ile mutant proteins would demonstrate altered ATP utilization. Therefore, we next probed the ATP requirement for catalytic activity using the kinetoplast DNA decatenation assay[159,183,361]. We assessed decatenation activity using a fixed enzyme concentration and decreasing concentrations of ATP (Figure 2.12 A and B). The wild type Top2α enzyme was able to decatenate kDNA at 25μM ATP whereas the Asp374Asn and Thr377Ile mutant proteins could decatenate kDNA at 13μM ATP.

The two previously characterized mutant proteins Asp48Asn and Tyr50Phe were reported to have defects in DNA-stimulated ATP hydrolysis[183,361]. Since this biochemical property was shared by the previously reported mutations along with hypersensitivity to etoposide, we next assessed ATP hydrolysis activity of the Asp374Gly mutant protein. We measured the rate of ATP hydrolysis in the Top2α Asp374Gly mutant protein with comparison to the wild type enzyme using the NADH-coupled ATPase assay[152,247,362,363]. The Asp374Gly mutant protein exhibited very low rates of ATP hydrolysis and lacked DNA stimulated ATP hydrolysis (Figure 2.12 B). We further analyzed the Asp374Gly mutant protein-ATP interaction with a recently reported plasmid relaxation FRET assay in collaboration with Dr. Fenfei Leng, at Florida International University[364]. This assay utilizes a specialized plasmid DNA developed by Dr. Leng that carries a fluorophore and quencher separated by DNA that forms a cruciform structure that is stabilized by negatively supercoiled DNA (Figure 2.12 C)[364,365]. In this plasmid relaxation FRET assay Top2α Asp374Gly mutant protein exhibited a faster rate of relaxation activity than the

wild type enzyme at low concentrations of ATP (Figure 2.12 D). Dr. Leng characterized

the catalytic activity of the Top2α Asp374Gly mutant protein for several ATP

concentrations and found that the Vmax of the Asp374Gly mutant protein was similar to

Vmax of wild type enzyme at saturating concentrations of ATP (Figure 2.12 E)[366].

Figure 2.12 Reduced ATP requirement for catalytic activity
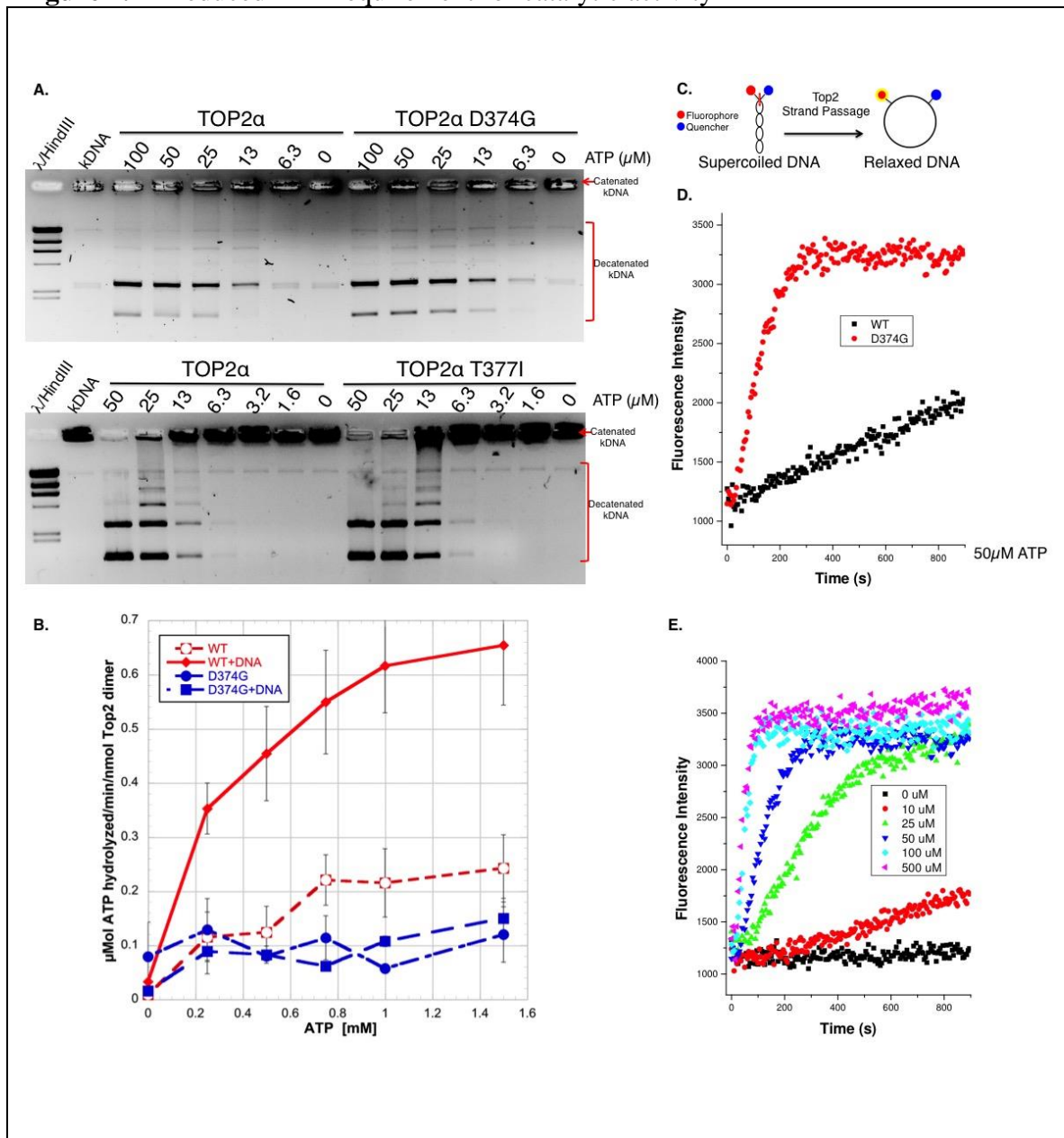
Figure 2.12 Reduced ATP requirement for catalytic activity **A.** The decatenation activity of D374G (top) and T377I (bottom) Top2α were assayed compared to wild type enzyme by incubating 200ng of kinetoplast DNA with 200ng of enzyme and decreasing concentrations of ATP. Decatenation activity was exhibited by the wild type enzyme at ~13-25μM ATP, whereas both mutant proteins D374G and T377I exhibited activity ~6.3-13μM ATP. **B**. The rate of ATP hydrolysis was assayed for the wild type and D374G proteins in the presence or absence of nucleotide. Rate of ATP hydrolysis was measured using a NADH-coupled ATPase assay for several concentrations of ATP. For each Top2α reaction, enzyme concentration was 50nM of dimer. Sonicated salmon sperm DNA (0.2mg/ml; ~2700bp per Top2 dimer) was added to reactions, as indicated, to stimulate ATP hydrolysis activity. D374G exhibited lower intrinsic levels of ATP hydrolysis activity than wild type enzyme at all concentrations of ATP and did not exhibit DNA stimulated ATP hydrolysis like the wild type enzyme. Error bars represent the standard deviation of three independent experiments. **C.** Schematic of FRET based plasmid relaxation assay using a specialized plasmid substrate. When the plasmid DNA is supercoiled the fluorophore is quenched and fluorescent signal intensity is low. When the plasmid DNA is relaxed fluorescent signal intensity is high. **D.** Time course FRET based plasmid relaxation activity with 23nM (~230ng) wild type and D374G Top2α at 50μM ATP. The D374G enzyme exhibited greater fluorescent intensity at a faster rate than the wild type enzyme, a maximum signal intensity was achieved by D374G after ~200 seconds. **E.** Time course FRET based plasmid relaxation activity with 23nM (~230ng) D374G Top2α at various ATP concentrations.

2.4.14 Top2α Asp374Gly nucleotide dependent etoposide induced DNA cleavage

The Asp374Gly and Thr377Ile mutant proteins exhibited changes to ATP utilization and hydrolysis by the enzymes, which could potentially delay the progression of the mutant proteins through the catalytic cycle. To probe the role in ATP in the sensitivity of the Asp374Gly mutant protein to etoposide we analyzed levels of DNA cleavage (with etoposide) in the presence of different nucleotides (ATP, ADP, AMP-PNP) (Figure 2.13). In the presence of ATP Asp374Gly demonstrated a dose-response increase in DNA cleavage with increasing concentrations of etoposide (Figure 2.13 A). As before, Asp374Gly mutant protein exhibited lower levels of plasmid linearization compared to the wild type enzyme. Elevated levels of nicked DNA were observed with the Asp374Gly mutant enzyme for all etoposide concentrations compared to wild type (Figure 2.13 B). As expected, a decrease in linearized plasmid DNA was exhibited with the wild type enzyme as multiple DNA double strand breaks in the plasmid will cause the DNA to run as multiple sizes in the electrophoresis gel.

In contrast, the levels of DNA cleavage for both the wild type and Asp374Gly mutant enzymes were reduced in the presence of ADP (Figure 2.13 C). The wild type enzyme showed increases in the populations of linear and nicked DNA with increased concentrations of etoposide. Asp374Gly did not exhibit any changes to linear or nicked DNA with etoposide except for a slight non-significant increase in nicked DNA at the highest concentration of etoposide (Figure 2.13 D).

The wild type enzyme and Asp374G both demonstrated high levels of DNA cleavage in the presence of AMP-PNP and etoposide (Figure 2.13 E). The wild type enzyme exhibited higher levels of linearized DNA in response to etoposide concentration.

114

The Asp374Gly mutant enzyme also demonstrated increased levels of linearized DNA in response to etoposide concentration (Figure 2.13 F). The Top2α wild type and Asp374Gly mutant proteins exhibited similar levels of DNA nicking in response to etoposide. Together these results suggest that Asp374Gly mutant protein etoposide mediated DNA cleavage was dependent on the presence of ATP or AMP-PNP. We additionally observed that the Asp374Gly mutant protein in the presence of AMP-PNP without etoposide exhibited elevated levels of DNA nicking and relatively low levels of linear DNA compared to the wild type enzyme (Figure 2.13 F).

Figure 2.13 Nucleotide stimulated etoposide induced DNA cleavage
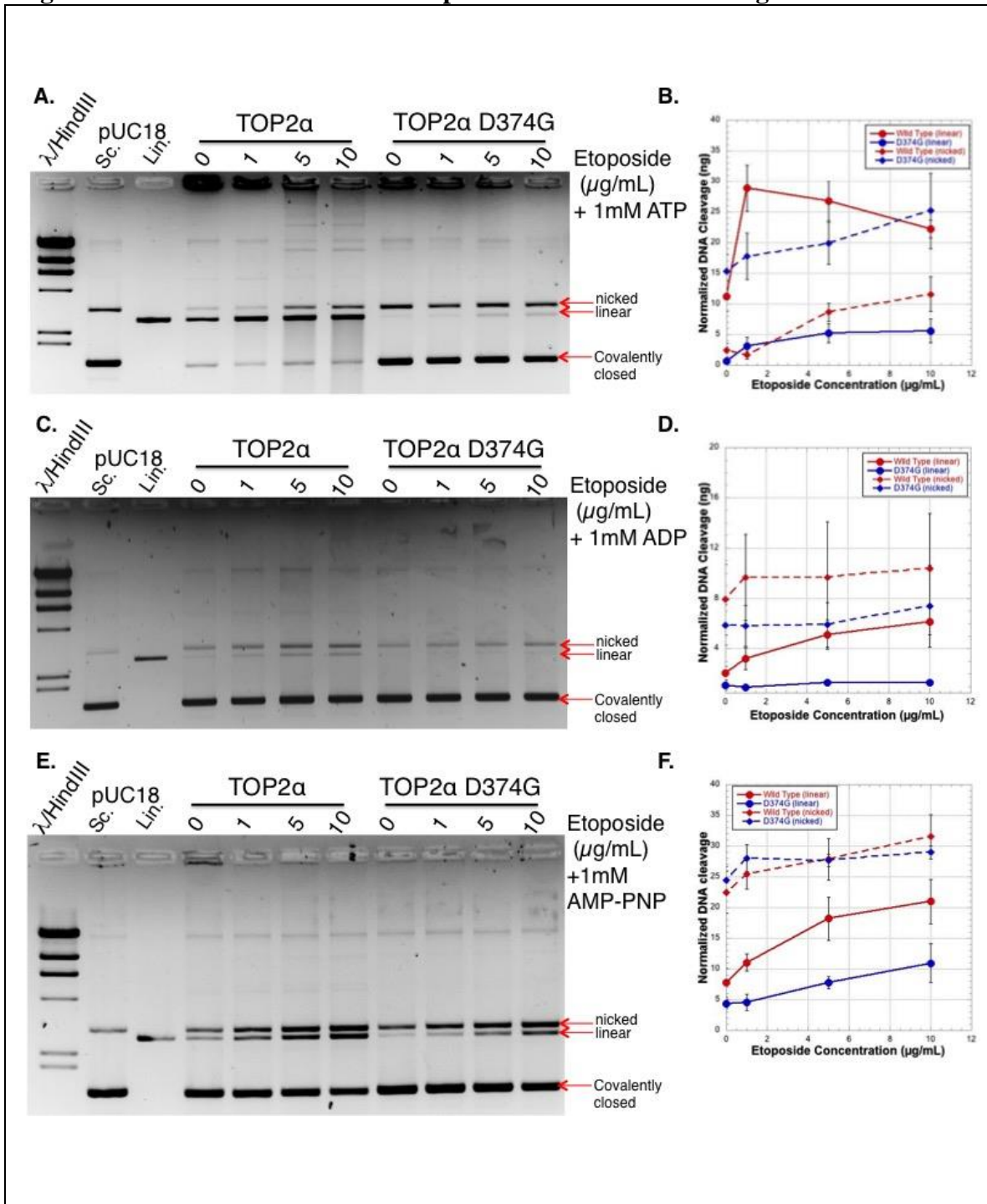
Figure 2.13 Nucleotide-dependent Top2α mutant protein mediated DNA cleavage of 200ng negatively supercoiled plasmid DNA (pUC18) in the presence of etoposide compared to wild type enzyme. The lanes labeled Sc. contain 200ng supercoiled pUC18 DNA and the lanes labeled Lin. contain 30ng ECORI linearized pUC18 DNA. The mobility of nicked, linearized and covalently closed DNA are labeled to the right of each gel. **A.** Plasmid cleavage assay with 500ng of Top2α enzyme (Wild type and D374G) with various concentrations of etoposide as indicated above each lane in 1mM ATP. 500ng of Top2α wild type enzyme produced innate levels of DNA cleavage (linear and nicked) with increasing amounts of etoposide the intensity of the linear and nicked DNA bands increased. **B.** Quantitation of etoposide induced DNA cleavage described in **A.**, error bars represent the standard deviation of three experiments. At higher concentrations of etoposide the amount of linearized plasmid DNA decreased because of plasmid DNA developed multiple Top2 mediated strand breaks and were therefore lost to quantitation. **C.** Plasmid cleavage assay with 500ng of Top2α enzyme (Wild type and D374G) with various concentrations of etoposide as indicated above each lane in 1mM ADP. 500ng of Top2α wild type enzyme produced innate levels of DNA cleavage (linear and nicked) with increasing amounts of etoposide the intensity of the linear and nicked DNA bands increased. **D.** Quantitation of etoposide induced DNA cleavage described in **C.**, error bars represent the standard deviation of three experiments. **E.** Plasmid cleavage assay with 500ng of Top2α enzyme (Wild type and D374G) with various concentrations of etoposide as indicated above each lane in 1mM AMP-PNP. 500ng of Top2α wild type enzyme produced innate levels of DNA cleavage (linear and nicked) with increasing amounts of etoposide the intensity of the linear and nicked DNA bands increased. **F.** Quantitation of etoposide induced DNA cleavage described in **E.**, error bars represent the standard deviation of three experiments.

2.4.15 AMP-PNP induced Top2α Asp374Gly DNA cleavage

We had observed that the Asp374Gly mutant protein generated a slightly different drug-independent DNA cleavage pattern in the presence of AMP-PNP with greater levels of DNA nicking and low levels of linearization. This finding led us to examine DNA cleavage induced by AMP-PNP. We assayed AMP-PNP stimulation of Top2-mediated DNA cleavage with the plasmid cleavage assay (Figure 2.14 A). We found that the presence of AMP-PNP trapped Top2α wild type and Asp374Gly as covalent complexes with differing levels of nicked and linear DNA. In the absence of nucleotide the wild type enzyme had higher innate levels of nicking and linearization that increased in response to increasing concentrations of AMP-PNP (Figure 2.14 B). Asp374Gly levels of linear DNA did not appreciably increase in the presence of AMP-PNP but the levels of nicked DNA increased to levels greater than wild type enzyme.

Figure 2.14 AMP-PNP dependent Top2 Asp374Gly cleavage
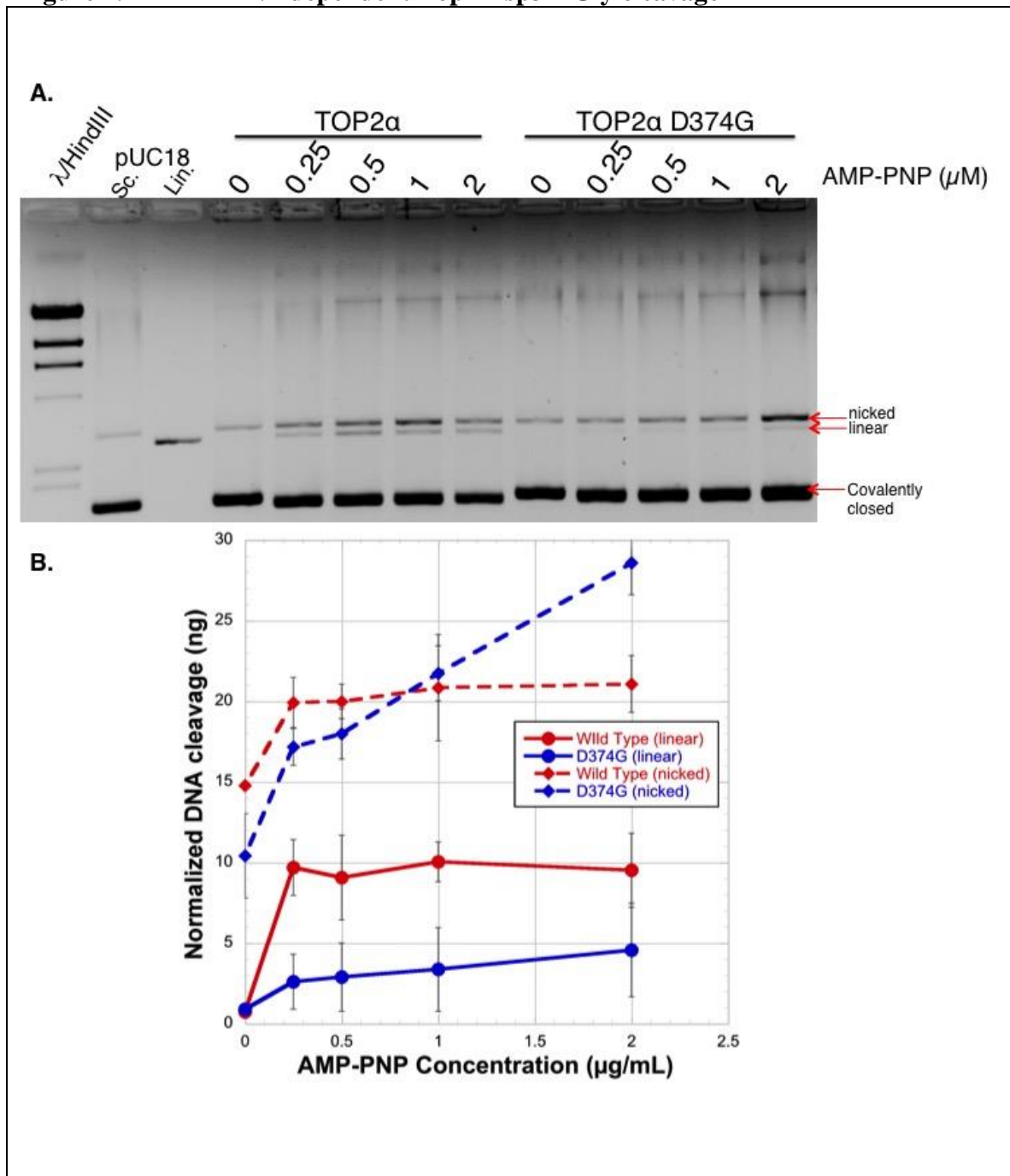
Figure 2.14 AMP-PNP-dependent Top2α mutant protein mediated DNA cleavage of 200ng negatively supercoiled plasmid DNA (pUC18) compared to wild type enzyme. The lanes labeled Sc. contain 200ng supercoiled pUC18 DNA and the lanes labeled Lin. contain 30ng ECORI linearized pUC18 DNA. The mobility of nicked, linearized and covalently closed DNA are labeled to the right of each gel. **A.** Plasmid cleavage assay with 400ng of Top2α enzyme (Wild type and D374G) with various concentrations of AMP-PNP as indicated above each lane. Top2α wild type enzyme produced measurable levels of DNA cleavage (linear and nicked) with increasing concentrations of AMP-PNP. **B.** Quantitation of AMP-PNP induced DNA cleavage described in **A.**, error bars represent the standard deviation of three experiments.

2.5   Discussion

Top2 drug-hypersensitive alleles have proven to be useful tools for exploring the mechanistic details of the Top2 catalytic mechanism and drug action[240,312,315,316]. In this study we have described a large range of mutations that confer greater levels of hypersensitivity to etoposide than previously described mutants of Top2α[316].

The interpretation of the positioning of these mutations has been greatly aided by the Top2α crystal structures of the ATPase/transducer domains and catalytic core of the enzyme (Figure 1.4)[72,159,178]. We identified etoposide sensitizing mutations located throughout the Top2 protein structure; this highlights the tight coordination of the Top2 machine involved in the catalytic mechanism and suggests a possible connection between the distal domains of Top2 and DNA cleavage/ligation[183,367].

The identification of clusters of mutations that confer etoposide hypersensitivity has helped to highlight regions of the protein that are likely important to sensitivity to Top2 targeting agents. Several mutation clusters were located near dimerization interfaces highlighting that these interactive regions of the enzyme could be important determinants of drug action.

Our screen identified mutations in the ATPase and Transducer domains that conferred high levels of sensitivity to etoposide and mAMSA in yeast. These findings were consistent with a previously described screen to detect fluoroquinolone resistant mutants of yTop2, Top2α and Top2β as many mutations were also identified in the ATPase and transducer domains[321]. These findings support an important role for the ATPase domain as a determinant of Top2 targeting drug sensitivity.

Several mutations in the ATPase domain have been characterized previously and have provided some insight into the molecular details of the ATPase and transducer domains. A mutation in *Drosophila* Top2 Lys359Glu/Gln (Lys376 Top2α) was identified to be critical to the utilization of ATP[368]. Structural analysis of this residue, located in the QTK-loop (a highly conserved region of Top2) identified the Lys359 residue as forming a hydrogen bond with the γ phosphate of the co-crystalized AMP-PNP[159].Deletion of the Top2α QTK-loop drastically reduced enzyme catalytic activity although the mutant enzyme exhibited increased steady-state levels of DNA cleavage[367]. This result suggested that the QTK-loop is not necessary for ATP hydrolysis and that alterations affected the way the enzyme interacts with DNA when not performing strand passage. These studies along with the simple observation that DNA cleavage is much higher *in vitro* when ATP is present support a role for the ATPase domain in the regulation of DNA cleavage.

To understand the importance of the ATPase and transducer domains to drug action, we characterized several of the etoposide-hypersensitive alleles carrying mutations in these domains. Our biochemical analysis focused primarily on Asp374Gly and revealed several unique biochemical properties. The Asp374Gly mutant protein lacked DNA stimulated ATP hydrolysis and exhibited reduced intrinsic levels of ATP hydrolysis. The absence of DNA stimulated ATP hydrolysis has been reported previously with several Top2α mutant alleles[183,361,367,369]. Of these the Arg162Gln and Asp48Asn mutant proteins exhibited elevated levels of DNA cleavage in the presence of etoposide *in vitro*[183,369]. Our results showed that Tyr50Phe and Asp48Asn also conferred etoposide hypersensitivity to yeast, potentially indicating this characteristic may be linked to processes that would sensitize the enzyme to etoposide.

The Asp48Asn, Asp374Gly and Thr377Ile mutant proteins also exhibited a reduced ATP requirement for catalytic activity. Several Top2α mutant proteins have been characterized that exhibited an increased ATP requirement for ATP hydrolysis as well as resistance to bisdioxopiperazines and vanadate[317,370,371]. In one, a human leukemia cell line (CCRF-CEM) passaged for resistance to teniposide exhibited an increased ATP requirement for unknotting activity in nuclear extracts[372]. These cells were later identified to carry Arg450Gln amino acid substitution and exhibited resistance to doxorubicin, teniposide, mAMSA and mitoxantrone[317]. Additionally, a bisdioxopiperazine resistance screen identified several mutations (Gly551Ser, Pro592Leu, Asp645Asn, and Thr996Leu) with high levels of resistance to several Top2 targeting agents (Etoposide, ICRF-187, mAMSA, Merbarone) and identified an increased ATP requirement for strand passage activity[370]. The Gln355His mutant protein was sensitive to etoposide but did not exhibit a reduced ATP requirement for strand passage activity, suggesting that this characteristic may be unique to mutations near the C1 cluster.

The binding of nucleotide exhibits a strong effect on Top2 enzyme dynamics. When bound to AMP-PNP, Top2 adopts a closed clamp conformation, carries out a single strand passage event but becomes trapped on the DNA G-segment[150,151,373]. When bound to ADP, Top2 adopts a closed clamp conformation but will not carry out strand passage[150]. During catalysis Top2 binds two ATP molecules and hydrolyzes them sequentially which revealed an asymmetric role for the two ATP hydrolysis events[151]. The role of the second ATP hydrolysis event in catalysis is predicted to be in resetting the enzyme for subsequent catalytic activity[151]. The first ATP hydrolysis event was proposed to accelerate the rate of DNA transport[373]. A mutant yeast Top2 Gly164Ile was identified

to block ATP binding[374]. Biochemical analysis of the purified yTop2 Gly164Ile/wild type heterodimer revealed the enzyme was able to slowly accomplish strand passage and lacked DNA stimulated ATP hydrolysis[374]. Supporting a role of the first ATP hydrolysis event in accelerating DNA transport. The yTop2 Gly164Ile/wild type heterodimer was also reported to convey elevated levels of DNA nicking and low relative levels of DNA linearization in the presence of AMP-PNP[374]. These data could suggest that the mutant protein has deranged the coordination of the first ATP hydrolysis event that drives stand passage. As the Asp374Gly mutant protein exhibits many of these same biochemical characteristics, dysregulation of the first ATP hydrolysis could lead to delays in DNA transport and the observed sensitivity to etoposide.

Top2 catalytic inhibition by vanadate has been demonstrated to inhibit the second ATP hydrolysis event[151]. Asp374Gly mutant protein was more sensitive to catalytic inhibition by vanadate potentially suggesting that the enzyme exhibits a defect in the first ATP hydrolysis event. The presence of a defect in this hydrolysis event could explain, the lack of DNA-stimulated ATP hydrolysis and the reduced requirement of ATP for strand passage activity.

The Asp48Asn mutant protein has high levels of drug independent DNA cleavage[183]. Increased steady-state levels of DNA cleavage could sensitize the enzyme to etoposide, as they are a substrate for anti-topoisomerase drug action. Additionally, the sensitivity of Thr372Asp and Asp374Leu connect observed etoposide sensitivity of QTK loop mutations with the previously reported altered steady-state levels of DNA cleavage in Asp48Asn[183]. Due to the close proximity to Thr377 and the shared biochemical characteristics between Asp48Asn, Thr377Ile, and Asp374Gly we suggest that these

mutations affect etoposide sensitivity by similar mechanisms. Furthermore, as the nearby Tyr50Phe also exhibited etoposide sensitivity a similar mechanism of etoposide sensitivity likely extends to this region of the protein.

I suggest that the ATPase domain of Top2 as a regulator of DNA cleavage could represent a therapeutic target that could reproduce the effects of Top2 poisons. This would allow the usage of alternate chemical scaffolds, which could mitigate existing side effects. This conclusion appears consistent with DNA cleavage stimulated by AMP-PNP. Additionally, several small molecules (salvicine and emodin) designed to target the ATPase domain of Top2 have been identified as agents that cause DNA damage[252,253]. This study provides a potential mechanistic basis for why this could occur. This model may predict that Top2 poisons like etoposide would synergize with salvicine or emodin.

The Asn445Asp and Val415Leu mutant proteins exhibited very low levels of catalytic activity and were located close to the catalytic core of the enzyme. Our time-course relaxation assay may suggest Asn445Asp carries out slow relaxation activity and could indicate that the mutant enzymes have difficulty progressing through the catalytic cycle. The Asn445Asp mutant protein exhibited high innate levels of DNA nicking in several DNA cleavage experiments potentially suggesting that the mutant enzyme persists as pre-strand passage complex. This mutant protein would be an excellent candidate for analysis with the FRET plasmid relaxation assay. We would speculate that the rate of relaxation will be far slower than the wild type enzyme; this is a potential mechanism that leads to increased levels of etoposide sensitivity because of a prolonged covalent complex during strand passage.

125

We selected several Top2α drug-sensitive mutant alleles to biochemically characterize in this study. Based on our findings we speculate that further studies of mutant proteins located in the etoposide hypersensitive mutation clusters we identified could provide interesting additional biochemical details regarding enzyme sensitivity to etoposide. Two candidates for further analysis would be Asn433Lys and Glu506Gly. Asn433 is not resolved on available crystal structures and other eukaryotic Top2 enzymes have serine at this position. However, given its extreme sensitivity to both etoposide and mAMSA, biochemical characterization of this mutant protein could reveal important details of drug action. By contrast the sensitivity of the Glu506Gly mutant allele appears specific to etoposide. Analysis of this allele may provide interesting details, particularly due to its proximity to the conserved PLRGK motif involved in resistance to fluoroquinolones[240,315,375]. Structural analysis of the co-crystal structure of Top2α bound to DNA and etoposide indicated the Glu506side chain is 4.3 Å from the polycyclic ring of etoposide[178]. The loss of this large negatively charged amino acid may promote increased sensitivity to etoposide through enhanced levels of drug binding. The PLRGK motif forms a loop that is positioned between Glu506 and the active site tyrosine of the opposing subunit. The loss of the large basic residue could allow greater displacement of the PLRGK motif upon etoposide binding thereby inhibiting religation. Further analysis of this mutation could assist with the rational design of more potent next generation Top2 poisons.

3 MUTAGENIC CONSEQUENCES OF ETOPOSIDE IN YEAST

3.1 <u>Summary</u>

The use of Top2 targeting agents in chemotherapeutic therapies is associated with a some severe side effects including the development of secondary malignancies typically presenting as acute myeloid leukemia (AML)[273,274,277,278]. The development of therapy associated AML (t-AML) is characterized by a latency period of ~2 years with Top2 targeting agents[277]. However, the molecular mechanisms that contribute to mutagenesis remain poorly understood. In this chapter we present work through which we explored the mutagenic consequences of yeast exposed to etoposide in order to expand current understanding of the molecular mechanisms responsible.

To approach this problem, we utilized the *CAN1* forward mutation assay to detect mutagenic consequences of exposure to etoposide in yeast. Additionally, we utilized a mutant yTop2 allele (Phe1025Tyr/Arg1128Gly) that exhibits elevated levels of drug-independent DNA cleavage to mimic Top2 targeting drug action. In these experiments we utilized the yeast genetic system to delete genes that participate in the repair of Top2 mediated DNA damage and then explored the consequences of that damage.

Our results indicated that the mutations induced by etoposide in yeast lead to a dramatic increase in the formation of tandem duplication events. Furthermore, our results indicated that the formation of tandem duplication events induced by Top2 mediated DNA damage likely occurred through the NHEJ double strand break repair pathway. These data also suggested that the *TDP1*, which is capable of hydrolyzing the DNA phosphotyrosyl linkage, might be involved in the formation of these tandem duplications.

TDP1 is known to play a role in the repair of etoposide induced DNA damage[376]. *TDP1* deficient yeast are sensitized to topoisomerase targeting agents[377–379]. These findings support *TDP1* as a viable target to boost the efficacy of topoisomerase targeting agents as well as highlight an added benefit to *TDP1* inhibition of the induction of genome instability.

3.2   Introduction

As discussed in chapter 1, usage of Top2 targeting agents in chemotherapy is associated with the development of secondary malignancies like AML. Therapy related AML (t-AML) is known to be caused by exposure to alkylating agents as well as Top2 targeting drugs[277]. The latency period of these two t-AML sources is distinct. Etoposide induced t-AML arises in 2-3% of patients with a latency period of about 2 years[277,380]. Alkylating agent associated t-AML occurs in ~5% of patients with a latency period of 5-7 years[380].

Patients with etoposide-induced t-AML typically present with translocations of the MLL1 gene 11q23, although translocations of other genes have also been observed[381]. The MLL1 gene translocations have been identified to fuse with many (>50) different partner loci [277]. The chromosomal rearrangements associated with etoposide induced t-AML are distinct from those associated with alkylating agents which typically involve the loss either parts of or all of chromosomes 5 and 7[382].

The MLL1 gene has a 8.3kb junction region that has been identified as a common breakpoint for the translocations[277,383,384]. This region which was analyzed to assist with the identification the DNA repair pathway involved in the mis-repair associated with the

genesis of these events[384–389]. Several mutation types were identified in this region (duplications, inversions, mini-direct tandem repeats)[387,389,390].

Translocations suggest the involvement of the NHEJ DNA repair pathway[268]. Some evidence from studying class switch recombination in B cells, suggests that translocations require alternative NHEJ (alt-NHEJ)[391,392]. The alt-NHEJ pathway uses XRCC1 and DNA ligase III, but its mechanisms are less well understood[393].Previous studies in yeast identified the NHEJ DNA repair pathway as important for yeast survival following etoposide induced DNA damage[268]. Mammalian cells deficient for NHEJ factors are also sensitive to Top2 targeting agents[394,395].

To repair Top2 mediated DNA damage cells must remove the covalently bound protein from DNA. This involves a nucleolytic mechanism through which cells may digest the covalently linked DNA or hydrolyze the 5' phosphotyrosyl protein-DNA linkage. Tyrosyl-DNA-phosphodiesterase 1 and 2 (TDP1 and TDP2) are capable of hydrolyzing the 5' phosphotyrosyl covalent protein-DNA bond[265,376,396,397]. Deletion of *tdp1* in yeast has been shown to increase sensitivity to topoisomerase targeting agents[27,265,376,397].

Yeast are particularly tractable tools as a model system for studying genetics. Through the work of Richard Kolodner the yeast system has developed profoundly sophisticated tools to study mutational spectra and rates[398–401]. Therefore we used a yeast-based system to explore the mutagenic consequences of exposure to etoposide. To accomplish this we used the genetic tools available in yeast such as the *CAN1* forward mutation assay, which allowed us to measure mutation frequency and rates as well as identify the types of mutations induced by etoposide[402]. Using this approach and the

genetic tools in yeast we hoped to identify the genetic requirements involved in etoposide induced mutagenesis.

3.3   Materials and methods

3.3.1   Yeast growth media

Yeast growth medium was made as described in chapter 2. L-canavanine medium was made by first making SC-Arg⁻ agar medium as outlined in described in chapter 2. After autoclaving, SC-Arg⁻ agar was supplemented with 60mg/L L-canavanine (dissolved in DMSO) after the sterilized agarose medium cooled to 55˚C in a water bath, mixed, then poured into 60mm petri dishes at room temperature to set.

3.3.2   Yeast vector and plasmid construction

The experiments described in this chapter study the mutagenic effects of poisoning Top2 in yeast. To accomplish this we utilized a yeast overexpression plasmid pDED1yTop2[311]. This plasmid is derived from YCP50 (described in chapter 2) and expresses yeast Top2 under the control of the *DED1* promoter, leading to the overexpression of the yeast Top2 (Table 3.1).

We also modified the pDED1yTop2 wild type plasmid to carry a set of mutations (Phe1025Tyr and Arg1128Gly) with oligonucleotide site directed mutagenesis. This set of mutations was identified in a follow up screen to characterize mutations of yTop2 that confer hypersensitivity to mAMSA[314].

Table 3.1 Yeast plasmids used in chapter 3

Yeast Plasmid	Description
pDED1yTop2	Yeast Top2 overexpression under control of the *DED1* promoter (10-20 fold)
pDED1yTop2 Phe1025Tyr/Arg1128Gly	Yeast Top2 Phe1025Tyr/Arg1128Gly overexpression under control of the *DED1* promoter
pGAL1TOP2	Yeast Top2 overexpression under control of the *GAL1* promoter
ypGAL:*RAD52*	*RAD52* under the control of the yeast *GAL1* promoter
YCP50	Yeast centromere containing shuttle vector (used as empty vector control)
Yeast gene deletion constructs *Δtdp1*::*LEU2* *ΔTop1*::*URA3* *Δdnl4*::*LEU2* *Δku70*::*LEU2*	Yeast gene replacement by gene disruption, these plasmids integrate into a target gene coding sequence and insert a selectable auxotrophic marker

3.3.3 Yeast strain

The YMM10 *S. cerevisiae* yeast strain described in chapter 2 was used for experiments in this chapter, the genotype of this strain is described in Table 2.3. Several gene deletion constructs were made in the YMM10 strain using standard gene replacement strategies as described in Table 3.1. The W303 *S. cerevisiae* yeast strain was used for experiments in this chapter and is a widely used haploid yeast strain[403]. The genotype of W303: *MATa RAD5 leu2-3,112 ura3 CAN1 his3-11,15 ade2-1*.

3.3.4 Canavanine forward mutation assay

The *CAN1* gene has been previously used for the detection of mutation events in yeast[398,399]. *CAN1* encodes an arginine permease protein that imports extracellular arginine and arginine analogs[404]. Canavanine (Tocris Bioscience, 2219-31-0) is a toxic analog of arginine that replaces the 3rd carbon of the aliphatic side chain with oxygen (Figure 3.1 A). Canavanine can be incorporated into proteins in place of arginine, leading to non-functional proteins through mis-folding[405]. Yeast strains that express functional

CAN1 are sensitive to canavanine and loss of function mutations in *CAN1* results in a canavanine resistance phenotype (CAN^R). We used the canavanine forward mutation assay to measure mutation rates and analyze mutations types in yeast (Figure 3.1 B).

Yeast (YMM10) carrying plasmids (pDEDyTop2, YCP50, pDEDyTop2 SNM, pDEDyTop2 Arg1128Gly Phe1025Tyr, or PMJ1) were grown in URA$^-$ media and exposed to Top2 poisons (0, 5, 10, 25, 50µg etoposide/ml) for 2,4, or 24 hours then plated onto SC-URA$^-$ and L-canavanine agar plates. The mutation frequency was calculated as the ratio of CAN^R colony forming yeast to the number of viable yeast cells. CAN^R yeast colonies were picked and expanded on an L-canavanine agarose plates. Mutation rates were determined in W303 pCAN-CAN1 yeast carrying plasmid DNA (empty vector, pDEDyTop2 wild type, or pDEDyTop2 Phe1025Tyr Arg1128Gly). Approximately 50-100 transformed yeast cells were inoculated into1ml of SC-URA media and grown at the appropriate temperature for 3 days then plated to selective media (SC-URA$^-$ and L-canavanine).

Figure 3.1 L-Canavanine forward mutation assay
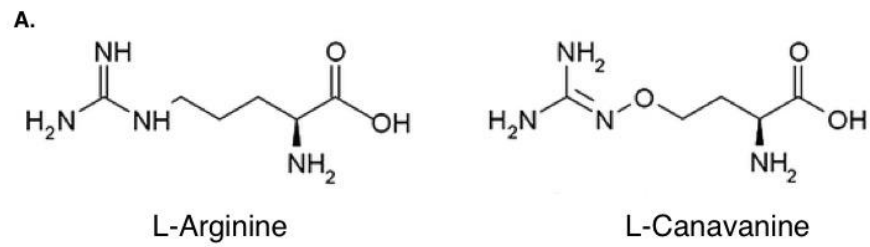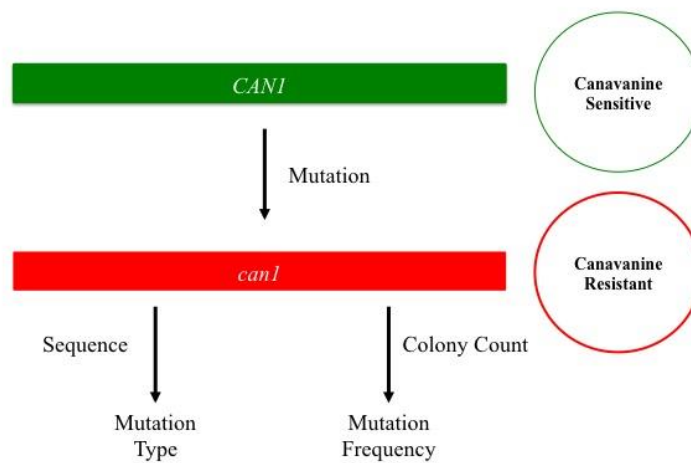
Figure 3.1 An illustration of the forward canavanine mutation assay. **A**. Comparison between L-Arginine (left) and L-canavanine (right). **B.** Schematic for the canavanine forward mutation assay. Yeast expressing a functional *CAN1* gene (arginine permease) are sensitive to L-canavanine containing media. Mutations that inactivate *CAN1* are resistant to L-canavanine containing media. The L-canavanine resistant yeast can be counted to estimate the mutation rate and *can1* can be sequenced to identify the mutation type responsible for *CAN1* inactivation.

3.3.5   Fluctuation analysis

To determine the rates and frequency of mutation in yeast we utilized fluctuation assays. The *CAN1* forward mutation assay was used to determine the mutation frequency in yeast in several different contexts. To measure the mutation frequency yeast strain YMM10 carrying *TOP2* wild type (pDEDyTop2) or empty vector (YCP50) were exposed to various concentrations of etoposide as indicated for a period of two hours at 30°C then plated to selective media (SC- Ura⁻ or L-canavanine). Alternatively, BY4741 yeast carrying *TOP2* wild type, Phe1025Tyr Arg1128Gly (pDEDyTop2) or empty vector (YCP50) were inoculated then grown for 3 days at 30°C then plated to selective media (SC- Ura⁻ or L-canavanine). The mutation frequency was calculated as the ratio of yeast colonies that formed on L-canavanine media compared to those that formed on SC- Ura⁻.

In collaboration with Sue-Jinks Robertson's laboratory, at Duke University, we determined the mutation frequency of yeast carrying *top2* Phe1025Tyr Arg1128Gly (pDEDyTop2). To measure the mutation frequency, yeast strain W303 carrying *top2* Phe1025Tyr Arg1128Gly (pDEDyTop2) ~50-100 yeast cells were inoculated and grown overnight then plated to selective media (SC- Ura⁻ or L-canavanine). The mutation rate was calculated from the measured mutation frequencies using the online fluctuation analysis calculator (FALCOR)[406]

3.3.6   Sanger sequencing and sequence analysis

Yeast genomic DNA was extracted from the CAN^R yeast by zymolase procedure[344,345]. The 2.4Kb *can1* gene was PCR amplified using the IPROOF high-fidelity PCR kit (Primers are shown in Table 3.2). Primer DNA was removed from the PCR product with the DNA gel extraction and PCR cleanup micro kit (Thermofisher,

K0831). DNA products were sent to UIC core facility iLAB for Sanger DNA sequencing. DNA sequences were analyzed for mutations against the known wild type *CAN1* coding sequence (NCBI RefSeq[407]) using DNA sequence alignment software (Snapgene[349], APE freeware, or DNASTAR Lasergene 9 'SeqMan'[350]).

Table 3.2 PCR conditions and primers used in chapter 3.

PCR conditions and Sequencing primers	Primer Name	DNA sequence (5' to 3')
CAN1 gene PCR: 46.6°C ann, 77 secs elong, 2.4 Kb product (Bio-Rad iProof)	5'CAN1PROM	GGCCACAGAACCGTATT
	CAN1 D	CTTTTCGGTGTATGACTTATGAGG
R1 (For Sequencing)	CAN1 R1	CCCAAAAAATACTAATCC
R2 (For Sequencing)	CAN1 R2	TCCTTGACAGGAATTTAG
R3 (For Sequencing)	CAN1 R3	GAGGGTGAGAATGCGAAATGG
F2 (For Sequencing)	CAN1 F2	TGGTTACATGTATTGGTTTTCTTG

3.3.7 Overexpression and purification of yeast *Top2* mutant proteins

As described in chapter 2, *S. cerevisiae* strain JEL1 *top1⁻* was used for protein overexpression and purification. Arg1128Gly and Phe1025Tyr/Arg1128Gly mutations were constructed in inducible yeast vector (pGAL1TOP2) by site directed mutagenesis. Cell growth and induction of yTop2 mutant protein was conducted as described in chapter 2[33]. Transformed JEL1 top1Δ strains were grown in URA⁻ induction media to a cell concentration measured by absorbance at 600nm ~0.7 ODU/mL. 20% Galactose was added to the cell culture (2% final concentration) to induce the yeast to produce *Top2* mutant protein, these yeast were incubated at 30°C for 10-14 hours, shaking at 280rpm. After the incubation yeast were harvested using the Beckman Coulter Avanti® J-E high-speed centrifuge, rotor JLA 10.500, 6000RPM for 15min at 4°C, frozen with liquid nitrogen and stored at -80°C. Yeast *Top2* proteins were purified using hydroxyapatite

(HAP) described in Chapter 2[351]. The *Top2* HAP purification protocol and buffer recipes are included in Appendix B.

3.3.8 Topoisomerase assays

The topoisomerase assays described in chapter 2 were carried out in this chapter as described.

3.3.9 Yeast modified *in vivo* complex of enzyme assay

The modified yeast in vivo complex of enzyme (ICE) assay was performed on yeast carrying plasmids that expressed yTop2 with a c-terminal hemagglutinin (HA) epitope tag[408]. Yeast cells were lysed using (1mM ETDA, 6M guanidinium thiocyanate, 1% Sarkosyl, 10mM Tris HCl, pH 7.5, 4% Triton X100) and mechanical glass bead homogenization. Cell debris was pelleted by centrifugation. The DNA was purified from the cell lysate supernatant by diluting 150% (w/v) CsCl then ultracentrifugation (18 hours, 42000 revolutions per minute at 25°C) (RPM) in NVT 65.2 rotor (Beckman Coulter). The DNA pellet was ethanol precipitated then resuspended in (10mM Tris, pH 8.0, 1mM EDTA buffer). The DNA concentration was quantified, and then digested with microccocal nuclease. Equal quantities of DNA (10μg) were loaded onto an SDS-PAGE gel for electrophoresesis then transferred to a nitrocellulose membrane. Top2cc were detected by immunoblot with anti-yTop2 antibody and anti-HA antibody (Santa Cruz). Double stranded DNA was immunodetected as a loading control with anti-dsDNA antibody (Abcam).

3.4 Results

3.4.1 Examination of the mutagenic consequences of exposure to etoposide

The goal of this project was to identify the mechanisms in yeast that drive the formation of mutations. To accomplish this I utilized two approaches-treating yeast cells with etoposide and using a newly characterized mutant top2 that generates high levels of drug independent cleavage. To characterize the development of mutations in yeast I utilized the yeast *CAN1* forward mutation assay to measure mutation frequency and analyze mutation types.

3.4.2 A yTop2 mutant allele (Phe1025Tyr Arg1128Gly) that mimics drug action

Previously characterized alleles of Top2 have proven to be incredibly useful tools for exploring numerous aspects of topoisomerase biology. In 2008 our lab published a genetic screen to identify mAMSA hypersensitive yeast alleles[314]. One of the mutants identified in the screen was near the C-terminal gate (Leu1052Ile) of yeast *Top2*. As this mutation was located distant from site of DNA cleavage and religation, our lab carried out an additional screen targeting amino acids 900-1250. This fragment the yTop2 coding sequence was PCR amplified with error-prone PCR and co-transformed with linearized plasmid (pDEDyTop2) into the JN362a t2-4 yeast strain[311]. The yeast *Top2* was reconstituted by homologous recombination *in vivo*. This approach identified two independent yeast isolates carrying mutations in the C-terminal gate (Arg1128Gly and Phe1025Tyr Arg1128Gly) that confer hypersensitivity to mAMSA and etoposide.

These mutations were constructed in pDEDyTop2 and transformed into recombination deficient yeast strain JN332at2-4, which is deleted for Δ*rad52*. This yeast strain additionally carried plasmid ypGAL:*RAD52*, which expresses *RAD52* under

control of the *GAL1* promoter. Therefore yeast that were transformed and grown on galactose containing media were DNA repair proficient and those that were grown on glucose were recombination deficient.

We found that the plasmids were transformed readily into yeast cells plated to galactose media (Figure 3.2 A) whereas only yeast carrying wild type yTop2 (pDEDyTop2) formed colonies on glucose. These results suggested that the Arg1128Gly and Phe1025Tyr Arg1128Gly mutant alleles were deleterious when expressed in recombination deficient yeast strains.

To verify this finding we streaked JN332at2-4 yeast carrying pGAL1RAD52 and (pDEDyTop2 wild type, Arg1128Gly or Phe1025Tyr/Arg1128Gly) on SC-URA⁻ glucose and galactose (Figure 3.2 B). We observed that yeast carrying the pDEDyTop2 wild type was able to grow on SC-URA⁻ galactose and glucose media. Yeast carrying Arg1128Gly or Phe1025Tyr/Arg1128Gly mutant alleles were not able to grow on glucose. These results suggested that the mutant yTop2 alleles were causing cytotoxic DNA damage in yeast cells.

Figure 3.2 Yeast *Top2* alleles that exhibit a Top2 self-poisoning phenotype
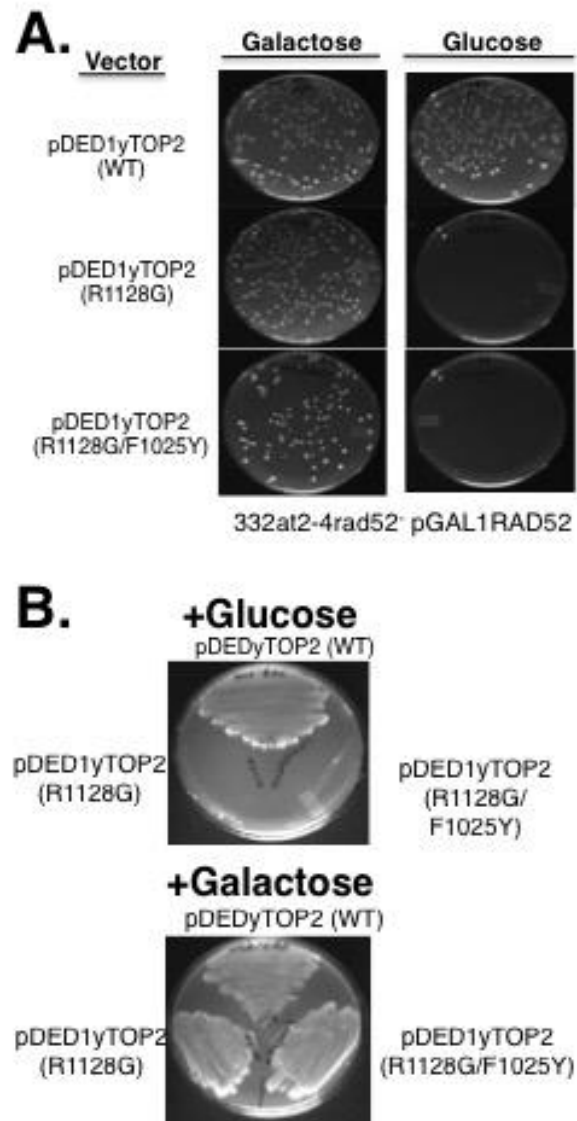
Figure 3.2 Evaluation of recombination deficient yeast expressing yTop2 wild type, Arg1128Gly, or Phe1025Tyr/Arg1128Gly. **A.** JN332at2-4 yeast carrying ypGAL:*RAD52* were independently introduced to pDEDyTop2 (wild type, Arg1128Gly, or Phe1025Tyr/Arg1128Gly) and then plated onto SC-URA⁻ media with glucose or galactose. Yeast carrying pDEDyTop2 wild type were able to form colonies on glucose and galactose. Yeast carrying Arg1128Gly, or Phe1025Tyr/Arg1128Gly mutant alleles were able to form colonies on SC-URA⁻ galactose but not on SC-URA⁻ glucose. **B.** JN332at2-4 yeast carrying ypGAL:*RAD52* and pDEDyTop2 (wild type, Arg1128Gly, or Phe1025Tyr/Arg1128Gly) were streaked onto SC-URA⁻ media with glucose or galactose. Yeast carrying Arg1128Gly, or Phe1025Tyr/Arg1128Gly mutant alleles were able to grow on SC-URA⁻ galactose but not on SC-URA⁻ glucose. Dr. Anna Rogojina carried out this experiment.

3.4.3   Biochemical properties of yTop2 Arg1128Gly and Phe1025Tyr/Arg1128Gly

The Arg1128Gly and Phe1025Tyr/Arg1128Gly mutant proteins were purified using Hydroxyapatite (HAP) chromatography. To assess the topoisomerase activity of the mutant proteins we assayed relaxation activity with negatively supercoiled pUC18 plasmid DNA. Purified Arg1128Gly and Phe1025Tyr/Arg1128Gly mutant proteins both exhibited reduced relaxation activity compared to the wild type enzyme (Figure 3.3 A). We observed complete relaxation activity of supercoiled plasmid at ~13-25ng of wild type yTop2 enzyme. The yTop2 mutant proteins (Arg1128Gly and Phe1025Tyr Arg1128Gly) exhibited slightly reduced levels of relaxation activity compared to wild type achieving complete relaxation with ~25ng of enzyme.

We next assessed the level of enzyme mediated DNA cleavage for the Arg1128Gly and Phe1025Tyr Arg1128Gly mutant proteins in the absence of drug with the plasmid cleavage assay (Figure 3.3 B). The wild type enzyme exhibited an increase in nicked DNA in response to increasing concentrations of enzyme. Both of the mutant proteins exhibited significant increases in DNA double strand breaks in response to increasing concentrations of enzyme (Figure 3.3 C). These findings indicated that the mutations confer a self-poisoning characteristic to yTop2 when expressed in cells.

Figure 3.3 Biochemical properties of Arg1128Gly/Phe1025Tyr
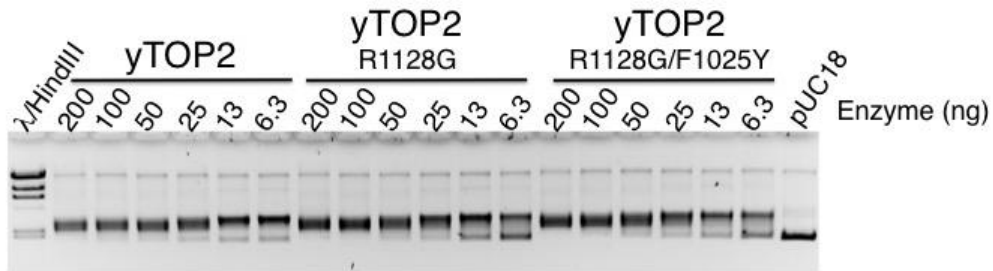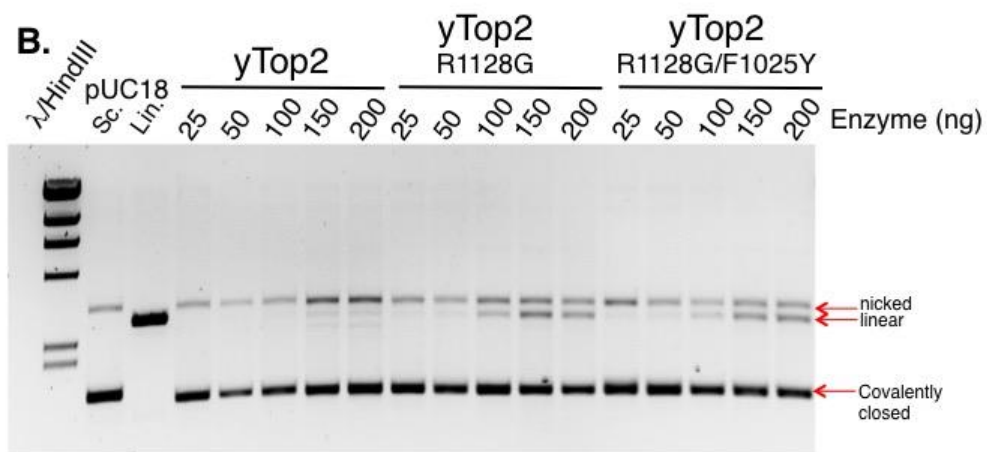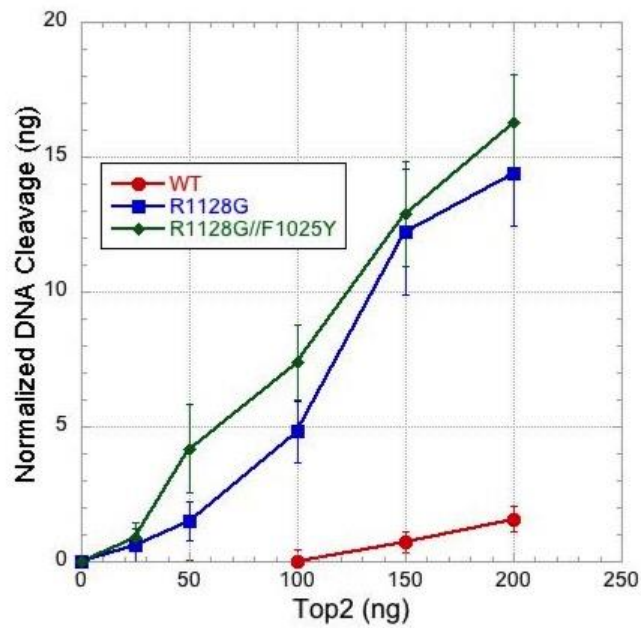
Figure 3.3 Catalytic strand passage activity of purified yTop2 R1128G and F1025Y R1128G mutant proteins compared to wild type enzyme using 200ng negatively supercoiled plasmid DNA (pUC18) and the amount of enzyme indicated above each well. All assays were carried out at least three times. **A.** Relaxation activity of purified yTop2 comparing wild type enzyme to purified mutant proteins (R1128G and F1025Y R1128G). The wild type yTOp2 exhibited complete relaxation of the 200ng of plasmid DNA at ~13-25ng of enzyme. The yTop2 R1128G and F1025Y R1128G mutant proteins exhibited a slightly reduced relaxation activity with complete relaxation of plasmid DNA at ~25ng of enzyme. **B.** ATP-dependent yTop2 mutant protein mediated DNA cleavage of 200ng negatively supercoiled plasmid DNA (pUC18) compared to wild type enzyme. The lanes labeled Sc. contain 200ng supercoiled pUC18 DNA and the lanes labeled Lin. contain 50ng ECORI linearized pUC18 DNA. The mobility of nicked, linearized and covalently closed DNA are labeled to the right of each gel. The level of drug independent, enzyme mediated DNA cleavage. The wild type enzyme exhibited increases in nicked DNA band intensity in response to DNA cleavage. **C.** Quantitation of Top2 mediated DNA cleavage described in **B.**, error bars represent the standard deviation of at least three experiments.

3.4.4 <u>The mutagenic consequences of etoposide exposure in yeast</u>

I set out to characterize the mutagenic consequences of exposure to etoposide in yeast. To increase the level of etoposide induced Top2 poisoning I used yeast carrying plasmid DNA (pDEDyTop2) to overexpress the yeast Top2 protein ~10 fold greater than the endogenous protein[311]. Plasmid DNA (empty vector or pDEDyTop2) was independently introduced into yeast strain YMM10. Yeast carrying plasmid DNA were exposed to various concentrations of etoposide (0 (DMSO), 5, 10, or 50 μg etoposide/mL) for 2 hours then plated to selective media (SC-URA⁻ or L-canavanine). The mutation frequency was calculated as the ratio of colonies that formed on L-canavanine media compared the colonies that grew on SC-URA⁻ Media.

I found that yeast carrying the overexpression vector for yTop2 exhibited increased mutation frequency for all concentrations of etoposide compared to yeast carrying the empty vector (Figure 3.4 A). At the highest concentration of etoposide (50μg etoposide/mL) the mutation frequency of yeast overexpressing yTop2 significantly increased (~5 fold) greater than yeast carrying empty vector (p-value:0.0166).

Genomic DNA was extracted from individual canavanine resistant (CAN^R) yeast colonies. The *can1* gene was PCR amplified and sequenced to identify the spectrum of *can1* mutations (Figure 3.4 B). Yeast exposed to DMSO exhibited primarily base substitutions (65.5%) and deletions (29.9%). However, yeast exposed to etoposide exhibited a substantial increase in the proportion of duplications (from 0% to 15.4%) and single base pair insertions (from 0% to 8.3%). These findings suggest that the observed *can1* mutations are from the mis-repair of etoposide induced DNA damage.

Figure 3.4 Etoposide induced mutations in *can1*
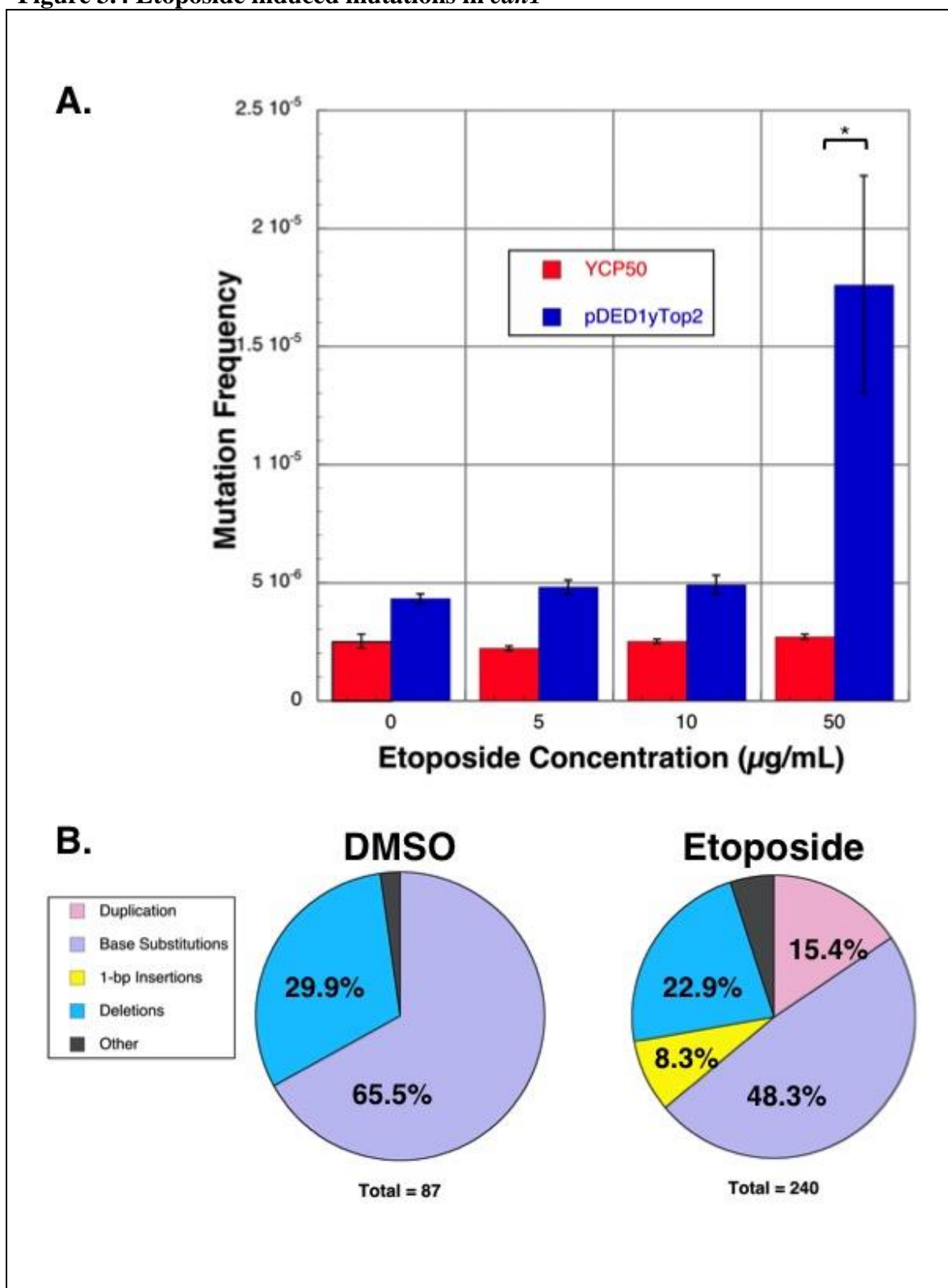
Figure 3.4 Etoposide induced mutation frequency and spectra using the *CAN1* forward mutation assay. **A.** Mutation frequency determined by the *CAN1* forward mutation assay of yeast cells exposed to etoposide. Yeast carrying empty vector (YCP50) or yTop2 (pDEDyTop2) plasmid DNA were exposed to various concentrations of etoposide (0 (DMSO), 5, 10, or 50 µg etoposide/mL) for 2 hours then plated to selective media (SC-URA⁻ and L-canavanine). Yeast over-expressing yTop2 exhibited elevated mutation frequency for all concentrations of etoposide, at the highest concentration of etoposide a significant ~5 fold increase was observed in mutation (p-value:0.0166). *Denotes a p-value: <0.05 calculated using student's t-test for independent samples.
B. The *can1* mutational spectra observed comparing yeast exposed to DMSO (left, number of mutations: 87) to yeast exposed to etoposide (right, number of mutations: 240). Yeast exposed to etoposide exhibited greater proportion of duplication (15.4%) and single base pair insertions (8.3%) compared to DMSO treated cells.

3.4.5   Role of NHEJ and *TDP1* in etoposide induced mutations

To probe the genetic requirements for the mutagenic consequences of etoposide I measured mutation frequency using the *CAN1* forward mutation assay using YMM10 yeast strains deleted for genes essential for NHEJ mediated DNA repair. Yeast deleted for *tdp1* were also examined as the *tdp1* protein can be involved in processing the trapped Top2 covalent complex by hydrolyzing the phosphotyrosyl protein-DNA covalent bond.

The yTop2 over expression vector pDEDyTop2 was introduced into YMM10 yeast strains carrying deletions for Δk*u70*, *dnl4*, or *tdp1*. Yeast were exposed to various concentrations of etoposide for 2 hours then plated to selective media (SC-URA⁻ or L-canavanine). The mutation frequency was calculated as the ratio of colonies that formed on L-canavanine media compared the colonies that grew on SC-URA⁻ media.

We observed a significant increase in the mutation frequency at the highest concentration of etoposide for Δ*tdp1* and Δ*dn4* yeast strains compared to wild type (p-value:0.005 and 0.0175 respectively) (Figure 3.5 A). These findings suggested that *TDP1* and *DNL4* are involved in the repair of Top2 mediated DNA damage and could influence DNA repair fidelity.

The mutational spectra observed in *tdp1* yeast comparing DMSO and etoposide exposure (Figure 3.5 B). There were no significant differences in the proportion of mutations observed in Δ*tdp1* yeast exposed to etoposide or DMSO. However, Δ*tdp1* yeast exhibited a large reduction in the proportion of etoposide-induced duplication events compared to wild type yeast (from 15.4% to 9.0%). These findings suggested that *TDP1* might be important for the formation of some etoposide induced DNA duplications and single base insertions in yeast.

Figure 3.5 Genetic details associated with etoposide induced mutation frequency
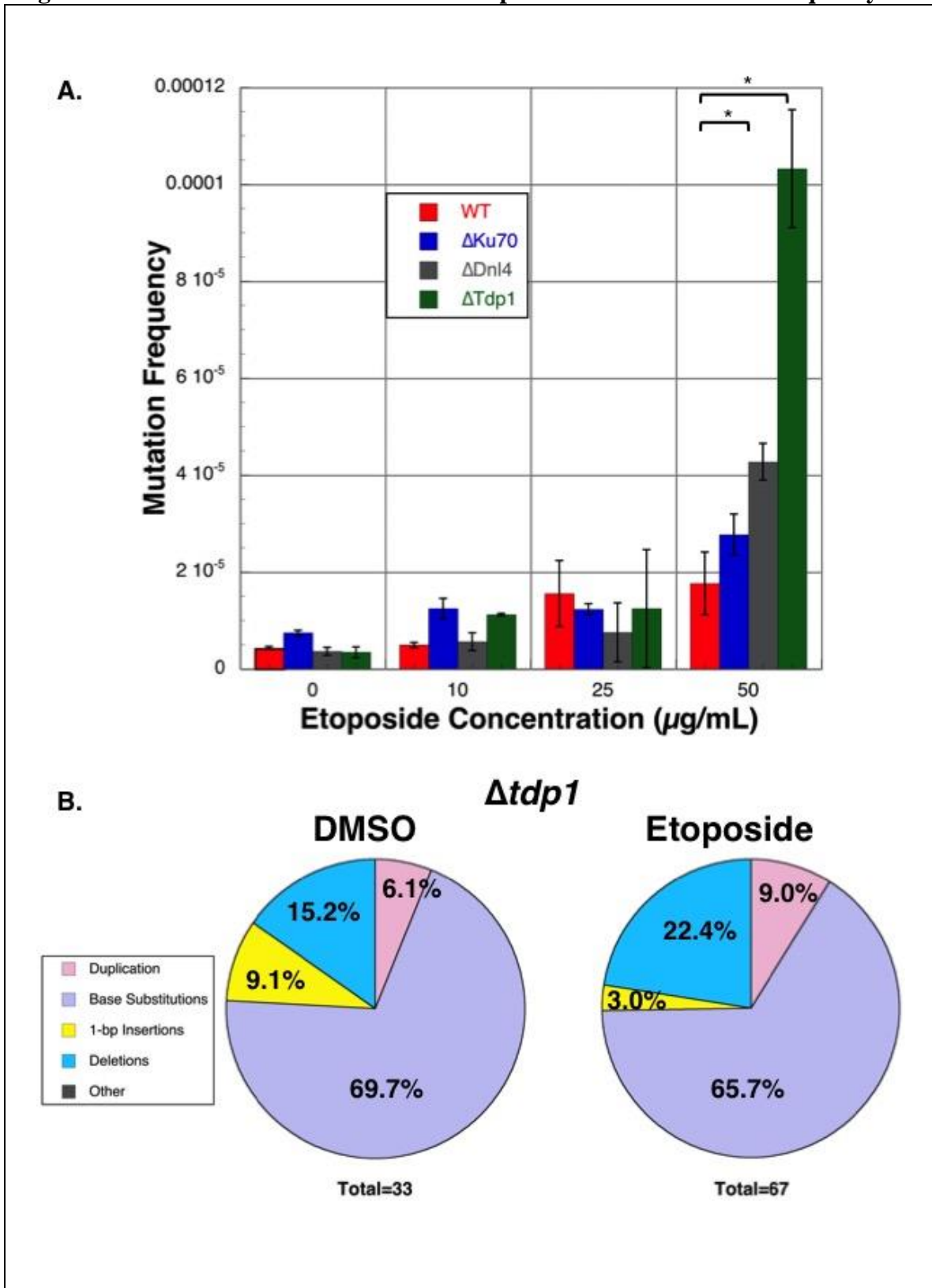
Figure 3.5 The role of NHEJ in the mis-repair of etoposide induced DNA damage. We measured the mutation frequency in yeast strain YMM10 deleted for important factors involved in NHEJ DNA repair (Δ*ku70*, *dnl4*, or *tdp1*). **A.** YMM10 yeast carrying these gene deletions were transformed with pDEDyTop2 to overexpress yTop2. Yeast were exposed to various concentrations of etoposide (0 (DMSO), 10, 25, or 50 μg etoposide/mL) for 2 hours then plated to selective media (SC-URA⁻ and L-canavanine). Mutation frequency was calculated as the ratio of yeast cells that grew on L-canavanine compared to those that grew on SC-URA⁻. **B.** The proportion of *can1* mutation spectra observed in YMM10 yeast carrying Δ*tdp1*-comparing DMSO exposed yeast (left, number of mutations: 33) to etoposide-exposed yeast (right, number of mutations: 67). There was no significant difference in the proportions of mutations observed in Δ*tdp1* yeast exposed to etoposide compared to DMSO.

       *Denotes a p-value: <0.05 calculated using student's t-test for independent samples.

3.4.6 <u>Unique mutation events observed in the *CAN1* forward mutation assay</u>

In the characterization of *can1* mutations in etoposide exposed yeast cells I identified several unique mutations including tandem duplications (ranging from 20-40 base-pairs) and deletions (ranging from 9 to 336 base-pairs) (Figure 3.6 A). We were interested in identifying more of these unique events.

Therefore, we next piloted an array of approaches to use the self-poisoning Top2 allele (Phe1025Tyr Arg1128Gly) to further characterize the mechanisms behind the genesis of these mutations. We expressed the yTop2 Phe1025Tyr/Arg1128Gly mutant allele as an etoposide mimic in yeast cells. Yeast carrying pDEDyTop2 Phe1025Tyr Arg1128Gly were grown for 3 days then plated to selective media (SC-URA⁻ or L-canavanine). With this approach we observed several unique mutations for yeast expressing the self-poisoning allele of top2 and yeast exposed to etoposide: large duplications (20-40 base-pairs) and deletions (7 to185 base-pairs) (Figure3.6 B). However, we quickly realized that these experiments would not generate enough of these unique mutations to draw strong conclusions. Therefore we collaborated with Sue Jinks-Robertson, at Duke University, to further pursue the mechanisms that drive these mutations in yeast.

Figure 3.6 Unique *can1* mutations identified in yeast

A. **Etoposide Induced Mutations**

336nt Deletion
1501 ...AGCATTTGGTGCGGCCAATGGTTACATGTA GGTTCTTAGGTTGGGTTTCCT
CTTTGATTA... 1845

TTGGTTTTCTTGGGCAATCACTTTT//ATATCTAAGGATAAAAACGAAGGGA

38nt Tandem Duplication
2561 ...ATGGTGTTAGCTTTGCTGCCGCCTATATCTCTATTTTCCTGTTCTTAGCT GTTTGGATCTTA
TTTCAATGCATATTCAGATG... 2640

TTGCTGCCGCCTATATCTCTATTTTCCTGTTCTTAGCT

B. **Self-poisoning Top2 Induced Mutations**

83nt Deletion
763 ...TGTGGTGCTGGGGTTACCGGCCCAGTTGGA TTCCTCTTTGATTAACGCTGCCTTCACATT... 876

TTCCGTTATTGGAGAAACCCAGGTG//ACGAAGGGAGGTTCTTAGGTTGGGT

185nt Deletion
1299 ...CGTTACTGCTGCATTTGGCGCTTTGGCTTA TTATGCGGCCACATTTATGACGATCATTAT... 1515

CATGGAGACATCTACTGGTGGTGAC//CTAAATTAATGCCCGGCTTGGCTTA

49nt Tandem Duplication
740 ...GTTTGTGGTGCTGGGGTTACCGGCCCAGTTGGATTCCGTTATTGGAGAAACCCAGGTGC CTGGGGTCCAGG
TATAATATCT...825

CTGGGGTTACCGGCCCAGTTGGATTCCGTTATTGGAGAAACCCAGGTGC

152

Figure 3.6 Unique *can1* mutations identified in YMM10 yeast exposed to etoposide or yeast overexpressing the self poisoning yTop2 allele Phe1025Tyr Arg1128Gly. **A.** Unique *can1* mutations identified in YMM10 yeast exposed to etoposide. Top: 336 base pair deletion, identified in YMM10 Δ*tdp1* yeast carrying pDEDyTop2 exposed to 50μg etoposide/mL yeast for 2 hours. Bottom: 38 base pair tandem duplication with microhomology (orange), identified in YMM10 Δ*tdp1* yeast carrying pDEDyTop2 exposed to 25μg etoposide/mL yeast for 4 hours **B.** Unique *can1* mutations identified in yeast carrying Phe1025Tyr Arg1128Gly. Top: 83 base pair deletion. Middle: 185 base pair deletion. Bottom: 49 base pair tandem duplication with microhomology (orange).

3.4.7 <u>Mutation spectra using self-poisoning etoposide mimetic</u>

In collaboration with Sue Jinks-Robertson's laboratory, at Duke University, we performed fluctuation assays using the *CAN1* forward mutation assay to measure mutation frequencies in yeast carrying the Phe1025Tyr/Arg1128Gly mutant allele. Plasmid (pDEDyTop2) DNA carrying the wild type yTop2, Phe1025Tyr/Arg1128Gly or empty vector were independently introduced into yeast strain W303[403]. The *CAN1* mutation rate was calculated from the median mutation frequency using the online fluctuation analysis calculator (FALCOR)[406].

The *CAN1* mutation rate exhibited by yeast overexpressing *TOP2* was similar to yeast carrying the empty vector (Figure 3.7 A). Yeast carrying the yTop2 Phe1025Tyr/Arg1128Gly mutant allele exhibited a (3.6 fold) higher mutation rate compared to those carrying the wild type enzyme.

The *can1* mutational spectra were characterized for yeast carrying empty vector, overexpressing yTop2 wild type or Phe1025Tyr/Arg1128Gly mutant allele (Figure 3.7 B). Yeast carrying empty vector or yTop2 wild type exhibited very similar proportions in their spectra of mutations, which were primarily base substitutions (75.6% and 74.7%, respectively) and deletions (19.7% and 19.1%, respectively). Yeast carrying the Phe1025Tyr/Arg1128Gly mutant allele exhibited a significantly higher proportion of duplications (38.6%) and single base insertions (10.5%) instead of base substitutions (33.8%) and deletions (16.2%). The spectrum of mutations observed in yeast carrying the Phe1025Tyr/Arg1128Gly mutant allele was highly similar to the etoposide induced mutation spectra identified (Figure 3.4 B).

Figure 3.7 Mutational spectra of yeast carrying etoposide mimetic yeast top2 allele
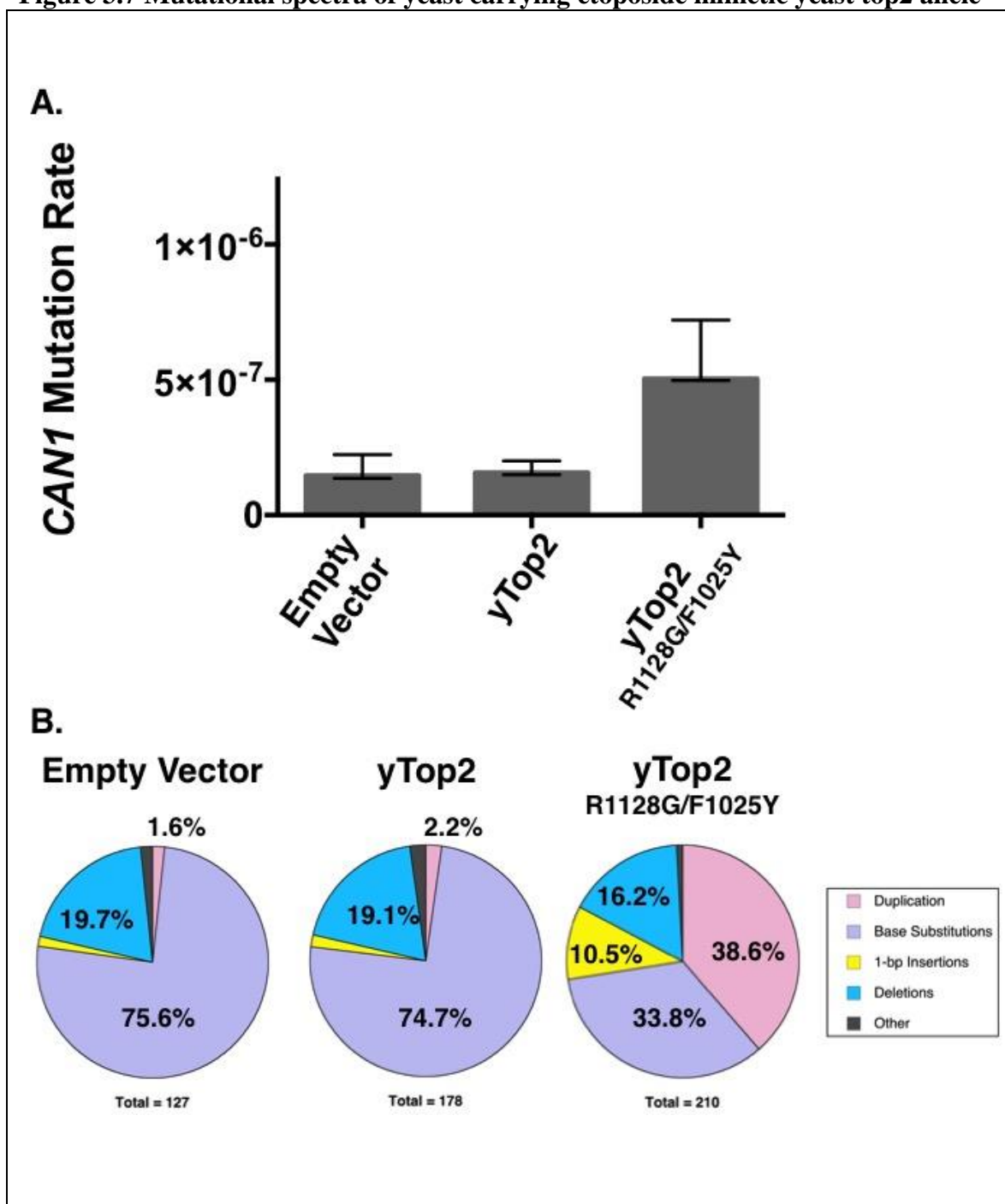
Figure 3.7 Evaluation of mutations induced yeast Top2. The *CAN1* mutation rates of yeast carrying empty vector (yCP50), yTop2 wild type or F1025Y/ R1128G mutant allele were compared. The proportion of *can1* mutations identified in these strains.
A. The mutation rate of yeast carrying empty vector (yCP50), yTop2 wild type or F1025Y R1128G. Mutation rate was calculated using the Fluctuation AnaLysis CalculatOR (FALCOR) available at: www.mitochondria.org/protocols/FALCOR.html. The mutation rate of yeast expressing the empty vector was 2.1×10^{-7}. The mutation rate of yeast overexpressing yTop2 wild type was 1.88×10^{-7}. The mutation rate of yeast overexpressing the F1025Y R1128G mutant allele was 6.68×10^{-7}. Error bars represent the 95% confidence interval of the mutation rate. **B.** The proportion of *can1* mutation spectra observed in yeast empty vector (yCP50) (left, number of mutations 127), yTop2 wild type (center, number of mutations 178) or F1025Y R1128G mutant allele (right, number of mutations 210). While yeast carrying empty vector (yCP50) and yTop2 wild type (pDEDyTop2) no significant difference in the proportions of mutations observed, yeast carrying yTop2 F1025Y R1128G mutant allele exhibited a significantly higher proportion of duplications (38.6%) and single base pair insertions (10.5%) instead of base substitutions (33.8%) and deletions (16.2%). Nicole Stantial from Sue Jinks-Robertson's laboratory, at Duke University, carried out these experiments.

.

3.4.8   <u>Genetic requirements for Top2 mediated mutagenesis</u>

In further collaboration with Sue Jinks-Robertson's laboratory, at Duke University, we next characterized the genetic requirements for Top2 induced mutagenesis. Based on the results we observed in exposing cells to etoposide several genes were examined that had the potential to contribute to the development of duplication events. The mutation frequency was measured using the *CAN1* forward mutation assay in yeast cells overexpressing the yTop2 Phe1025Tyr/Arg1128Gly mutant allele. Yeast mutation rates and mutation spectra were examined in yeast deleted for *dnl4*, *pol4*, or *tdp1*.

Similar mutation rates were observed wild type yeast cells overexpressing the yTop2 Phe1025Tyr/Arg1128Gly mutant allele compared to those deleted for *tdp1* (Figure 3.8 A). The median mutation rates for *dnl4*, *tdp1*, and *pol4* overexpressing the yTop2 Phe1025Tyr/Arg1128Gly mutant allele were (5.04×10^{-7}, 3.88×10^{-7}, and 2.91×10^{-7}, respectively) compared to wild type yeast cells 6.68×10^{-7}.

The *can1* mutations were characterized for wild type yeast cells overexpressing the yTop2 Phe1025Tyr/Arg1128Gly mutant allele and compared to those deleted for *tdp1* (Figure 3.8 B). Yeast cells deleted for *tdp1* exhibited decreases in duplication events (from 38.6% to 6.6%). These data suggest that *TDP1* mediated repair of Top2 induced DNA damage may participate in the formation of tandem duplications and single base insertions. The repair of Top2 induced DNA damage in yeast cells deleted for *tdp1* instead introduces base substitutions and deletions. Yeast cells deleted for *dnl4* and *pol4* exhibited altered proportions of duplications (from 38.6% to 6.7% and 16.9%,

respectively). These findings suggested that NHEJ plays an important role in the formation of the duplication events and the mis-repair of Top2 induced DNA damage.

To validate this finding Sue Jinks-Robertson's laboratory, utilized an *mre11* allele (Asp56Asn) that lacks endonuclease activity, which is capable of removing the phosphotyrosyl-DNA lesion by cleaving the DNA strand to release a phosphotyrosyl linked oligonucleotide[409]. Yeast carrying *mre11* Asp56Asn as well as the yTop2 Phe1025Tyr/Arg1128Gly mutant allele exhibited an increase in the proportion of duplications events (from 38.6% to 59.6%). This result strongly suggests that NHEJ was responsible for the genesis of many of the duplication mutations observed in cells carrying a self-poisoning Top2 allele.

Figure 3.8 *TDP1* is required for DNA duplications induced by self-poisoning yTop2
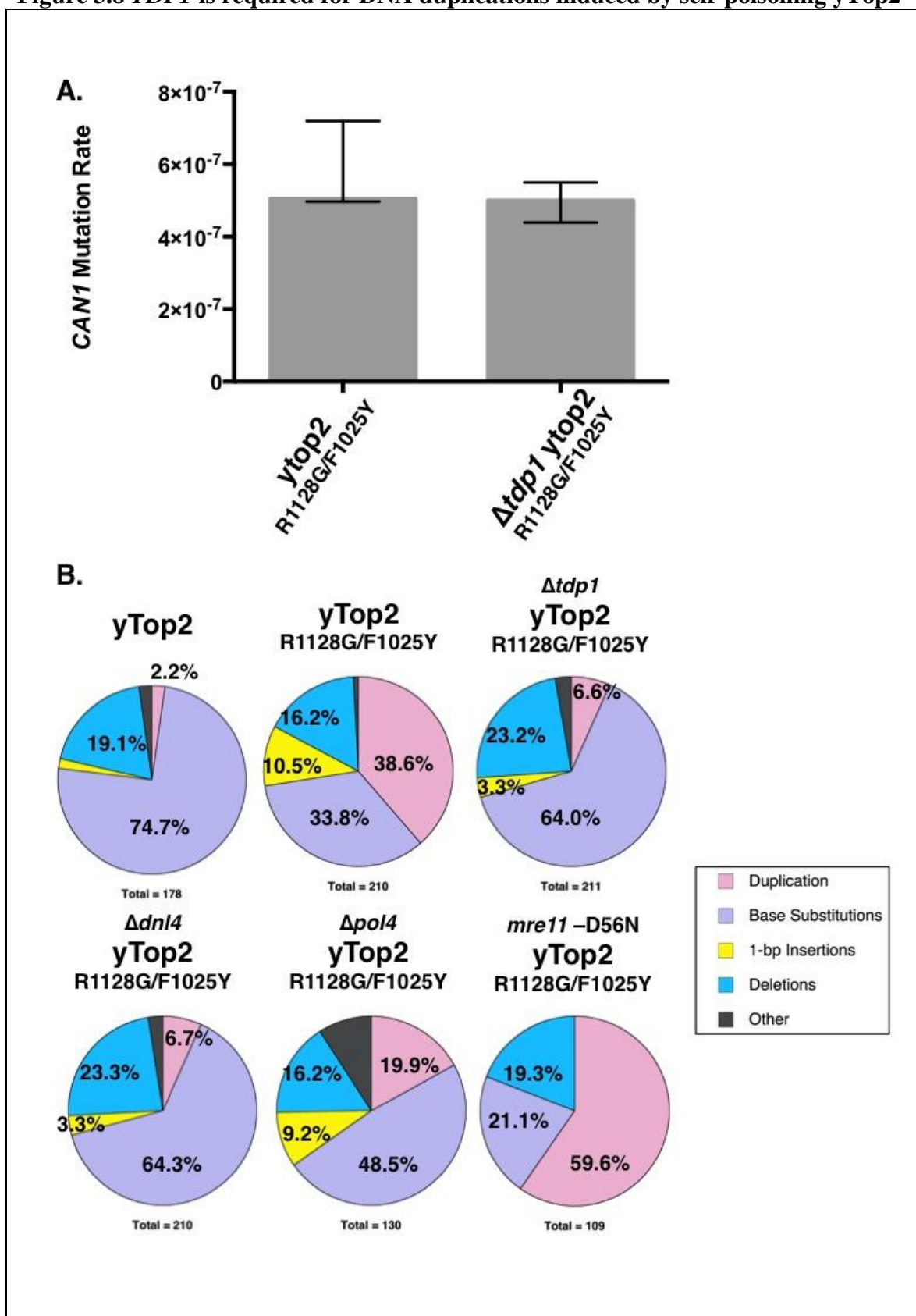
Figure 3.8 Evaluation of mutations induced yeast Top2. The *CAN1* mutation rates of yeast (*tdp1⁻* or *TDP1⁺*) carrying the yTop2 F1025Y/R1128G mutant allele were compared. **A.** The mutation rates of yeast (*tdp1⁻* or *TDP1⁺*) carrying the yTop2 F1025Y/R1128G mutant allele. Mutation rate was calculated using the Fluctuation AnaLysis CalculatOR (FALCOR) available at: www.mitochondria.org/protocols/FALCOR.html. The mutation rate of yeast overexpressing the F1025Y R1128G mutant allele was 6.68×10^{-7}. The mutation rate of $\Delta tdp1$ yeast overexpressing the F1025Y R1128G mutant allele was 5.04×10^{-7}. Error bars represent the 95% confidence interval. **B.** The proportion of *can1* mutation spectra observed in yeast carrying the yTop2 wild type or F1025Y R1128G mutant allele. Top row:yTop2 wild type (left, number of mutations 178), F1025Y R1128G mutant allele (center, number of mutations 210), or $\Delta tdp1$ yeast carrying the F1025Y R1128G mutant allele (right, number of mutations 211). Bottom row: yeast carrying the yeast Top2 F1025Y R1128G mutant allele and a deletion of (right, $\Delta dnl4$, number of mutations 210), (center, $\Delta pol4$, number of mutations 130), or (left, *mre11* Asp56Asn, number of mutations 109). Nicole Stantial from Sue Jinks-Robertson's laboratory, at Duke University, carried out these experiments.

3.5   Discussion

We set out to characterize mutations induced by etoposide in yeast and identify the mechanisms associated with their genesis. Our initial studies revealed that yeast deficient in *dnl4* or *tdp1* exposed to etoposide exhibited higher mutation frequencies. Previous studies have identified that these factors play an important role in the repair of the trapped Top2 covalent complex [268,376]. As expected, we observed that yeast deficient for *dnl4* or *tdp1* were sensitized to etoposide. The increase in mutation frequency we observed in *dnl4* yeast suggested that mis-repair of etoposide induced DNA damage could involve the participation of alternative NHEJ (alt-NHEJ) pathways, which are less well characterized. Alt-NHEJ typically involves the participation of XRCCI and either DNA ligase I or DNA ligase III[393].

Yeast deficient for *tdp1* exhibited a reduced proportion of etoposide induced duplications events suggesting that *TDP1* processing of the trapped Top2 could be involved in generating these mutations. Therefore, we would predict that a *TDP1* inhibitor would similarly reduce the proportion of etoposide induced duplication events. This finding contrasts with findings that suggest that *TDP1* plays a role in regulating the fidelity of NHEJ[410]. However, a yeast screen exploring gene overexpression and the induction of chromosomal instability identified *TDP1* overexpression as capable of inducing chromosomal instability[411].

We collaborated with Sue Jinks-Robertson's laboratory to explore the mutagenic effects more rigorously. To accomplish this we utilized a mutant allele of yeast Top2 characterized by our laboratory that exhibits high levels of nicking and double strand breaks *in vitro* as well as leads to high levels Top2 covalent complexes *in vivo*. Yeast

deficient for the *rad52* gene were not able to express this allele of yTop2. We found that yeast carrying the self-poisoning mutant exhibited elevated mutation rates suggesting this allele has strong mutagenic properties. Yeast carrying the self-poisoning mutant exhibited unique classes of *can1* mutations (duplications and singled base pair insertions).

Haploid yeast cells are known to rely on NHEJ for the repair of etoposide induced DNA damage[268,412,413]. Therefore the mutagenic consequences of trapped Top2 were explored in yeast cells deficient for key elements of NHEJ (*dnl4* or *ku70*)[393]. We found that the unique set of *can1* mutations induced by the self-poisoning mutant required NHEJ. These results suggest that the NHEJ pathway is likely the mechanism drives the formation of these unique mutations associated with Top2 mediated DNA damage. We also found that the unique set of *can1* mutations induced by the self-poisoning mutant required *TDP1*, indicating an important role for *TDP1* in the formation of these unique mutations. We found that yeast carrying *mre11* Asp56Asn antagonized to the formation of these unique mutations. The unique set of *can1* mutations induced by the self-poisoning mutant (duplications and singled base pair insertions) was very similar to those that were observed in etoposide exposed yeast cells. We speculate that the mechanisms of mutations may be similar to translocations. Together these data support the conclusion that trapped Top2 induced genome instability is dependent on NHEJ and *TDP1* in yeast.

A limitation of this study was that the conditions under which we used the *CAN1* forward mutation assay did not allow for the easy detection of chromosomal translocations. An approach to identify gross chromosomal rearrangements was developed through the work of Richard Kolodner[398,399,401,414].

In this chapter we used a self-poisoning allele of yeast Top2 in wild type cells to study the mutagenic effects of Top2 poisoning in yeast. We observed strong mutagenic properties in yeast cells carrying this allele. These data show that top2 mutations can be genotoxic and cytotoxic. Therefore these data predict that certain top2 mutations could play a role in human disease. In the next chapter we characterized a mutant allele that causes human disease and has these properties.

4   A SELF POISONING MUTATION IN TOP2 LINKED TO HUMAN DISEASE

4.1   <u>Summary</u>

In a recent case report, a patient exhibiting global developmental delay and autism spectrum disorder (ASD), a *de novo* mutation was identified in Top2β[1]. This mutation conferred by a single amino acid substitution that replaced His63 with tyrosine. While the case report suggested that the mutation may have been causative for the disease, other potential mutations were not described in the case report. Therefore it was important to examine the potential biochemical consequences of this mutation. His63 is located in a highly conserved region of the ATPase domain of Top2β. Our lab previously characterized several mutations in Top2α (Tyr50Phe and Asp48Asn) located near this residue and we wondered whether this mutation was a loss-of-function allele. Results with a heterozygous knockout mouse mouse did not report haploinsufficiency of Top2β, suggesting that a more detailed characterization of this allele would be of interest[66].

We constructed Top2β His63Tyr in a yeast expression vector and characterized the consequences of expressing the mutant allele in yeast. Top2β His63Tyr failed to complement a *top2-4* allele at the non-permissive temperature, potentially indicating that the mutant protein lacks catalytic activity. However, expression of the Top2β His63Tyr allele in DNA recombination deficient yeast strain was deleterious, which suggested that expression of the mutant allele may cause DNA damage. Yeast expressing the Top2β His63Tyr mutant allele exhibited significantly elevated recombination rates suggesting that the expression of Top2β His63Tyr potentially misfunctions rather than having a complete lack of catalytic activity.

Based on these results, we undertook a characterization of Top2β His63Tyr by overexpression and purification of the mutant protein. The purified Top2β His63Tyr mutant protein was catalytically active but had reduced levels of strand passage activity. In a plasmid cleavage assay, the mutant protein generated drug-independent DNA nicking. During the course of these studies, we had difficulties in purifying both wild type and mutant Top2β, in part due to the presumed poor expression of Top2β in yeast. While we continue to carry analyses of Top2β, we decided to examine the effects of the orthologous mutant protein in the other human Top2 isoform.

We constructed the orthologous mutation in the conserved residue of Top2α (His42Tyr) and found that the expression of this mutant protein was deleterious in all yeast strains, even strains proficient in repair of DNA damage. We hypothesized that expression of Top2α His42Tyr conferred high levels of DNA damage that could not be tolerated in repair proficient yeast strains. We also found that the Top2α His42Tyr could not be expressed in yeast strains overexpressing yeast Top2, suggesting that the cytotoxic mechanism was not due to an interference with normal Top2 function.

We purified Top2α His42Tyr and showed that the mutant protein was catalytically active, although it exhibited slightly reduced levels of strand passage activity. We found that the Top2α His42Tyr mutant protein exhibited high levels of drug-independent DNA cleavage, particularly single strand nicking. The levels of drug independent nicking observed was greater than for any Top2α mutant that we have observed to date.

Based on our characterization of Top2β His63Tyr and the orthologous Top2α mutant protein, we suggest that the phenotype conferred by this mutant Top2 arises from

165

its ability to generate DNA damage, rather than a loss of topoisomerase activity. Previous work from our laboratory showed that trapped topoisomerases in the central nervous system can have neurotoxic consequences. We hypothesize that *de novo* mutations in topoisomerase genes may cause neurotoxicity due to enzyme-induced DNA damage.

Finally, this work has allowed us to identify a topoisomerase mutation that cannot be expressed in repair proficient yeast cells. Our work in the previous chapter described a "self-poisoning" Top2 allele that required repair proficiency; the work described in this chapter describes a stronger damage inducing allele. This serendipitous discovery may provide additional insights into how topoisomerases are constrained from inducing genotoxic DNA damage.

4.2   <u>Introduction</u>

A *de novo* mutation in Top2β was identified by whole exome sequencing (WES) in a 15-year-old patient exhibiting global developmental delay and autism spectrum disorder[1]. This novel mutation was identified as a single amino acid substitution that replaced His63 with tyrosine. While this case report did not provide a mechanistic link between the identified mutation and disease pathology there is evidence linking Top2β to the development neurological diseases[92,125,140,396,415].

Top2β plays important roles in transcription[164]. Top2β activity appears to be especially critical to cells in the nervous system as Top2β^{-/-} mice are stillborn since they fail to innervate the diaphragm[66]. Further analysis of the Top2β^{-/-} mice revealed that cortical neurons in the embryonic nervous system undergo apoptosis at differentiation[140]. Loss of Top2β in cells was also observed to decrease transcription of genes important to neuronal differentiation and longevity[140]. Conditional Top2β^{-/-} mouse embryos exhibited

166

aberrant lamination in neurons and aberrant neurogenesis[416]. However, heterozygous Top2β^{+/-} mice were not reported to exhibit a deleterious phenotype[66]. These studies call into question whether the neurological disease observed in the patient described above is due to the His63Tyr mutation encoding an inactive protein since haploinsufficiency would be predicted not to carry a phenotype. However, since Top2β is a dimer, expression of an inactive subunit would be predicted to have a larger effect on Top2β activity than a null allele, if one assumes that the wild type/mutant heterodimer lacks catalytic activity.

Top2β and Top1 have been identified to play a critical role in the transcription of long genes[125]. Many of the long genes affected are among those identified as Autism Spectrum Disorder (ASD) risk factors[125]. Therefore these findings suggest a connection between loss of topoisomerase function (Top1 and Top2β) and ASD/neurological development[92,396].

Autism spectrum disorders are a heterogeneous group of neurodevelopmental diseases[417]. Research in twins and population cohorts has identified a strong heritable component to these diseases[417]. While over 100 genes have been identified as rare risk factors, ASD pathogenesis remains poorly understood[418]. Some ASD patients (5-10%) present with chromosomal rearrangements, deletions, duplications and or copy number variations (CNVs)[419–421].

Ataxia telangiectasia mutated (ATM) is a protein kinase that is well known for its role in DNA damage response signaling[422]. The mutation of the ATM gene is associated with genomic instability syndrome ataxia-telangiectasia[422,423]. This neurodegenerative

syndrome caused by a deficiency in DNA repair response is phenotypically related to a number of other neuronal phenotypes associated with deficiencies in DNA repair[424].

The generation of DNA damage or defects in aspects of DNA repair has been studied in several contexts and can confer a hyper-recombination phenotype[425–427]. Hyper-recombination phenotypes (mutators) are associated with gene conversion events and genome instability[426,428–430]. One example of this phenotype is yeast cells carrying a mutant *RAD3* gene (*rad3-101* or *rad3-102*), which exhibit single strand DNA gaps that are converted into double strand breaks. The hyper-recombination phenotype is also relevant in human cells, one recently identified variant of RAD51 (Gly151Asp), involved in homologous recombination DNA repair, is associated with aggressive and therapy-resistant breast carcinomas[427].

Top2 mediated DNA damage results in a 5' phosphotyrosyl residue at the break. Specialized repair enzymes (TDP1 and TDP2) are capable of hydrolyzing the covalent bond to allow the repair of the broken DNA ends to proceed[265,377,396,397,431,432]. Loss of function mutations in TDP1 are associated with the rare neurological disease, Spinocerebellar Ataxia with Axonal Neuropathy SCAN1)[396,433–435]. Similarly, loss of function mutations in TDP2 are associated with seizures, intellectual delay and ataxia[396,436,437]. This indicates a clear mechanism for topoisomerase-induced damage to affect neuronal development.

In the previous chapter we described the characterization of a Top2 mutant allele that leads to DNA damage in a yeast system. We hypothesized that the Top2β His63Tyr that was identified recently as a neurological disease causing mutation will produce elevated levels of drug independent DNA damage. Therefore, we examined this scenario

using a yeast system to characterize potential phenotypic consequence of expressing the Top2β His63Tyr allele.

In this chapter we discuss mutant alleles of both Top2β and Top2α at the His63 of Top2β. One interesting aspect, not explored here, is that there are two alternatively spliced isoforms of Top2β, differing by five amino acids at the extreme amino terminus. The literature is unclear whether the two isoforms have differing biochemical activities, and genomic databases have been inconsistent which isoform should be considered the canonical sequence. In this chapter, I have chosen the longer isoform as the canonical sequence. Work in collaboration with the laboratory of James Berger, at Johns Hopkins University, has failed to identify significant differences between the two differentially spliced isoforms. All of the experiments in this chapter have used the shorter isoform.

4.3 Materials and methods

4.3.1 Yeast growth media

Yeast growth medium used in these experiments were described in chapter 2.

4.3.2 Yeast vector and plasmid construction

The yeast expression plasmids used for expressing mutant Top2β and Top2α alleles are summarized in Table 4.1. We used a yeast overexpression plasmid pKN17 that carries Top2β under the control of the *TPI* promoter. Due to toxicity in *E. coli,* we also modified the plasmid to include an internal *ACT1* intron at amino acid position 133. Expression of Top2βwith this construct was verified by Western blotting, and by demonstration that the intron containing plasmid complemented a yeast *top2-4* allele. The pKN17 plasmid was constructed by Dr. Karin Nitiss (plasmid map Appendix E). The pKN17 Top2β wild type plasmid was further modified to carry an amino acid substitution

to carry a His63Tyr in Top2β by oligonucleotide directed mutagenesis (Table 4.2). The

pKN17 plasmid was also modified to carry a N-terminally deleted Top2β (amino acids 1-

449), Top2β-ΔATPase. The Top2β-ΔATPase mutant was constructed using Gibson

assembly (PCR conditions and primers Table 4.3)[438].

The plasmid pMJ1 was described in chapter 2. This plasmid carries Top2α under

the control of the *TOP1* promoter. The pMJ1 plasmid was modified by oligonucleotide

directed mutagenesis to carry an amino acid substitution His42Tyr in Top2α (Table 4.2).

Table 4.1 Yeast expression plasmids used in chapter 4

Yeast expression plasmid	Description
α12URAB	Top2α with N-Terminal 6xHis tag under the control of the yeast GAL1 promoter
β12URAB	Top2β with N-Terminal 6xHis tag under the control of the yeast GAL1 promoter
ΔJMB1	Top2α with N-Terminal 6xHis tag under the control of the yeast GAL1 promoter
pKN17 with ACT1 intron	Top2β overexpression the control of the yeast *TPI* promoter
pMJ1	Top2α overexpression the control of the yeast *TOP1* promoter
yCP50	Yeast centromere containing shuttle vector (used as empty vector control)
yCPlac33	Yeast centromere containing shuttle vector (used as empty vector control)

4.3.1 Site directed mutagenesis

Plasmid DNA (pKN17 or pMJ1) was amplified using high-fidelity PCR (New

England Biolabs, Q5 PCR Kit) using a mutagenic oligonucleotide primer. PCR reactions

were treated with the DPN1 restriction enzyme for 1 hour at 37°C to digest the parental

plasmids, and then transformed in to high-efficiency *E. coli*. The incorporation of the

specific mutations in the Top2 coding sequence was confirmed by Sanger sequencing.

Table 4.2 Site directed mutagenesis primers and PCR conditions

Site directed mutagenesis PCR conditions	Primer Name	Primer Sequence (5'-3')
pKN17 Top2β His63Tyr: 56°C annealing, 240 seconds elongation, 12 Kb product (NEB Q5)	hTop2bH58Y_F	ACAACTTGAATACATTCTTC TTC
	hTop2bH58_R	GTCTTCTTCTGATACACTC
pMJ1 Top2α His42Tyr: 57°C annealing, 240 seconds elongation, 11 Kb product (NEB Q5)	hTop2aH42Y_F	ACAATTGGAATATATTTTGC TCC
	hTop2aH42_R	GTTTTCTTTTGATAGATTCTT TCAAC

4.3.2 Gibson assembly of purification vectors

Gibson assembly is a molecular cloning technique used to join multiple DNA fragments together as one reaction[438]. The ΔJMB1 and β12URAB plasmid are inducible overexpression plasmids for Top2α and Top2β, respectively[247]. These plasmids express the Top2 protein under the control of the *GAL1* promoter with a 6x histidine tag attached to the amino terminus of the protein by a peptide linker that is a substrate for a TEV protease. These plasmids were modified by using Gibson assembly to carry an amino acid substitution Top2α His42Tyr and Top2β His63Tyr (PCR conditions and primers Table 4.3)[438]. Plasmid DNA fragments were PCR amplified using high-fidelity PCR (New England Biolabs, Q5 PCR Kit), these reactions incorporated a base change to the Top2 coding sequence. PCR reactions were treated with the Dpn1 restriction enzyme for 1 hour at 37°C to digest the parental plasmids. The DNA fragments were assembled using the Gibson assembly protocol and buffer recipes included in Appendix E. Plasmid assembly and incorporation of the specific Top2 mutation was verified by Sanger sequencing.

Table 4.3 Gibson assembly primers and PCR conditions

DNA Frag. And PCR conditions	DNA Frag.	Primer Name	Primer Sequence (5'-3')
pKN17 Top2β: ΔATPase (Δaa 1-449): 59.1°C ann, 240 secs elong, Kb product (NEB Q5)	1 of 2	URA3_to_TPI_fwd	AACACATGTGGATATCTTGACTGATTTTTCCATGGAGG
		headless_Top2b_to_URA3_fwd	TTCCTGCAGCCCCATGTCATCAGTAAAATACAGTAAAATC
pKN17 Top2β: ΔATPase (Δaa 1-449): 59.1°C ann, 240 secs elong, Kb product (NEB Q5)	2 of 2	URA3_to_TPI_rev	TTACTGATGACATGGGGCTGCAGGAATTCCTG
		headless_Top2b_to_URA3_rev	AATCAGTCAAGATATCCACATGTGTTTTTAGTAAAC
ΔJMB1 His42Tyr: 59°C ann, 165 secs elong, 6 Kb product (NEB Q5)	1 of 2	hTop2aH42Y_F	ACAATTGGAAtATATTTTGCTCC
		F-URA3	AGGGCTCCCTATCTACTGGAGAATATACTAAGGG
ΔJMB1 His42Tyr: 59°C ann, 165 secs elong, 5.8 Kb product (NEB Q5)	2 of 2	hTop2aH42_R	GTTTTCTTTTGATAGATTCTTTCAAC
		R-URA3	ATATTCTCCAGTAGATAGGGAGCCCTTGCATG
β12URAB H63Y: 64°C ann, 155 secs elong, 6.2 Kb product (NEB Q5)	1 of 2	F-H63Y	ACAACTTGAAtACATTCTTCTTC
		F-URA3	AGGGCTCCCTATCTACTGGAGAATATACTAAGGG
β12URAB H63Y 63°C ann, 155 secs elong, 7 Kb product (NEB Q5)	2 of 2	R-H63Y	GTCTTCTTCTGATACACTC
		R-URA3	ATATTCTCCAGTAGATAGGGAGCCCTTGCATG

4.3.3 Yeast strains

The *S. cerevisiae* yeast strains used for experiments in this chapter . CG2009 *S. cerevisiae* yeast strain was used for experiments in this chapter, the genotype is (*a/α lys2-1/lys2-2 tyr1-1/tyr1-2 his 7-2/his7-1 leu2D/leu2D ura3D/ura3-1 trp5-d/trp5-c met13-d/met13-c ade5/ADE5 ade2/ade2*). This yeast strain was used to characterize the frequency or rate of homologous recombination gene conversion events.

Table 4.4 Yeast parental strain genotype

Yeast Strain	MAT (a/α)	Genotype	Year Published (Citation)
CG2009	a/α	*lys2-1/lys2-2 tyr1-1/tyr1-2 his 7-2/his7-1 leu2D/leu2D ura3D/ura3-1 trp5-d/trp5-c met13-d/met13-c ade5/ADE5 ade2/ade2*	Gift from C. Giroux
JEL1t1	a	*trp1, leu2, ura3-52, pbr1-1122, pep4-3, his3:: pGAL10GAL4, top1::LEU*	1993[152]
JN362a	a	*ura3-52 leu2 trp1, his7 adel-2, ISE2*	1992[311]
JN332a	a	As JN362a but *rad52::TRP1*	1992[311]
JN394t2-4	a	As JN362a but *rad52::LEU2 top2-4*	1992[311]
YMM10	a	*ura3-52; his3-Δ200; leu2-Δ1; trp1-Δ63; lys2-801amb; ade2-101oc; Δpdr18::hisG-URA3-hisG; Δpdr12::hisG; Δsnq2::hisG; pdr5::TRP1; Δpdr10::hisG; Δpdr15::loxP-KANMX-loxP; Δyor1::HIS3; Δbat1::HIS3; Δycf1::HIS3*	2001[343]
YMM10 t2-4	a	As YMM10 but *top2-4*	2001[343]

4.3.4 Fluctuation analysis

To determine the rates and frequency of homologous recombination gene conversion events in yeast we used fluctuation assay. Fluctuation assays were used to measure the frequency of recombination in yeast strains carrying various plasmids[439]. The CG2009 yeast strain is diploid and carries heteroallelic markers for several genes. Heteroallelic markers are heterozygous alleles of genes; in this case the alleles carry different inactivating mutations. To determine the recombination frequency Top2β wild type, His63Tyr (pKN17) or empty vector (YCPlac33) plasmid DNA were introduced into the CG2009 yeast strain. 50-100 yeast cells were inoculated and grown overnight at 30°C and then plated to selective media (SC- Ura⁻, His⁻, Lys⁻, or Trp⁻). The recombination frequency was calculated as the ratio of yeast colonies that formed on SC- His⁻, Lys⁻, or Trp⁻ media compared to those that formed on SC- Ura⁻. The rate of HIS+, LYS+, and

TRP+ yeast colonies was calculated using the online fluctuation analysis calculator for each of the heteroallelic markers (FALCOR)[406].

4.3.5 Overexpression and purification of human Top2 proteins in yeast

S. cerevisiae strain JEL1 *top1⁻* was used for protein overexpression prior to protein purification. We constructed the Top2α His42Tyr and Top2β His63Tyr mutants in inducible yeast plasmid vectors (ΔJMB1 or β12URAB, respectively) by Gibson assembly. Cell growth and induction of Top2α and Top2β mutant protein were conducted as described in chapter 2[33]. Briefly, JEL1 top1Δ strains with the appropriate expression vectors were grown in URA⁻ induction media to a cell concentration measured by absorbance at 600nm ~0.7 ODU/mL. 20% Galactose was added to the cell culture (2% final concentration) to induce the yeast to produce Top2α or Top2β protein; Cells were incubated at 30°C with shaking at 280rpm. Incubation times were 10-14 hours for Top2α expressing cells or for 8 hours for Top2β expressing cells, After the incubation yeast were harvested using the Beckman Coulter Avanti® J-E high-speed centrifuge, rotor JLA 10.500, 6000RPM for 15min at 4°C, frozen with liquid nitrogen and stored at -80°C.

Ni-NTA purification. Ni-NTA affinity purification was described in chapter 2[353]. These proteins carried a 6x His tag attached to the amino terminus of the Top2 protein by a peptide linker that is recognizable by a *Tobacco etched virus* (TEV) protease. After protein purification the 6x His tag was cleaved from the protein[354].

A modified Ni-NTA purification protocol was used to purify the Top2α wild type and His42Tyr proteins. The modified Ni-NTA protocol and buffer recipes are included in Appendix B. The modification to the original Ni-NTA purification protocol involved replacing the overnight protein dialysis step with a SP-Sepharose cation exchange

column. Top2α protein sample was eluted from Ni-NTA resin with a low-salt elution

buffer containing 200mM imidazole and loaded onto SP-Sepharose. As before the

purified enzyme was the 6x His tag was cleaved from the protein with TEV protease[354].

Purified protein was concentrated with Amicon Ultra Centrifuge filters; purified protein

was loaded into the filter then centrifuged for 20 minutes at 3000rpm at 4°C.

4.3.6   **Topoisomerase assays**

The topoisomerase assays described in chapter 2 were carried out in this chapter

as described above.

4.4   Results

4.4.1   Top2β His63Tyr fails to complement the topoisomerase deficiency of yeast *top2-4* strains

To measure the activity of Top2β mutant alleles expressed in yeast we first
assessed for the ability to complement the topoisomerase deficiency of yeast *top2-4*
strains. We first confirmed that expression of the wild type Top2β could complement the
topoisomerase deficiency of yeast *top2-4* strains. The pKN17 plasmid, which expresses
Top2β under the control of the *TPI* promoter, was introduced into yeast strain JN362a t_{2-4}. At the non-permissive temperature of the *top2-4* allele, 34°C, yeast carrying Top2β
wild type supported growth (Figure 4.1 A). This indicated that expression of Top2β wild
type could complement the topoisomerase deficiency in yeast. We next introduced a
mutation (His63Tyr) in the pKN17 vector by site directed mutagenesis. The pKN17
His63Tyr, wild type and empty vector were introduced into yeast strains (YMM10 t_{2-4}
and JN362a t_{2-4}) carrying a temperature sensitive allele of yTop2. At the non-permissive
temperature of the *top2-4* allele, 34°C, yeast carrying Top2β wild type supported growth
while yeast carrying Top2β His63Tyr or empty vector did not (Figure 4.1 A). Failure to
complement temperature sensitive yTop2 may indicate that the mutant allele is not active,
fails to properly localize or is unstable.

Figure 4.1 Top2β His63Tyr fails to complement *ts* yTop2
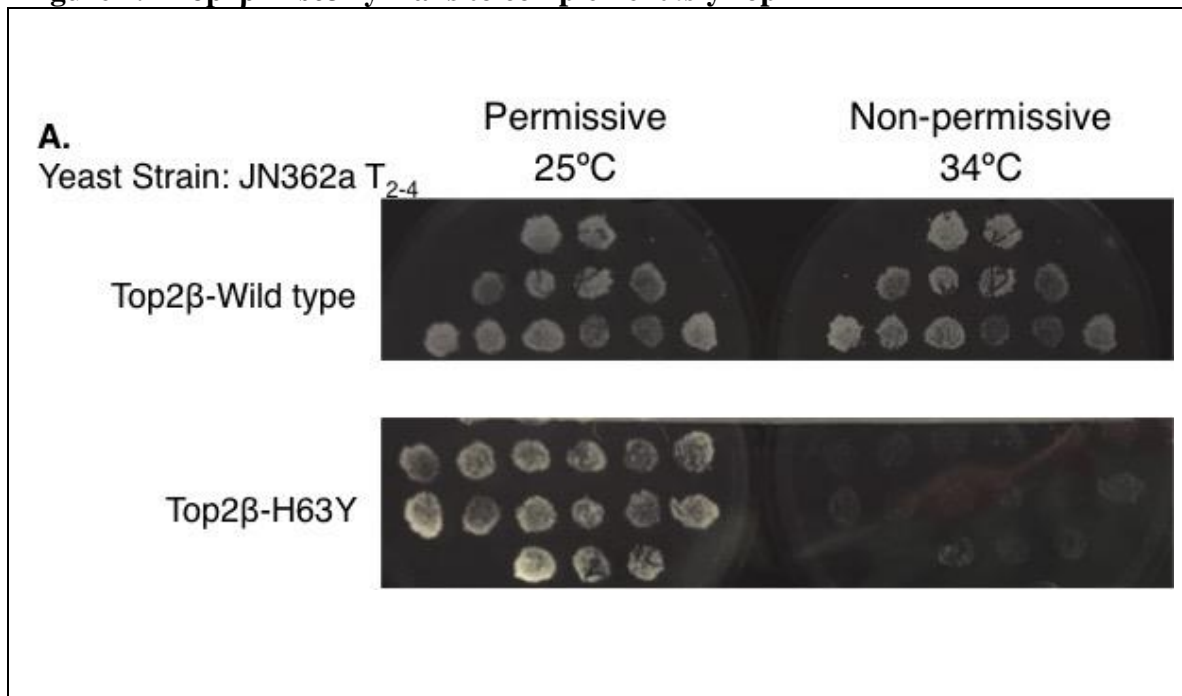
Figure 4.1 Evaluation of Top2β His63Tyr expression in yeast. The functional expression of the Top2β mutant allele was assessed by checking for complementation at the non-permissive temperature in yeast carrying temperature sensitive yTop2 allele. **A.** Independent JN362a *top2-4* yeast isolates carrying pKN17 (Top2β wild type or His63Tyr) were replica-plated from a master plate onto naïve SC-URA⁻ plates and grown at 25°C or 34°C for ~24hours. Yeast isolates carrying Top2β His63Tyr were unable to grow at 34°C which indicated that the yeast could not complement for the temperature sensitive yeast allele (*top2-4*).

4.4.2 <u>Expression of Top2β His63Tyr is deleterious in yeast</u>

We hypothesized that the mutant Top2β His63Tyr would generate DNA damage. Therefore, we next assessed if the expression of Top2β His63Tyr was deleterious in recombination deficient yeast strains. We transformed the Top2β His63Tyr plasmid (pKN17) into JN362a and JN394 yeast strains, which are isogenic except for the deletion of *RAD52* in JN394[311]. In these experiments, the yeast strains carry the wild type Top2 allele, and the ability to complement a Top2 deficiency is not a factor in these experiments. The wild type plasmid or an empty vector were readily transformed into both strains. By contrast, Top2β His63Tyr produced fewer colonies in the *rad52*⁻ strain per microgram of transforming DNA (Figure 4.2 A). Based on the results presented in chapter 3 and previous studies, Top2 alleles that exhibit high intrinsic levels of DNA damage are not tolerated in *rad52*- yeast strains[183]. Therefore, as a positive control we also introduced a truncated Top2β allele lacking the ATPase domain (amino acids:1-449) (Top2β ΔATPase), which is known to exhibit high intrinsic levels of DNA cleavage[321]. JN394 Yeast transformed with Top2β ΔATPase did not form colonies (Figure 4.2 A). These results indicated that the expression of the Top2β His63Tyr mutant allele was deleterious when expressed in a recombination deficient yeast strain.

Figure 4.2 Expression the Top2β His63Tyr alleles was deleterious in yeast
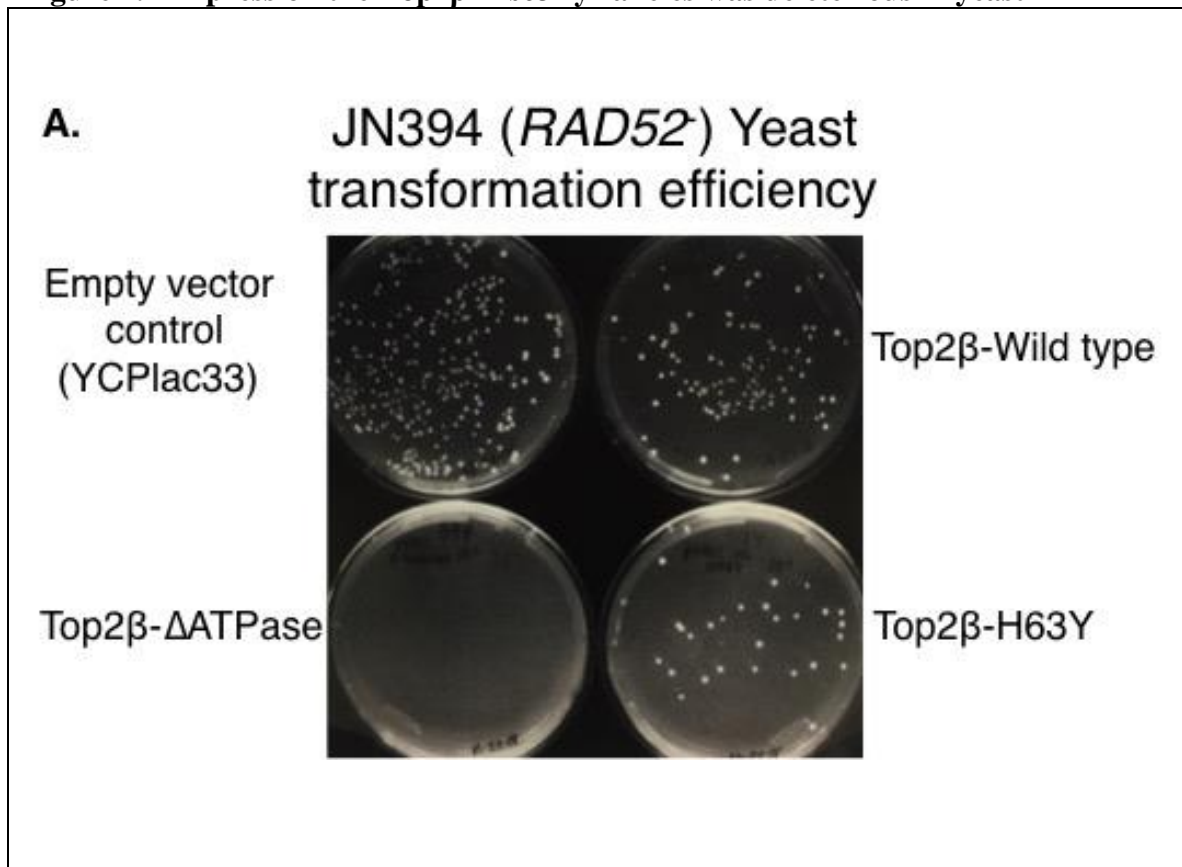
Figure 4.2 Evaluation of Top2β His63Tyr expression in yeast. The genetic requirements for expression of Top2β His63Tyr was tested by introducing the mutant alleles into yeast strains (JN362 and JN394). **A.** The results of a quantitative yeast transformation where an equal concentration and volume of plasmid DNA was introduced into yeast carrying RAD52$^+$ (JN362a) or RAD52$^-$ (JN394). Yeast transformed with pKN17 Top2β H63Y formed fewer colonies than yeast transformed with pKN17 Top2β wild type or empty vector (yCPlac33) in the RAD52$^-$ yeast strain (JN394) compared to the RAD52$^+$ (JN362a). These results showed a reduction in the transformation efficiency for Top2β His63Tyr and indicated that the expression of the mutant allele may be deleterious in yeast. As a positive control for recombination, yeast strain JN394 was also transformed with pKN17 Top2β ΔATPase, as expected this control transformation produced no colonies.

4.4.3   Top2β His63Tyr confers a hyper-recombinant phenotype in yeast

Since we found the Top2β His63Tyr was deleterious when expressed in a recombination deficient yeast strain, we hypothesized that the expression of Top2β His63Tyr would exhibit a hyper-recombination phenotype. Therefore, we independently introduced plasmids expressing Top2β alleles (pKN17) or empty vector (yCPlac33) into yeast strain CG2009, a diploid strain that carries several heteroallelic markers. Heteroallelic markers are heterozygous alleles of genes; in this case the alleles carry different inactivating mutations. We carried out fluctuation assays to determine recombination rates in yeast expressing different alleles of Top2β using *HIS7*, *LYS2* and *TRP5* genetic markers. CG2009 yeast that were able to grow and form colonies on SC-His⁻, Lys⁻, or Trp⁻ selective media underwent a recombination event that reconstitutes the associated genetic marker to restore gene function (*HIS7*, *LYS2* or *TRP5*).

To perform fluctuation assays we introduced Top2β wild type (pKN17), Top2β His63Tyr and empty vector (yCPlac33) into yeast strain CG2009. To determine the recombination rates of the transformed CG2009 yeast, ~50-100 yeast cells of 12 independent CG2009 clones were inoculated and grown overnight at 30°C then plated to selective media (SC- Ura⁻, His⁻, Lys⁻, or Trp⁻). The recombination rate was calculated using the online fluctuation analysis calculator (FALCOR)[406]. As expected, yeast carrying the Top2β wild type exhibited a slightly higher recombination rate for each of the genetic markers than those carrying the control empty vector (Figure 4.3 A). Yeast carrying Top2β His63Tyr exhibited a much higher (~3-4 fold) recombination rate than the yeast carrying Top2β wild type for each of the genetic markers. These results

indicated that expression of the Top2β His63Tyr mutant protein leads to a hyper-recombinant, mutator phenotype in yeast.

Figure 4.3 Top2β H63Y confers a hyper-recombinant phenotype in yeast
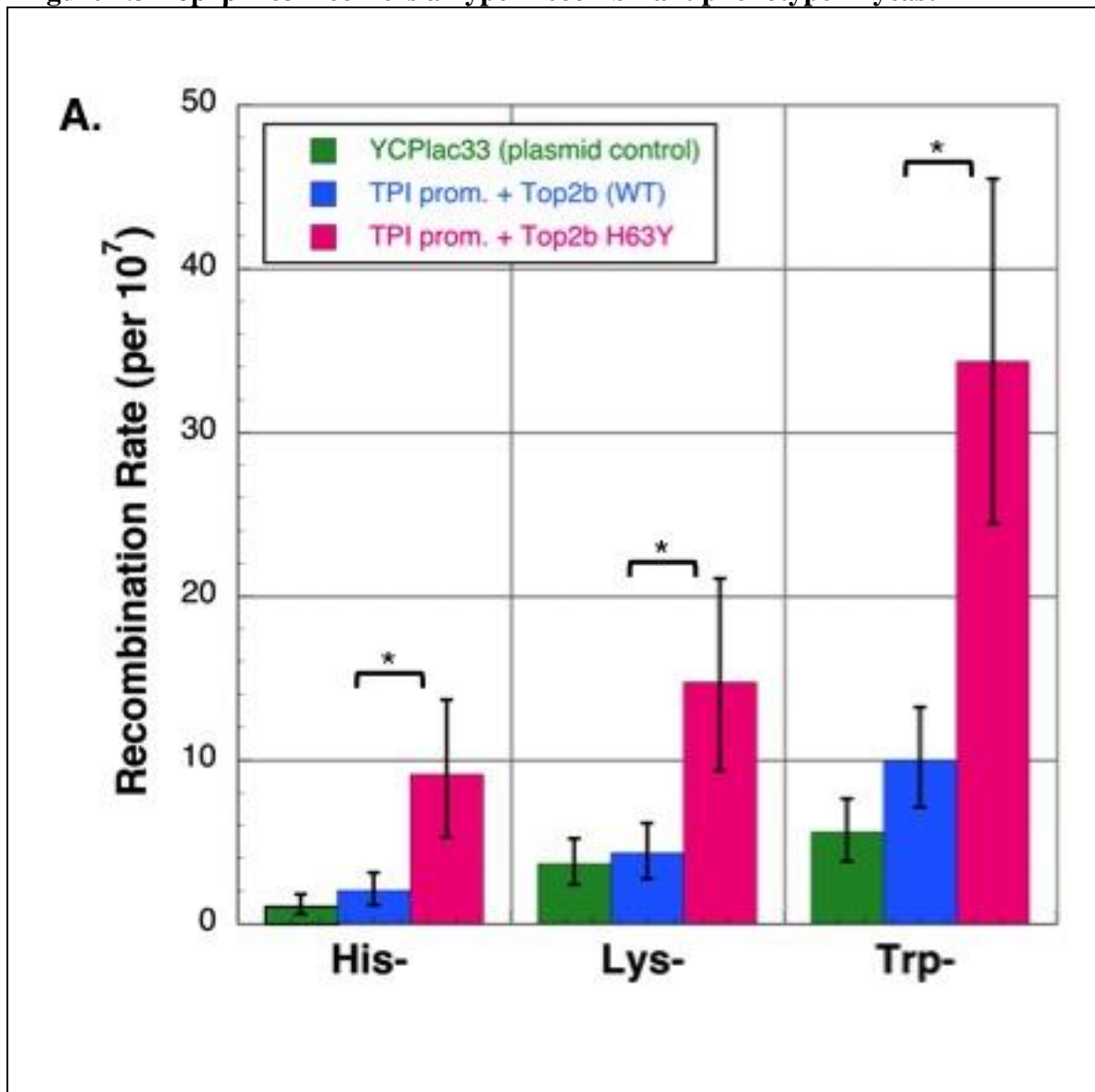
Figure 4.3 Expression of Top2β His63Tyr increased recombination rate in CG2009 yeast. **A.** The recombination rate of CG2009 yeast carrying Top2β wild type, Top2β His63Tyr or empty vector (yCPlac33). Between 50 and100 yeast cells from 12 CG2009 yeast clones carrying plasmid DNA as indicated were inoculated and grown over night then plated to selective media, the number of colonies formed on the selective media (SC-His⁻, Lys⁻, Trp⁻, and Ura⁻) were counted and used to determine the rate of recombination. Recombination rate was calculated using the Fluctuation AnaLysis CalculatOR (FALCOR) available at: www.mitochondria.org/protocols/FALCOR.html. Error bars represent the 95% confidence interval of the recombination rate.

    *Denotes a p-value: <0.05 calculated using student's t-test for independent samples.

4.4.4 Biochemical properties of Top2β His63Tyr

Based on the characteristics exhibited by yeast carrying these mutant alleles we next evaluated the biochemical characteristics of purified Top2β His63Tyr mutant protein. We introduced the His63Tyr mutation into a Top2β inducible expression plasmid (β12URAB). This vector was used to overexpress and purify the mutant Top2β protein in yeast strain JEL1t1. The mutant protein was purified using nickel affinity chromatography (Appendix B).

To assess the topoisomerase activity of the mutant protein we assayed decatenation activity with catenated kDNA. The His63Tyr Top2β purified mutant protein exhibited reduced kDNA decatenation activity compared to the wild type enzyme (Figure 4.4 A). The Top2β wild type enzyme exhibited complete decatenation activity at 13ng of enzyme. The Top2β His63Tyr enzyme did not completely decatenate kDNA with 200ng of enzyme. While these results indicated that Top2β His63Tyr exhibits reduced decatenation activity they are based on a single experiment with the Top2β His63Tyr mutant protein. After purification, the Top2 protein was stored in liquid nitrogen for subsequent experiments; this greatly reduced Top2β His63Tyr mutant topoisomerase activity. Subsequent efforts to freshly purify active mutant protein have not succeeded.

We next measured the level of DNA cleavage induced by the Top2β His63Tyr mutant protein in the presence of etoposide using the plasmid cleavage assay. Using a fixed protein concentration we added increasing concentrations of etoposide. The Top2β His63Tyr mutant protein exhibited lower levels of DNA double strand breaks in the presence of etoposide compared to wild type enzyme (Figure 4.4 B). However, the Top2β His63Tyr mutant protein exhibited high levels of drug independent DNA single strand

breaks. Unfortunately, the level of etoposide induced DNA cleavage could only be measured in two independent experiments as the storage of Top2β His63Tyr in liquid nitrogen for subsequent experiments greatly reduced Top2β His63Tyr mutant topoisomerase activity.

The His63 residue is located in the region of etoposide hypersensitive Top2α mutant proteins described in chapter 2. These mutant proteins were found to exhibit alterations to ATP utilization and lacked DNA-stimulated ATP hydrolysis. Therefore we next characterized the ATPase activity of the Top2β His63Tyr mutant protein and compared to wild type (Figure 4.4 C). As expected, Top2β His63Tyr had altered ATPase activity and lacked DNA-stimulated ATPase activity. Rather, DNA independent ATPase activity was elevated and reflected activity similar to the DNA-stimulated wild type enzyme.

We observe a large reduction in topoisomerase activity with the Top2β His63Tyr mutant protein after the enzyme was stored in liquid nitrogen. Our subsequent attempts at purification for this mutant protein have been unsuccessful.

Figure 4.4 Biochemical activity purified Top2β His63Tyr mutant protein
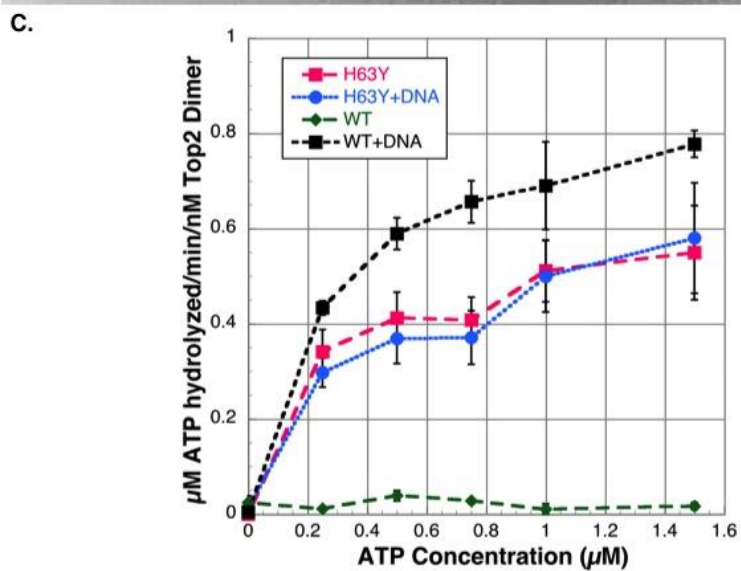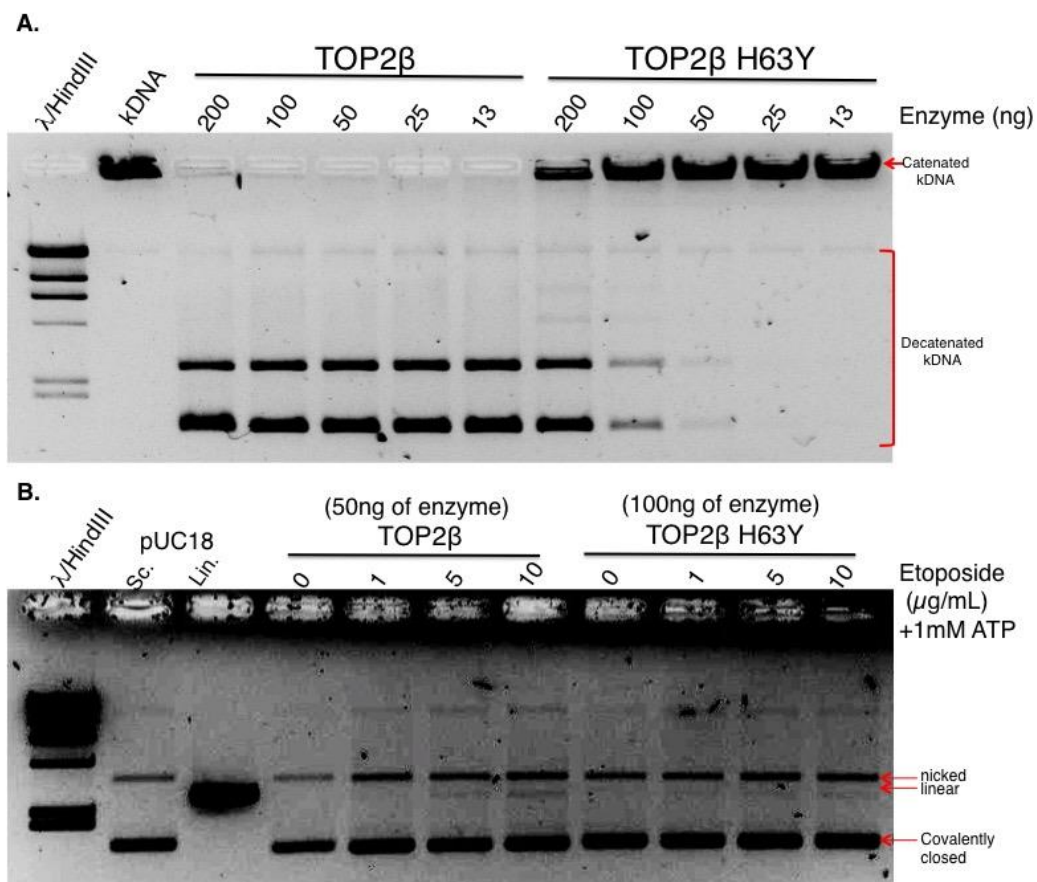
Figure 4.4 Biochemical properties of purified Top2β H63Y mutant protein compared to wild type enzyme. **A.** Decatenation of 150ng catenated kinetoplast DNA (kDNA) and the amount of enzyme indicated above each well. Decatenation activity of the Top2β H63Y mutant protein compared to wild type enzyme. Complete decatenation activity was observed with 13ng wild type Top2β and partial decatenation activity was observed with 200ng of Top2β H63Y. This experiment could only be carried out once due to extenuating circumstances highlighted in the text. **B.** ATP-dependent Top2 mutant protein mediated DNA cleavage of 200ng negatively supercoiled plasmid DNA (pUC18) in the presence of etoposide compared to wild type enzyme. The lanes labeled Sc. contain 200ng supercoiled pUC18 DNA and the lanes labeled Lin. contain 30ng ECORI linearized pUC18 DNA. The mobility of nicked, linearized and covalently closed DNA are labeled to the right of each gel. Plasmid cleavage assay with 100ng of Top2β H63Y enzyme and 50ng Top2β wild type and various concentrations of etoposide as indicated above each lane. 50ng of Top2β wild type enzyme induced DNA cleavage (nicked and linear) as a dose response increase with etoposide concentrations. 100ng of Top2β H63Y enzyme exhibited high drug independent levels of single strand breaks and a modest response to increases in etoposide concentration. **C**. ATP hydrolysis activity of Top2β H63Y compared to wild type enzyme. The rate of ATP hydrolysis was assayed for the Top2β wild type and H63Y proteins in the presence or absence of nucleotide. Rate of ATP hydrolysis was measured using a NADH-coupled ATPase assay for several concentrations of ATP. For each Top2α reaction, enzyme concentration was 50nM of dimer. Sonicated salmon sperm DNA (0.2mg/ml; ~2700bp per Top2 dimer) was added to reactions, as indicated, to stimulate ATP hydrolysis activity. H63Y exhibited higher intrinsic levels of ATP hydrolysis activity than wild type enzyme at all concentrations of ATP and did not exhibit DNA stimulated ATP hydrolysis like the wild type enzyme. Error bars represent the standard deviation of three independent experiments.

4.4.5   Expression of Top2α His42Tyr is deleterious in yeast

Because of the difficulties we experienced in subsequent purification attempts with Top2β His63Tyr we constructed the orthologous Top2α mutation (His42Tyr) in plasmid pMJ1. To determine if Top2α His42Tyr could complement the topoisomerase deficiency of yeast *top2-4* strains, we introduced the Top2α His42Tyr mutant allele into yeast strains (JN362a t_{2-4} and YMM10 t_{2-4}). We quickly noticed that the DNA repair proficient yeast strains JN362a t_{2-4} and YMM10 t_{2-4} produced very few pMJ1 Top2α His42Tyr colonies compared to pMJ1 wild type (Figure 4.5 A). These results suggested that the expression of Top2α His42Tyr may be extremely deleterious in yeast.

We tested the rare colonies obtained in YMM10 t_{2-4} carrying pMJ1 Top2α His42Tyr for the ability to complement the temperature sensitive topoisomerase deficiency. Similar to the Top2β allele, yeast (YMM10 t2-4) carrying Top2α His42Tyr failed to complement a temperature sensitive allele of yTop2 (Figure 4.5 B). Based on the extremely deleterious nature we observed with this allele it is likely that the rare colonies used in this experiment could have acquired additional alterations that affect topoisomerase activity.

190

Figure 4.5 Expression of Top2α His42Tyr is deleterious in yeast
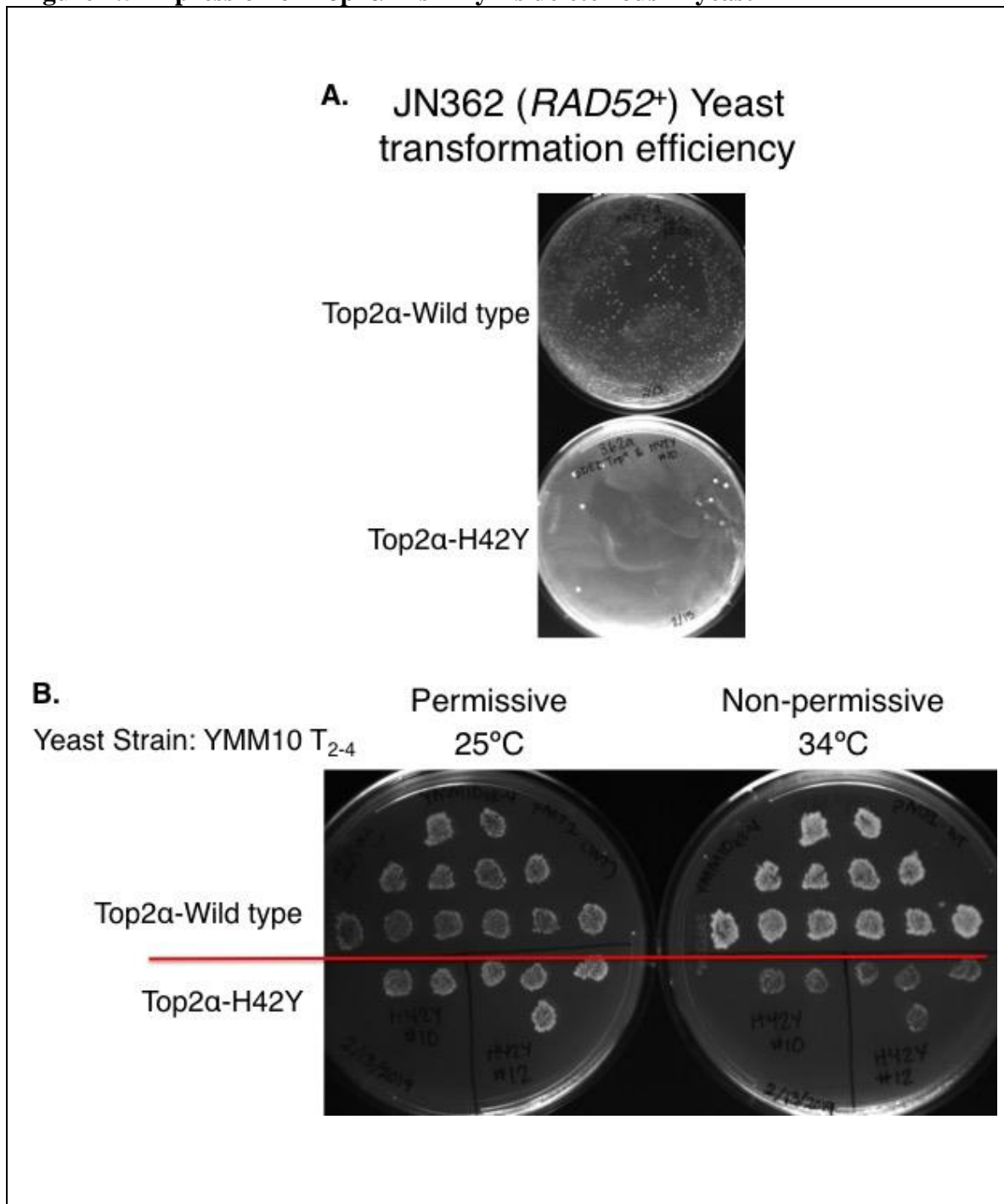
Figure 4.5 Evaluation of and Top2α His42Tyr expression in yeast. The functional expression of Top2α mutant alleles was assessed by checking for complementation at the non-permissive temperature in yeast carrying temperature sensitive yTop2 allele.
A. The results of a quantitative yeast transformation comparing transformation efficiency for Top2α wild type and His42Tyr in yeast strains carrying RAD52+ (JN362a). Fewer yeast colonies were found expressing the Top2α H42Y, suggesting the expression was deleterious. **B.** Independent YMM10 top2-4 yeast isolates carrying pMJ1 (Top2α wild type or His42Tyr) were replica-plated from a master plate onto naïve SC-URA- plates and grown at 25°C or 34°C for ~24hours. Yeast isolates carrying Top2α His42Tyr were unable to grow at 34°C which indicated that the yeast could not complement for the temperature sensitive yeast allele (*top2-4*).

4.4.6   <u>Biocehmical properties of Top2α His42Tyr</u>

Based on the characteristics exhibited by yeast carrying the Top2α His42Tyr

mutant allele and the biochemical properties of the Top2β His63Tyr mutant protein. We

purified the Top2α His42Tyr mutant protein. We introduced the His42Tyr mutation into a

Top2α inducible expression plasmid (JMB1). This vector was used to overexpress and

purify the mutant Top2α protein in yeast strain JEL1t1. The mutant protein was purified

using nickel affinity chromatography (Appendix B).

To assess the topoisomerase activity of the mutant protein we first assayed

relaxation activity with negatively supercoiled puUC18 plasmid DNA. The Top2α wild

type enzyme exhibited complete relaxation activity at 100ng of enzyme whereas the

Top2α His42Tyr enzyme requires 200ng of enzyme (Figure 4.6 A). We next assessed the

topoisomerase activity of Top2α His42Tyr mutant protein by assaying decatenation

activity with catenated kDNA (Figure 4.6 B). The Top2α wild type enzyme exhibited

complete decatenation activity at 25ng of enzyme whereas the Top2α His42Tyr enzyme

requires 100ng of enzyme.

We next assayed the levels of DNA cleavage induced by the Top2α His42Tyr

mutant protein in the presence of etoposide compared to wild type enzyme (Figure 4.6

C). As expected the Top2α wild type enzyme exhibited a dose response in levels of DNA

cleavage (nicked and linear) to etoposide concentration. The Top2α His42Tyr mutant

protein exhibited higher levels of drug independent DNA double strand breaks and higher

levels of etoposide induced DNA double strand breaks (Figure 4.6 D). These results were

quite striking and suggested that Top2α His42Tyr could be a self-poisoning allele of

Top2α.

Figure 4.6 Biochemical properties of Top2α His42Tyr
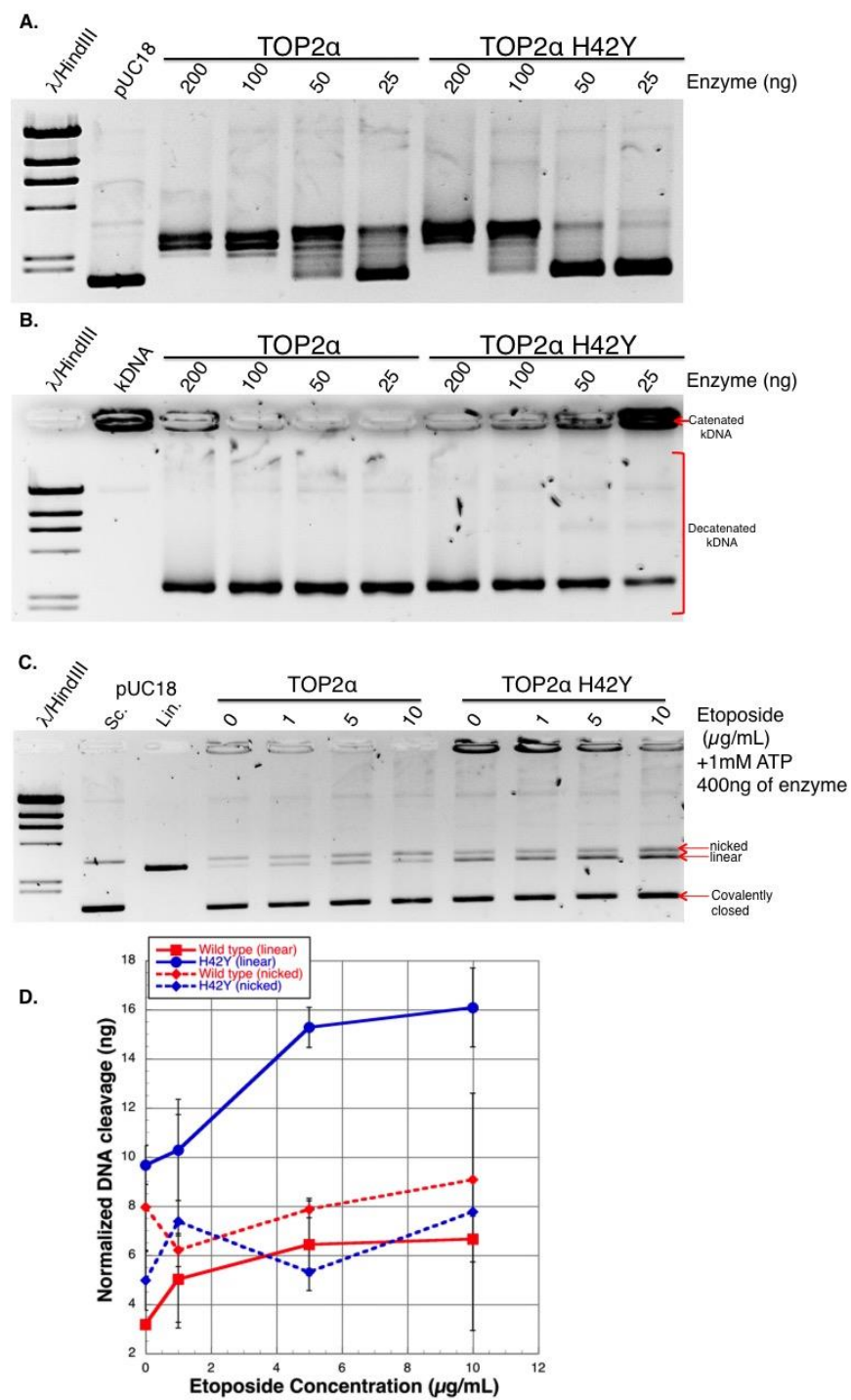
Figure 4.6 Biochemical properties of Top2α His42Tyr mutant protein compared to wild type. All assays were carried out as two independent experiments. **A**. Relaxation activity of Top2α H42Y mutant protein compared to wild type enzyme. Complete decatenation activity was observed with 100ng wild type Top2α and 200ng of Top2α H42Y. **B.** Decatenation activity of the Top2α H42Y mutant protein compared to wild type enzyme. Complete decatenation activity was observed with 25ng wild type Top2α and 100ng of Top2α H42Y. **C.** Plasmid cleavage assay with 400ng of Top2α enzyme (Wild type and H42Y) and various concentrations of etoposide as indicated above each lane. 400ng of Top2α wild type enzyme produced low innate levels of DNA linearization and exhibited a dose response increase of DNA cleavage with etoposide concentrations and the intensity of the linear and nicked DNA bands. 400ng of Top2α H42Y enzyme produced higher innate levels of DNA linearization and exhibited a dose response increase of DNA cleavage (nicked and linear) with etoposide concentrations. **D.** Quantitation of etoposide induced DNA cleavage described in **C.**, error bars represent the standard deviation of two experiments.

4.4.7 <u>Validation of His42Tyr drug independent DNA cleavage</u>

Based on the striking level of DNA cleavage observed with the Top2α His42Tyr mutant protein, we decided to further probe the level of drug-independent DNA cleavage using the plasmid cleavage assay. Using 200ng of negatively supercoiled plasmid (pUC18) DNA and a variable amount of purified protein we compared the level of ATP-dependent DNA cleavage of the Top2α His42Tyr mutant protein to the wild type.

Figure 4.7 shows the results of the drug independent cleavage assay. In the presence of 8mM Mg^{2+} the Top2α wild type enzyme induced low levels of DNA double strand breaks visible at 400ng of enzyme (Figure 4.7 A). Because of topoisomerase strand passage activity some of the DNA became catenated with 200-500ng of the wild type enzyme and remained outside the agarose gel. The Top2α His42Tyr mutant protein induced higher levels of linear DNA cleavage (Figure4.7 C).

The DNA cleavage reaction is strongly affected by the divalent cation[173,174]. Therefore we assayed drug-independent DNA cleavage in the presence of 8mM Ca^{2+}. In the presence of 8mM Ca^{2+} the Top2α wild type enzyme induced low levels of DNA double strand breaks (Figure 4.7 B). As before due to topoisomerase strand passage activity some of the DNA became catenated with 200-500ng of the wild type enzyme and remained outside the agarose gel. The Top2α His42Tyr mutant protein induced higher levels of DNA double strand breaks as well as much higher levels of single strand breaks (Figure4.7 B and D). We observed modest levels of drug independent cleavage with the mutant enzyme in the presence of Mg^{2+}. However, the Top2α His42Tyr exhibited extraordinary levels of drug independent DNA cleavage in the Ca^{2+}.
These plasmid cleavage assays were carried out as two independent experiments.

Figure 4.7 Top2α His42Tyr drug independent DNA cleavage with Mg^{2+} or Ca^{2+}
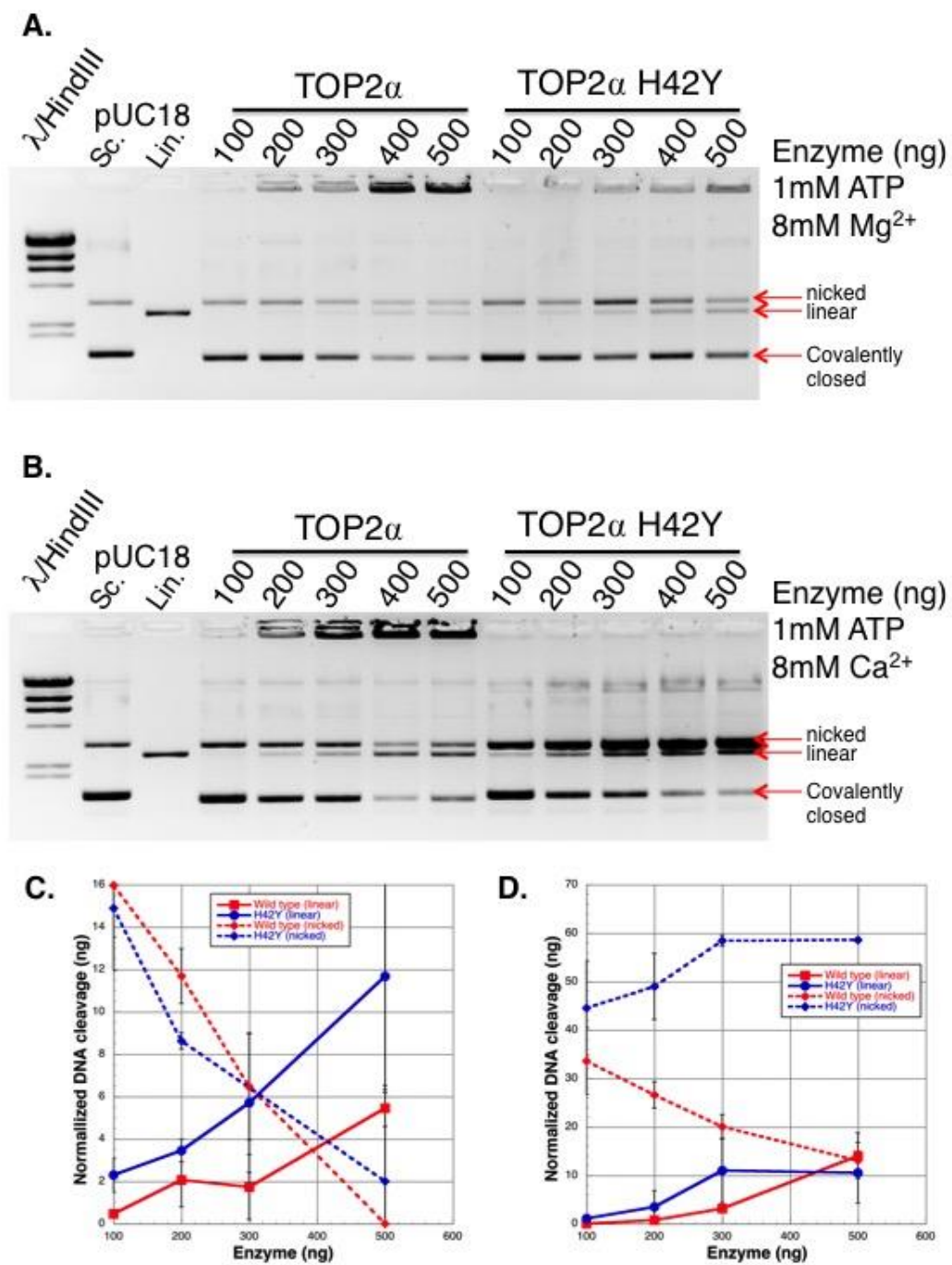
Figure 4.7 ATP-dependent Top2 mutant protein mediated DNA cleavage of 200ng negatively supercoiled plasmid DNA (pUC18) compared to wild type enzyme. The lanes labeled Sc. contain 200ng supercoiled pUC18 DNA and the lanes labeled Lin. contain 30ng ECORI linearized pUC18 DNA. The mobility of nicked, linearized and covalently closed DNA are labeled to the right of each gel. All assays were carried out as two independent experiments. **A.** Plasmid cleavage assay in 8mM Mg^{2+} with Top2α enzyme (Wild type and H42Y) ng of Top2 as indicated above each lane. Top2α wild type enzyme induced DNA double strand breaks are visible at 400ng of enzyme. Top2α H42Y enzyme induced DNA double strand breaks are visible at 200-300ng of enzyme. **B.** Plasmid cleavage assay in 8mM Ca^{2+} with Top2α enzyme (Wild type and H42Y) ng of Top2 as indicated above each lane. Top2α wild type enzyme induced DNA double strand breaks are visible at 200ng of enzyme. Top2α H42Y enzyme induced DNA double strand breaks are visible at 100 of enzyme. Higher levels of Top2α H42Y induced DNA single strand breaks were observed compared to wild type enzyme. **C.** Quantitation of Mg^{2+} Top2 mediated drug independent DNA cleavage described in **A.**, error bars represent the standard deviation of two experiments. **D.** Quantitation of Ca^{2+} Top2 mediated drug independent DNA cleavage described in **B.**, error bars represent the standard deviation of two experiments.

4.5   Discussion

In this chapter we characterized the consequences of expressing a Top2β mutant allele that was identified in a human neurological disease which presented as developmental delay and autism[1]. While at first we demonstrated that Top2β His63Tyr does not complement a temperature sensitive yeast allele the explanation of a catalytically inactive Top2β did not appear to sufficiently explain the disease state. Therefore we probed the cellular consequences of Top2β His63Tyr expression further and revealed a genetic requirement for the expression of Top2β His63Tyr. These findings suggested that the expression of the enzyme is deleterious to yeast deficient for recombination. This was type of characteristic observed in the self-poisoning yeast Top2 allele described in chapter 3 and was observed in yeast expressing the Top2β ΔATPase allele.

Fluctuation analysis of yeast expressing the Top2β His63Tyr mutant allele revealed that the enzyme conferred a high recombination rate to yeast. These results along with our findings that suggest the enzyme incurs intrinsic levels of drug-independent Top2 mediated DNA damage suggest that the Top2β His63Tyr mutant allele is a mutator. As a mutator Top2β could play a role in tumorigenesis or tumor progression, as it could be a potential of source mutations in cells[440]. The implications of this therefore link Top2β to oncogenesis.

This finding is especially important as it provides strong evidence in support of Top2β His63Tyr generating DNA damage within cells. As a mechanism for developing neurological disease, high levels of Top2 mediated DNA damage induced by a self poisoning Top2 allele would be similar to a loss of either TDP1 or TDP2, which are

already linked to the development of neurological disease[265,377,396,397,431–435]. Therefore our evidence suggests that the Top2β His63Tyr mutation causes neurological disease by exhibiting high intrinsic levels of Top2 mediated DNA damage.

Surprisingly, expression of the Top2α His42Tyr allele was deleterious in yeast proficient for DNA repair, suggesting a greater amount of DNA damage. We observed high levels of drug independent DNA damage *in vitro*, which indicated that this mutant protein is a potent self-poisoning mutant. The Top2α His42Tyr mutant protein exhibited extremely high levels of drug independent DNA cleavage in the presence of Ca^{2+}, this result was expected based on results from Joseph Deweese's laboratory exploring the relative cleavage using other divalent cations (Mn^{2+} and Co^{2+})[148,171–173]. We speculate that Top2β His63Tyr would also exhibit high levels of drug independent DNA cleavage in the presence of Ca^{2+}.

The characterization of Top2α His42Tyr as a self-poisoning allele was fortuitous. A previously characterized Top2α mutant Asp48Asn also the self-poisoning characteristic[183]. These two residues are located in the N-gate dimerization interface. Figure 4.8 illustrates the proximity of these residues on the Top2α crystal structure bound to ADP[159].

Figure 4.8 Top2α ATPase structure His42 and Asp48
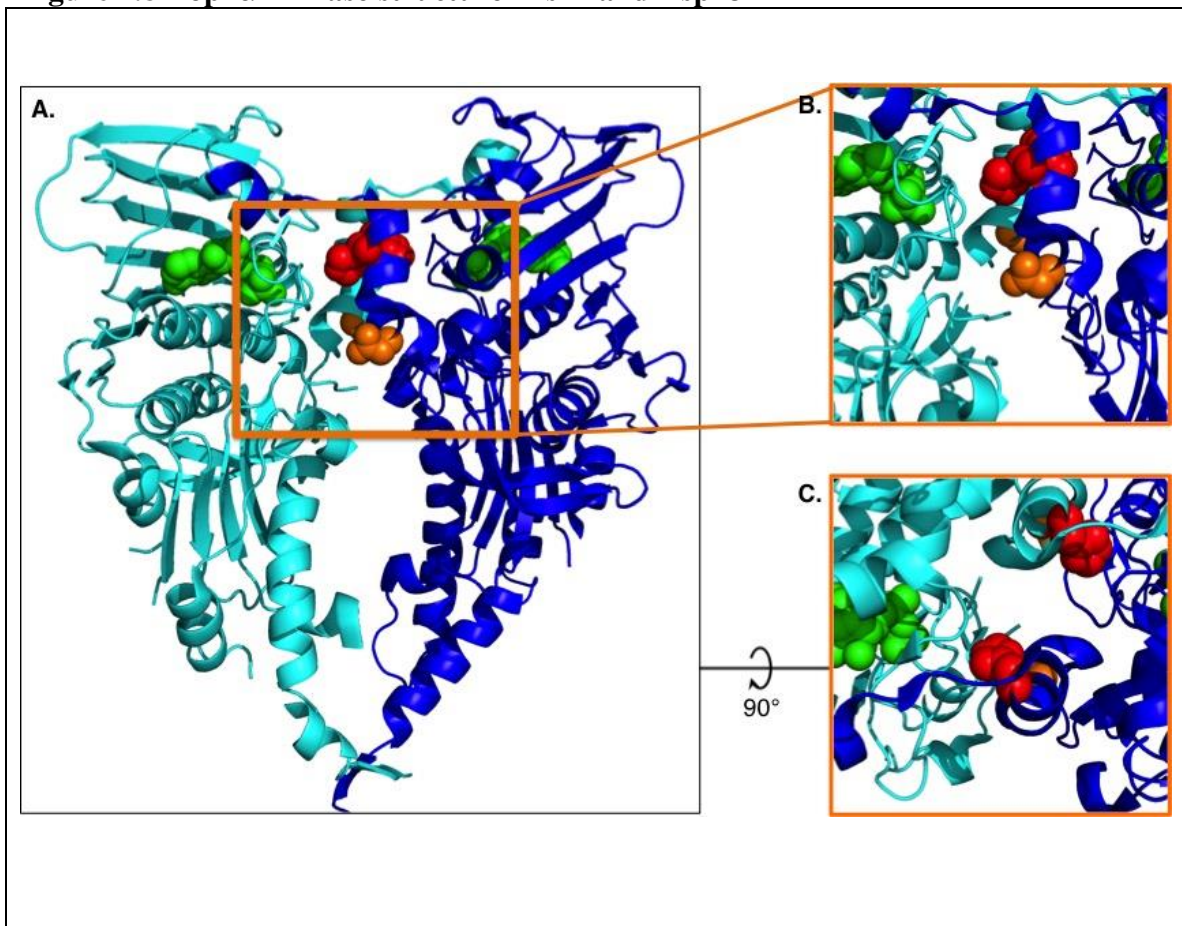
Figure 4.8 Top2α ATPase domain crystal structure (1ZXN) in complex with ADP (Green) with screen identified amino acid residues highlighted (His42: red, Asp48: Orange)[159]. **A.** Top2α ATPase domain crystal structure (1ZXN). **B.** Closer view of the highlighted residues in the Top2α ATPase domain (His42: red, Asp48: Orange). **C.** Closer view of the highlighted residues in the Top2α ATPase domain (His42: red, Asp48: Orange) rotated for a top view.

The histidine residue at amino acid position 42 of Top2α is located in close proximity with two tyrosines on opposing subunit of the Top2 homodimer (4.0Å and 3.4Å with Tyr165 and Tyr151, respectively). A substitution to tyrosine in this position could disrupt interactions in the N-terminal dimerization interface. The change to tyrosine could have an impact on the ATP binding pocket increasing intrinsic levels of ATP hydrolysis. The proximity of His 42 to the previously identified Asp48Asn in Top2α further suggests that some set of perturbations to this region of the protein leads to elevated levels of drug independent cleavage.

The expression of these mutant alleles in yeast was demonstrated to be deleterious. The discovery of two mutations in the ATPase domain in close proximity that exhibit high intrinsic levels of DNA cleavage implicates aberrant enzyme activity by promoting DNA cleavage. Therefore, our data suggest that Top2β His63Tyr exhibits aberrant activity and induces DNA damage. We hypothesize that Top2β His63Tyr could contribute to neurological disease through its induction of DNA damage. These findings suggest that mutations in the ATPase domain of Top2 can lead to a self-poisoning phenotype in human cells, linking certain mutations in Top2 to the induction of genome instability.

5 DISCUSSION

5.1 The role of the ATPase domain in DNA cleavage

Our research has highlighted a relationship between the utilization of ATP and sensitivity to etoposide. We identified several amino acid changes that appeared to dysregulate the catalytic mechanism of the enzyme. Our findings could be explained by the discoordination of the catalytic cycle that leads to prolonged DNA breakage during strand passage. Mutations in this domain seem to affect the utilization of ATP and lead to elevated levels of DNA nicking. This research leads us to echo speculations about the function of the first ATP hydrolysis event being linked to the transport of the DNA T-segment[373].

These conclusions were also supported by evidence presented in chapter 4. If these conclusions correctly interpret details of the ATPase domains function then they infer that the ATPase domain of Top2 may also be targeted with small molecules to improve the effects of Top2 targeting agents. Our results showed the induction of high levels of DNA cleavage with AMP-PNP in the absence of a Top2 targeting drug. DNA cleavage experiments with ADP did not reveal similar levels of DNA cleavage potentially suggesting that AMP-PNP traps Top2 in a way that promotes DNA cleavage. These findings suggest that targeting the ATPase domain of Top2 could promote elevated levels of DNA cleavage and likely do so with ATP during catalysis. We speculate that a small molecule that stabilizes the conformation adopted in the Top2α AMP-PNP bound ATPase domain crystal structure might replicate the DNA cleavage, observed with agents like etoposide[159].

5.2   Mutagenic consequences of targeting Top2

Our research identified mechanisms that contribute to the formation of unique mutations induced by etoposide exposure. The formations of etoposide induced tandem duplications and insertions was dependent on NHEJ and TDP1.We speculate the mechanisms that generated these mutations similar to those involved in the formation of chromosomal translocations. Consistent with our findings, previous research has highlighted a role for NHEJ in the formation of chromosomal translocations[268,441].

A potential strategy for decreasing secondary malignancies would be to co-target pathways associated with the generation of mutations associated with those malignancies alongside etoposide treatment. Defects in the NHEJ pathway have been identified previously as leading to higher levels of sensitivity to topoisomerase targeting drugs in yeast and mammalian cells[268,394,395]. Many efforts have been made to identify small molecule inhibitors of this pathway, as they would be valuable co-therapies along with DNA damaging agents[442]. Prior to this research TDP1 was known to play a role in the removal of Top1 and Top2 covalent complexes, its loss is associated with higher levels of sensitivity to topoisomerase targeting drugs[17,27,376]. Therefore, studies to identify small molecule inhibitors of TDP1 are already underway[431,443]. If small molecule inhibitors are discovered they will likely have the added benefit of potentially ameliorating the secondary malignancies associated with Top2 targeting agents as well as sensitizing the cells to the Top2 targeting agent. A major benefit of this approach is that these therapies have the potential to sensitize cells to Top2 targeting agents and therefore could result in a reduction in etoposide dosing required to achieve similar therapeutic efficacy. This

strategy could reduce the overall patient exposure to etoposide. Our research stresses the importance and potential advantages of these therapies.

5.3   Self-poisoning Top2 alleles and novel enzyme targeting strategies

The identification of a second ATPase domain mutation in Top2 that leads to high levels of drug independent DNA cleavage was fortuitous. The His42Tyr and Asp48Asn mutations in Top2α are located in the C1 cluster identified in the etoposide sensitivity screen (Figure 2.4 and Figure 4.8). Further characterization of the details that lead to this self-poisoning phenotype could be beneficial to the rational design of therapies targeting this area of the protein.

These self-poisoning mutants suggest that there can be a catastrophic failure in Top2 activity such that the enzyme is slow or incapable of DNA ligation. During its catalytic cycle the Top2 dimer must sequentially dissociate each of its interaction points to accomplish DNA strand passage. Based on the available crystal structure and a wide array of experimental data we know that there are three major locations that hold the Top2 dimer together. These dimerization interfaces are located in the ATPase domain, Breakage/Reunion Core, and coiled coil domain. The published crystal structures for the Breakage/Reunion Core have shown two conformational states for the coiled-coil domain either with the C-gate open or closed. The difference between these two states is a 17˚ bend[72]. The self-poisoning mutations we have identified in the eukaryotic top2 protein thus far, are located in the N-gate and C-gate but not in the DNA breakage reunion enzyme core. This evidence leads us to speculate that mutations that disrupt the integrity of any of the three domains will cause potentially catastrophic failure in the enzyme.

Based on the severely cytotoxic characteristics exhibited by Top2α His42Tyr mutant allele in yeast cells, it is not surprising that this class of Top2 mutant has not been previously described. The self-poisoning mutants that have been identified in Top2 thus far (Top2α: Asp48Asn, His42Tyr, yTop2: Arg1128Gly Phe1025Tyr) have exhibited different levels of self-poisoning with Top2α His42Tyr producing the highest levels of drug independent cleavage *in vitro*. The etoposide genetic screen described here identified many mutant alleles of Top2a that confer hypersensitivity to etoposide. We suspect it is likely that some of the mutations that were identified by our screen could exhibit self-poisoning characteristics. We speculate that there are certain Top2 mutations that would cause the enzyme to bind irreversibly to DNA after cleavage.

5.4   Top2 mediated DNA damage and human disease

Self-poisoning mutations of Top2 clearly mimic the effects of Top2 targeting drugs. One of the most striking findings of the research presented here was the biochemical characterization of the Top2β His63Tyr mutant proteins. This research established the Top2β His63Tyr mutant protein as a self-poisoning allele of Top2β. Thereby linking aberrant enzyme activity and autism, which has helped to broaden our understanding of how Top2 can contribute to human diseases. Particularly striking was that these data suggested that expression of the Top2β His63Tyr mutant proteins lead to a mutator phenotype.

A variant of Top2β (His63Asn) was identified in the cells of a thyroid tumor in the Catalog Of Somatic Mutations In Cancer database (COSMIC)[444]. Given our findings that indicated His63Tyr has increased levels of drug independent DNA cleavage and we would speculate the Top2β His63Asn could have acted as a mutator in oncogenesis.

Single nucleotide variations have been identified for both human Top2 isoforms in tumors (COSMIC)[444]. Several mutant alleles have been identified in multiple tumors (Top2α: Lys743Asn, Ile1064Val; Top2β: Arg651His), these mutant alleles are strong candidates for biochemical characterization studies. We hypothesize that some of these mutations may also exhibit the mutator phenotypes we observed in yeast with Top2β His63Tyr. Top2α copy number is amplified in some tumors (breast and ovarian), this is likely due to a co-amplification along with HER2[445]. Etoposide has been observed to be highly effective in breast and ovarian cancers, likely due to Top2α copy number amplifications[446–448].

5.5   Conclusions

This research has provided evidence supporting a role for the ATPase domain of the Top2 protein in regulating the DNA cleavage reaction. The ATPase domain of Top2 belongs to the GHKL superfamily with high profile members like Gyrase, HSP90 and Histidine kinases. Numerous small molecule agents are known to target these proteins[252,253,256,449,450]. Analysis of these agents has been explored by comparing catalytic inhibitors of HSP90 and Top2, assessing commonalities to find a pharmacophore[256]. A careful examination of GHKL ATPase inhibitors could reveal that some have the ability to promote DNA cleavage and act as poisons to Top2.

The identification of several amino acid substitutions (Asp48Asn and His42Tyr) in the same region of the ATPase domain of Top2α that are able to mimic the action of Top2 poisons represents an extremely fortuitous discovery. Future biochemical studies will probe the particular details associated with the generation of DNA damage in the mutants. It is hoped that the understanding of the behavior of these mutants will lead to

the development of novel factors that could target the ATPase domain for therapeutic anti-cancer activity.

Currently the Nitiss laboratory is in the process of carrying out a screen for etoposide hypersensitive alleles of Top2β. Notably, a etoposide hypersensitive isolate identified in the Top2α screen carrying Arg736Gly Gly852Cys (MLC<10μg etoposide/mL) had its conserved residue identified in the Top2β genetic screen (Arg757Trp). The characterization of etoposide hypersensitive mutants identified in both screens should provide a useful perspective for analysis of topoisomerase function and biochemistry.

CITED LITERATURE

1.   Lam, C.-W., Yeung, W.-L. & Law, C.-Y. Global developmental delay and intellectual disability associated with a de novo TOP2B mutation. *Clin. Chim. Acta.* **469**, 63–68 (2017).
2.   Watson, J. D. & Crick, F. H. The structure of DNA. *Cold Spring Harb. Symp. Quant. Biol.* **18**, 123–131 (1953).
3.   Vos, S. M., Tretter, E. M., Schmidt, B. H. & Berger, J. M. All tangled up: how cells direct, manage and exploit topoisomerase function. *Nat Rev Mol Cell Biol* **12**, 827–841 (2011).
4.   Uzman, A. Molecular biology of the cell: Alberts, B., Johnson, A., Lewis, J., Raff, M., Roberts, K., and Walter, P. (2003).
5.   CAIRNS, J. THE FORM AND DUPLICATION OF DNA. *Endeavour* **22**, 141–145 (1963).
6.   Cairns, J. & Davern, C. I. The mechanics of DNA replication in bacteria. *J. Cell. Physiol.* **70**, Suppl:65-76 (1967).
7.   MESELSON, M. & STAHL, F. W. The replication of DNA. *Cold Spring Harb. Symp. Quant. Biol.* **23**, 9–12 (1958).
8.   Wang, J. C. Interaction between DNA and an Escherichia coli protein omega. *J. Mol. Biol.* **55**, 523–533 (1971).
9.   Champoux, J. J. & Dulbecco, R. An activity from mammalian cells that untwists superhelical DNA--a possible swivel for DNA replication (polyoma-ethidium bromide-mouse-embryo cells-dye binding assay). *Proc. Natl. Acad. Sci. U. S. A.* **69**, 143–146 (1972).
10.   Gellert, M., Mizuuchi, K., O'Dea, M. H. & Nash, H. A. DNA gyrase: an enzyme that introduces superhelical turns into DNA. *Proc. Natl. Acad. Sci. U. S. A.* **73**, 3872–3876 (1976).
11.   Vinograd, J., Lebowitz, J., Radloff, R., Watson, R. & Laipis, P. The twisted circular form of polyoma viral DNA. *Proc. Natl. Acad. Sci. U. S. A.* **53**, 1104–1111 (1965).
12.   Spengler, S. J., Stasiak, A. & Cozzarelli, N. R. The stereostructure of knots and catenanes produced by phage lambda integrative recombination: implications for mechanism and DNA structure. *Cell* **42**, 325–334 (1985).
13.   Dorman, C. J. & Dorman, M. J. DNA supercoiling is a fundamental regulatory principle in the control of bacterial gene expression. *Biophys. Rev.* **8**, 89–100 (2016).
14.   Wang, J. C. DNA TOPOISOMERASES. *Annu. Rev. Biochem.* **65**, 635–692 (1996).
15.   Champoux, J. J. DNA topoisomerases: structure, function, and mechanism. *Annu. Rev. Biochem.* **70**, 369–413 (2001).
16.   Bush, N. G., Evans-Roberts, K. & Maxwell, A. DNA Topoisomerases. *EcoSal Plus* **6**, (2015).
17.   Pommier, Y. Drugging topoisomerases: lessons and challenges. *ACS Chem. Biol.* **8**, 82–95 (2013).
18.   Nitiss, J. L. Targeting DNA topoisomerase II in cancer chemotherapy. *Nat Rev Cancer* **9**, 338–350 (2009).

19. Pommier, Y., Leo, E., Zhang, H. & Marchand, C. DNA Topoisomerases and Their Poisoning by Anticancer and Antibacterial Drugs. *Chem. Biol.* **17**, 421–433 (2010).

20. Lindsey, R. H. *et al.* Catalytic Core of Human Topoisomerase IIŒ±: Insights. *Biochemistry* **53**, 6595–6602 (2014).

21. Smith, N. A., Byl, J. A. W., Mercer, S. L., Deweese, J. E. & Osheroff, N. Etoposide Quinone Is a Covalent Poison of Human Topoisomerase. *Biochemistry* **53**, 3229–3236 (2014).

22. Mondrala, S. & Eastmond, D. A. Topoisomerase II inhibition by the bioactivated benzene metabolite hydroquinone involves multiple mechanisms. *Chem Biol Interact* **184**, 259–268 (2010).

23. Lindsey Jr., R. H., Bromberg, K. D., Felix, C. A. & Osheroff, N. 1,4-Benzoquinone is a topoisomerase II poison. *Biochemistry* **43**, 7563–7574 (2004).

24. Bender, R. P., Ham, A. J. & Osheroff, N. Quinone-induced enhancement of DNA cleavage by human topoisomerase IIalpha: adduction of cysteine residues 392 and 405. *Biochemistry* **46**, 2856–2864 (2007).

25. Horwitz, S. B. & Loike, J. D. A comparison of the mechanisms of action of VP-16-213 and podophyllotoxin. *Lloydia* **40**, 82–89 (1977).

26. Deweese, J. E., Osheroff, M. A. & Osheroff, N. DNA Topology and Topoisomerases: Teaching a 'Knotty' Subject. *Biochem Mol Biol Educ* **37**, 2–10 (2008).

27. Pommier, Y., Sun, Y., Huang, S.-Y. N. & Nitiss, J. L. Roles of eukaryotic topoisomerases in transcription, replication and genomic stability. *Nat. Rev. Mol. Cell Biol.* **17**, 703–721 (2016).

28. Schoeffler, A. J. & Berger, J. M. DNA topoisomerases: harnessing and constraining energy to govern chromosome topology. *Q. Rev. Biophys.* **41**, 41–101 (2008).

29. Tse, Y. C., Kirkegaard, K. & Wang, J. C. Covalent bonds between protein and DNA. Formation of phosphotyrosine linkage between certain DNA topoisomerases and DNA. *J. Biol. Chem.* **255**, 5560–5565 (1980).

30. Champoux, J. J. DNA is linked to the rat liver DNA nicking-closing enzyme by a phosphodiester bond to tyrosine. *J. Biol. Chem.* **256**, 4805–4809 (1981).

31. Horowitz, D. S. & Wang, J. C. Mapping the active site tyrosine of Escherichia coli DNA gyrase. *J. Biol. Chem.* **262**, 5339–5344 (1987).

32. Lynn, R. M. & Wang, J. C. Peptide sequencing and site-directed mutagenesis identify tyrosine-319 as the active site tyrosine of Escherichia coli DNA topoisomerase I. *Proteins Struct. Funct. Bioinforma.* **6**, 231–239 (1989).

33. Worland, S. T. & Wang, J. C. Inducible overexpression, purification, and active site mapping of DNA topoisomerase II from the yeast Saccharomyces cerevisiae. *J. Biol. Chem.* **264**, 4412–4416 (1989).

34. Champoux, J. J. Type IA DNA topoisomerases: strictly one step at a time. *Proc. Natl. Acad. Sci. U. S. A.* **99**, 11998–12000 (2002).

35. Redinbo, M. R., Stewart, L., Kuhn, P., Champoux, J. J. & Hol, W. G. Crystal structures of human topoisomerase I in covalent and noncovalent complexes with DNA. *Science* **279**, 1504–1513 (1998).

36. Stewart, L., Redinbo, M. R., Qiu, X., Hol, W. G. & Champoux, J. J. A model for

the mechanism of human topoisomerase I. *Science* **279**, 1534–1541 (1998).

37. Lima, C. D., Wang, J. C. & Mondragon, A. Three-dimensional structure of the 67K N-terminal fragment of E. coli DNA topoisomerase I. *Nature* **367**, 138–146 (1994).

38. Cheng, C., Kussie, P., Pavletich, N. & Shuman, S. Conservation of structure and mechanism between eukaryotic topoisomerase I and site-specific recombinases. *Cell* **92**, 841–850 (1998).

39. Redinbo, M. R., Champoux, J. J. & Hol, W. G. Structural insights into the function of type IB topoisomerases. *Curr. Opin. Struct. Biol.* **9**, 29–36 (1999).

40. Brown, P. O. & Cozzarelli, N. R. Catenation and knotting of duplex DNA by type 1 topoisomerases: a mechanistic parallel with type 2 topoisomerases. *Proc. Natl. Acad. Sci. U. S. A.* **78**, 843–847 (1981).

41. Koster, D. A., Croquette, V., Dekker, C., Shuman, S. & Dekker, N. H. Friction and torque govern the relaxation of DNA supercoils by eukaryotic topoisomerase IB. *Nature* **434**, 671–674 (2005).

42. Zhang, H. *et al.* Human mitochondrial topoisomerase I. *Proc. Natl. Acad. Sci. U. S. A.* **98**, 10608–10613 (2001).

43. Roca, J., Berger, J. M., Harrison, S. C. & Wang, J. C. DNA transport by a type II topoisomerase: direct evidence for a two-gate mechanism. *Proc. Natl. Acad. Sci.* **93**, 4057–4062 (1996).

44. Roca, J. & Wang, J. C. The capture of a DNA double helix by an ATP-dependent protein clamp: A key step in DNA transport by type II DNA topoisomerases. *Cell* **71**, 833–840 (1992).

45. Roca, J. & Wang, J. C. DNA transport by a type II DNA topoisomerase: Evidence in favor of a two-gate mechanism. *Cell* **77**, 609–616 (1994).

46. Williams, N. L. & Maxwell, A. Probing the two-gate mechanism of DNA gyrase using cysteine cross-linking. *Biochemistry* **38**, 13502–13511 (1999).

47. Wang, J. C. DNA topoisomerases. *Annu. Rev. Biochem.* **54**, 665–697 (1985).

48. Cozzarelli, N. R. & Wang, J. C. *DNA topology and its biological effects*. (Cold Spring Harbor Laboratory Press, 1990).

49. Osheroff, N. Biochemical basis for the interactions of type I and type II topoisomerases with DNA. *Pharmacol. Ther.* **41**, 223–241 (1989).

50. Reece, R. J. & Maxwell, A. DNA gyrase: structure and function. *Crit. Rev. Biochem. Mol. Biol.* **26**, 335–375 (1991).

51. Osheroff, N., Zechiedrich, E. L. & Gale, K. C. Catalytic function of DNA topoisomerase II. *Bioessays* **13**, 269–273 (1991).

52. Sharma, A. & Mondragon, A. DNA topoisomerases. *Curr. Opin. Struct. Biol.* **5**, 39–47 (1995).

53. Andersen, A. H., Svejstrup, J. Q. & Westergaard, O. The DNA binding, cleavage, and religation reactions of eukaryotic topoisomerases I and II. *Adv. Pharmacol.* **29A**, 83–101 (1994).

54. Watt, P. M. & Hickson, I. D. Structure and function of type II DNA topoisomerases. *Biochem. J.* **303 (Pt 3**, 681–695 (1994).

55. Berger, J. M. Structure of DNA topoisomerases. *Biochim. Biophys. Acta* **1400**, 3–18 (1998).

56. Dong, K. C. & Berger, J. M. Structural basis for gate-DNA recognition and

bending by type IIA topoisomerases. *Nature* **450**, 1201–1205 (2007).

57. Nitiss, J. L. DNA topoisomerase II and its growing repertoire of biological functions. *Nat Rev Cancer* **9**, 327–337 (2009).

58. Forterre, P., Gribaldo, S., Gadelle, D. & Serre, M.-C. Origin and evolution of DNA topoisomerases. *Biochimie* **89**, 427–446 (2007).

59. Keeney, S., Giroux, C. N. & Kleckner, N. Meiosis-specific DNA double-strand breaks are catalyzed by Spo11, a member of a widely conserved protein family. *Cell* **88**, 375–384 (1997).

60. Bergerat, A. *et al.* An atypical topoisomerase II from Archaea with implications for meiotic recombination. *Nature* **386**, 414–417 (1997).

61. Corbett, K. D. & Berger, J. M. Structure of the topoisomerase VI-B subunit: implications for type II topoisomerase mechanism and evolution. *EMBO J.* **22**, 151–163 (2003).

62. Corbett, K. D. & Berger, J. M. Emerging roles for plant topoisomerase VI. *Chem. Biol.* **10**, 107–111 (2003).

63. Morham, S. G., Kluckman, K. D., Voulomanos, N. & Smithies, O. Targeted disruption of the mouse topoisomerase I gene by camptothecin selection. *Mol. Cell. Biol.* **16**, 6804–6809 (1996).

64. Douarre, C. *et al.* Mitochondrial topoisomerase I is critical for mitochondrial integrity and cellular energy metabolism. *PLoS One* **7**, e41094 (2012).

65. Akimitsu, N. *et al.* Enforced cytokinesis without complete nuclear division in embryonic cells depleting the activity of DNA topoisomerase IIalpha. *Genes Cells* **8**, 393–402 (2003).

66. Yang, X., Li, W., Prescott, E. D., Burden, S. J. & Wang, J. C. DNA topoisomerase IIbeta and neural development. *Science* **287**, 131–134 (2000).

67. Li, W. & Wang, J. C. Mammalian DNA topoisomerase IIIalpha is essential in early embryogenesis. *Proc. Natl. Acad. Sci. U. S. A.* **95**, 1010–1013 (1998).

68. Kwan, K. Y. *et al.* Development of autoimmunity in mice lacking DNA topoisomerase 3beta. *Proc. Natl. Acad. Sci. U. S. A.* **104**, 9242–9247 (2007).

69. Goto, T. & Wang, J. C. Yeast DNA topoisomerase II is encoded by a single-copy, essential gene. *Cell* **36**, 1073–1080 (1984).

70. Wyckoff, E. & Hsieh, T. S. Functional expression of a Drosophila gene in yeast: genetic complementation of DNA topoisomerase II. *Proc. Natl. Acad. Sci.* **85**, 6272 LP – 6276 (1988).

71. Austin, C. A. & Marsh, K. L. Eukaryotic DNA topoisomerase II beta. *Bioessays* **20**, 215–226 (1998).

72. Wendorff, T. J., Schmidt, B. H., Heslop, P., Austin, C. A. & Berger, J. M. The structure of DNA-bound human topoisomerase II alpha: conformational mechanisms for coordinating inter-subunit interactions with DNA cleavage. *J Mol Biol* **424**, 109–124 (2012).

73. Wu, C. C. *et al.* Structural basis of type II topoisomerase inhibition by the anticancer drug etoposide. *Science (80-.).* **333**, 459–462 (2011).

74. Wu, C.-C., Li, Y.-C., Wang, Y.-R., Li, T.-K. & Chan, N.-L. On the structural basis and design guidelines for type II topoisomerase-targeting anticancer drugs. *Nucleic Acids Res.* **41**, 10630–10640 (2013).

75. Lang, A. J. *et al.* Structural organization of the human TOP2A and TOP2B genes.

Gene **221**, 255–266 (1998).

76. Sng, J. H. *et al.* Molecular cloning and characterization of the human topoisomerase IIalpha and IIbeta genes: evidence for isoform evolution through gene duplication. *Biochim. Biophys. Acta* **1444**, 395–406 (1999).

77. Tan, K. B. *et al.* Topoisomerase II alpha and topoisomerase II beta genes: characterization and mapping to human chromosomes 17 and 3, respectively. *Cancer Res.* **52**, 231–234 (1992).

78. Chung, T. D. *et al.* Characterization and immunological identification of cDNA clones encoding two human DNA topoisomerase II isozymes. *Proc. Natl. Acad. Sci. U. S. A.* **86**, 9431–9435 (1989).

79. Jenkins, J. R. *et al.* Isolation of cDNA clones encoding the beta isozyme of human DNA topoisomerase II and localisation of the gene to chromosome 3p24. *Nucleic Acids Res.* **20**, 5587–5592 (1992).

80. Drake, F. H. *et al.* Purification of topoisomerase II from amsacrine-resistant P388 leukemia cells. Evidence for two forms of the enzyme. *J. Biol. Chem.* **262**, 16739–16747 (1987).

81. Austin, C. A., Sng, J. H., Patel, S. & Fisher, L. M. Novel HeLa topoisomerase II is the II beta isoform: complete coding sequence and homology with other type II topoisomerases. *Biochim. Biophys. Acta* **1172**, 283–291 (1993).

82. Austin, C. A. & Fisher, L. M. Isolation and characterization of a human cDNA clone encoding a novel DNA topoisomerase II homologue from HeLa cells. *FEBS Lett.* **266**, 115–117 (1990).

83. Woessner, R. D., Mattern, M. R., Mirabelli, C. K., Johnson, R. K. & Drake, F. H. Proliferation- and cell cycle-dependent differences in expression of the 170 kilodalton and 180 kilodalton forms of topoisomerase II in NIH-3T3 cells. *Cell Growth Differ.* **2**, 209–214 (1991).

84. Onoda, A. *et al.* Nuclear dynamics of topoisomerase IIbeta reflects its catalytic activity that is regulated by binding of RNA to the C-terminal domain. *Nucleic Acids Res.* **42**, 9005–9020 (2014).

85. Grue, P. *et al.* Essential mitotic functions of DNA topoisomerase IIalpha are not adopted by topoisomerase IIbeta in human H69 cells. *J. Biol. Chem.* **273**, 33660–33666 (1998).

86. Holm, C., Goto, T., Wang, J. C. & Botstein, D. DNA topoisomerase II is required at the time of mitosis in yeast. *Cell* **41**, 553–563 (1985).

87. Heck, M. M. & Earnshaw, W. C. Topoisomerase II: A specific marker for cell proliferation. *J. Cell Biol.* **103**, 2569–2581 (1986).

88. Hsiang, Y. H., Wu, H. Y. & Liu, L. F. Proliferation-dependent regulation of DNA topoisomerase II in cultured human cells. *Cancer Res.* **48**, 3230–3235 (1988).

89. Heck, M. M., Hittelman, W. N. & Earnshaw, W. C. Differential expression of DNA topoisomerases I and II during the eukaryotic cell cycle. *Proc. Natl. Acad. Sci. U. S. A.* **85**, 1086–1090 (1988).

90. Kimura, K., Saijo, M., Ui, M. & Enomoto, T. Growth state- and cell cycle-dependent fluctuation in the expression of two forms of DNA topoisomerase II and possible specific modification of the higher molecular weight form in the M phase. *J. Biol. Chem.* **269**, 1173–1176 (1994).

91. McClendon, A. K., Rodriguez, A. C. & Osheroff, N. Human topoisomerase IIalpha

rapidly relaxes positively supercoiled DNA: implications for enzyme action ahead of replication forks. *J. Biol. Chem.* **280**, 39337–39345 (2005).

92. Lyu, Y. L. *et al.* Role of topoisomerase IIbeta in the expression of developmentally regulated genes. *Mol. Cell. Biol.* **26**, 7929–7941 (2006).

93. Linka, R. M. *et al.* C-terminal regions of topoisomerase IIalpha and IIbeta determine isoform-specific functioning of the enzymes in vivo. *Nucleic Acids Res.* **35**, 3810–3822 (2007).

94. Lodish, H. *et al. Molecular cell biology*. (Macmillan, 2008).

95. Levene, S. D. & Crothers, D. M. Topological distributions and the torsional rigidity of DNA. A Monte Carlo study of DNA circles. *J. Mol. Biol.* **189**, 73–83 (1986).

96. Peter, B. J., Ullsperger, C., Hiasa, H., Marians, K. J. & Cozzarelli, N. R. The structure of supercoiled intermediates in DNA replication. *Cell* **94**, 819–827 (1998).

97. Chaly, N., Chen, X., Dentry, J. & Brown, D. L. Organization of DNA topoisomerase II isotypes during the cell cycle of human lymphocytes and HeLa cells. *Chromosome Res.* **4**, 457–466 (1996).

98. Meyer, K. N. *et al.* Cell cycle-coupled relocation of types I and II topoisomerases and modulation of catalytic enzyme activities. *J. Cell Biol.* **136**, 775–788 (1997).

99. Kim, R. A. & Wang, J. C. Function of DNA topoisomerases as replication swivels in Saccharomyces cerevisiae. *J. Mol. Biol.* **208**, 257–267 (1989).

100. Brill, S. J., DiNardo, S., Voelkel-Meiman, K. & Sternglanz, R. Need for DNA topoisomerase activity as a swivel for DNA replication for transcription of ribosomal RNA. *Nature* **326**, 414–416 (1987).

101. Bermejo, R. *et al.* Top1- and Top2-mediated topological transitions at replication forks ensure fork progression and stability and prevent DNA damage checkpoint activation. *Genes Dev.* **21**, 1921–1936 (2007).

102. Postow, L., Crisona, N. J., Peter, B. J., Hardy, C. D. & Cozzarelli, N. R. Topological challenges to DNA replication: conformations at the fork. *Proc. Natl. Acad. Sci. U. S. A.* **98**, 8219–8226 (2001).

103. Lucas, I., Germe, T., Chevrier-Miller, M. & Hyrien, O. Topoisomerase II can unlink replicating DNA by precatenane removal. *EMBO J.* **20**, 6509–6519 (2001).

104. Carpenter, A. J. & Porter, A. C. G. Construction, characterization, and complementation of a conditional-lethal DNA topoisomerase IIalpha mutant human cell line. *Mol. Biol. Cell* **15**, 5700–5711 (2004).

105. Isaacs, R. J. *et al.* Physiological regulation of eukaryotic topoisomerase II. *Biochim. Biophys. Acta* **1400**, 121–137 (1998).

106. Baxter, J. & Diffley, J. F. X. Topoisomerase II inactivation prevents the completion of DNA replication in budding yeast. *Mol. Cell* **30**, 790–802 (2008).

107. Fachinetti, D. *et al.* Replication termination at eukaryotic chromosomes is mediated by Top2 and occurs at genomic loci containing pausing elements. *Mol. Cell* **39**, 595–605 (2010).

108. Bell, S. P. & Dutta, A. DNA replication in eukaryotic cells. *Annu. Rev. Biochem.* **71**, 333–374 (2002).

109. Sundin, O. & Varshavsky, A. Terminal stages of SV40 DNA replication proceed via multiply intertwined catenated dimers. *Cell* **21**, 103–114 (1980).

110. Sundin, O. & Varshavsky, A. Arrest of segregation leads to accumulation of highly intertwined catenated dimers: dissection of the final stages of SV40 DNA replication. *Cell* **25**, 659–669 (1981).

111. Li, H., Wang, Y. & Liu, X. Plk1-dependent phosphorylation regulates functions of DNA topoisomerase IIalpha in cell cycle progression. *J. Biol. Chem.* **283**, 6209–6221 (2008).

112. Belmont, A. S. Mitotic chromosome structure and condensation. *Curr. Opin. Cell Biol.* **18**, 632–638 (2006).

113. Uuskula-Reimand, L. *et al.* Topoisomerase II beta interacts with cohesin and CTCF at topological domain borders. *Genome Biol.* **17**, 182 (2016).

114. Manville, C. M. *et al.* Genome-wide ChIP-seq analysis of human TOP2B occupancy in MCF7 breast cancer epithelial cells. *Biol. Open* **4**, 1436–1447 (2015).

115. Canela, A. *et al.* Genome Organization Drives Chromosome Fragility. *Cell* **170**, 507-521.e18 (2017).

116. Kouzine, F. *et al.* Transcription-dependent dynamic supercoiling is a short-range genomic force. *Nat. Struct. Mol. Biol.* **20**, 396–403 (2013).

117. Dawlaty, M. M. *et al.* Resolution of sister centromeres requires RanBP2-mediated SUMOylation of topoisomerase IIalpha. *Cell* **133**, 103–115 (2008).

118. Deming, P. B. *et al.* The human decatenation checkpoint. *Proc. Natl. Acad. Sci. U. S. A.* **98**, 12044–12049 (2001).

119. Gonzalez, R. E. *et al.* Effects of conditional depletion of topoisomerase II on cell cycle progression in mammalian cells. *Cell Cycle* **10**, 3505–3514 (2011).

120. Downes, C. S. *et al.* A topoisomerase II-dependent G2 cycle checkpoint in mammalian cells/. *Nature* **372**, 467–470 (1994).

121. Kaufmann, W. K. & Kies, P. E. DNA signals for G2 checkpoint response in diploid human fibroblasts. *Mutat. Res.* **400**, 153–167 (1998).

122. Luo, K., Yuan, J., Chen, J. & Lou, Z. Topoisomerase IIalpha controls the decatenation checkpoint. *Nat. Cell Biol.* **11**, 204–210 (2009).

123. Lou, Z., Minter-Dykhouse, K. & Chen, J. BRCA1 participates in DNA decatenation. *Nat. Struct. Mol. Biol.* **12**, 589–593 (2005).

124. Kang, X. *et al.* PTEN stabilizes TOP2A and regulates the DNA decatenation. *Sci. Rep.* **5**, 17873 (2015).

125. King, I. F. *et al.* Topoisomerases facilitate transcription of long genes linked to autism. *Nature* **501**, 58–62 (2013).

126. Hayashi, M. A DNA-RNA complex as an intermediate of in vitro genetic transcription. *Proc. Natl. Acad. Sci. U. S. A.* **54**, 1736–1743 (1965).

127. Wang, J. C. & Lynch, A. S. Effects of DNA Supercoiling on Gene Expression BT - Regulation of Gene Expression in Escherichia coli. in (eds. Lin, E. C. C. & Lynch, A. S.) 127–147 (Springer US, 1996). doi:10.1007/978-1-4684-8601-8_7

128. Wang, J. C. & Lynch, A. S. Transcription and DNA supercoiling. *Curr. Opin. Genet. Dev.* **3**, 764–768 (1993).

129. Hirose, S. & Matsumoto, K. Possible Roles of DNA Supercoiling in Transcription BT - DNA Conformation and Transcription. in (ed. Ohyama, T.) 138–143 (Springer US, 2005). doi:10.1007/0-387-29148-2_10

130. Gartenberg, M. R. & Wang, J. C. Positive supercoiling of DNA greatly diminishes

mRNA synthesis in yeast. *Proc. Natl. Acad. Sci. U. S. A.* **89**, 11461–11465 (1992).

131. Liu, L. F. & Wang, J. C. Supercoiling of the DNA template during transcription. *Proc. Natl. Acad. Sci. U. S. A.* **84**, 7024–7027 (1987).

132. Bermudez, I., Garcia-Martinez, J., Perez-Ortin, J. E. & Roca, J. A method for genome-wide analysis of DNA helical tension by means of psoralen-DNA photobinding. *Nucleic Acids Res.* **38**, e182 (2010).

133. Brill, S. J. & Sternglanz, R. Transcription-dependent DNA supercoiling in yeast DNA topoisomerase mutants. *Cell* **54**, 403–411 (1988).

134. Haffner, M. C. *et al.* Androgen-induced TOP2B-mediated double-strand breaks and prostate cancer gene rearrangements. *Nat. Genet.* **42**, 668–675 (2010).

135. Ju, B.-G. *et al.* A topoisomerase IIbeta-mediated dsDNA break required for regulated transcription. *Science* **312**, 1798–1802 (2006).

136. Perillo, B. *et al.* DNA oxidation as triggered by H3K9me2 demethylation drives estrogen-induced gene expression. *Science* **319**, 202–206 (2008).

137. Wong, R. H. F. *et al.* A role of DNA-PK for the metabolic gene regulation in response to insulin. *Cell* **136**, 1056–1072 (2009).

138. Mo, X. & Dynan, W. S. Subnuclear localization of Ku protein: functional association with RNA polymerase II elongation sites. *Mol. Cell. Biol.* **22**, 8088–8099 (2002).

139. Haffner, M. C., De Marzo, A. M., Meeker, A. K., Nelson, W. G. & Yegnasubramanian, S. Transcription-induced DNA double strand breaks: both oncogenic force and potential therapeutic target? *Clin. Cancer Res.* **17**, 3858–3864 (2011).

140. Tiwari, V. K. *et al.* Target genes of Topoisomerase IIbeta regulate neuronal survival and are defined by their chromatin state. *Proc. Natl. Acad. Sci. U. S. A.* **109**, E934-43 (2012).

141. Collins, I., Weber, A. & Levens, D. Transcriptional consequences of topoisomerase inhibition. *Mol. Cell. Biol.* **21**, 8437–8451 (2001).

142. Iossifov, I. *et al.* De novo gene disruptions in children on the autistic spectrum. *Neuron* **74**, 285–299 (2012).

143. Neale, B. M. *et al.* Patterns and rates of exonic de novo mutations in autism spectrum disorders. *Nature* **485**, 242–245 (2012).

144. Fass, D., Bogden, C. E. & Berger, J. M. Quaternary changes in topoisomerase II may direct orthogonal movement of two DNA strands. *Nat Struct Mol Biol* **6**, 322–326 (1999).

145. Burden, D. A. & Osheroff, N. Mechanism of action of eukaryotic topoisomerase II and drugs targeted to the enzyme. *Biochim. Biophys. Acta - Gene Struct. Expr.* **1400**, 139–154 (1998).

146. Wang, J. C. Moving one DNA double helix through another by a type II DNA topoisomerase: the story of a simple molecular machine. *Q. Rev. Biophys.* **31**, 107–144 (1998).

147. Zechiedrich, E. L., Christiansen, K., Andersen, A. H., Westergaard, O. & Osheroff, N. Double-stranded DNA cleavage/religation reaction of eukaryotic topoisomerase II: evidence for a nicked DNA intermediate. *Biochemistry* **28**, 6229–6236 (1989).

148. Deweese, J. E. & Osheroff, N. The DNA cleavage reaction of topoisomerase II:

wolf in sheep's clothing. *Nucleic Acids Res.* **37**, 738–748 (2009).

149. Hammonds, T. R. & Maxwell, A. The DNA dependence of the ATPase activity of human DNA topoisomerase IIalpha. *J Biol Chem* **272**, 32696–32703 (1997).

150. Hu, T., Sage, H. & Hsieh, T. S. ATPase domain of eukaryotic DNA topoisomerase II. Inhibition of ATPase activity by the anti-cancer drug bisdioxopiperazine and ATP/ADP-induced dimerization. *J Biol Chem* **277**, 5944–5951 (2002).

151. Harkins, T. T., Lewis, T. J. & Lindsley, J. E. Pre-steady-state analysis of ATP hydrolysis by Saccharomyces cerevisiae DNA topoisomerase II. 2. Kinetic mechanism for the sequential hydrolysis of two ATP. *Biochemistry* **37**, 7299–7312 (1998).

152. Lindsley, J. E. & Wang, J. C. On the coupling between ATP usage and DNA transport by yeast DNA topoisomerase II. *J. Biol. Chem.* **268**, 8096–8104 (1993).

153. Halligan, B. D., Edwards, K. A. & Liu, L. F. Purification and characterization of a type II DNA topoisomerase from bovine calf thymus. *J. Biol. Chem.* **260**, 2475–2482 (1985).

154. Maxwell, A. & Gellert, M. The DNA dependence of the ATPase activity of DNA gyrase. *J. Biol. Chem.* **259**, 14472–14480 (1984).

155. West, K. L., Turnbull, R. M., Willmore, E., Lakey, J. H. & Austin, C. A. Characterisation of the DNA-dependent ATPase activity of human DNA topoisomerase IIbeta: mutation of Ser165 in the ATPase domain reduces the ATPase activity and abolishes the in vivo complementation ability. *Nucleic Acids Res.* **30**, 5416–5424 (2002).

156. Liu, Q. & Wang, J. C. Identification of active site residues in the 'GyrA' half of yeast DNA topoisomerase II. *J. Biol. Chem.* **273**, 20252–20260 (1998).

157. Berger, J. M., Gamblin, S. J., Harrison, S. C. & Wang, J. C. Structure and mechanism of DNA topoisomerase II. *Nature* **379**, 225–232 (1996).

158. Chen, S.-F. *et al.* Structural insights into the gating of DNA passage by the topoisomerase II DNA-gate. *Nat. Commun.* **9**, 3085 (2018).

159. Wei, H., Ruthenburg, A. J., Bechis, S. K. & Verdine, G. L. Nucleotide-dependent domain movement in the ATPase domain of a human type IIA DNA topoisomerase. *J Biol Chem* **280**, 37041–37047 (2005).

160. Marx, G., Zhou, H., Graves, D. E. & Osheroff, N. Covalent Attachment of Ethidium to DNA Results in Enhanced Topoisomerase II-Mediated DNA Cleavage. *Biochemistry* **36**, 15884–15891 (1997).

161. Huang, W.-C., Lee, C.-Y. & Hsieh, T.-S. Single-molecule Forster resonance energy transfer (FRET) analysis discloses the dynamics of the DNA-topoisomerase II (Top2) interaction in the presence of TOP2-targeting agents. *J. Biol. Chem.* **292**, 12589–12598 (2017).

162. Olland, S. & Wang, J. C. Catalysis of ATP hydrolysis by two NH(2)-terminal fragments of yeast DNA topoisomerase II. *J. Biol. Chem.* **274**, 21688–21694 (1999).

163. Morris, S. K. & Lindsley, J. E. Yeast topoisomerase II is inhibited by etoposide after hydrolyzing the first ATP and before releasing the second ADP. *J. Biol. Chem.* **274**, 30690–30696 (1999).

164. Austin, C. A. *et al.* TOP2B: The First Thirty Years. *Int. J. Mol. Sci.* **19**, (2018).

165. Martin, E. *et al.* Evaluation of the topoisomerase II-inactive bisdioxopiperazine

ICRF-161 as a protectant against doxorubicin-induced cardiomyopathy. *Toxicology* **255**, 72–79 (2009).

166. Pulleyblank, D. E., Shure, M., Tang, D., Vinograd, J. & Vosberg, H. P. Action of nicking-closing enzyme on supercoiled and nonsupercoiled closed circular DNA: formation of a Boltzmann distribution of topological isomers. *Proc. Natl. Acad. Sci. U. S. A.* **72**, 4280–4284 (1975).

167. Rybenkov, V. V, Ullsperger, C., Vologodskii, A. V & Cozzarelli, N. R. Simplification of DNA topology below equilibrium values by type II topoisomerases. *Science* **277**, 690–693 (1997).

168. Vologodskii, A. V *et al.* Mechanism of topology simplification by type II DNA topoisomerases. *Proc. Natl. Acad. Sci. U. S. A.* **98**, 3045–3049 (2001).

169. Smiley, R. D., Collins, T. R. L., Hammes, G. G. & Hsieh, T.-S. Single-molecule measurements of the opening and closing of the DNA gate by eukaryotic topoisomerase II. *Proc. Natl. Acad. Sci. U. S. A.* **104**, 4840–4845 (2007).

170. Collins, T. R. L., Hammes, G. G. & Hsieh, T.-S. Analysis of the eukaryotic topoisomerase II DNA gate: a single-molecule FRET and structural perspective. *Nucleic Acids Res.* **37**, 712–720 (2009).

171. Fortune, J. M. & Osheroff, N. Topoisomerase II as a target for anticancer drugs: when enzymes stop being nice. *Prog. Nucleic Acid Res. Mol. Biol.* **64**, 221–253 (2000).

172. Deweese, J. E., Burgin, A. B. & Osheroff, N. Using 3'-bridging phosphorothiolates to isolate the forward DNA cleavage reaction of human topoisomerase IIalpha. *Biochemistry* **47**, 4129–4140 (2008).

173. Deweese, J. E., Burgin, A. B. & Osheroff, N. Human topoisomerase IIalpha uses a two-metal-ion mechanism for DNA cleavage. *Nucleic Acids Res.* **36**, 4883–4893 (2008).

174. Schmidt, B. H., Burgin, A. B., Deweese, J. E., Osheroff, N. & Berger, J. M. A novel and unified two-metal mechanism for DNA cleavage by type II and IA topoisomerases. *Nature* **465**, 641–644 (2010).

175. Schultz, P., Olland, S., Oudet, P. & Hancock, R. Structure and conformational changes of DNA topoisomerase II visualized by electron microscopy. *Proc Natl Acad Sci U S A* **93**, 5936–5940 (1996).

176. Classen, S., Olland, S. & Berger, J. M. Structure of the topoisomerase II ATPase region and its mechanism of inhibition by the chemotherapeutic agent ICRF-187. *Proc Natl Acad Sci U S A* **100**, 10629–10634 (2003).

177. Schmidt, B. H., Osheroff, N. & Berger, J. M. Structure of a topoisomerase II-DNA-nucleotide complex reveals a new control mechanism for ATPase activity. *Nat Struct Mol Biol* **19**, 1147–1154 (2012).

178. Wang, Y.-R. *et al.* Producing irreversible topoisomerase II-mediated DNA breaks by site-specific Pt(II)-methionine coordination chemistry. *Nucleic Acids Res.* **45**, 10861–10871 (2017).

179. Dutta, R. & Inouye, M. GHKL, an emergent ATPase/kinase superfamily. *Trends Biochem. Sci.* **25**, 24–28 (2000).

180. Stanger, F. V, Dehio, C. & Schirmer, T. Structure of the N-terminal Gyrase B fragment in complex with ADPPi reveals rigid-body motion induced by ATP hydrolysis. *PLoS One* **9**, e107289 (2014).

181. Vaughn, J. *et al.* Stability of the topoisomerase II closed clamp conformation may influence DNA-stimulated ATP hydrolysis. *J Biol Chem* **280**, 11920–11929 (2005).

182. Wigley, D. B., Davies, G. J., Dodson, E. J., Maxwell, A. & Dodson, G. Crystal structure of an N-terminal fragment of the DNA gyrase B protein. *Nature* **351**, 624–629 (1991).

183. Walker, J. V *et al.* A mutation in human topoisomerase II alpha whose expression is lethal in DNA repair-deficient yeast cells. *J Biol Chem* **279**, 25947–25954 (2004).

184. Oestergaard, V. H., Giangiacomo, L., Bjergbaek, L., Knudsen, B. R. & Andersen, A. H. Hindering the strand passage reaction of human topoisomerase IIalpha without disturbing DNA cleavage, ATP hydrolysis, or the operation of the N-terminal clamp. *J. Biol. Chem.* **279**, 28093–28099 (2004).

185. Oestergaard, V. H. *et al.* The transducer domain is important for clamp operation in human DNA topoisomerase IIalpha. *J. Biol. Chem.* **279**, 1684–1691 (2004).

186. Bjergbaek, L. *et al.* Communication between the ATPase and cleavage/religation domains of human topoisomerase IIalpha. *J. Biol. Chem.* **275**, 13041–13048 (2000).

187. Roca, J. The path of the DNA along the dimer interface of topoisomerase II. *J. Biol. Chem.* **279**, 25783–25788 (2004).

188. Aravind, L., Leipe, D. D. & Koonin, E. V. Toprim--a conserved catalytic domain in type IA and II topoisomerases, DnaG-type primases, OLD family nucleases and RecR proteins. *Nucleic Acids Res.* **26**, 4205–4213 (1998).

189. Morais Cabral, J. H. *et al.* Crystal structure of the breakage-reunion domain of DNA gyrase. *Nature* **388**, 903–906 (1997).

190. Caron, P. R., Watt, P. & Wang, J. C. The C-terminal domain of Saccharomyces cerevisiae DNA topoisomerase II. *Mol Cell Biol* **14**, 3197–3207 (1994).

191. Lambert, J.-P. *et al.* Interactome Rewiring Following Pharmacological Targeting of BET Bromodomains. *Mol. Cell* **73**, 621-638.e17 (2019).

192. Kumar, S., Kandavelu, P. & Rathod, P. Crystal structure of Plasmodium falciparum topoisomerase II DNA-binding, cleavage and re-ligation domain. *Unpubl. Manuscr.* (2019).

193. Liu, L. F. & Wang, J. C. Interaction between DNA and Escherichia coli DNA topoisomerase I. Formation of complexes between the protein and superhelical and nonsuperhelical duplex DNAs. *J. Biol. Chem.* **254**, 11082–11088 (1979).

194. Liu, L. F. DNA topoisomerase poisons as antitumor drugs. *Annu Rev Biochem* **58**, 351–375 (1989).

195. Montecucco, A., Zanetta, F. & Biamonti, G. Molecular mechanisms of etoposide. *EXCLI J.* **14**, 95–108 (2015).

196. Carvalho, C. *et al.* Doxorubicin: the good, the bad and the ugly effect. *Curr. Med. Chem.* **16**, 3267–3285 (2009).

197. Tacar, O., Sriamornsak, P. & Dass, C. R. Doxorubicin: an update on anticancer molecular action, toxicity and novel drug delivery systems. *J. Pharm. Pharmacol.* **65**, 157–170 (2013).

198. Nitiss, J. L., Liu, Y. X. & Hsiung, Y. A temperature sensitive topoisomerase II allele confers temperature dependent drug resistance on amsacrine and etoposide: a

genetic system for determining the targets of topoisomerase II inhibitors. *Cancer Res.* **53**, 89–93 (1993).

199. Nitiss, J. L. Using yeast to study resistance to topoisomerase II-targeting drugs. *Cancer Chemother. Pharmacol.* **34 Suppl**, S6-13 (1994).

200. Ishida, R. *et al.* Inhibition of intracellular topoisomerase II by antitumor bis(2,6-dioxopiperazine) derivatives: mode of cell growth inhibition distinct from that of cleavable complex-forming type inhibitors. *Cancer Res.* **51**, 4909–4916 (1991).

201. Kerrigan, D., Pommier, Y. & Kohn, K. W. Protein-linked DNA strand breaks produced by etoposide and teniposide in mouse L1210 and human VA-13 and HT-29 cell lines: relationship to cytotoxicity. *NCI Monogr.* 117–121 (1987).

202. Covey, J. M., Kohn, K. W., Kerrigan, D., Tilchen, E. J. & Pommier, Y. Topoisomerase II-mediated DNA damage produced by 4'-(9-acridinylamino)methanesulfon-m-anisidide and related acridines in L1210 cells and isolated nuclei: relation to cytotoxicity. *Cancer Res.* **48**, 860–865 (1988).

203. Maxwell, A. The molecular basis of quinolone action. *J. Antimicrob. Chemother.* **30**, 409–414 (1992).

204. Corbett, A. H. & Osheroff, N. When good enzymes go bad: conversion of topoisomerase II to a cellular toxin by antineoplastic drugs. *Chem. Res. Toxicol.* **6**, 585–597 (1993).

205. Pommier, Y. DNA topoisomerase I and II in cancer chemotherapy: update and perspectives. *Cancer Chemother. Pharmacol.* **32**, 103–108 (1993).

206. Chen, A. Y. & Liu, L. F. DNA topoisomerases: essential enzymes and lethal targets. *Annu. Rev. Pharmacol. Toxicol.* **34**, 191–218 (1994).

207. Kreuzer, K. N. & Cozzarelli, N. R. Escherichia coli mutants thermosensitive for deoxyribonucleic acid gyrase subunit A: effects on deoxyribonucleic acid replication, transcription, and bacteriophage growth. *J. Bacteriol.* **140**, 424–435 (1979).

208. Gupta, M., Fujimori, A. & Pommier, Y. Eukaryotic DNA topoisomerases I. *Biochim. Biophys. Acta* **1262**, 1–14 (1995).

209. Beck, W. T., Kim, R. & Chen, M. Novel actions of inhibitors of DNA topoisomerase II in drug-resistant tumor cells. *Cancer Chemother. Pharmacol.* **34 Suppl**, S14-8 (1994).

210. Pommier, Y. *et al.* Cellular determinants of sensitivity and resistance to DNA topoisomerase inhibitors. *Cancer Invest.* **12**, 530–542 (1994).

211. Kaufmann, S. H. Cell death induced by topoisomerase-targeted drugs: more questions than answers. *Biochim. Biophys. Acta* **1400**, 195–211 (1998).

212. Hsiang, Y. H., Lihou, M. G. & Liu, L. F. Arrest of replication forks by drug-stabilized topoisomerase I-DNA cleavable complexes as a mechanism of cell killing by camptothecin. *Cancer Res.* **49**, 5077–5082 (1989).

213. Howard, M. T., Neece, S. H., Matson, S. W. & Kreuzer, K. N. Disruption of a topoisomerase-DNA cleavage complex by a DNA helicase. *Proc. Natl. Acad. Sci. U. S. A.* **91**, 12031–12035 (1994).

214. Drlica, K., Malik, M., Kerns, R. J. & Zhao, X. Quinolone-mediated bacterial death. *Antimicrob. Agents Chemother.* **52**, 385–392 (2008).

215. Sinha, B. K. Topoisomerase inhibitors. A review of their therapeutic potential in cancer. *Drugs* **49**, 11–19 (1995).

216. Staker, B. L. *et al.* The mechanism of topoisomerase I poisoning by a camptothecin analog. *Proc. Natl. Acad. Sci. U. S. A.* **99**, 15387–15392 (2002).

217. Osheroff, N. Effect of antineoplastic agents on the DNA cleavage/religation reaction of eukaryotic topoisomerase II: inhibition of DNA religation by etoposide. *Biochemistry* **28**, 6157–6160 (1989).

218. Freudenreich, C. H. & Kreuzer, K. N. Localization of an aminoacridine antitumor agent in a type II topoisomerase-DNA complex. *Proc. Natl. Acad. Sci. U. S. A.* **91**, 11007–11011 (1994).

219. Beck, W. T., Danks, M. K., Wolverton, J. S., Kim, R. & Chen, M. Drug resistance associated with altered DNA topoisomerase II. *Adv. Enzyme Regul.* **33**, 113–127 (1993).

220. Beck, W. T. *et al.* Resistance of mammalian tumor cells to inhibitors of DNA topoisomerase II. *Adv. Pharmacol.* **29B**, 145–169 (1994).

221. Bjornsti, M. A., Knab, A. M. & Benedetti, P. Yeast Saccharomyces cerevisiae as a model system to study the cytotoxic activity of the antitumor drug camptothecin. *Cancer Chemother. Pharmacol.* **34 Suppl**, S1-5 (1994).

222. Froelich-Ammon, S. J., Patchan, M. W., Osheroff, N. & Thompson, R. B. Topoisomerase II binds to ellipticine in the absence or presence of DNA. Characterization of enzyme-drug interactions by fluorescence spectroscopy. *J. Biol. Chem.* **270**, 14998–15004 (1995).

223. Nabiev, I. *et al.* Molecular interactions of DNA-topoisomerase I and II inhibitor with DNA and topoisomerases and in ternary complexes: binding modes and biological effects for intoplicine derivatives. *Biochemistry* **33**, 9013–9023 (1994).

224. Capranico, G. & Zunino, F. DNA topoisomerase-trapping antitumour drugs. *Eur. J. Cancer* **28A**, 2055–2060 (1992).

225. Bandele, O. J. & Osheroff, N. Bioflavonoids as poisons of human topoisomerase II alpha and II beta. *Biochemistry* **46**, 6097–6108 (2007).

226. Bandele, O. J. & Osheroff, N. The efficacy of topoisomerase II-targeted anticancer agents reflects the persistence of drug-induced cleavage complexes in cells. *Biochemistry* **47**, 11900–11908 (2008).

227. Toyoda, E. *et al.* NK314, a topoisomerase II inhibitor that specifically targets the alpha isoform. *J. Biol. Chem.* **283**, 23711–23720 (2008).

228. Capranico, G. & Binaschi, M. DNA sequence selectivity of topoisomerases and topoisomerase poisons. *Biochim Biophys Acta* **1400**, 185–194 (1998).

229. Pommier, Y., Capranico, G., Orr, A. & Kohn, K. W. Local base sequence preferences for DNA cleavage by mammalian topoisomerase II in the presence of amsacrine or teniposide. *Nucleic Acids Res* **19**, 5973–5980 (1991).

230. Capranico, G., Kohn, K. W. & Pommier, Y. Local sequence requirements for DNA cleavage by mammalian topoisomerase II in the presence of doxorubicin. *Nucleic Acids Res* **18**, 6611–6619 (1990).

231. Chabner, B. A. & Longo, D. L. *Cancer chemotherapy and biotherapy: principles and practice*. (Lippincott Williams & Wilkins, 2011).

232. Pommier, Y. *DNA topoisomerases and cancer*. (Springer, 2012).

233. Evison, B. J., Sleebs, B. E., Watson, K. G., Phillips, D. R. & Cutts, S. M. Mitoxantrone, More than Just Another Topoisomerase II Poison. *Med. Res. Rev.* **36**, 248–299 (2016).

234. Nitiss, J. L. & Beck, W. T. Antitopoisomerase drug action and resistance. *Eur J Cancer* **32A**, 958–966 (1996).

235. Stone, R. M. *et al.* Phase III open-label randomized study of cytarabine in combination with amonafide L-malate or daunorubicin as induction therapy for patients with secondary acute myeloid leukemia. *J. Clin. Oncol.* **33**, 1252–1257 (2015).

236. Hooper, D. C. & Wolfson, J. S. Fluoroquinolone antimicrobial agents. *N. Engl. J. Med.* **324**, 384–394 (1991).

237. Ross, W., Rowe, T., Glisson, B., Yalowich, J. & Liu, L. Role of topoisomerase II in mediating epipodophyllotoxin-induced DNA cleavage. *Cancer Res.* **44**, 5857–5860 (1984).

238. Hevener, K., Verstak, T. A., Lutat, K. E., Riggsbee, D. L. & Mooney, J. W. Recent developments in topoisomerase-targeted cancer chemotherapy. *Acta Pharm. Sin. B* **8**, 844–861 (2018).

239. Bjorkholm, M. Etoposide and teniposide in the treatment of acute leukemia. *Med. Oncol. Tumor Pharmacother.* **7**, 3–10 (1990).

240. Hsiung, Y., Elsea, S. H., Osheroff, N. & Nitiss, J. L. A mutation in yeast TOP2 homologous to a quinolone-resistant mutation in bacteria. Mutation of the amino acid homologous to Ser83 of Escherichia coli gyrA alters sensitivity to eukaryotic topoisomerase inhibitors. *J. Biol. Chem.* **270**, 20359–20364 (1995).

241. Hooper, D. C. & Wolfson, J. S. The fluoroquinolones: pharmacology, clinical uses, and toxicities in humans. *Antimicrob. Agents Chemother.* **28**, 716–721 (1985).

242. Robinson, M. J. *et al.* Effects of quinolone derivatives on eukaryotic topoisomerase II. A novel mechanism for enhancement of enzyme-mediated DNA cleavage. *J. Biol. Chem.* **266**, 14585–14592 (1991).

243. Ravandi, F. *et al.* Phase 3 results for vosaroxin/cytarabine in the subset of patients >/=60 years old with refractory/early relapsed acute myeloid leukemia. *Haematologica* **103**, e514–e518 (2018).

244. Kane, R. C., McGuinn, W. D. J., Dagher, R., Justice, R. & Pazdur, R. Dexrazoxane (Totect): FDA review and approval for the treatment of accidental extravasation following intravenous anthracycline chemotherapy. *Oncologist* **13**, 445–450 (2008).

245. Roca, J., Ishida, R., Berger, J. M., Andoh, T. & Wang, J. C. Antitumor bisdioxopiperazines inhibit yeast DNA topoisomerase II by trapping the enzyme in the form of a closed protein clamp. *Proc. Natl. Acad. Sci. U. S. A.* **91**, 1781–1785 (1994).

246. Jensen, L. H. *et al.* A novel mechanism of cell killing by anti-topoisomerase II bisdioxopiperazines. *J. Biol. Chem.* **275**, 2137–2146 (2000).

247. Lee, J. H., Wendorff, T. J. & Berger, J. M. Resveratrol: A novel type of topoisomerase II inhibitor. *J. Biol. Chem.* **292**, 21011–21022 (2017).

248. Jensen, P. B. & Sehested, M. DNA topoisomerase II rescue by catalytic inhibitors: a new strategy to improve the antitumor selectivity of etoposide. *Biochem. Pharmacol.* **54**, 755–759 (1997).

249. Yang, S.-Y. *et al.* Inhibition of topoisomerase II by 8-chloro-adenosine triphosphate induces DNA double-stranded breaks in 8-chloro-adenosine-exposed

human myelocytic leukemia K562 cells. *Biochem. Pharmacol.* **77**, 433–443 (2009).

250. Chene, P. *et al.* Catalytic inhibition of topoisomerase II by a novel rationally designed ATP-competitive purine analogue. *BMC Chem. Biol.* **9**, 1 (2009).

251. Buettner, R. *et al.* 8-Chloro-Adenosine Inhibits Molecular Poor-Risk Acute Myeloid Leukemia (AML) and Leukemic Stem Cells (LSC) Growth Via Novel RNA- and ATP-Directed Mechanisms: A Novel Therapeutic Approach for AML. *Blood* **126**, 792 LP – 792 (2015).

252. Li, Y. *et al.* Emodin triggers DNA double-strand breaks by stabilizing topoisomerase II-DNA cleavage complexes and by inhibiting ATP hydrolysis of topoisomerase II. *Toxicol. Sci.* **118**, 435–443 (2010).

253. Hu, C.-X. *et al.* Salvicine functions as novel topoisomerase II poison by binding to ATP pocket. *Mol. Pharmacol.* **70**, 1593–1601 (2006).

254. Sorensen, B. S. *et al.* Mode of action of topoisomerase II-targeting agents at a specific DNA sequence. Uncoupling the DNA binding, cleavage and religation events. *J. Mol. Biol.* **228**, 778–786 (1992).

255. Fortune, J. M. & Osheroff, N. Merbarone inhibits the catalytic activity of human topoisomerase IIalpha by blocking DNA cleavage. *J. Biol. Chem.* **273**, 17643–17650 (1998).

256. Jun, K.-Y. & Kwon, Y. Proposal of Dual Inhibitor Targeting ATPase Domains of Topoisomerase II and Heat Shock Protein 90. *Biomol. Ther. (Seoul).* **24**, 453–468 (2016).

257. Jensen, L. H. *et al.* Characterisation of cytotoxicity and DNA damage induced by the topoisomerase II-directed bisdioxopiperazine anti-cancer agent ICRF-187 (dexrazoxane) in yeast and mammalian cells. *BMC Pharmacol.* **4**, 31 (2004).

258. Liu, L. F., Rowe, T. C., Yang, L., Tewey, K. M. & Chen, G. L. Cleavage of DNA by mammalian DNA topoisomerase II. *J. Biol. Chem.* **258**, 15365–15370 (1983).

259. Walker, J. V & Nitiss, J. L. DNA topoisomerase II as a target for cancer chemotherapy. *Cancer Invest.* **20**, 570–589 (2002).

260. Sander, M. & Hsieh, T. Double strand DNA cleavage by type II DNA topoisomerase from Drosophila melanogaster. *J. Biol. Chem.* **258**, 8421–8428 (1983).

261. Isik, S. *et al.* The SUMO pathway is required for selective degradation of DNA topoisomerase IIbeta induced by a catalytic inhibitor ICRF-193(1). *FEBS Lett.* **546**, 374–378 (2003).

262. Mao, Y., Desai, S. D. & Liu, L. F. SUMO-1 conjugation to human DNA topoisomerase II isozymes. *J. Biol. Chem.* **275**, 26066–26073 (2000).

263. Bachant, J., Alcasabas, A., Blat, Y., Kleckner, N. & Elledge, S. J. The SUMO-1 isopeptidase Smt4 is linked to centromeric cohesion through SUMO-1 modification of DNA topoisomerase II. *Mol. Cell* **9**, 1169–1182 (2002).

264. Azuma, Y., Arnaoutov, A. & Dasso, M. SUMO-2/3 regulates topoisomerase II in mitosis. *J. Cell Biol.* **163**, 477–487 (2003).

265. Nitiss, J. L. & Nitiss, K. C. Tdp2: a means to fixing the ends. *PLoS Genet.* **9**, e1003370 (2013).

266. Neale, M. J., Pan, J. & Keeney, S. Endonucleolytic processing of covalent protein-linked DNA double-strand breaks. *Nature* **436**, 1053–1057 (2005).

267. Sartori, A. A. *et al.* Human CtIP promotes DNA end resection. *Nature* **450**, 509–514 (2007).

268. Malik, M., Nitiss, K. C., Enriquez-Rios, V. & Nitiss, J. L. Roles of nonhomologous end-joining pathways in surviving topoisomerase II-mediated DNA damage. *Mol. Cancer Ther.* **5**, 1405–1414 (2006).

269. Powell, S. N. & Kachnic, L. A. Therapeutic exploitation of tumor cell defects in homologous recombination. *Anticancer. Agents Med. Chem.* **8**, 448–460 (2008).

270. Lund, B., Hansen, O. P., Hansen, H. H. & Hansen, M. Combination therapy with carboplatin/cisplatin/ifosfamide/etoposide in ovarian cancer. *Semin. Oncol.* **19**, 26–29 (1992).

271. Pautier, P. *et al.* Combination of bleomycin, etoposide, and cisplatin for the treatment of advanced ovarian granulosa cell tumors. *Int. J. Gynecol. Cancer* **18**, 446–452 (2008).

272. Zhang, S. *et al.* Identification of the molecular basis of doxorubicin-induced cardiotoxicity. *Nat. Med.* **18**, 1639–1642 (2012).

273. Rowley, J. D. & Olney, H. J. International workshop on the relationship of prior therapy to balanced chromosome aberrations in therapy-related myelodysplastic syndromes and acute leukemia: overview report. *Genes, chromosomes & cancer* **33**, 331–345 (2002).

274. Allan, J. M. & Travis, L. B. Mechanisms of therapy-related carcinogenesis. *Nat. Rev. Cancer* **5**, 943–955 (2005).

275. Errington, F., Willmore, E., Leontiou, C., Tilby, M. J. & Austin, C. A. Differences in the longevity of topo IIalpha and topo IIbeta drug-stabilized cleavable complexes and the relationship to drug sensitivity. *Cancer Chemother. Pharmacol.* **53**, 155–162 (2004).

276. Willmore, E., Frank, A. J., Padget, K., Tilby, M. J. & Austin, C. A. Etoposide targets topoisomerase IIalpha and IIbeta in leukemic cells: isoform-specific cleavable complexes visualized and quantified in situ by a novel immunofluorescence technique. *Mol. Pharmacol.* **54**, 78–85 (1998).

277. Felix, C. A. Secondary leukemias induced by topoisomerase-targeted drugs. *Biochim. Biophys. Acta* **1400**, 233–255 (1998).

278. Cowell, I. G. *et al.* Model for MLL translocations in therapy-related leukemia involving topoisomerase IIbeta-mediated DNA strand breaks and gene proximity. *Proc. Natl. Acad. Sci. U. S. A.* **109**, 8989–8994 (2012).

279. Pendleton, M., Lindsey Jr., R. H., Felix, C. A., Grimwade, D. & Osheroff, N. Topoisomerase II and leukemia. *Ann N Y Acad Sci* **1310**, 98–110 (2014).

280. Smith, M. A., Rubinstein, L. & Ungerleider, R. S. Therapy-related acute myeloid leukemia following treatment with epipodophyllotoxins: estimating the risks. *Med. Pediatr. Oncol.* **23**, 86–98 (1994).

281. Ezoe, S. Secondary leukemia associated with the anti-cancer agent, etoposide, a topoisomerase II inhibitor. *Int. J. Environ. Res. Public Health* **9**, 2444–2453 (2012).

282. Kollmannsberger, C. *et al.* Secondary leukemia following high cumulative doses of etoposide in patients treated for advanced germ cell tumors. *J. Clin. Oncol.* **16**, 3386–3391 (1998).

283. Smith, K. A., Cowell, I. G., Zhang, Y., Sondka, Z. & Austin, C. A. The role of

topoisomerase II beta on breakage and proximity of RUNX1 to partner alleles RUNX1T1 and EVI1. *Genes. Chromosomes Cancer* **53**, 117–128 (2014).

284. Azarova, A. M. *et al.* Roles of DNA topoisomerase II isozymes in chemotherapy and secondary malignancies. *Proc Natl Acad Sci U S A* **104**, 11014–11019 (2007).

285. Volkova, M. & Russell, R. 3rd. Anthracycline cardiotoxicity: prevalence, pathogenesis and treatment. *Curr. Cardiol. Rev.* **7**, 214–220 (2011).

286. Hortobagyi, G. N. Anthracyclines in the treatment of cancer. An overview. *Drugs* **54 Suppl 4**, 1–7 (1997).

287. Singal, P. K., Li, T., Kumar, D., Danelisen, I. & Iliskovic, N. Adriamycin-induced heart failure: mechanism and modulation. *Mol. Cell. Biochem.* **207**, 77–86 (2000).

288. Damrot, J. *et al.* Lovastatin protects human endothelial cells from the genotoxic and cytotoxic effects of the anticancer drugs doxorubicin and etoposide. *Br. J. Pharmacol.* **149**, 988–997 (2006).

289. Nitiss, K. C. & Nitiss, J. L. Twisting and ironing: doxorubicin cardiotoxicity by mitochondrial DNA damage. *Clin. Cancer Res.* **20**, 4737–4739 (2014).

290. Sepe, D. M., Ginsberg, J. P. & Balis, F. M. Dexrazoxane as a cardioprotectant in children receiving anthracyclines. *Oncologist* **15**, 1220–1226 (2010).

291. Hensley, M. L. *et al.* American Society of Clinical Oncology 2008 clinical practice guideline update: use of chemotherapy and radiation therapy protectants. *J. Clin. Oncol.* **27**, 127–145 (2009).

292. Swain, S. M. *et al.* Delayed administration of dexrazoxane provides cardioprotection for patients with advanced breast cancer treated with doxorubicin-containing therapy. *J. Clin. Oncol.* **15**, 1333–1340 (1997).

293. Swain, S. M. *et al.* Cardioprotection with dexrazoxane for doxorubicin-containing therapy in advanced breast cancer. *J. Clin. Oncol.* **15**, 1318–1332 (1997).

294. Sawyer, D. B. Anthracyclines and heart failure. *N. Engl. J. Med.* **368**, 1154–1156 (2013).

295. Jungwirth, H. & Kuchler, K. Yeast ABC transporters-- a tale of sex, stress, drugs and aging. *FEBS Lett.* **580**, 1131–1138 (2006).

296. Shukla, S., Ohnuma, S. & Ambudkar, S. V. Improving cancer chemotherapy with modulators of ABC drug transporters. *Curr. Drug Targets* **12**, 621–630 (2011).

297. Shukla, S., Wu, C.-P. & Ambudkar, S. V. Development of inhibitors of ATP-binding cassette drug transporters: present status and challenges. *Expert Opin. Drug Metab. Toxicol.* **4**, 205–223 (2008).

298. Wang, F., Jiang, X., Yang, D. C., Elliott, R. L. & Head, J. F. Doxorubicin-gallium-transferrin conjugate overcomes multidrug resistance: evidence for drug accumulation in the nucleus of drug resistant MCF-7/ADR cells. *Anticancer Res.* **20**, 799–808 (2000).

299. Perez-Soler, R. *et al.* Annamycin circumvents resistance mediated by the multidrug resistance-associated protein (MRP) in breast MCF-7 and small-cell lung UMCC-1 cancer cell lines selected for resistance to etoposide. *Int. J. cancer* **71**, 35–41 (1997).

300. Choi, C.-H. ABC transporters as multidrug resistance mechanisms and the development of chemosensitizers for their reversal. *Cancer Cell Int.* **5**, 30 (2005).

301. Beck, W. T., Mueller, T. J. & Tanzer, L. R. Altered surface membrane glycoproteins in Vinca alkaloid-resistant human leukemic lymphoblasts. *Cancer*

Res. **39**, 2070–2076 (1979).

302. Cho, S. *et al.* Notch1 regulates the expression of the multidrug resistance gene ABCC1/MRP1 in cultured cancer cells. *Proc. Natl. Acad. Sci. U. S. A.* **108**, 20778–20783 (2011).

303. Politi, P. M. & Sinha, B. K. Role of differential drug uptake, efflux, and binding of etoposide in sensitive and resistant human tumor cell lines: implications for the mechanisms of drug resistance. *Mol. Pharmacol.* **35**, 271–278 (1989).

304. Beck, W. T. Mechanisms of multidrug resistance in human tumor cells. The roles of P-glycoprotein, DNA topoisomerase II, and other factors. *Cancer Treat. Rev.* **17 Suppl A**, 11–20 (1990).

305. Danks, M. K., Yalowich, J. C. & Beck, W. T. Atypical multiple drug resistance in a human leukemic cell line selected for resistance to teniposide (VM-26). *Cancer Res.* **47**, 1297–1301 (1987).

306. Vassetzky, Y. S., Alghisi, G. C., Roberts, E. & Gasser, S. M. Ectopic expression of inactive forms of yeast DNA topoisomerase II confers resistance to the anti-tumour drug, etoposide. *Br. J. Cancer* **73**, 1201–1209 (1996).

307. Jiang, X. Random mutagenesis of the B'A' core domain of yeast DNA topoisomerase II and large-scale screens of mutants resistant to the anticancer drug etoposide. *Biochem Biophys Res Commun* **327**, 597–603 (2005).

308. Hohl, A. M. *et al.* Restoration of topoisomerase 2 function by complementation of defective monomers in Drosophila. *Genetics* **192**, 843–856 (2012).

309. Ishida, R. *et al.* DNA topoisomerase II is the molecular target of bisdioxopiperazine derivatives ICRF-159 and ICRF-193 in Saccharomyces cerevisiae. *Cancer Res.* **55**, 2299–2303 (1995).

310. Wasserman, R. A. & Wang, J. C. Analysis of yeast DNA topoisomerase II mutants resistant to the antitumor drug amsacrine. *Cancer Res.* **54**, 1795–1800 (1994).

311. Nitiss, J. L. *et al.* Amsacrine and etoposide hypersensitivity of yeast cells overexpressing DNA topoisomerase II. *Cancer Res.* **52**, 4467–4472 (1992).

312. Dong, J., Walker, J. & Nitiss, J. L. A mutation in yeast topoisomerase II that confers hypersensitivity to multiple classes of topoisomerase II poisons. *J Biol Chem* **275**, 7980–7987 (2000).

313. Elsea, S. H., Hsiung, Y., Nitiss, J. L. & Osheroff, N. A yeast type II topoisomerase selected for resistance to quinolones. Mutation of histidine 1012 to tyrosine confers resistance to nonintercalative drugs but hypersensitivity to ellipticine. *J. Biol. Chem.* **270**, 1913–1920 (1995).

314. Rogojina, A. T. & Nitiss, J. L. Isolation and characterization of mAMSA-hypersensitive mutants. Cytotoxicity of Top2 covalent complexes containing DNA single strand breaks. *J Biol Chem.* **283**, 29239–50. doi: 10.1074/jbc.M804058200. Epub 2008 A (2008).

315. Strumberg, D., Nitiss, J. L., Rose, A., Nicklaus, M. C. & Pommier, Y. Mutation of a conserved serine residue in a quinolone-resistant type II topoisomerase alters the enzyme-DNA and drug interactions. *J Biol Chem* **274**, 7292–7301 (1999).

316. Strumberg, D., Nitiss, J. L., Dong, J., Kohn, K. W. & Pommier, Y. Molecular analysis of yeast and human type II topoisomerases. Enzyme-DNA and drug interactions. *J Biol Chem* **274**, 28246–28255 (1999).

317. Bugg, B. Y., Danks, M. K., Beck, W. T. & Suttle, D. P. Expression of a mutant

DNA topoisomerase II in CCRF-CEM human leukemic cells selected for resistance to teniposide. *Proc. Natl. Acad. Sci. U. S. A.* **88**, 7654–7658 (1991).

318. Hinds, M. *et al.* Identification of a point mutation in the topoisomerase II gene from a human leukemia cell line containing an amsacrine-resistant form of topoisomerase II. *Cancer Res.* **51**, 4729–4731 (1991).

319. Liu, Y. X., Hsiung, Y., Jannatipour, M., Yeh, Y. & Nitiss, J. L. Yeast topoisomerase II mutants resistant to anti-topoisomerase agents: identification and characterization of new yeast topoisomerase II mutants selected for resistance to etoposide. *Cancer Res.* **54**, 2943–2951 (1994).

320. Sabourin, M., Byl, J. A., Hannah, S. E., Nitiss, J. L. & Osheroff, N. A mutant yeast topoisomerase II (top2G437S) with differential sensitivity to anticancer drugs in the presence and absence of ATP. *J. Biol. Chem.* **273**, 29086–29092 (1998).

321. Blower, T. *et al.* Quinolone susceptibility landscape of eukaryotic type II topoisomerases determined by next-generation sequencing. *Unpubl. Manuscr.* (2019).

322. Sreedharan, S., Oram, M., Jensen, B., Peterson, L. R. & Fisher, L. M. DNA gyrase gyrA mutations in ciprofloxacin-resistant strains of Staphylococcus aureus: close similarity with quinolone resistance mutations in Escherichia coli. *J. Bacteriol.* **172**, 7260–7262 (1990).

323. Gruger, T. *et al.* A mutation in Escherichia coli DNA gyrase conferring quinolone resistance results in sensitivity to drugs targeting eukaryotic topoisomerase II. *Antimicrob. Agents Chemother.* **48**, 4495–4504 (2004).

324. Hicks, J., Sherman, F. & Fink, G. Methods in Yeast Genetics. (1979).

325. Rose, M. D., Novick, P., Thomas, J. H., Botstein, D. & Fink, G. R. A Saccharomyces cerevisiae genomic plasmid bank based on a centromere-containing shuttle vector. *Gene* **60**, 237–243 (1987).

326. Hsiung, Y. *et al.* Functional expression of human topoisomerase II alpha in yeast: mutations at amino acids 450 or 803 of topoisomerase II alpha result in enzymes that can confer resistance to anti-topoisomerase II agents. *Cancer Res.* **56**, 91–99 (1996).

327. Dornfeld, K. J. & Livingston, D. M. Effects of controlled RAD52 expression on repair and recombination in Saccharomyces cerevisiae. *Mol. Cell. Biol.* **11**, 2013–2017 (1991).

328. Gietz, D., St Jean, A., Woods, R. A. & Schiestl, R. H. Improved method for high efficiency transformation of intact yeast cells. *Nucleic Acids Res.* **20**, 1425 (1992).

329. Stepanov, A., Nitiss, K. C., Neale, G. & Nitiss, J. L. Enhancing drug accumulation in Saccharomyces cerevisiae by repression of pleiotropic drug resistance genes with chimeric transcription repressors. *Mol. Pharmacol.* **74**, 423–431 (2008).

330. Ito, H., Fukuda, Y., Murata, K. & Kimura, A. Transformation of intact yeast cells treated with alkali cations. *J. Bacteriol.* **153**, 163–168 (1983).

331. Rothstein, R. J. [12] One-step gene disruption in yeast. in *Recombinant DNA Part C* **101**, 202–211 (Academic Press, 1983).

332. Lindsley, J. E. & Wang, J. C. Proteolysis patterns of epitopically labeled yeast DNA topoisomerase II suggest an allosteric transition in the enzyme induced by ATP binding. *Proc. Natl. Acad. Sci. U. S. A.* **88**, 10485–10489 (1991).

333. Gleeson, M. A., White, C. E., Meininger, D. P. & Komives, E. A. Generation of

protease-deficient strains and their use in heterologous protein expression. *Methods Mol. Biol.* **103**, 81–94 (1998).

334. Schultz, L. D. *et al.* Regulated overproduction of the GAL4 gene product greatly increases expression from galactose-inducible promoters on multi-copy expression vectors in yeast. *Gene* **61**, 123–133 (1987).

335. Scherer, S. & Davis, R. W. Replacement of chromosome segments with altered DNA sequences constructed in vitro. *Proc. Natl. Acad. Sci. U. S. A.* **76**, 4951–4955 (1979).

336. Nitiss, J. & Wang, J. C. DNA topoisomerase-targeting antitumor drugs can be studied in yeast. *Proc Natl Acad Sci U S A* **85**, 7501–7505 (1988).

337. Eng, W. K., Faucette, L., Johnson, R. K. & Sternglanz, R. Evidence that DNA topoisomerase I is necessary for the cytotoxic effects of camptothecin. *Mol. Pharmacol.* **34**, 755–760 (1988).

338. Nitiss, J. L. & Wang, J. C. Yeast as a genetic system in the dissection of the mechanism of cell killing by topoisomerase-targeting anti-cancer drugs. *DNA topoisomerases cancer. Oxford Univ. Press. London, United Kingdom* 77–91 (1991).

339. Schild, D., Konforti, B., Perez, C., Gish, W. & Mortimer, R. Isolation and characterization of yeast DNA repair genes : I. Cloning of the RAD52 gene. *Curr. Genet.* **7**, 85–92 (1983).

340. Schuetzer-Muehlbauer, M., Willinger, B., Egner, R., Ecker, G. & Kuchler, K. Reversal of antifungal resistance mediated by ABC efflux pumps from Candida albicans functionally expressed in yeast. *Int. J. Antimicrob. Agents* **22**, 291–300 (2003).

341. Sipos, G. & Kuchler, K. Fungal ATP-binding cassette (ABC) transporters in drug resistance & detoxification. *Curr. Drug Targets* **7**, 471–481 (2006).

342. Tombline, G. *et al.* Effects of an unusual poison identify a lifespan role for Topoisomerase 2 in Saccharomyces cerevisiae. *Aging (Albany. NY).* **9**, 68–97 (2017).

343. Tong, A. H. *et al.* Systematic genetic analysis with ordered arrays of yeast deletion mutants. *Science* **294**, 2364–2368 (2001).

344. Karas, B. J. *et al.* Transferring whole genomes from bacteria to yeast spheroplasts using entire bacterial cells to reduce DNA shearing. *Nat. Protoc.* **9**, 743–750 (2014).

345. Rodriguez, A., Benito, B. & Cagnac, O. Using heterologous expression systems to characterize potassium and sodium transport activities. *Methods Mol. Biol.* **913**, 371–386 (2012).

346. Sanders, E. R. Aseptic laboratory techniques: plating methods. *J. Vis. Exp.* e3064 (2012). doi:10.3791/3064

347. Kwolek-Mirek, M. & Zadrag-Tecza, R. Comparison of methods used for assessing the viability and vitality of yeast cells. *FEMS Yeast Res.* **14**, 1068–1079 (2014).

348. O'Leary, N. A. *et al.* Reference sequence (RefSeq) database at NCBI: current status, taxonomic expansion, and functional annotation. *Nucleic Acids Res.* **44**, D733-45 (2016).

349. Snapgene. No Title. *SnapGene software (from GSL Biotech; available at snapgene.com)*

350. DNASTAR. No Title. *SeqMan NGen®. Version 12.0. DNASTAR. Madison, WI.*

351. Goto, T., Laipis, P. & Wang, J. C. The purification and characterization of DNA topoisomerases I and II of the yeast Saccharomyces cerevisiae. *J. Biol. Chem.* **259**, 10422–10429 (1984).

352. Schroder, E., Jonsson, T. & Poole, L. Hydroxyapatite chromatography: altering the phosphate-dependent elution profile of protein as a function of pH. *Anal. Biochem.* **313**, 176–178 (2003).

353. Bornhorst, J. A. & Falke, J. J. Purification of proteins using polyhistidine affinity tags. *Methods Enzymol.* **326**, 245–254 (2000).

354. Kapust, R. B., Tozser, J., Copeland, T. D. & Waugh, D. S. The P1' specificity of tobacco etch virus protease. *Biochem. Biophys. Res. Commun.* **294**, 949–955 (2002).

355. Robinson, M. J. & Osheroff, N. Effects of antineoplastic drugs on the post-strand-passage DNA cleavage/religation equilibrium of topoisomerase II. *Biochemistry* **30**, 1807–1813 (1991).

356. Robinson, M. J., Corbett, A. H. & Osheroff, N. Effects of topoisomerase II-targeted drugs on enzyme-mediated DNA cleavage and ATP hydrolysis: evidence for distinct drug interaction domains on topoisomerase II. *Biochemistry* **32**, 3638–3643 (1993).

357. Burden, D. A., Froelich-Ammon, S. J. & Osheroff, N. Topoisomerase II-mediated cleavage of plasmid DNA. *Methods Mol. Biol.* **95**, 283–289 (2001).

358. Lindsley, J. E. Use of a real-time, coupled assay to measure the ATPase activity of DNA topoisomerase II. *Methods Mol Biol* **95**, 57–64 (2001).

359. Nitiss, J. L., Soans, E., Rogojina, A., Seth, A. & Mishina, M. Topoisomerase assays. *Curr Protoc Pharmacol* **Chapter 3**, Unit 3 3 (2012).

360. Marini, J. C., Miller, K. G. & Englund, P. T. Decatenation of kinetoplast DNA by topoisomerases. *J. Biol. Chem.* **255**, 4976–4979 (1980).

361. Sehested, M. *et al.* Chinese Hamster Ovary Cells Resistant to the Topoisomerase II Catalytic Inhibitor ICRF-159: A Tyr49Phe Mutation Confers High-Level Resistance to Bisdioxopiperazines. *Cancer Res.* **58**, 1460 LP – 1468 (1998).

362. Morrical, S. W., Lee, J. & Cox, M. M. Continuous association of Escherichia coli single-stranded DNA binding protein with stable complexes of recA protein and single-stranded DNA. *Biochemistry* **25**, 1482–1494 (1986).

363. Tamura, J. K. & Gellert, M. Characterization of the ATP binding site on Escherichia coli DNA gyrase. Affinity labeling of Lys-103 and Lys-110 of the B subunit by pyridoxal 5'-diphospho-5'-adenosine. *J. Biol. Chem.* **265**, 21342–21349 (1990).

364. Gu, M. *et al.* Fluorescently labeled circular DNA molecules for DNA topology and topoisomerases. *Sci. Rep.* **6**, 36006 (2016).

365. Courey, A. J. & Wang, J. C. Cruciform formation in a negatively supercoiled DNA may be kinetically forbidden under physiological conditions. *Cell* **33**, 817–829 (1983).

366. Wang, Y. *et al.* Steady-state kinetics of DNA topoisomerases. *Unpubl. Manuscr.* (2019).

367. Bendsen, S. *et al.* The QTK loop is essential for the communication between the N-terminal atpase domain and the central cleavage--ligation region in human

topoisomerase IIalpha. *Biochemistry* **48**, 6508–6515 (2009).

368. Hu, T., Chang, S. & Hsieh, T. Identifying Lys359 as a critical residue for the ATP-dependent reactions of Drosophila DNA topoisomerase II. *J. Biol. Chem.* **273**, 9586–9592 (1998).

369. Wessel, I. *et al.* Human small cell lung cancer NYH cells selected for resistance to the bisdioxopiperazine topoisomerase II catalytic inhibitor ICRF-187 demonstrate a functional R162Q mutation in the Walker A consensus ATP binding domain of the alpha isoform. *Cancer Res.* **59**, 3442–3450 (1999).

370. Jensen, L. H. *et al.* N-terminal and core-domain random mutations in human topoisomerase II alpha conferring bisdioxopiperazine resistance. *FEBS Lett.* **480**, 201–207 (2000).

371. Sorensen, T. K., Grauslund, M., Jensen, P. B., Sehested, M. & Jensen, L. H. Separation of bisdioxopiperazine- and vanadate resistance in topoisomerase II. *Biochem. Biophys. Res. Commun.* **334**, 853–860 (2005).

372. Danks, M. K., Schmidt, C. A., Deneka, D. A. & Beck, W. T. Increased ATP requirement for activity of and complex formation by DNA topoisomerase II from human leukemic CCRF-CEM cells selected for resistance to teniposide. *Cancer Commun.* **1**, 101–109 (1989).

373. Baird, C. L., Harkins, T. T., Morris, S. K. & Lindsley, J. E. Topoisomerase II drives DNA transport by hydrolyzing one ATP. *Proc. Natl. Acad. Sci. U. S. A.* **96**, 13685–13690 (1999).

374. Skouboe, C. *et al.* A human topoisomerase II alpha heterodimer with only one ATP binding site can go through successive catalytic cycles. *J. Biol. Chem.* **278**, 5768–5774 (2003).

375. Yoshida, H., Bogaki, M., Nakamura, M., Yamanaka, L. M. & Nakamura, S. Quinolone resistance-determining region in the DNA gyrase gyrB gene of Escherichia coli. *Antimicrob. Agents Chemother.* **35**, 1647–1650 (1991).

376. Nitiss, K. C., Malik, M., He, X., White, S. W. & Nitiss, J. L. Tyrosyl-DNA phosphodiesterase (Tdp1) participates in the repair of Top2-mediated DNA damage. *Proc. Natl. Acad. Sci. U. S. A.* **103**, 8953–8958 (2006).

377. El-Khamisy, S. F. *et al.* Defective DNA single-strand break repair in spinocerebellar ataxia with axonal neuropathy-1. *Nature* **434**, 108–113 (2005).

378. Interthal, H. *et al.* SCAN1 mutant Tdp1 accumulates the enzyme--DNA intermediate and causes camptothecin hypersensitivity. *EMBO J.* **24**, 2224–2233 (2005).

379. Miao, Z.-H. *et al.* Hereditary ataxia SCAN1 cells are defective for the repair of transcription-dependent topoisomerase I cleavage complexes. *DNA Repair (Amst).* **5**, 1489–1494 (2006).

380. Krishnan, A. *et al.* Predictors of therapy-related leukemia and myelodysplasia following autologous transplantation for lymphoma: an assessment of risk factors. *Blood* **95**, 1588–1593 (2000).

381. Pedersen-Bjergaard, J. & Philip, P. Balanced translocations involving chromosome bands 11q23 and 21q22 are highly characteristic of myelodysplasia and leukemia following therapy with cytostatic agents targeting at DNA-topoisomerase II. *Blood* **78**, 1147–1148 (1991).

382. Smith, S. M. *et al.* Clinical-cytogenetic associations in 306 patients with therapy-

related myelodysplasia and myeloid leukemia: the University of Chicago series. *Blood* **102**, 43–52 (2003).

383. Blanco, J. G., Edick, M. J. & Relling, M. V. Etoposide induces chimeric Mll gene fusions. *FASEB J. Off. Publ. Fed. Am. Soc. Exp. Biol.* **18**, 173–175 (2004).

384. Broeker, P. L. *et al.* Distribution of 11q23 breakpoints within the MLL breakpoint cluster region in de novo acute leukemia and in treatment-related acute myeloid leukemia: correlation with scaffold attachment regions and topoisomerase II consensus binding sites. *Blood* **87**, 1912–1922 (1996).

385. Super, H. G. *et al.* Identification of complex genomic breakpoint junctions in the t(9;11) MLL-AF9 fusion gene in acute leukemia. *Genes. Chromosomes Cancer* **20**, 185–195 (1997).

386. Langer, T. *et al.* Analysis of t(9;11) chromosomal breakpoint sequences in childhood acute leukemia: almost identical MLL breakpoints in therapy-related AML after treatment without etoposides. *Genes. Chromosomes Cancer* **36**, 393–401 (2003).

387. Reichel, M. *et al.* Biased distribution of chromosomal breakpoints involving the MLL gene in infants versus children and adults with t(4;11) ALL. *Oncogene* **20**, 2900–2907 (2001).

388. Gillert, E. *et al.* A DNA damage repair mechanism is involved in the origin of chromosomal translocations t(4;11) in primary leukemic cells. *Oncogene* **18**, 4663–4671 (1999).

389. Reichel, M. *et al.* Rapid isolation of chromosomal breakpoints from patients with t(4;11) acute lymphoblastic leukemia: implications for basic and clinical research. *Cancer Res.* **59**, 3357–3362 (1999).

390. Zody, M. C. *et al.* DNA sequence of human chromosome 17 and analysis of rearrangement in the human lineage. *Nature* **440**, 1045–1049 (2006).

391. Panchakshari, R. A. *et al.* DNA double-strand break response factors influence end-joining features of IgH class switch and general translocation junctions. *Proc. Natl. Acad. Sci. U. S. A.* **115**, 762–767 (2018).

392. Boboila, C. *et al.* Alternative end-joining catalyzes robust IgH locus deletions and translocations in the combined absence of ligase 4 and Ku70. *Proc. Natl. Acad. Sci. U. S. A.* **107**, 3034–3039 (2010).

393. Chiruvella, K. K., Liang, Z. & Wilson, T. E. Repair of double-strand breaks by end joining. *Cold Spring Harb. Perspect. Biol.* **5**, a012757 (2013).

394. Adachi, N., Suzuki, H., Iiizumi, S. & Koyama, H. Hypersensitivity of nonhomologous DNA end-joining mutants to VP-16 and ICRF-193: implications for the repair of topoisomerase II-mediated DNA damage. *J. Biol. Chem.* **278**, 35897–35902 (2003).

395. Jin, S., Inoue, S. & Weaver, D. T. Differential etoposide sensitivity of cells deficient in the Ku and DNA-PKcs components of the DNA-dependent protein kinase. *Carcinogenesis* **19**, 965–971 (1998).

396. Gomez-Herreros, F. *et al.* TDP2 protects transcription from abortive topoisomerase activity and is required for normal neural function. *Nat. Genet.* **46**, 516–521 (2014).

397. Ashour, M. E., Atteya, R. & El-Khamisy, S. F. Topoisomerase-mediated chromosomal break repair: an emerging player in many games. *Nat. Rev. Cancer*

15, 137–151 (2015).

398. Putnam, C. D. & Kolodner, R. D. Determination of gross chromosomal rearrangement rates. *Cold Spring Harb. Protoc.* **2010**, pdb.prot5492 (2010).

399. Myung, K., Datta, A., Chen, C. & Kolodner, R. D. SGS1, the Saccharomyces cerevisiae homologue of BLM and WRN, suppresses genome instability and homeologous recombination. *Nat. Genet.* **27**, 113–116 (2001).

400. Fishel, R. *et al.* The human mutator gene homolog MSH2 and its association with hereditary nonpolyposis colon cancer. *Cell* **75**, 1027–1038 (1993).

401. Kolodner, R. D., Putnam, C. D. & Myung, K. Maintenance of genome stability in Saccharomyces cerevisiae. *Science* **297**, 552–557 (2002).

402. Whelan, W. L., Gocke, E. & Manney, T. R. The CAN1 locus of Saccharomyces cerevisiae: fine-structure analysis and forward mutation rates. *Genetics* **91**, 35–51 (1979).

403. Lippert, M. J. *et al.* Role for topoisomerase 1 in transcription-associated mutagenesis in yeast. *Proc. Natl. Acad. Sci. U. S. A.* **108**, 698–703 (2011).

404. Hoffmann, W. Molecular characterization of the CAN1 locus in Saccharomyces cerevisiae. A transmembrane protein without N-terminal hydrophobic signal sequence. *J. Biol. Chem.* **260**, 11831–11837 (1985).

405. Rodgers, K. J. & Shiozawa, N. Misincorporation of amino acid analogues into proteins by biosynthesis. *Int. J. Biochem. Cell Biol.* **40**, 1452–1466 (2008).

406. Hall, B. M., Ma, C.-X., Liang, P. & Singh, K. K. Fluctuation analysis CalculatOR: a web tool for the determination of mutation rate using Luria-Delbruck fluctuation analysis. *Bioinformatics* **25**, 1564–1565 (2009).

407. Mortimer, R. K., Schild, D., Contopoulou, C. R. & Kans, J. A. Genetic map of Saccharomyces cerevisiae, edition 10. *Yeast* **5**, 321–403 (1989).

408. Anand, J., Sun, Y., Zhao, Y., Nitiss, K. C. & Nitiss, J. L. Detection of Topoisomerase Covalent Complexes in Eukaryotic Cells. *Methods Mol. Biol.* **1703**, 283–299 (2018).

409. Lewis, L. K. *et al.* Role of the nuclease activity of Saccharomyces cerevisiae Mre11 in repair of DNA double-strand breaks in mitotic cells. *Genetics* **166**, 1701–1713 (2004).

410. Heo, J. *et al.* TDP1 promotes assembly of non-homologous end joining protein complexes on DNA. *DNA Repair (Amst).* **30**, 28–37 (2015).

411. Duffy, S. *et al.* Overexpression screens identify conserved dosage chromosome instability genes in yeast and human cancer. *Proc. Natl. Acad. Sci. U. S. A.* **113**, 9967–9976 (2016).

412. Li, X. C. & Tye, B. K. Ploidy dictates repair pathway choice under DNA replication stress. *Genetics* **187**, 1031–1040 (2011).

413. Frank-Vaillant, M. & Marcand, S. NHEJ regulation by mating type is exercised through a novel protein, Lif2p, essential to the ligase IV pathway. *Genes Dev.* **15**, 3005–3012 (2001).

414. Chen, C. & Kolodner, R. D. Gross chromosomal rearrangements in Saccharomyces cerevisiae replication and recombination defective mutants. *Nat. Genet.* **23**, 81–85 (1999).

415. Khan, F. A. & Ali, S. O. Physiological Roles of DNA Double-Strand Breaks. *J. Nucleic Acids* **2017**, 6439169 (2017).

416. Lyu, Y. L. & Wang, J. C. Aberrant lamination in the cerebral cortex of mouse embryos lacking DNA topoisomerase IIbeta. *Proc. Natl. Acad. Sci. U. S. A.* **100**, 7123–7128 (2003).

417. Kleijer, K. T. E., Huguet, G., Tastet, J., Bourgeron, T. & Burbach, J. P. H. Anatomy and Cell Biology of Autism Spectrum Disorder: Lessons from Human Genetics. *Adv. Anat. Embryol. Cell Biol.* **224**, 1–25 (2017).

418. Huguet, G., Ey, E. & Bourgeron, T. The genetic landscapes of autism spectrum disorders. *Annu. Rev. Genomics Hum. Genet.* **14**, 191–213 (2013).

419. Pinto, D. *et al.* Functional impact of global rare copy number variation in autism spectrum disorders. *Nature* **466**, 368–372 (2010).

420. Pinto, D. *et al.* Convergence of genes and cellular pathways dysregulated in autism spectrum disorders. *Am. J. Hum. Genet.* **94**, 677–694 (2014).

421. Vorstman, J. A. S. *et al.* Identification of novel autism candidate regions through analysis of reported cytogenetic abnormalities associated with autism. *Mol. Psychiatry* **11**, 1,18-28 (2006).

422. Shiloh, Y. & Ziv, Y. The ATM protein kinase: regulating the cellular response to genotoxic stress, and more. *Nat. Rev. Mol. Cell Biol.* **14**, 197–210 (2013).

423. Lavin, M. F. Ataxia-telangiectasia: from a rare disorder to a paradigm for cell signalling and cancer. *Nat. Rev. Mol. Cell Biol.* **9**, 759–769 (2008).

424. McKinnon, P. J. ATM and the molecular pathogenesis of ataxia telangiectasia. *Annu. Rev. Pathol.* **7**, 303–321 (2012).

425. Friedberg, E. C. *et al.* DNA repair: from molecular mechanism to human disease. *DNA Repair (Amst).* **5**, 986–996 (2006).

426. Aguilera, A. & Klein, H. L. Genetic control of intrachromosomal recombination in Saccharomyces cerevisiae. I. Isolation and genetic characterization of hyper-recombination mutations. *Genetics* **119**, 779–790 (1988).

427. Marsden, C. G. *et al.* The Tumor-Associated Variant RAD51 G151D Induces a Hyper-Recombination Phenotype. *PLoS Genet.* **12**, e1006208 (2016).

428. Golin, J. E. & Esposito, M. S. Evidence for joint genic control of spontaneous mutation and genetic recombination during mitosis in Saccharomyces. *Mol. Gen. Genet.* **150**, 127–135 (1977).

429. Klein, H. L. Genetic control of intrachromosomal recombination. *Bioessays* **17**, 147–159 (1995).

430. Schiestl, R. H., Igarashi, S. & Hastings, P. J. Analysis of the mechanism for reversion of a disrupted gene. *Genetics* **119**, 237–247 (1988).

431. Pommier, Y. *et al.* Tyrosyl-DNA-phosphodiesterases (TDP1 and TDP2). *DNA Repair (Amst).* **19**, 114–129 (2014).

432. Caldecott, K. W. Single-strand break repair and genetic disease. *Nat. Rev. Genet.* **9**, 619–631 (2008).

433. Takashima, H. *et al.* Mutation of TDP1, encoding a topoisomerase I-dependent DNA damage repair enzyme, in spinocerebellar ataxia with axonal neuropathy. *Nat. Genet.* **32**, 267–272 (2002).

434. McKinnon, P. J. Maintaining genome stability in the nervous system. *Nat. Neurosci.* **16**, 1523–1529 (2013).

435. Ciccia, A. & Elledge, S. J. The DNA damage response: making it safe to play with knives. *Mol. Cell* **40**, 179–204 (2010).

436. Cortes Ledesma, F., El Khamisy, S. F., Zuma, M. C., Osborn, K. & Caldecott, K. W. A human 5'-tyrosyl DNA phosphodiesterase that repairs topoisomerase-mediated DNA damage. *Nature* **461**, 674–678 (2009).

437. McKinnon, P. J. Topoisomerases and the regulation of neural function. *Nat. Rev. Neurosci.* **17**, 673–679 (2016).

438. Gibson, D. G. *et al.* Enzymatic assembly of DNA molecules up to several hundred kilobases. *Nat. Methods* **6**, 343–345 (2009).

439. Luria, S. E. & Delbruck, M. Mutations of Bacteria from Virus Sensitivity to Virus Resistance. *Genetics* **28**, 491–511 (1943).

440. Loeb, L. A. Mutator phenotype may be required for multistage carcinogenesis. *Cancer Res.* **51**, 3075–3079 (1991).

441. Yu, X. & Gabriel, A. Reciprocal translocations in Saccharomyces cerevisiae formed by nonhomologous end joining. *Genetics* **166**, 741–751 (2004).

442. Ceccaldi, R., Rondinelli, B. & D'Andrea, A. D. Repair Pathway Choices and Consequences at the Double-Strand Break. *Trends Cell Biol.* **26**, 52–64 (2016).

443. Marchand, C. *et al.* Biochemical assays for the discovery of TDP1 inhibitors. *Mol. Cancer Ther.* **13**, 2116–2126 (2014).

444. Tate, J. G. *et al.* COSMIC: the Catalogue Of Somatic Mutations In Cancer. *Nucleic Acids Res.* **47**, D941–D947 (2019).

445. Jacot, W., Fiche, M., Zaman, K., Wolfer, A. & Lamy, P.-J. The HER2 amplicon in breast cancer: Topoisomerase IIA and beyond. *Biochim. Biophys. Acta* **1836**, 146–157 (2013).

446. Yuan, P. *et al.* Efficacy of oral Etoposide in pretreated metastatic breast cancer: a multicenter phase 2 study. *Medicine (Baltimore).* **94**, e774 (2015).

447. Yuan, P. *et al.* Oral etoposide monotherapy is effective for metastatic breast cancer with heavy prior therapy. *Chin. Med. J. (Engl).* **125**, 775–779 (2012).

448. Kucukoner, M. *et al.* Oral etoposide for platinum-resistant and recurrent epithelial ovarian cancer: a study by the Anatolian Society of Medical Oncology. *Asian Pac. J. Cancer Prev.* **13**, 3973–3976 (2012).

449. Wilke, K. E., Francis, S. & Carlson, E. E. Inactivation of multiple bacterial histidine kinases by targeting the ATP-binding domain. *ACS Chem. Biol.* **10**, 328–335 (2015).

450. Velikova, N. *et al.* Putative histidine kinase inhibitors with antibacterial effect against multi-drug resistant clinical isolates identified by in vitro and in silico screens. *Sci. Rep.* **6**, 26085 (2016).

451. Thomas, W., Spell, R. M., Ming, M. E. & Holm, C. Genetic analysis of the gyrase A-like domain of DNA topoisomerase II of Saccharomyces cerevisiae. *Genetics* **128**, 703–716 (1991).

452. Oestergaard, V. H., Knudsen, B. R. & Andersen, A. H. Dissecting the cell-killing mechanism of the topoisomerase II-targeting drug ICRF-193. *J. Biol. Chem.* **279**, 28100–28105 (2004).

453. Leontiou, C., Lakey, J. H., Lightowlers, R., Turnbull, R. M. & Austin, C. A. Mutation P732L in Human DNA Topoisomerase IIbeta Abolishes DNA Cleavage in the Presence of Calcium and Confers Drug Resistance. *Mol. Pharmacol.* **69**, 130–139 (2006).

454. Gilroy, K. L., Leontiou, C., Padget, K., Lakey, J. H. & Austin, C. A. mAMSA

resistant human topoisomerase IIbeta mutation G465D has reduced ATP hydrolysis activity. *Nucleic Acids Res.* **34**, 1597–1607 (2006).

455. Mao, Y. *et al.* Mutations of human topoisomerase II alpha affecting multidrug resistance and sensitivity. *Biochemistry* **38**, 10793–10800 (1999).

456. Nitiss, J. L., Vilalta, P. M., Wu, H. & McMahon, J. Mutations in the gyrB domain of eukaryotic topoisomerase II can lead to partially dominant resistance to etoposide and amsacrine. *Mol. Pharmacol.* **46**, 773–777 (1994).

457. Wasserman, R. A. & Wang, J. C. Mechanistic studies of amsacrine-resistant derivatives of DNA topoisomerase II. Implications in resistance to multiple antitumor drugs targeting the enzyme. *J. Biol. Chem.* **269**, 20943–20951 (1994).

458. Patel, S., Keller, B. A. & Fisher, L. M. Mutations at arg486 and glu571 in humPatel, S., Keller, B. A., & Fisher, L. M. (2000). Mutations at arg486 and glu571 in human topoisomerase IIalpha confer resistance to amsacrine: relevance for antitumor drug resistance in human cells. Molecular Pharmaco. *Mol. Pharmacol.* **57**, 784–791 (2000).

459. Leontiou, C., Lakey, J. H. & Austin, C. A. Mutation E522K in human DNA topoisomerase IIbeta confers resistance to methyl N-(4'-(9-acridinylamino)-phenyl)carbamate hydrochloride and methyl N-(4'-(9-acridinylamino)-3-methoxy-phenyl) methane sulfonamide but hypersensitivity to etoposide. *Mol. Pharmacol.* **66**, 430–439 (2004).

460. Patel, S., Sprung, A. U., Keller, B. A., Heaton, V. J. & Fisher, L. M. Identification of yeast DNA topoisomerase II mutants resistant to the antitumor drug doxorubicin: implications for the mechanisms of doxorubicin action and cytotoxicity. *Mol. Pharmacol.* **52**, 658–666 (1997).

461. Yoshida, H., Bogaki, M., Nakamura, M. & Nakamura, S. Quinolone resistance-determining region in the DNA gyrase gyrA gene of Escherichia coli. *Antimicrob. Agents Chemother.* **34**, 1271–1272 (1990).

462. Willmott, C. J. & Maxwell, A. A single point mutation in the DNA gyrase A protein greatly reduces binding of fluoroquinolones to the gyrase-DNA complex. *Antimicrob. Agents Chemother.* **37**, 126–127 (1993).

463. Strumberg, D. *et al.* Importance of the fourth alpha-helix within the CAP homology domain of type II topoisomerase for DNA cleavage site recognition and quinolone action. *Antimicrob. Agents Chemother.* **46**, 2735–2746 (2002).

464. Okada, Y. *et al.* Assignment of functional amino acids around the active site of human DNA topoisomerase IIalpha. *J. Biol. Chem.* **275**, 24630–24638 (2000).

465. Bromberg, K. D., Hendricks, C., Burgin, A. B. & Osheroff, N. Human topoisomerase IIalpha possesses an intrinsic nucleic acid specificity for DNA ligation. Use of 5' covalently activated oligonucleotide substrates to study enzyme mechanism. *J. Biol. Chem.* **277**, 31201–31206 (2002).

466. DiNardo, S., Voelkel, K. & Sternglanz, R. DNA topoisomerase II mutant of Saccharomyces cerevisiae: topoisomerase II is required for segregation of daughter molecules at the termination of DNA replication. *Proc. Natl. Acad. Sci. U. S. A.* **81**, 2616–2620 (1984).

467. Elsea, S. H., Osheroff, N. & Nitiss, J. L. Cytotoxicity of quinolones toward eukaryotic cells. Identification of topoisomerase II as the primary cellular target for the quinolone CP-115,953 in yeast. *J. Biol. Chem.* **267**, 13150–13153 (1992).

468. Jannatipour, M., Liu, Y. X. & Nitiss, J. L. The top2-5 mutant of yeast topoisomerase II encodes an enzyme resistant to etoposide and amsacrine. *J. Biol. Chem.* **268**, 18586–18592 (1993).
469. Chang, S., Hu, T. & Hsieh, T. S. Analysis of a core domain in Drosophila DNA topoisomerase II. Targeting of an antitumor agent ICRF-159. *J. Biol. Chem.* **273**, 19822–19828 (1998).

CURRICULUM VITA

Education
Masters of Public Health in Epidemiology and Global Communicable Diseases,
Graduate Certificate in Biostatistics, University of South Florida, *2012*

Bachelor of Arts in Biology and Biomedical Studies, Saint Olaf College, *2009*

Poster Abstracts Published:
When topoisomerases fail, Cold Spring Harbor Symposium on Quantitative Biology,
2017.

Podia and Seminars:
Gilbertson, M. University of Illinois at Chicago, Rockford Research Day, Student podia presentation, Etoposide hypersensitivity mediated by mutations in the ATPase domain of hTop2 alpha, 2019.
Gilbertson, M. University of Illinois at Chicago, Biopharmaceutical Sciences Department Seminar, Breaking Badly: Topoisomerase 2 Proteins that are Etoposide Hypersensitive, 2017
Gilbertson, M. University of Illinois at Chicago, Biopharmaceutical Sciences Department Seminar, Regulation of DNA cleavage by the ATPase domain of DNA Topoisomerase II, **Anticipated: 2019**

AWARDS AND HONORS
Eagle Scout
2nd place Poster Session Award: Biology, UIC College of Pharmacy Research Day, 2016
2nd place Poster Session Award: Biology, UIC College of Pharmacy Research Day, 2017
2nd place Poster Session Award: Biology, UIC College of Pharmacy Research Day, 2019
Outstanding Poster Award: Pharmacy, UIC College of Pharmacy, Rockford Research
Day 2017

PUBLICATIONS
Tombline, G, Millen JI, Polevoda, B, Rapaport, M, Baxter, B, Van Meter, M, Gilbertson, M, Madrey, J, Piazza, GA, Rasmussen, L, Wennerberg, K, White, EL, Nitiss, JL, Goldfarb, DS. Effects of an unusual poison identify a lifespan role for Topoisomerase 2 in Saccharomyces cerevisiae. *Aging (Albany. NY).* **9,** 68–97 (2017).

Ray, JA, Detman, LA, Chavez, M, Gilbertson, M & Berumen, J. Improving Data, Enhancing Enrollment: Florida Covering Kids & Families CHIPRA Data System. *Maternal Child Health J.* **20,** 749–753 (2016).

Gonzalez, LE, Sutton, SK, Pratt, C, Gilbertson, M, Antonia, S, Quinn, GP. The bottleneck effect in lung cancer clinical trials. *J. Cancer Education* **28,** 488–493 (2013).

APPENDIX A PREVIOUSLY CHARACTERIZED EUKARYOTIC

TOPOISOMERASES

Top2 Amino acid substitution studied					Biochemical Properties /Annotation	Year (Source)
DM Top2	Gyrase A	Human Beta	Human Alpha	*Sc* Top2		
		Ser165 Arg	Ser149	Ser128	Reduced Catalytic Activity, Reduced ATP hydrolysis	2002[155]
			Arg162 Lys	Arg141	Resistant: Vanadate Reduced DNA stimulated ATP hydrolysis	2005[371]
			Arg162 Gln	Arg141	Resistant: Vanadate Reduced DNA stimulated ATP hydrolysis	2005[371]
				Gly164Ile heterodimer	Heterodimer capable of binding one ATP Lacks DNA-stimulated ATP hydrolysis Sensitive to ICRF-187	2003[374]
			Tyr165 Ser	Tyr144	Resistant: Bisdioxopiperazines, Vanadate Reduced DNA stimulated ATP hydrolysis	2005[371]
			Leu169 Ile	Leu148	Resistant: Bisdioxopiperazines, Vanadate Reduced DNA stimulated ATP hydrolysis	2005[371]
			Leu169 Phe	Leu148	Resistant: Bisdioxopiperazines, Vanadate Increased ATP requirement for catalysis Reduced DNA stimulated ATP hydrolysis	2005[371] 2000[370]
				Top2-828Δ Del	Reduced catalytic activity <30°C Temperature Sensitive (*Top2-18*)	1991[451]
			Asp48 Asn	Asp26	No change in sensitivity (Bisdioxopiperazines) Hypersensitive: Etoposide	2004[183]
			Tyr50 Phe	Tyr28	Resistant: Bisdioxopiperazines Sensitivity Unchanged:	1998[361]

					(Etoposide and mAMSA)	
			351i	Val340	Confer sensitivity to mAMSA but not ICRF-193	2004[452]
		Gly465 Asp		Thr358	Resistant: DACA, Doxorubicin, Ellipticine, Etoposide, mAMSA 3-fold decreased ATP affinity Altered requirement for Mg2+ in Decatenation Assays	2006[453,454]
				Cys381Arg	Resistant: Etoposide <50% of catalytic activity	2005[307]
				Tyr387Asn	Resistant: Etoposide >4fold Decrease in catalytic activity	2005[307]
				Thr394Pro	Resistant: Etoposide, mAMSA <50% of catalytic activity	2005[307]
				Leu396Trp	Resistant: Etoposide >4fold Decrease in catalytic activity	2005[307]
			408i	Ala397	Confer sensitivity to mAMSA but not ICRF-193	2004[452]
				Arg399Gly	Resistant: Etoposide >4fold Decrease in catalytic activity	2005[307]
				Asn407Lys	Resistant: Etoposide >4fold Decrease in catalytic activity	2005[307]
				Glu408Gly	Resistant: Etoposide, mAMSA >4fold Decrease in catalytic activity	2005[307]
				Lys413Glu	Resistant: Etoposide >4fold Decrease in catalytic activity	2005[307]
				Asp416Glu	>4fold Decrease in catalytic activity	2005[307]
				Asp416Val	Resistant: Etoposide <50% of catalytic activity	2005[307]
				Arg422Lys	Resistant: Etoposide >4fold Decrease in catalytic activity	2005[307]

				Gly437 Glu	Asn425	Hypersensitive: Adriamycin (ATP-), mAMSA (ATP-), Mitoxantrone (ATP-), Teniposide (ATP-) No Change in sensitivity (ATP+) ATP utilization defect	1999[455]
					Asn425Lys	Resistant: Etoposide, mAMSA >4fold Decrease in catalytic activity	2005[307]
					Gly437Ser	Resistant: CP115,953, mAMSA, Etoposide, Ellipticine (*in vivo*) Hypersensitive: (*in vitro*) Mutant Protein is unstable and is resistant because cell titer is depleted *in vivo*	1998[320]
				Arg450 Gln	Lys438	Resistant: mAMSA, Teniposide Increased ATP requirement for activity	1991[317]
				Arg450 Gln// Pro803 Ser	Lys438// Ala780	Resistant: Teniposide	1999[455]
				Arg450	Lys439Asn	Slightly Resistant: Etoposide, mAMSA	1994[456]
				Arg450 Gln	Lys439Gln	Resistant: Adriamycin, Etoposide, ICRF-193, mAMSA, Mitoxantrone, Teniposide Resistant (yeast): mAMSA	1994[199,456] 1996[326] 1999[455]
				Arg450	Lys439Glu	Resistant: Etoposide, mAMSA	1994[456] 1996[326]
					Asp461Glu	Resistant: Etoposide, mAMSA	2005[307]
					Pro473Leu	Hypersensitive: mAMSA Resistant: Etoposide Possible Mechanism: Nicking (*trans*)	2008[314]
					Pro473Leu// Tyr782Phe	Hypersensitive: mAMSA, Etoposide	2008[314]
					Leu475Ala// Arg476Gly	Resistant: mAMSA Slower Catalytic activity No Cleavage with Cacium ions Decreased ATP hydrolysis	1994[457]
					Leu475Ala// Arg476Lys	Resistant: Etoposide, mAMSA	1994[310]

				Leu475Ala// Leu480Pro	Resistant: mAMSA Slow Catalytic activity No Cleavage with Cacium ions Decreased ATP hydrolysis	1994[457]
				Leu475Ala// Lys478Ala	Resistant: Etoposide, mAMSA	1994[310]
		Arg486 Lys		Arg476Lys	Resistant: Etoposide, mAMSA (Human) No change in sensitivity (Yeast)	1991[318] 2000[458]
				Ala484Pro	Hypersensitive: mAMSA, Etoposide	2008[314]
				Lys491Glu	Resistant: Etoposide >4fold Decrease in catalytic activity	2005[307]
				Asn492Asp	Resistant: Etoposide, mAMSA <50% of catalytic activity	2005[307]
		Glu522 Lys		Glu494	Resistant: mAMSA, mAMCA Hypersensitive: Etoposide, Ellipticine	2004[459]
				Lys499Arg	Resistant: Etoposide, mAMSA <50% of catalytic activity	2005[307]
				His506Arg	Resistant: Etoposide <50% of catalytic activity	2005[307]
				His507Tyr// His521Tyr	Resistant: Etoposide, mAMSA	1994[199]
				Glu511Asp	Resistant: Etoposide, mAMSA <50% of catalytic activity	2005[307]
		Gly550 Arg		Gly519	Resistant: mAMCA	2004[459]
				Thr525Ser	Resistant: Etoposide, mAMSA <50% of catalytic activity	2005[307]
		Gly551 Ser		Gly536	Resistant: Etoposide, ICRF-187, mAMSA, Merbarone Increased ATP requirement for catalysis Purified protein ICRF-187 sensitivity unchanged	2000[370]
				Asn540Ser	Resistant: Etoposide >4fold Decrease in catalytic activity	2005[307]
				Ser545Leu	Resistant: Etoposide >4fold Decrease in catalytic activity	2005[307]

			Glu571 Lys	Leu557	Resistant: Etoposide, mAMSA	2000[458]
		Ala596 Thr		Val566	Resistant: mAMCA	2004[459]
			Pro592 Leu	Pro581	Resistant: ICRF-187 Purified protein ICRF-187 sensitivity unchanged	2000[370]
				Glu591Asp	Resistant: Etoposide >4fold Decrease in catalytic activity	2005[307]
				Phe595Leu	Resistant: Etoposide <50% of catalytic activity	2005[307]
				Leu630Met	Resistant: Etoposide >4fold Decrease in catalytic activity	2005[307]
			Asp645 Asn	Asp632	Resistant: Etoposide, ICRF-187, mAMSA, Merbarone Increased ATP requirement for catalysis Purified protein ICRF-187 sensitivity unchanged	2000[370]
		Asp661Asn		Asp634	Resistant: mAMCA	2004[459]
				Tyr637Asn	Resistant: Etoposide >4fold Decrease in catalytic activity	2005[307]
				Ala642Gly	Resistant: Etoposide, mAMSA Decreased ATP hydrolysis	1994[457]
				Ala642Ser	Resistant: Doxorubicin, Etoposide, mAMSA	1997[460]
				Ala642Thr	Resistant: Etoposide, mAMSA	1994[310]
				Lys644Met	Resistant: Etoposide, mAMSA <50% of catalytic activity	2005[307]
				Lys644Thr	Resistant: Etoposide <50% of catalytic activity	2005[307]
				Lys645Ile	Resistant: Etoposide <50% of catalytic activity	2005[307]
				Asp648Val	Resistant: Etoposide, mAMSA <50% of catalytic activity	2005[307]
				Lys651Arg	Resistant: Etoposide >4fold Decrease in catalytic activity	2005[307]
				Glu669Lys	Resistant: Etoposide	2005[307]
				Glu669Lys// Ser740Trp	Resistant: Etoposide <50% of catalytic activity	2005[307]

				Leu685Trp// Ser740Trp	Resistant: Etoposide, mAMSA <50% of catalytic activity	2005[307]
				Arg690Ala// Tyr782Phe heterodimer	Heterodimer indicates that the dimers work in *Trans*	1998[156]
	Pro732 Leu			Pro693	Resistant: mAMSA, All tested Top2 poisons Decreased catalytic activity Decreased DNA binding capacity Requires Mg^{2+} for catalysis, Ca^{2+} insufficient Structural Analysis: Modeling indicates a shift in the local peptide backbone	2006[453]
				Leu708Pro	Reduced catalytic activity <30˚C Temperature Sensitive (*Top2-19*)	1991[451]
				Phe711Ile	Hypersensitive: mAMSA, Etoposide	2008[314]
				Leu720Pro	Reduced catalytic activity <30˚C Temperature Sensitive (*Top2-14*)	1991[451]
Ala67 Ser				*Ala722*	Resistant: Ciprofloxacin, Enoxacin, Nalidixic acid, Norfloxacin, Ofloxacin, Pipimidic acid	1990[461] 1993[462]
				Glu730Gly// Ser740Trp	Resistant: Etoposide <50% of catalytic activity	2005[307]
Gly81 Cys				*Gly737*	Resistant: Ciprofloxacin, Enoxacin, Nalidixic acid, Norfloxacin, Ofloxacin, Pipimidic acid	1990[461] 1993[462]
				Gly737Val	Hypersensitive: mAMSA Resistant: Etoposide, CP115,953 Possible Mechanism: Double Strand Break (*cis*)	2008[314]
				Gly738Asn	Resistant: Etoposide	1994[319]
				Gly738Ser	Resistant: CP115,953, Etoposide Sensitive: mAMSA	1994[199]
Ser83 Ala			Ser763	Ser740Ala	Resistant: CP-115,953 Homologous yTop2 Ser740Ala Sensitivity unaffected: Quinolones	1995[240]

	Ser83 Leu		Ser763	Ser740Leu	Resistant: CP-115,953 Homologous yTop2 Ser740Leu Sensitivity unaffected: Quinolones	1995[240]
	Ser83 Trp		Ser763 Trp	Ser740Trp	Hypersensitive: Etoposide Resistant: Ciprofloxicin, CP115,953, Enoxacin, Fluoroquinolones, Nalidixic acid, Norfloxacin, Pipimidic Acid Enhanced Heat/Salt Stability of Top2cc	1990[461] 1995[240] 1999[315]
				Ser740Trp// Asn845Thr	Resistant: Etoposide >4fold Decrease in catalytic activity	2005[307]
				Ser740Trp// Lys775Gln	Resistant: Etoposide >4fold Decrease in catalytic activity	2005[307]
				Ser740Trp// Tyr827Ala	Resistant: Etoposide >4fold Decrease in catalytic activity	2005[307]
	Ala84 Pro			*Leu741*	Resistant: Ciprofloxacin,Enoxacin, Nalidixic acid, Norfloxacin, Ofloxacin , Pipimidic acid	1990[461] 1993[462]
	Asp87 Asn			*Gln743*	Resistant: Ciprofloxacin,Enoxacin, Nalidixic acid, Norfloxacin, Ofloxacin , Pipimidic acid	1990[461] 1993[462]
				Thr744Pro	Hypersensitive: mAMSA, CP115,953 Sensitive: Norfloxacin, Oxolinic Acid Sensitivity unaffected: Etoposide *in vitro* Enhanced DNA cleavage: mAMSA, Flouroquinolones Suggested mechanism: Displacement of key residues	2000[312] 2002[463]
				Gly748Glu	Resistant: Doxorubicin, Etoposide, mAMSA	1997[460]
				Gln750Ala	Complements Temperatire Sensitivity	1998[156]
	Gln106 His			*Asp764*	Resistant: Ciprofloxacin,Enoxacin, Nalidixic acid, Norfloxacin, Ofloxacin , Pipimidic acid	1990[461] 1993[462]
			Lys798	Lys775	Resistant: Etoposide	2000[464]

			Leu		
			Lys798 Pro	Lys775	Resistant: Etoposide	2000[464]
				Ala779Glu	Resistant: Etoposide, mAMSA <50% of catalytic activity	2005[307]
			Pro803 Ser	Ala780	Resistant: Teniposide (ATP-), Etoposide No Change in sensitivity (ATP+)	1999[455] 2000[464]
			Tyr805 Phe	Tyr782	Active site Tyrosine Incapable of Celavage Proficient for ligation of nicked DNA substrate	2002[465]
			Tyr805 Ala	Tyr782	Active site Tyrosine Incapable of Celavage Proficient for ligation of nicked DNA substrate	2002[465]
				Leu787Ser	Hypersensitive: mAMSA, Etoposide	2008[314]
				Pro824Ser	Resistant: Etoposide, mAMSA	1994[199,319]
				Gly829Asp	Reduced catalytic activity <30˚C Temperature Sensitive (*Top2-1*)	1984[466] 1992[467]
				Pro831Gln	Reduced catalytic activity >30˚C Temperature Sensitive (*Top2-4*)	1985[86]
				Arg884Pro	Resistant: Etoposide, mAMSA, Mitoxantrone	1993[468]
				Arg884Pro// Arg886Ile// Met887Ile	Resistant: Etoposide, mAMSA, Mitoxantrone Reduced catalytic activity >30˚C Temperature Sensitive (*Top2-5*)	1985[86] 1993[468]
				Arg886Ile	Resistant: Etoposide, mAMSA, Mitoxantrone	1993[468]
				Met887Ile	Resistant: Etoposide, mAMSA, Mitoxantrone	1993[468]
				Leu967Pro	Reduced catalytic activity >30˚C Temperature Sensitive (*Top2-2*)	1985[86]
			Thr996 Leu	Ser971	Resistant: Etoposide, ICRF-187, mAMSA, Merbarone	2000[370]

					Increased ATP requirement for catalysis Purified protein ICRF-187 sensitivity unchanged	
			Leu1032 Phe	Leu1007	Mutation identified in HL-60 and HL-60/AMSA resistant cell lines not associated with resistance	1991[318]
				His1011Tyr	Hypersensitive: Ellipticine Resistant: Etoposide, CP115,953 Sensitive: mAMSA Small Decrease in catalytic activity	1995[313]
				Ile1030Phe	Reduced catalytic activity <30˚C Temperature Sensitive (*Top2-17*)	1991[451]
				Leu1052Ile	Hypersensitive: mAMSA, Etoposide	2008[314]
				Gly1119Ala // Met1120Ile	Reduced catalytic activity <30˚C Temperature Sensitive (*Top2-15*)	1991[451]
				Trp1123Arg // Ser1124Thr	Reduced catalytic activity <25˚C Temperature Sensitive (*Top2-13*)	1991[451]
				Tyr1166Δdel	Resistant: mAMSA Loss of nuclear localization	1994[457]
				Arg1195Lys	Resistant: Etoposide, mAMSA	1994[199]
Δ1-408					Sensitive: ICRF-159 Lacks relaxation/decatenation/ATPase activity Retains DNA cleavage N-Clamp formation dependent on ATPase domain	1998[469]
Δ1-408 // Δ1207-1447					Sensitive: ICRF-159 Lacks relaxation/decatenation/ATPase activity Retains DNA cleavage N-Clamp formation dependent on ATPase domain	1998[469]

			ΔQTK Loop		Increased DNA cleavage Lacks DNA-Stimulated ATPase Low intrinsic ATP hydrolysis activity	2009[367]

APPENDIX B Protocol Index

5.6   Yeast lithium transformation protocol and buffer recipes

Protocol:

1. Inoculate yeast in the appropriate media (typically, YPDA) and grow overnight at the appropriate temperature (25°C for top2-4, 30°C for all other yeast) shaking vigorously ~250rpm.

2. Dilute yeast cultures to OD 0.6 (10mL per transformation condition) and grow for ~2-3 hours.

3. Pellet yeast culture by centrifugation (3000 rpm for 5 minutes) and wash in 5mL Lithium solution (1 mM EDTA, pH 8.0, 0.1 M LiOAC, and 10mM Tris HCl, pH 8.0). Pellet yeast again by centrifugation 3000 rpm for 5 minutes, then resuspend in 5-10mL of Lithium solution and incubate at room temperature for 1 hour.

4. Pellet yeast culture by centrifugation (3000 rpm for 5 minutes) and resuspend in the appropriate volume of Lithium solution (100μL/10mL of culture in step 2). Prepare sterile eppendorf tubes for different transformation conditions, Add 200μg of heterologous denatured carrier DNA (Sonicated salmon sperm DNA) and ~1μg of target DNA (plasmid). Include a negative control transformation condition that lacks target DNA. To the DNA add 100μL of yeast culture in lithium solution and incubate for 30 minutes at room temperature.

5. Add 700μL of PEG solution (1 mM EDTA, pH 8.0, 0.1 M LiOAc, 40% PEG 3350, and 10mM Tris HCL, pH 8.0) to each transformation and incubate at room temperature for 1 hour.

6. Heat shock the yeast transformations at 42°C for 5 minutes, then plate to the appropriate selective media.

Buffers:

1. Lithium solution: (1 mM EDTA, pH 8.0, 0.1 M LiOAC, and 10mM Tris HCl, pH 8.0)

2. PEG solution: (1 mM EDTA, pH 8.0, 0.1 M LiOAc, 40% PEG 3350, and 10mM Tris HCL, pH 8.0).

Protocol Reference:[328–330]

5.7   HAP purification protocol

Yeast lithium transformation protocol and buffer recipes

Protocol:

1. Inoculate yeast in the appropriate media (typically, YPDA) and grow overnight at the appropriate temperature (25°C for top2-4, 30°C for all other yeast) shaking vigorously ~250rpm.

2. Dilute yeast cultures to OD 0.6 (10mL per transformation condition) and grow for ~2-3 hours.

3. Pellet yeast culture by centrifugation (3000 rpm for 5 minutes) and wash in 5mL Lithium solution (1 mM EDTA, pH 8.0, 0.1 M LiOAC, and 10mM Tris HCl, pH 8.0). Pellet yeast again by centrifugation 3000 rpm for 5 minutes, then resuspend in 5-10mL of Lithium solution and incubate at room temperature for 1 hour.

4. Pellet yeast culture by centrifugation (3000 rpm for 5 minutes) and resuspend in the appropriate volume of Lithium solution (100µL/10mL of culture in step 2). Prepare sterile eppendorf tubes for different transformation conditions, Add 200µg of heterologous denatured carrier DNA (Sonicated salmon sperm DNA) and ~1µg of target DNA (plasmid). Include a negative control transformation condition that lacks target DNA. To the DNA add 100µL of yeast culture in lithium solution and incubate for 30 minutes at room temperature.

5. Add 700µL of PEG solution (1 mM EDTA, pH 8.0, 0.1 M LiOAc, 40% PEG 3350, and 10mM Tris HCL, pH 8.0) to each transformation and incubate at room temperature for 1 hour.

6. Heat shock the yeast transformations at 42°C for 5 minutes, then plate to the

appropriate selective media.

<u>Buffers:</u>

1. Lithium solution: (1 mM EDTA, pH 8.0, 0.1 M LiOAC, and 10mM Tris HCl, pH 8.0)

2. PEG solution: (1 mM EDTA, pH 8.0, 0.1 M LiOAc, 40% PEG 3350, and 10mM Tris

HCL, pH 8.0)

DAY ZERO:

1. Make Buffers:

   1000mL Buffer I + 25mM KCl

   250mL Buffer I + 150mM KCl

   250mL Buffer I + 1M KCl

   900mL H-KP 100 (no PMSF, DTT)

   Boil 2L of Deionized H_2O

   <u>Measure conductivity of buffers</u>

Buffer I + KCl

	Buffer I +25mM KCl	Buffer I +150mM KCl	Buffer I +1000mM KCl
Total volume	**1000mL**	**250mL**	**250mL**
2x Buffer I	500 mL	125 mL	125 mL
3M KCl	8.33 mL	12.5 mL	83.33 mL
1mM PMSF	17.5 mL	4.38 mL	4.38 mL
2-BME	70µl	17.5µl	17.5µl
0.5µg/ml leupeptin	0.5mL	125µl	125µl
1µg/ml pepstatin	1mL	250µl	250µl
QS with Boiled MilliQ	**~472.6ml 1L**	**~107.7275 250 mL**	**~36.89 250 mL**
Conductivity	95 µSemen	204 µSemen	1100 µSemen

2. Pour HAP Column **(No protease inhibitors)**

   a. Measure ~10g of Hydroxyapatite (HAP)

   b. Hydrate resin in a large beaker (~1L) using H-KP 100 (enough to cover

   the resin). Gently swirl the resin and allow crystals to settle. Pour off fines

   (dust-like particles) add more buffer and repeat 2-3 times.

c. Swirl the resin in the H-KP 100 buffer and pour a 1.5 x 8 cm (15 ml)(try 18 ml - 1.5x10 cm) packed bed volume column.

  i. Allow 2-3cm to settle before opening the stopcock and let gravity pack the HAP column.

  ii. **DO NOT LET THE HAP DRY OUT**!!! Watch column closely Apply more H-KP 100 as needed

  iii. Leave 3-5cm head space above the packed resin

  iv. Once the column has settled you can swirl with a pipet and remove resin but cannot add more!

d. Gently move HAP column to 4°C, be sure to have a small amount of buffer in the headspace on the column**.**

Hydroxylapapitite Buffer Recipes

Chemicals	H-KP$_{100}$	H-KP$_{200}$	H-KP$_{600}$	1X conc.	BufIw/NaP
.5M NaP, pH 7.7	**27 ml**	12 ml	12 ml	15 mM	12 ml
50% Glycerol	**180 ml**	80 ml	80 ml	10%	80 ml
0.5M NaEDTA				1 mM	0.8 ml
0.25M EGTA				1 mM	1.6 ml
1.5M KP, pH 7.7	**60 ml**	53.3ml	160 ml	100,200,600mM	
57 mM PMSF	**0.9 ml**	0.4 ml	0.4 ml	1, 0.1 mM	7ml
1 mM BME					0.028 ml
Leupeptin					0.2ml
Pepstatin					0.4 ml
0.5 mM DTT	**0.9 ml**	0.4 ml	0.4 ml	0.5mM	
1M Na$_2$SO$_5$	**9.0 ml**	4.0 ml	4.0 ml	10 mM	
qs with Boiled Milli-Q	**~622.2 900 ml**	~249.9 400 ml	~143.2 400 ml		~297.972 400 ml
CONDUCTIVITY		**350-400 µSemen**	**1000 µSemen**		

Protein Purification:

Additional Notes:

Also: It will require between 3-5hours to load the HAP column.

To Prepare for the purification procedure

1. Make P-cell Slurry as described in the protocol book.

2. Check the conductivity of all purification buffers. To check the conductivity you must bring the volume up to ~7.0mL with water in a 14mL tube

3. Note that the conductivity of the following buffers are important

Buffer	Conductivity
Buffer I+25mM KCl	95 µsemens
Buffer I+150mM KCl	204 µsemens
Buffer I+1M KCl	1,100 µsemens
HAP 200	350-400 µsemens
HAP 600	1000 µsemens
P200	350 µsemens
P600	1000 µsemens

Checking the conductivity of Buffer I w/NaPi and stock 2x Buffer I is unnecessary.

The following outlines the list of reagents that should be made and available for

purification Prior to Day Zero:

Reagent	Minimum amount (ie. perfect pipetting)
1M Tris-HCl pH 7.7	2.5mL
0.5M EDTA pH 8.0	4.9mL
0.25M EGTA pH 8.0	4.9mL
50% Glycerol	570mL
3M KCl	144.2mL
100mM PMSF	42.36mL
3mg/ml Leupeptin	1.15mL
3mg/mL Pepstatin	2.3mL
25mg/mL Trypsin inhibitor	XXX
0.5M NaPi buffer pH 7.7	78mL
0.5M DTT	2.3mL
1M Na2SO5	14mL
1.5M KP pH 7.7	253.3mL
2-ME	0.105mL

Protein Extraction

1. Thaw cell suspension (30-50g as described in Induction Protocol) on ice. Add all
    cells to bead beater vial, add 150-200 ml glass beads (if using large container, 50 ml
    if using small chamber), and add Buffer I+25 mM KCl to fill chamber. It is best if
    you have at least 1:1 beads to cells (more beads works great). Bead beat for 1 min
    with 2 min rest intervals, repeat ~5-6x.

    > Note: It is important not to overheat the cells. It is a good ideal to look at
    > the cells after the third 1 min beating under the microscope (especially if new
    > glass bead are used). Make a 1:10 dilution of bead beated cells to buffer and pipet
    > 10 μL on hemocytometer for physical observation. The objective is to break up
    > 80% to 90% of the cells. If more bead beatings are needed, check cells under the
    > microscope after each beating. This is a very important step and should be done
    > with care.

2. Transfer supernatant to a large beaker, wash the remaining glass beads twice with
    ~10mL of BufferI+25 mM KCl and pour the supernatant into the beaker as well.
    Allow the glass beads to settle, and then carefully pour into an appropriate graduated
    cylinder to measure volume, and then transfer to a 400mL Beckman Centrifuge tube.
    Top2 is in supernatant.

    a. <u>Suggestion:</u> If you are starting out with a lot of cells 40 grams or more, take
        the extra time at this step wash beads with more buffer. In step 5, the sample
        will have to be diluted to 5 mg/mL and it would be better to dilute with extra
        bead washes (might extract more top2) than buffer.

3. Measure protein concentration with Bradford assay (Take a 0.25mL extract Sample before diluting). Dilute supernatant to ~5 mg/ml protein with Buffer I plus 25 mM KCl. May need to dulite sample 1:2.

4. For each ml of extract, add 20 µl of 10% Polymin P slowly w/stirring (about 2 ml in 100 ml) at 4° C. Allow to stir 30 min at 4°C.

5. Spin in JLA 16.25 rotor for 10 min. at 4° C at 9000 rpm. Pour off clear Polymin P supernatant into grad cylinder and save. (Save an aliquot - 1 mL as Polymin P.) Top2 should be in the pellet.

   a. Wash pellet with 90 ml Buffer I plus 150 mM KCl, stir 15 min (if you used two centrifuge tubes, combine the pellets at this point). Take sample (.5 mL) of supernatant. Centrifuge as above.

   b. Resuspend pellet (may be a little clumpy) in 90 ml Buffer I plus 1000 mM KCl, stir for 15 to 25 min., centrifuge as above. Pellets can be resuspended with a glass dounce to help in these extractions steps. Centrifuge for 10 min at 4°C at 9000 rpm. Take a sample of supernatant (0.5 mL).   The Top2 should now be in the supernatant.

   c. Start making your HAP buffers and make sure to cool them down.

6. Slowly and with stirring add 0.197 g ground up ammonium sulfate/ml of Polymin P extraction. This is a 35% cut. Stir in a small glass beaker in a cold water in the fridge. Stir for 30 min. once all of the ammonium sulfate is in solution.

7. Spin in JLA16.25 rotor for 25 min. at 4° C at 13500 rpm. Pour off clear 35% supernatant from the pellet and record volume. Top2 should be in the supernatant.

8. Slowly and with stirring add 0.187 g of ground up ammonium sulfate/ ml of 35% supernatant. This is a 65% cut. Stir in a small glass beaker in a cold water in the fridge. Stir for 30 min. at 4° C once all of the ammonium sulfate is in solution. Try to pour the HAP column at this time.

9. Spin in JLA16.25 for 25 min. at 4° C at 13500 rpm Immediately pour off clear 65% supernatant from the pellet and wipe the walls to remove the last of the supernatant.

Note: Since 65% pellet can easily resuspend, it is best to pour off sup right after the spin has stopped at the centrifuge. Top2 should be in the pellet.

10. Gently re-dissolve the 65% ammonium sulfate pellet in Buffer I w/ NaP using about 2.5 ml/ 1 g of cells (~50 ml) - a spatula might be needed to gently mash the ammonium sulfate pellet.

11. Adjust the conductivity of the solution (to a little less than the conductivity of H-KP 100) by additional dilution if required. (Probably to about 200 mls). Conductivity of solution should be <400 (~370-390) μsemens (10 μl/ml dilution). (Save aliquot as 65% PELLET.)

12. Load on HAP column with gravity pump (~100 mls/hr). Wash column and collect fractions. (see HAP column protocol)

Hydroxyapatite Column Protocol

Prepare buffers the day of use. Use only boiled Milli-Q water (to remove CO_2) that has

been cooled to RT.

	H-KP$_{100}$	H-KP$_{200}$	H-KP$_{600}$		BufIw/NaP
Chemicals				**1X conc.**	
.5M NaP, pH 7.7	18 ml	12 ml	12 ml	15 mM	12 ml
50% Glycerol	120 ml	80 ml	80 ml	10%	80 ml
0.5M NaEDTA				1 mM	0.8 ml
0.25M EGTA				1 mM	1.6 ml
1.5M KP, pH 7.7	40 ml	53.3ml	160 ml	100,200,600mM	
57 mM PMSF	0.6 ml	0.4 ml	0.4 ml	1, 0.1 mM	7ml
1 mM BME					0.028 ml
Leupeptin					0.2ml
Pepstatin					0.4 ml
0.5 mM DTT	0.6 ml	0.4 ml	0.4 ml	0.5mM	
1M Na$_2$SO$_5$	6.0 ml	4.0 ml	4.0 ml	10 mM	
qs with Boiled Milli-Q	~414.8 600 ml	~249.9 400 ml	~143.2 400 ml		~297.972 400 ml
CONDUCTIVITY		**350-400** μSemen	**1000** μSemen		

Protocol

1. Pour a 1.5 x 8 cm (15 ml)(try 18 ml - 1.5x10 cm) packed bed volume column

   following Bio-Rad protocol using HTP grade HAP in H-KP100 buffer. (Use 15

   g. HAP into 175 ml, c, etc.)

2. Pass through at least 2 column volumes H-KP100 (~40mL)

3. Apply 65% pellet soln. in Buf I with NaP. Collect eluent in 250 ml erlenmeyer

   flask.

4. Wash with 3 column volumes H-KP100 (~60ml). Wash with 2 column volumes of H-KP200 (40ml).

5. Run a 10 (150 ml or 180 ml) column volume gradient of H-KP200 (90mL) to H-KP600 (90ml) collecting (80) 1.875 - 2.25 ml fractions. Run the gradient with pump set ~1 (just barely over 1 on 10x) (less than 50 mL/hr). The slower the gradient run, the better separation of Top2.

Day Two:
HAP Column continued:

6. Assay salt conc of every 10th tube by conductivity (10µl/ml dilution). Assay fractions for enzyme by SDS PAGE gel. Use fractions 20, 23, 26, 29, 32, 35, 38, 41, 44, 47, 50, 54, 60, 70. Dilute fractions 1:1 (5 µL sample and 5 µL 2x PAGE sample dye) with dye.   Also run load on and standard.

7. Pool fractions with Top2 activity. (Label 0.1 ml aliquot as HAP and save before diluting to the appropriate conductivity.)

NOTE: Top2 should elute @ salt conc of 400 mM.

Conductivity of H-KP100 should be ~350 µsemen (10µl/ml dilution).

**Conductivity of H-KP600 should be about ~1000 µsemen (10µl/ml dilution).

Record the lot number of the hydroxyapatite

Concentrate Pooled fractions with a PCELL column:

Phosphocellulose Collection Column (Cation Exchange)

P200	1L	400mL	1x Conc.
0.5 M NaP, pH 7.7	30.0 mL	12 mL	15mM
0.25 M EDTA, pH 8.0	4.0mL	1.6mL	1mM
0.25 M EGTA, pH 8.0	4.0mL	1.6mL	1mM
50% Glycerol	200.0 mL	80 mL	10%
3M KCl	66.67mL	26.7mL	200mM
0.5M DTT	1.0 mL	0.4mL	0.5mM
57mM PMSF	1.75mL	0.7mL	
QS with Boiled MilliQ H$_2$O	~692.58mL 1L	~277mL 400mL	
Conductivity	350 μSemen		

Regenerating P-Cell

Wear gloves and laboratory coat

Need: 2 buchner funnels with Whatman #4 filter paper*

                2 L flask

                1 L beaker (or graduated cylinder)

                stopwatch

                500 ml graduated cylinder

                litmus paper

1. Add 100mL 0.5M NaOH to regenerate phosphocellulose (10g) in a 1 L beaker (250-300ml of NaOH)

2. Let sit for 1 min., then swirl and add ~150-200mL of 0.5M NaOH

    START TIMER

3. Soak while swirling and wait 5 minutes

4. Filter to dryness (may need to change filters due to clogging)

5. Rinse with H2O (up to 2L) to pH≤10 (measure with pH strips)

6. Repeat above only use 200-250ml of 0.5N HCl

7. Scoop P-cell into a beaker, add HCl and swirl gently

   <u>START TIMER</u>

8. Filter as above, rinse with H2O (up to 2L) to pH≥3

9. Scoop resin into 600ml beaker (in as little volume as possible)

10. Add 1.5 M KP dibasic stir slowly w/stir bar ~250-300 ml, to reach pH 7.7

11. Let equilibrate in P200 buffer (change buffer a couple of times) before placing P-cell in the cold room.

PROTOCOL

Pouring the P-cell Column:

1. Swirl P200 buffer containing P-cell resin pipet 5-10mL onto the column.

2. Wait ~15min then open stopcock to pack the column.

3. Wash with 2 column volumes of fresh P200 (depends on size poured ~4-8ml)

4. Ready to load sample

Mini Phosphocellulose Column

1. Dilute HAP pool with an ~equal volume of Buffer I w/ NaP to a final conductivity equal to or less than that of the P_{200} buffer.

2. Pass over a 2 x 1.8 cm (~4 ml) P-cell column in P_{200}. Size of column depends on how much Top2 there is present in HAP pool.

3. Wash column with ~4 column volumes of P_{200}.

4. Elute Top2 with 3 column volumes P750 and X% glycerol collecting 3 or 4 drop fractions (load at 1-2 drops at a time for three tubes before loading the bulk of the buffer). Collect fractions by gravity if concentrated Top2 is desired (This is probably the best method. To make it less painful, time how long it take to collect 3 or 4 drop fractions. Then you can wait outside the cold room for that length time and come back in to move the temp block to the next tube). One can also use positive force of concentration of Top2 is not an issue. The # of fraction depends on how much Top2 is present and the size of column. The usual rule is :
The more Top2 means the bigger the P-cell column which in turn means

more fractions need to be collected. Example : the smallest P-cell column (5

cm, 1 mL) - collect 15 fractions, 2 mL - collect 20 fractions, etc.

5.   Assay each sample for protein content by Bradford assay (1µl/1000µl dilution)

and pool samples in the peak of protein presence. Top2 is usually in fractions ~4-

9.

6.   Measure Topoisomerase Activity (Plasmid relaxation assay)

7.   Freeze as aliquots in liquid Nitrogen

P750+X%Glyc.	P_{750} +30%	P_{750} +5%	**P_{750} +40%**	P_{750}+50%
Tris, pH 7.7	2.5 ml (50 mM)			
0.5 M DTT	50 µl (.5 mM)			
EDTA	20 µl (.1 mM)			
3M KCl	12.5 ml (750 mM)			
50% glycerol	30mL	5mL	20mL**	25mL**
QS To 50mL				
with Boiled milliQ H_2O				

**100%Glycerol

5.8   Ni-NTA purification protocol and buffers

Lysis

1. Resuspend induced yeast pellet in an equal volume Equilibration Buffer (+protease inhibitors). Load into the Bead beating chamber, add ~1:1 glass beads to cells, additional beads works great. Bead beat for 1 min with 2 min rest intervals. ~5-6x

   Important Note: Do not overheat the cells. Look at the cells after a few bead beatings (5x) Objective it to break open 80-90% of the cells.

2. Spin down debris for 10 min at ~18,500 x g at 4°C. Take 50µl Sample-Cell Soluble and Insoluble lysate.

Ni-NTA Equilibration

3. Pipet ~3-4 mL per 10 g wet weight cells of Ni-NTA agarose slurry into a small chromatography column. Equilibrate the column with 5-10ml Equilibration buffer. (don't let the resin dry!)

Ni-NTA Column Loading

4. Transfer cleared Cell Lysate from step 2 and collect flow through.

Column Wash

5. Wash Ni-NTA column with 40CVs Medium Salt Wash buffer and collect flow through).

Ni-NTA Elution

6. Equilibrate Ni-NTA column with Low Salt wash buffer ~1-2 CVs.

7. Elute Ni-NTA column with elution buffer column ~15mls. Collect 500µl to 1ml fractions

8. Take 5µL sample of each fraction (for analysis by SDS-PAGE). After combining, remove 5 µL of the "total" elution to an Eppendorf tube.

9. Equilibrate Dialysis Cassette. Submerge the cassette in dialysis buffer for approximately 2min.

Dialysis

10. Load combined Ni-NTA elution fractions into dialysis cassette with a syringe. Add 500µl 1M DTT to buffer before dialysis. Dialyze sample at 4°C in 1L 1x dialysis buffer for 2 hrs.

11. Change buffer, dialyze at 4°C for an additional 2 hrs. Add 500µl 1M DTT to buffer before dialysis.

12. Detect protein concentration by Bradford assay. Add 1mg TEV protease per 20mg Top2 protein. Dialyze overnight at 4°C in dialysis buffer. Add 500μl DTT.

13. Determine protein concentration by Bradford assay after overnight dialysis protein concentration by Bradford assay and assess activity.

14. Concentrate sample with Millipore Centricon samples, Or remove TEV with small eppendorf of Ni-NTA washed with final high salt elution buffer.

5.8.1 <u>Modified Ni-NTA purification protocol and buffers</u>

Lysis

15. Resuspend induced yeast pellet in an equal volume Equilibration Buffer (+protease inhibitors). Load into the Bead beating chamber, add ~1:1 glass beads to cells, additional beads works great. Bead beat for 1 min with 2 min rest intervals. ~5-6x

    <u>Important Note:</u> Do not overheat the cells. Look at the cells after a few bead beatings (5x) Objective it to break open 80-90% of the cells.

16. Spin down debris for 10 min at ~18,500 x *g* at 4°C. Take 50μl Sample-Cell Soluble and Insoluble lysate.

Ni-NTA Equilibration

17. Pipet ~3-4 mL per 10 g wet weight cells of Ni-NTA agarose slurry into a small chromatography column. Equilibrate the column with 5-10ml Equilibration buffer. (don't let the resin dry!)

Ni-NTA Column Loading

18. Transfer cleared Cell Lysate from step 2 and collect flow through.

Column Wash

19. Wash Ni-NTA column with 40CVs Medium Salt Wash buffer and collect flow through).

Sepharose column transfer and elution

20. Equilibrate Ni-NTA column with Low Salt wash buffer ~1-2 CVs.

21. Elute Ni-NTA column with Low Salt elution buffer column ~15mls. Collect a sample and load elutant onto SP sepharose column

22. Elute from SP Sepharose with 50ml gradient from Low Salt elution (-imidazole) to high salt elution buffer. Collect 10-15 drop fractions (1.5mL)

23. Detect protein concentration by Bradford assay. Add 1mg TEV protease per 20mg Top2 protein and gently shake overnight.

24. Concentrate sample with Millipore Centricon samples, Or remove TEV with small eppendorf of Ni-NTA washed with final high salt elution buffer.

Optional

25. Run 2 µg and 5 µg on a 7.5% PAGE gel to see purification vs. quantification (and whether degradation occurred during concentrating). Run another purified topoisomerase IIα sample of known concentration as a standard for 2 µg and 5 µg comparison.

Buffers

Equilibration Buffer
20mM Tris HCl pH: 7.7
300mM KCl
10mM Imidazole
10% Glycerol
1 mM βME
1 mM PMSF
1µg/ml Leupeptin
1µg/ml Pepstatin A

Wash Buffer 1 (Medium Salt)
20mM Tris HCl pH: 7.7
300mM KCl
20mM Imidazole
10% Glycerol
1 mM βME
1 mM PMSF
1µg/ml Leupeptin
1µg/ml Pepstatin A

Wash Buffer 2 (Low Salt)
20mM Tris HCl pH: 7.7
150mM KCl
20mM Imidazole
10% Glycerol
1 mM βME

1 mM PMSF
1µg/ml Leupeptin
1µg/ml Pepstatin A

Ni-NTA Elution Buffer (Low Salt)
20mM Tris HCl pH: 7.7
150mM KCl
200mM Imidazole
10% Glycerol
1 mM βME
1 mM PMSF
1µg/ml Leupeptin
1µg/ml Pepstatin A

Low Salt Wash Buffer 2
20mM Tris HCl pH: 7.7
150mM KCl
10% Glycerol
1 mM βME
1 mM PMSF
1µg/ml Leupeptin
1µg/ml Pepstatin A

1x dialysis buffer
20mM Tris-HCl, pH 7.7
750mM KCl
100µM EDTA
20% glycerol
500µM DTT

p750+20%Glycerol-50mL
20mM Tris HCl, pH:7.7
750mM KCl
1mM EDTA
20% Glycerol
0.5mM DTT

Protease Inhibitors:
1M Di0thiothreitol (DTT): Dissolve 15.45 g of dithiothreitol in 100 mL of water to obtain a final concentration of 1 M (154.5 mg/mL). Aliquot into 1.6 mL tubes and store the tubes at -20 °C.
100mM PMSF (Phenyl Methyl Sulfonyl Flouride): Dissolve 174.2mg in 10mL of 100%Ethanol (17.4mg/mL). Aliquot and store at -20 °C.
1mg/ml Pepstatin: Dissolve 10mg in DMSO and QS to 10mL. Store in 1mL aliquots at -20 °C.

1mg/ml Leupeptin: Dissolve 10mg in water and QS to 10mL. Store in 1mL aliquots at -20 °C.

5.9   Gibson Assembly Protocol

Protocol for Gibson assembly (GA) master mix preparation and GA reaction set-up

5X isothermal reaction buffer (IRB):

Components*	Stock conc - M	Amt/Vol - g/ml	Final conc - %/M
PEG- 8000	powder	**0.75**	**25**
DTT	1	0.15	0.05
NAD**	0.05	0.3	0.005
dNTPs mix	0.1	0.03	0.001
MgCl2	1	0.15	0.05
Tris/HCl, pH 7.5	1	1.5	0.5

H2O   **add water up to final 3 ml**

If separate dNTP stocks are used:

Components*	Stock - M	Amt/Vol - g/ml	Final conc - %/M
PEG- 8000	powder	**0.75**	**25**
DTT	1	0.15	0.05
NAD**	0.05	0.3	0.005
dATP	0.1	0.03	0.001
dTTP	0.1	0.03	0.001
dCTP	0.1	0.03	0.001
dGTP	0.1	0.03	0.001
MgCl2	1	0.15	0.05
Tris/HCl, pH 7.5	1	1.5	0.5

H2O   **add water up to final 3 ml** (there's usually no room for water!)

Don't autoclave and don't filter the final mix
Split freshly made unused 5X IRB into 400 or 700-ul aliquots and store at -80oC for no longer than 1 year
Upon thawing an aliquot to make master mix, discard the left-over, use a fresh one every time

*   Use sterile high quality reagents and stocks
**   NAD (B-nicotinamideadenine dinucleotide) - we prefer to use Sigma's powder form C# N0632 to make fresh stock in water
       instead of pre-made solution C# N8535 that isn't very stable

3.2X GA Master Mix

Components

	Vol - ul	Vol -- ul
IRB, 5X	320	640
T5 Exonuclease, 10U/ul*	0.64	1.28
Taq DNA Ligase, 40U/ul**	160	320
Phusion Hi-Fi DNA Pol, 2U/ul***	20	40
Total volume	**500.64**	**1001.28**

Don't filter the final mix
Store at -80oC preferably in one-time use aliquots (any convenient volume), repeated freeze-thaw should be avoided
A thawed aliquot can be reused without too much loss in activity when stored at -20oC up to 2 - 4 weeks after thawing

*   T5 Exonuclease, 10U/ul, Epicentre C# T5E4111K or through Fisher Sci C# NC9847399
**   Taq DNA Ligase, 40U/ul, NEB C# M0208L
***   Phusion High-Fidelity DNA Polymerase, 2U/ul, NEB C# M0530L

GA reaction set-up and transformation

Components per 1 reaction	Vol - ul	Vol - ul
GA Master Mix, 3.2X	15	7.5
DNA fragments**	X	X
H2O	X	X
Total	**48**	**24***

Incubate at 50oC for 60 min (we incubate in PCR machine)

You can transform competent cells directly with the GA or store it at — 20oC if transformation is to be done later
We use 1 ul of GA reaction per each 10 ul of homemade RBCl-- or electro— competent cells
(we have used so far POP2136, BL21(DE3) and SQ171 E. coli strains with good results)
*   We found 24— ul reaction volume sufficient in our cloning experiments but it can be scaled up from the original 48 ul
**   I use NEB's recommendations regarding amount of DNA fragments per reaction
1.   50–100 ng of vectors with 2–3 fold of excess inserts
2.   5 times more of inserts if insert size is less than 200 bps
3.   In 2–3 fragment assembly use 0.02–0.5 pmols/ — ul rxn
4.   In 4–6 fragment assembly use 0.2–1 pmols/ — ul rxn

The above protocol was adopted directly from :
"Protocol for Gibson assembly" by Eric Carlson (graduate student, Michael Jewen's lab, Northwestern University in Chicago)
Both used reference to:
D. G. Gibson et al., Enzyma.c assembly of DNA molecules up to several hundred kilobases. Nat. Methods 6, 343 (2009)

APPENDIX C SCREEN RESULTS

Top2α genetic etoposide hypersensitivity screen: Results						
Yeast Isolate #	**Mutated Region**	**Mutated Amino Acids**	**Yeast Relative Survival (%)**			
			Etoposide Concentration (µg/mL)			
			0	**5**	**10**	**20**
XXX	**Null**	**PMJ1 WT**	**550**	**510**	**450**	**480**
3455, 3415	Δ199-386	Q292R (CAA to CGA)	550	500	240	50
3578	Δ199-386	D374G	660	200	51	10
3576	Δ199-386	D374G	760	280	90	5.6
3542	Δ199-386		1300	890	560	TMTC
3541	Δ902-1161	E1109K (GAA to AAA)	2000	240	130	9.0
3540	Δ902-1161	L1025V (CTC to GTC)	1300	430	110	9.7
3539	Δ902-1161	T920T (ACC to ACT), E1024E (GAA to GAG), K1070E (AAG to GAG)	660	590	160	24
3538	Δ902-1161		1200	760	720	TMTC
3537	Δ902-1161	S891G (AGT to GGT)	860	290	180	18
3536	Δ902-1161	L1144V (CTC to GTC), V966M GTG to ATG, L1048L (CTG to CTT)	2700	790	250	26
3535	Δ902-1161	No Mutations (aa734-1284 good seq data)	2500	950	550	130
3534	Δ902-1161	A1043D (GCT to GAT)	340	180	100	17
3533	Δ902-1161	A1043D (GCT to GAT)	350	200	120	35
3532	Δ902-1161	R1146T (AGG to ACG), K1151Q (AAA to CAA)	430	270	130	63
3531	Δ902-1161	Y960C (TAC to TGC), K1161E (AAG to GAG)	1100	620	230	78
3530	Δ902-1161	E1109K (GAA to AAA)	330	120	46	20
3529	Δ902-1161	T920T (ACC to ACT), E1024E (GAA to GAG), K1070E (AAG to GAG),	330	140	77	26

		D1170N (GAC to AAC)				
3528	Δ902-1161	T920T (ACC to ACT), E1024E (GAA to GAG), K1070E (AAG to GAG), D1170N (GAC to AAC)	580	470	24	39
3527	Δ902-1161		1100	840	440	TMTC
3526	Δ902-1161	No mutations in PCR product	1000	830	550	190
3524	Δ902-1161	E1109K (GAA to AAA)	550	240	110	30
3523	Δ902-1161	E1109K (GAA to AAA)	1100	420	130	16
3522	Δ902-1161	D1120G (GAT to GGT)	1100	690	400	150
3521	Δ902-1161		1500	570	330	100
3520	Δ902-1161	I842V (ATT to GTT)	1200	710	410	86
3519	Δ902-1161		320	180	130	40
3518	Δ902-1161	No mutations found in coding sequence	230	100	66	16
3517	Δ902-1161	No mutations in PCR product	530	480	290	67
3516	Δ902-1161	T955R (ACA to AGA), E1113E (GAA to GAG), Y1135N (TAT to AAT)	1200	450	250	71
3515	Δ902-1161	S1045F (TCT to TTT)	1400	540	270	60
3514	Δ902-1161		420	360	310	210
3513	Δ902-1161	F1003L (TTT to TTA)	850	650	500	200
3512	Δ359-756	N445D (AAT to GAT)	1500	40	2.7	1.1
3511	Δ359-756	N445D (AAT to GAT)	440	21	2.1	0.60
3510	Δ902-1161		790	480	350	180
3509	Δ902-1161	V869M (GTG to ATG), N1067D (AAT to GAT)	350	200	140	74
3508	Δ902-1161	T955I (ACA to ATA), V966A (GTG to GCG)	1400	550	300	60
3507	Δ902-1161	S891G (AGT to GGT)	1600	420	180	34
3502	Δ359-756	D479Y, N413N (AAC to AAT)	1100	220	65	14
3501	Δ359-756	D479Y, N413N (AAC to	510	51	4.1	0.83

278

		AAT), A429A (GCT to GCA)				
3500	Δ359-756	N370S (AAC to AGC), I399T (ATC to ACC)	540	140	360	89
3499	Δ359-756	N370S (AAC to AGC), I399T (ATC to ACC)	470	390	240	91
3498	Δ359-756	D479Y (GAC to TAC), Q422Q (CAG to CAA)	660	65	4.4	0.52
3497	Δ359-756	D479Y (GAC to TAC)	510	52	2.8	0.51
3496	Δ902-1161	D956Y (GAC to TAC)	1100	230	120	10
3495	Δ902-1161	D956Y (GAC to TAC)	400	160	70	17
3494	Δ359-756		740	380	230	64
3493	Δ359-756		440	310	180	63
3492	Δ359-756		520	260	160	51
3491	Δ359-756	V470L (GTT to CTT), H498Y (CAT to TAT), G437E (GGA to GAG)	380	60	11	2.5
3490	Δ359-756	V470L (GTT to CTT), H498Y (CAT to TAT), G437E (GGA to GAG)	340	49	13	1.2
3489	Δ359-756	V470G (GTT to GGT), L531L (CTT to CTC)	310	140	68	52
3488	Δ359-756	V470G (GTT to GGT), L531L (CTT to CTC)	390	120	57	25
3487	Δ359-756	D280E (GAT to GAG), E281K (GAA to AAA)	660	100	66	10
3486	Δ359-756	D374E (GAC to GAG), S387G (AGC to GGC)	420	210	92	20
3485	Δ359-756	D374E (GAC to GAG), S387G (AGC to GGC)	410	100	49	8.8
3481	Δ359-756	M502L (ATG to TTG)	680	160	34	6.9
3480	Δ359-756	M502L (ATG to TTG), S224F (TCT to TTT)	400	140	43	4.7
3479	Δ359-756	D442G (GAT to GGT)	560	110	27	1.1
3478	Δ359-756	D442G (GAT to GGT)	540	91	28	1.9
3477	Δ359-756	V415L (GTG to CTG)	600	89	40	8.8
3476	Δ359-756	V415L (GTG to CTG)	760	68	23	2.3

3475	Δ199-386	Q355H (CAG to CAT)	670	82	30	13
3474	Δ199-386	Q355H (CAG to CAT)	640	340	190	46
3473	Δ359-756		540	350	290	85
3472	Δ359-756		690	360	230	55
3471	Δ359-756	V364I (GTA to ATA)	720	230	110	13
3470	Δ359-756	V364I, S471P	380	210	110	10
3469	Δ359-756		590	390	260	71
3468	Δ359-756		830	520	330	92
3467	Δ359-756		1000	630	410	120
3466	Δ359-756		590	410	260	100
3463	Δ199-386	L275M (TTG to ATG)	970	270	100	9.0
3462	Δ199-386	L275M (TTG to ATG)	570	230	110	8.0
3459	Δ199-386	No mutations in PCR product	340	210	140	45
3458	Δ199-386	No mutations in PCR product	490	260	150	49
3456	Δ199-386		1100	560	200	110
3454	Δ199-386	Q292R (CAA to CGA)	620	330	200	70
3452	Δ199-386		370	170	130	28
3450	Δ199-386		610	370	230	84
3449	Δ199-386	L275M (TTG to ATG)	1400	560	390	87
3448	Δ199-386		960	TMTC	TMTC	TMTC
3446	Δ199-386		1100	580	470	160
3444	Δ199-386		100	320	140	120
3442	Δ199-386		670	350	190	63
3440	Δ199-386		1200	670	450	TMTC
3439	Δ199-386		1000	510	280	TMTC
3438	Δ199-386	K278K, N508T	630	380	230	75
3437	Δ902-1161	S891G (AGT to GGT),	1300	330	110	24

		L1155L (CTG to TTG), T1157I (ACA to ATA)				
3436	Δ902-1161	T920T (ACC to ACT), E1024E (GAA to GAG), K1070E (AAG to GAG)	1100	510	210	18
3435	Δ902-1161	No mutations in PCR product	890	490	240	130
3434	Δ902-1161		790	470	310	TMTC
3433	Δ199-386	No mutations in PCR product	880	220	290	85
3432	Δ199-386	No mutations in PCR product	740	460	310	97
3431	Δ199-386	T377I (ACA to ATA)	850	200	87	18
3430	Δ199-386	T377I (ACA to ATA)	740	400	250	75
3427	Δ199-386	L223F (TTG to TTC) Q220Q (CAG to CAA), G323G (GGC to GGT)	610	330	140	39
3426	Δ199-386	L223F (TTG to TTC) Q220Q (CAG to CAA), G323G (GGC to GGT)	840	340	160	43
3425	Δ199-386	G347G	470	330	230	96
3424	Δ199-386	G347G	730	340	220	81
3422	Δ199-386	L140L (CTC to CTT)	470	330	400	94
3420	Δ902-1161	P904R (CAA to CGA), N1108K (AAC to AAG)	1300	480	250	67
3419	Δ902-1161		1400	670	370	76
3418	Δ902-1161	K1161E (AAG to GAG)	1900	1100	360	29
3417	Δ902-1161	T920I (ACC to ATC)	430	640	280	95
3416	Δ902-1161	T920I (ACC to ATC)	840	640	340	83
3415	Δ902-1161	Q292R (CAA to CGA)	550	500	240	50
3412	Δ199-386	D374D	470	320	190	91
3410	Δ199-386	R268H (CGT to CAT), S285S (TCC to TCA), K352R (AAA to AGA), P385H (CCC to CAC)	560	390	230	93
3408	Δ199-386	No mutations in PCR product	600	280	200	66

3405	Δ199-386	P221S (CTT to TCT), V253V (GTC to GTT), D339N (GAT to AAT)	120	130	110	68
3404	Δ199-386	E281D (GAA to GAT)	510	210	130	47
3403	Δ199-386	E203K (GAG to AAG)	340	160	170	91
3402	Δ199-386		650	360	230	140
3401	Δ199-386	G211G (GGA to GGG), K278M (AAT to ATG), T377I (ACA to ATA)	290	180	94	30
3400	Δ199-386		380	400	230	TMTC
3399	Δ902-1161		460	240	160	38
3398	Δ902-1161		370	320	260	80
3397	Δ902-1161		530	260	120	31
3396	Δ902-1161	No Mutations found in coding sequence	780	250	120	16
3395	Δ902-1161		1400	660	320	54
3394	Δ902-1161		900	530	220	62
3391	Δ902-1161	A1052G (GCT to GGT)	4300	870	80	26
3390	Δ902-1161	Y960C (TAC to TGC), K1161E (AAG to GAG)	640	180	25	2.6
3389	Δ902-1161	H986G (CAC to CAT), V988F (GTC to TTC), P952P (CCT to CCC)	630	260	140	35
3388	Δ902-1161	H986G (CAC to CAT), V988F (GTC to TTC), P952P (CCT to CCC)	570	240	160	35
3387	Δ902-1161		750	360	180	41
3199-386	Δ902-1161	No mutations in PCR product	520	440	110	54
3385	Δ902-1161		750	390	310	TMTC
3384	Δ902-1161		990	420	290	120
3383	Δ902-1161		910	420	TMTC	TMTC
3382	Δ902-1161		1500	650	630	140
3381	Δ902-1161		310	290	170	83

3380	Δ902-1161		1000	830	540	270
3379	Δ902-1161		1100	500	320	104
3378	Δ902-1161		830	440	230	120
3376	Δ902-1161		500	260	160	42
3375	Δ902-1161		980	600	360	TMTC
3374	Δ902-1161		830	370	250	TMTC
3373	Δ902-1161		560	360	210	TMTC
3372	Δ902-1161		740	330	270	TMTC
3369	Δ902-1161		650	180	240	100
3368	Δ902-1161		1400	800	790	250
3366	Δ199-386	V329V (GTA to GTT), V338A (GTT to GCT)	400	270	250	140
3365	Δ199-386	No mutations in PCR product	520	230	140	54
3364	Δ199-386	No mutations in PCR product	730	390	250	73
3358	Δ359-756	A330V, D374G	670	270	120	18
3357	Δ199-386	N258D (AAT to GAT), A350G (GCA to GGA)	1200	260	88	10.0
3350	Δ359-756	A350A (GCA to GCC), D442N (GAT to AAT)	330	140	43	21
3348	Δ359-756	V415V (GTG to GTA), V470A (GTT to GCT)	1600	270	54	4.4
3346	Δ359-756	D463N (GAT to AAT), K466I (AAA to ATA)	440	68	5.9	0.84
3344	Δ359-756	N424N (AAC to AAT), K466R (AAA to AGA), K499K (AAG to AAA)	130	110	41	3.0
3342	Δ199-386		200	160	100	61
3341	Δ359-756	A444T (GCC to ACC)	800	240	97	22
3338	Δ199-386	No mutations found in coding sequence	820	220	60	20.0
3336	Δ199-386		540	440	370	TMTC
3334	Δ359-756	No mutations in PCR product	800	500	390	TMTC

3332	Δ199-386		730	670	590	TMTC
3330	Δ199-386		490	380	180	52
3328	Δ199-386		650	520	350	210
3326	Δ199-386		380	230	190	81
3324	Δ199-386		350	190	130	49
3323	Δ199-386	A330V (GCT to GTT), D374G (GAC to GGC)	1200	260	88	10
3322	Δ199-386	A330V (GCT to GTT), D374G (GAC to GGC)	670	270	120	18
3320	Δ199-386		1000	590	290	130
3694	Δ359-756	T377R (ACA to AGA)	180	76	32	5.9
3692	Δ359-756		600	470	340	170
3691	Δ359-756	V415A (GTG to GCG), V476V (GTT to GTC), I511I (ATC to ATT)	770	30	10	7.9
3689	Δ359-756	V364I (GTA to ATA), D442Y (GAT to TAT)	910	21	2.5	1.0
3687	Δ359-756	E503G (GAA to GGA), M539V (ATG to GTG)	260	110	40	3.8
3685	Δ359-756	D479Y (GAC to TAC)	330	56	11.5	1.2
3683	Δ359-756	N433K (AAT to AAA), S471S (TCA to TCT)	320	5.0	2.7	0.60
3681	Δ359-756	N445I (AAT to ATT)	290	160	50	18
3675	Δ576-925	I787F (ATT to TTT), G911C (GGT to TGT), T808T (ACA TO ACG)	580	360	210	51
3674	Δ576-925	I787F (ATT to TTT), G911C (GGT to TGT), T808T (ACA TO ACG)	840	450	280	75
3673	Δ576-925	M669T (ATG to ACG), Q938H (CAA to CAC), R793R (AGG to AGA)	870	570	430	180
3671	Δ576-925	A652V (GCC to GTC), G852S (GGT to AGT), K936N (AAA to AAT)	750	110	16	1.7
3670	Δ576-925	A652V (GCC to GTC), G852S (GGT to AGT), K936N (AAA to AAT)	1000	150	11	2.0

3669	Δ576-925	P576L (CCC to CTC), A814V (GCT to GTT), H795H (CAT to CAC)	790	340	66	10
3667	Δ576-925	V751M (GTG to ATG), A814V (GCT to GTT)	880	740	280	TMTC
3665	Δ576-925	T792A (ACC to GCC), F818Y (TTT to TAT)	520	170	54	3.5
3663	Δ576-925	R736G (CGG to GGG), G852C (GGT to TGT), S650S (AGC to AGT), Q674Q (CAA to CAG)	520	62	4.8	0.50
3662	Δ576-925	R736G (CGG to GGG), G852C (GGT to TGT), S650S (AGC to AGT), Q674Q (CAA to CAG)	690	150	41	1.4
3660	Δ576-925	N866K (AAC to AAA)	430	92	32	8.7
3658	Δ576-925	H634L (CAT to CTT), L783I (CTC TO ATC), E854G (GAA to GGA)	860	360	160	41
3655	Δ576-925	Y640H (TAT to CAT), G760S (GGT to AGT)	2600	92	15	2.9
3653	Δ576-925	V742L (GTA to CTA), E839K (GAA to AAA)	440	91	20	2.6
3651	Δ576-925	E623K (GAA to AAA), V751A (GTG to GCG)	410	180	79	34
3650	Δ576-925	L651M (CTG to ATG), C862C (TGC to TGT)	460	290	160	55
3648	Δ576-925	I577V (ATT to GTT), Q674H (CAA to CAC), L730M (TTG to ATG)	330	190	110	49
3646	Δ576-925	F790S (TTT to TCT), T858I (ACT to ATT)	560	170	63	13
3643	Δ359-756	T372N (ACC to AAC), D442Y (GAT to TAT), A469T (GCT to ACT), E523V (GAA to GTA)	180	96	30	8.9
3641	Δ359-756	E506G (GAG to GGG), A469A (GCT to GCA)	700	28	2.3	1.0
3639	Δ359-756	D442G (GAT to GGT), I490V (ATA to GTA)	403.3	83.5	25.7	1.2
3637	Δ359-756	V476I (GTT to ATT)	770	590	350	39
3635	Δ359-756	D478E (GAC to GAG)	1200	590	160	29
3633	Δ359-756	R434K (AGA to AAA), E505V (GAG to GTG)	840	680	200	72

3632	Δ359-756	H432R (CAT to CGT)	580	260	60	12
3697	Δ576-925	S763S (TCA to TCG)	490	240	220	71
3695	Δ576-925	T694I (ACA to ATA), Y612C (TAT to TGT)	740	230	94	19
3698	Δ576-925	F807F (TTT to TTC), K622E (AAG to GAG)	580	150	53	9.2
3701	Δ359-756		430	240	140	26
3703	Δ359-756	N504Y (AAT to TAT)	710	410	290	100

*TMTC- Too many to count, indicates that the cells were too plentiful to count for the serial dilution of culture plated. Given the experimental parameters this was interpreted to mean that the yeast isolate was not appreciably sensitive to etoposide

APPENDIX D FIGURE PERMISSIONS

Figure 1.1 Deweese J.E.,Osheroff M.A., & Osheroff N. DNA topology and topoisomerases: Teaching a "knotty" subject. *Biochemistry and Molecular Biology Education*, John Wiley & Sons (2009) License # 4563130776724.

Figure 1.2 Nitiss J.L.. DNA topoisomerase II and its growing repertoire of biological functions. *Nature Cancer Reviews*, Springer Nature (2009) License # 4581480500666
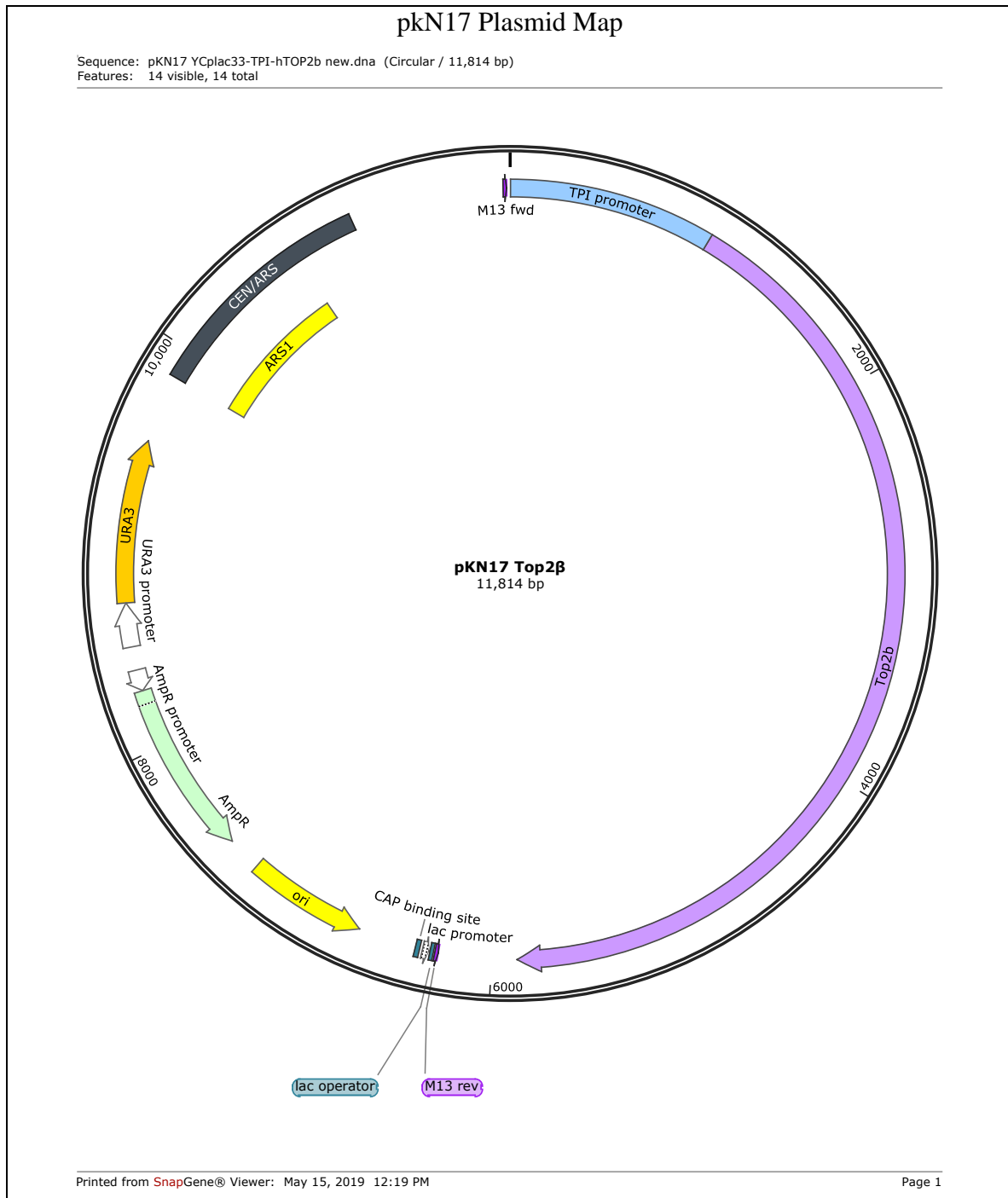
Figure 2.1A Wendorff T.J. et al., The Structure of DNA-Bound Human Topoisomerase II Alpha: Conformational Mechanisms for Coordinating Inter-Subunit Interactions with DNA Cleavage, *Journal of Molecular Biology* (2012), License # 4595461272332

Used in Dissertation Defense, Deweese J.E. and Osheroff N., The DNA cleavage reaction of topoisomerase II: wolf in sheep's clothing, *Nucleic Acids Research* (2008), License#4595460268502

Used in Dissertation Defense, Jeppsson K. et al, The maintenance of chromosome structure: positioning and functioning of SMC complexes, *Nature reviews Molecular Cell Biology* (2014), License# 4590360984520

Used in Dissertation Defense, Skouboe C et al., A Human Topoisomerase IIα Heterodimer with Only One ATP Binding Site Can Go through Successive Catalytic Cycles, Journal of Biological Chemistry, (2003) License# 4596650171228

pkN17 Plasmid Map

Sequence: pKN17 YCplac33-TPI-hTOP2b new.dna (Circular / 11,814 bp)
Features: 14 visible, 14 total

pKN17 Top2β
11,814 bp

M13 fwd
TPI promoter
2000
Top2b
4000
lac promoter
CAP binding site
6000
ori
AmpR
AmpR promoter
8000
URA3 promoter
URA3
ARS1
10,000
CEN/ARS

lac operator
M13 rev

ΔJMB1 Plasmid Map

Sequence: JMB-hTop2a .dna (Circular / 13,681 bp)
Features: 17 visible, 17 total

ΔJMB1 Top2α
13,681 bp